NTNU – Trondheim
Norwegian University of
Science and Technology

Sea State Limitations for the Deployment of Subsea Compression Station Modules

Ingvild Roti

Abstract

Deployment of a large box structure in many sea states has been investigated. Two deployment methods are compared; crane installation over the side and through moonpool installation. The structure is 12 [m] long, 6 [m] wide and 12 [m] high with a mass of 250 [t]. Normand Subsea is used as installation vessel. Both JONSWAP and Torsethaugen wave spectra are used for crane lowering while only JONSWAP is used for moonpool installation.

Splash zone lowering is seen as the most critical stage of the installation because hydrodynamic forces are largest at the surface. Hydrodynamic uplift is assumed limiting for the deployment, i.e "slack slings". Slings are the lower part of the lift rigging. The operation limit is that dynamic uplift should not exceed 90 % of the modules static weight. Forces in z-direction are hence most interesting. Minimum wire tension for the lowering is therefore calculated at two time instances; when the module bottom end is at mean water level and when the module is fully submerged with its top end 0.5 [m] below mean water level. These time instances are referred to as time instance 1 and 2 in the report respectively.

Design significant wave heights, H_s, are taken from plots of minimum wire tension for different wave peak periods T_p and wave headings. Based on these design H_s values, which equals the operation limits, operability rosettes are plotted. It is seen that wave headings 90° and 120° are most critical with lowest operability for crane installation while wave heading 90° is worst for moonpool deployment.

The lowest design H_s for all T_p values considering wave headings 0° ±30° is used as overall operation limit for deployment when weather window statistics are computed. Time instance 1 is worst for crane deployment with resulting forecasted weather operational criterion $H_s = 2.8$ [m]. Time instance 2 is worst for moonpool deployment with forecasted operational criterion $H_s = 2.5$ [m] and $T_p \geq 13.0$ [s]. Reference time for deployment, hence the time needed from the weather forecast is issued to the module is landed on the seabed, is 6 hours. Based on reference time and forecasted operation limits weather window statistics are estimated.

Moonpool deployment annual operability is 7.24 days, hence 2.0 % of the year, and can naturally not be used. Crane deployment annual operability is 213.22 days, 58.4 % of the year. This is much better but still not very good as it is theoretically desirable to be able to install the module any day year round.

Sammendrag

I denne hovedoppgaven har nedsenkning av en stor boksformet struktur blitt undersøkt for mange sjøtilstander. To nedsenkningsmetoder er sammenlignet; kraninstallasjon over skutesida og nedsekning gjennom moonpool. Strukturen er 12 [m] lang, 6 [m] bred og 12 [m] høy med en masse på 250 [t]. Normand Subsea er brukt som installasjonsfartøy. Både JONSWAP og Torsethaugen bølgespektra er brukt ved krannedsenkning mens bare JONSWAP er brukt ved moonpoolnedsenkning.

Nedsenkning gjennom plaskesonen er sett på som mest kritisk for installasjonen siden hydrodynamiske krefter er størst ved vannoverflaten. Hydrodynamisk løft er antatt begrensende for å få gjennomført installasjon, det vil si slakke løftestropper. Løftestropper er den nederste delen av løfteriggingen. Operasonsgrensen er at dynamisk løft av strukturen ikke skal overskride 90 % av strukturens vekt. Krefter i z-retning er da mest interessante siden. Minimum vaierstrekk er derfor beregnet ved to tidspunkt: når modulens bunn er ved stillevannslinja og når modulen er fullt nedsenket med dens topp 0.5 [m] under stillevannslinja. Disse tidspunktene er omtalt som henholdsvis tidspunkt 1 og 2 i rapporten.

Design signifikante bølgehøyder, H_s, er funnet fra plott av minimum vaierstrekk for ulike bølgetopp-perioder T_p og bølgeretninger. Basert på disse design H_s verdiene, som tilsvarer operasjonsgrensene, er tilgjengelighetsrosetter plottet. Det viser seg at 90^0 og 120^0 er de mest kritiske bølgeretningene med lavest tilgjengelighet for kraninstallasjon mens 90° er mest kritisk for moonpoolinstallasjon.

Den laveste design H_s-verdien for alle T_p-verdier ved bølgeretning $0^o \pm30^o$ er brukt som generell operasjonsgrense når værvindustatistikk beregnes. Tidspunkt 1 er verst for kraninstallasjon og gir meteorologisk varslet operasjonsgrense på $H_s = 2.8$ [m]. Tidspunkt 2 er verst for moonpoolinstallasjon og gir meteorologisk varslet operasjonsgrense på $H_s = 2.5$ [m] og $T_p \geq$ 13.0 [s]. Referansetid for nedsenkningen, altså tiden som trengs fra værvarselet er utstedt til modulen er landet på havbunnen, er 6 [timer]. Basert på referansetid og meteorologisk varslede operasjonsgrenser er værvindustatistikk estimert.

Årlig tilgjengelighet for moonpoolinstallasjon er kun 7.24 [dager], altså 2.0 % av året, og denne installasjonsmetoden kan derfor naturlig nok ikke brukes. Årlig tilgjengelighet for kraninstallasjon over skipssida er 213.22 [dager], 58.4 % av året. Dette er mye bedre men likevel ikke veldig bra med tanke på at det optimale vil være å kunne installere modulen en hvilken som helst dag i løpet av året.

MASTER THESIS IN MARINE TECHNOLOGY

SPRING 2012

FOR

STUD. TECHN. INGVILD ROTI

Seastate Limitations for the Deployment of Subsea Compression Station Modules

Shell is presently considering the implementation of subsea gas compression for the Ormen Lange field. Should this project proceed it will be one of the first such developments in the world. The scale of the project is unprecedented in terms of size and complexity for a subsea development. The subsea compression system will include compressor, pump, variable speed drive, UPS and switchgear modules. Modules are installable individually and range in weight up to 250 tonnes.

Once installed, a high degree of system availability is essential. In the event of a module failure, the ability to deliver replacement modules in high seastates will extend the intervention window thereby increasing system up-time.

Vessel delivery of heavy and highly instrumented equipment packages is challenging from a number of viewpoints. Deployment of equipment with a large 'sail area' through the air/water interface is possibly the most critical aspect of the installation sequence. Wave induced uplift of the package and subsequent snap-loading of wire lines can result in critical dynamic amplification of tensions. Additionally, wave slam and inertial forces in open structures can result in high accelerations and consequent damage to susceptible components within the modules. Deployment of such large packages through a moonpool is technically feasible but will be subject to its own unique considerations. Delineation of such factors is central to the demonstration of feasibility of the mode of deployment.

The objective of this thesis will be to calculate responses for a typical installation vessel in a range of characteristic seastates thereby determining the conditions under which deployment of the subsea compression modules is feasible. Further, the study will seek to determine the optimal means of delivering modules through the air/water interface considering both 'over-the-side' and through-moonpool deployment techniques.

The outcomes of the study will provide preliminary data on the influence of maintenance intervention on overall system availability in the event of module malfunction, thus providing important grounding for more detailed analytical work on deployment issues.

The student shall:

1. Give a background of the concept.
2. Define the air/water interface problem and key parameters.
3. Review deployment methods for large modules.
4. Evaluate the hydrodynamic flow field including moonpool and free-surface effects in the splash-zone.
5. Assess slack slings and consequences for operability and weather windows.
6. Evaluate the deployment methods based on the resulting weather window statistics.

In the thesis the candidate shall present his/her personal contribution to the resolution of problem within the scope of the thesis work.

Theories and conclusions should be based on mathematical derivations and/or logic reasoning identifying the various steps in the deduction.

The candidate should utilize the existing possibilities for obtaining relevant literature.

The thesis should be organized in a rational manner to give a clear exposition of results, assessments, and conclusions. The text should be brief and to the point, with a clear language. Telegraphic language should be avoided.

The thesis shall contain the following elements: A text defining the scope, preface, list of contents, summary, main body of thesis, conclusions with recommendations for further work, list of symbols and acronyms, reference and (optional) appendices. All figures, tables and equations shall be numerated.

The supervisor may require that the candidate, in an early stage of the work, present a written plan for the completion of the work. The plan should include a budget for the use of computer and laboratory resources that will be charged to the department. Overruns shall be reported to the supervisor.

The original contribution of the candidate and material taken from other sources shall be clearly defined. Work from other sources shall be properly referenced using an acknowledged referencing system.

The thesis shall be submitted in two copies:

- Signed by the candidate
- The text defining the scope included
- In bound volume(s)
- Drawings and/or computer prints that cannot be bound should be organized in a separate folder.
- The bound volume shall be accompanied by a CD or DVD containing the written thesis in Word or PDF format. In case computer programs have been made as part of the thesis work, the source code shall be included. In case of experimental work, the experimental results shall be included in a suitable electronic format.

Contact   : Bruce Wilson, AS Norske Shell
Advisors   : Professor Bernt J. Leira
                    Professor Dag Myrhaug

Deadline   : 10.06.2012:

Dag Myrhaug
Supervisor

1. Preface

This report is the Master's Thesis in Marine Hydrodynamics for Ingvild Roti written during the spring of 2012 in Stavanger. It counts the last 30 credits to complete the Master of Science Study at the department of Marine Technology at the Norwegian University of Science and Technology (NTNU) in Trondheim, Norway.

The Thesis is written for AS Norske Shell and I have therefore been located in Stavanger at their Norwegian main office. Norske Shell has no in-house capability for in-depth analyses and there are few with marine hydrodynamics as their field of excellence. Getting help has therefore been a challenge. But my NTNU supervisors professors Dag Myrhaug and Bernt J. Leira have been very helpful and answered all my emails and calls, and for that I am grateful.

I will also like to thank Shell supervisor Bruce Wilson for his support, encouragement and advices, Bjarte Landa for helping me with MACSI2 and the analyses in general, Rasmus Kulseng for helping me with the computer program Metocean Tool Box and fellow Shell intern Tor Ivar Gjære for meaningful discussions.

In addition I appreciate that both Peter Christian Sandvik and Knut Torsethaugen have taken the time to answer my questions regarding MACSI2 and the Torsethaugen wave spectrum respectively.

The analysis program MACSI2 and methodology to compute slamming forces are rather simple, but there are good reasons for this approach. MACSI2 was the program to use if I wanted to ensure timely support in the office. Besides time is limited so each analysis has to be quite fast.

It is worth mentioning that with two weeks left of the Thesis I discovered a mistake in the moonpool analyses. The wire length was set about 6 [m] too long, which in practice means that the deployed module was below the ship hull. All MACSI2 moonpool analyses had therefore to be rerun and post-processed all over again. This was a frustrating occurrence since MACSI2 could not handle the analyses with the new wire length at first, and because it was discovered during Pentecost no one was available for answering my questions. But after some trying and failing with changing parameters it finally worked for most sea states and the results are as good as they can get with the limited time left. But I am glad the mistake was discovered as it changed the conclusion completely; from moonpool installation being much better than crane installation to crane installation being much better than moonpool installation.

Stavanger, 05.06.2012

Ingvild Roti

Ingvild Roti

Table of Contents

List of Figures

List of Tables

List of Equations

Nomenclature

$A(\omega)$ – Real part of complex transfer function

A_i – Uncoupled added mass in direction i (i = x, y, z) [kg]

A_w – Circumscribed area of lift wire [m^2]

A_{mi} – Projected area of the module in direction i (i = x, y, z) [m^2]

$A_{moonpool}$ – Projected area of the moonpool in z-direction [m^2]

A_s – Slamming area [m^2]

A_{33wp} – Added mass of water plug in heave direction [kg]

a_i – i-component of acceleration (i = x, y, z) [m/s^2]

$B(\omega)$ – Imaginary part of complex transfer function

B – Buoyancy of module [N]

$B_1{}'$ – Linear drag at velocity = 1

$B_2{}'$ – Quadratic drag at velocity = 1

C_{Ai} – Module added mass coefficient in direction i (i = x, y, z)

C_{Ai_corr} – Position correction factor to the added mass coefficient in direction i (i = x, y, z)

C_b – Damping of relative motion between water plug and body in moonpool [kg/m]

C_{Di} – Module quadratic drag coefficient in direction i (i = x, y, z)

C_{DDi} – Total module drag coefficient in direction i (i = x, y, z)

$C_{resilience}$ – Total crane system resilience [m/N]

C_{ps} – Damping of relative motion between water plug and ship moonpool walls [kg/m]

C_{ps1} – Linearised damping of relative motion between water plug and ship moonpool walls [kg/m]

C_s – Slamming coefficient

ct$_i$ – Crane tip coordinate compared to vessels CoG at MWL in direction i (i = x, y, z) [m]

D – Characteristic length of object when calculating R_e [m]

D – Ship draught [m]

d – The distance from MWL to center of gravity of the submerged part of the object [m]

d_W – Lift wire diameter [m^2]

E_W – Wire cross-sectional Young's modulus [GPa]

F(t) – Excitation force on water plug [N]

F_D – Drag force [N]

F_G – Weight of module in air including rigging and water in structural volumes [N]

F_{hyd} – Hydrodynamic forces on the structure being lowered [N]

F_M – Hydrodynamic mass force [N]

F_{slam} – Slamming impact force [N]

F_{snap} – Characteristic snap load [N]

F_S – Module submerged weight [N]

$F_{static_{min}}$ – Minimum static weight of lowered structure [N]

F_{Wi} – Winch wire forces including drag [N]

F_ρ – Varying buoyancy force [N]

f – Wave frequency [Hz]

g – Acceleration of gravity [m/s^2]

$H(\omega)$ – General complex transfer function

H_S – Significant wave height [m]

h – Water depth [m]

h_m – Height of module [m]

K – Total system stiffness [N/m]

$K_{moonpool}$ – Water plane stiffness in moonpool [N/m]

k – Wave number [1/m]

k_{block} – Stiffness of multiple lines in a block if used [N/m]

k_{boom} – Stiffness of crane boom [N/m]

k_{crane} – Total crane system stiffness, which equals total stiffness minus wire stiffness [N/m]

k_{other} – Other stiffness contributions if any [N/m]

$k_{rigging}$ – Stiffness of rigging [N/m]

k_{soft} – Stiffness of soft strop or passive heave compensation system if used [N/m]

k_w – Stiffness of lifting wire(s) [N/m]

l_m – Length of module [m]

l_w – Length of lift wire between crane tip and module volume center in z-direction [m]

M – Total mass including added mass [kg]

M_m – Mass of module in air [kg]

M_{min} – Minimum module mass, hence mass before the module is flooded [t]

M_{wp} – Mass of water plug in moonpool [kg]

$M_{wp_{TOT}}$ – Total mass of the water plug, including added mass [kg]

m_n – Spectral moments

ms_i – Main sheave coordinate compared to the vessels CoG at MWL in direction i (i = x, y, z) [m]

$N^+(0)$ – Expected zero up-crossing frequency [Hz]

p – Module perforation ratio %

p_o – Atmospheric pressure [Pa]

p_d – Dynamic pressure [Pa]

R_e – Reynolds number

$S(\omega)$ – Wave spectrum [m²s]

s – Motion of any point on the ship [m]

T – Wave period [s]

T_C – Contingency period hours

T_p – Spectral peak period [s]

T_{POP} – Planned operation time hours

T_R – Operation reference period hours

T_Z – Mean zero up-crossing period [s]

T_0 – Eigenperiod and hence resonance period [s]

t – Time variable [s]

U_∞ – Inflow velocity [m/s]

U_e – Tangential velocity [m/s]

u_r – Relative water velocity [m/s]

V_m – Volume of the unit being lowered [m³]

V_m' – Submerged volume at a given time instance [m³]

V_{wind} – Wind velocity 19.5 [m] above MWL [m/s]

v_c – Hook lowering velocity [m/s]

v_{ct} – Characteristic single amplitude vertical velocity of crane tip [m/s]

v_i – i-component of velocity (i = x, y, z) [m/s]

v_s – Slamming impact velocity [m/s]

v_{snap} – Characteristic snap velocity [m/s]

v_w – Characteristic vertical water particle velocity [m/s]

W – Module weight [N]

w_m – Width of module [m]

$x_i, \dot{x}_i, \ddot{x}_i$ – Module position, velocity and acceleration in direction in direction i (i = x, y, z) [m] / [m/s] / [m/s²]

Greek letters

α – Spectral parameter for the JONSWAP spectrum

β – Form parameter for the JONSWAP spectrum

γ – Peakedness parameter for the JONSWAP spectrum

γ_{SF} – Nominal safety factor

ΔT – Time increment for MACSI2 analyses [s]

ϵ – Random phase angle [rad]

$\zeta, \dot{\zeta}$ – Wave profile and surface elevation velocity [m] / [m/s]

ζ_a – Wave amplitude [m]

ζ_b – Displacement of body in moonpool [m]

ζ_s – Ship heave motion [m]

$\zeta_{wp}, \dot{\zeta}_{wp}$ – Water plug displacement and velocity [m] / [m/s]

η – Relative damping ratio to critical damping

η_i – Ship mode of motion

θ – Angular coordinate used for explaining drag [degrees]

λ – Wavelength [m]

ν – Kinematic water viscosity [m^2/s]

ρ_{mp} – Density of water in moonpool [kg/m^3]

ρ_{steel} – Steel density [kg/m^3]

ρ_w – Seawater density [kg/m^3]

σ – Spectral parameter for the JONSWAP spectrum

φ – Wave heading [Degrees]

φ – Velocity potential [m^2/s]

ψ – Phase angle between response and excitation

ω_0 – Eigenfrequency and hence resonance frequency [rad/s]

ω – Wave frequency [rad/s]

ω_p – Spectrum peak frequency [rad/s]

Abbreviations

AHC – Active Heave Compensation

AP – Aft Perpendicular

CAPEX – Capital Expenditure

CM – Choke Module

CoF – Center of Flotation

CoG – Center of Gravity

DAF – Dynamic Amplification Factor

DNV – Det Norske Veritas

DP – Dynamic Positioning

EPC – Engineering, Procurement and Construction

FBS – Foundation Bottom Structure

FEM – Federation Europeenne de la Manutention

ICP – Independent Competent Person

IMR – Inspection, Maintenance and Repair

KC – Keulegan-Carpenter

LCG – Longitudinal Center of Gravity

MBL – Minimum Breakage Load

MDV – Meg Dosage Valve

MEG – Mono-Ethylene Glycol

MHS – Module Handling System

MTB – Metocean Tool Box

MWL – Mean Water Level

NS – Norsk Standard

OL – Ormen Lange

OPEX – Operating Expenditure

PLET – Pipeline End Termination System

PM – Pierson-Moskowitz

RAO – Response Amplitude Operator

ROV – Remotely Operated Vehicle

SCM – Subsea Control Module

SWL – Safe Working Load

UPS – Uninterruptible Power Supply

VCG – Vertical Center of Gravity

VIV – Vortex Induced Vibration

VSD – Variable Speed Drive

2. Scope of Work

Annual operability for deployment of the largest module envisaged for the Ormen Lange subsea future compression station is to be compared for two deployment methods; over the side using a crane and via moonpool.

To give a better understanding of the installation and operational background, information on the future compression concept and the Ormen Lange field will be given. Also some typical deployment methods of modules this size are reviewed. Then the free-surface and moonpool flow fields together with the ship motions are used to compute minimum wire tension in the lifting wire during deployment of the structure. This is done to see whether slack slings and hence snap loads will be a problem. The "slack sling" condition is in this report considered to be the operability limit. Operability limits can therefore be found based on minimum wire tension results. These operability limits are then used to compute annual weather window statistics allowing the two deployment methods, crane over the side and moonpool lowering, to be compared.

2.1 Analyses methodology

The limiting criterion for installing the structure is to avoid hydrodynamic uplift, i.e. "slack slings". Analyses are run for the two deployment methods at two different time instances with zero winch speed as seen in Figure 1.

1. When the lower end of the unit is at mean water level (MWL).
2. When the unit is fully submerged. The top of the module is taken to be 0.5 [m] below MWL.
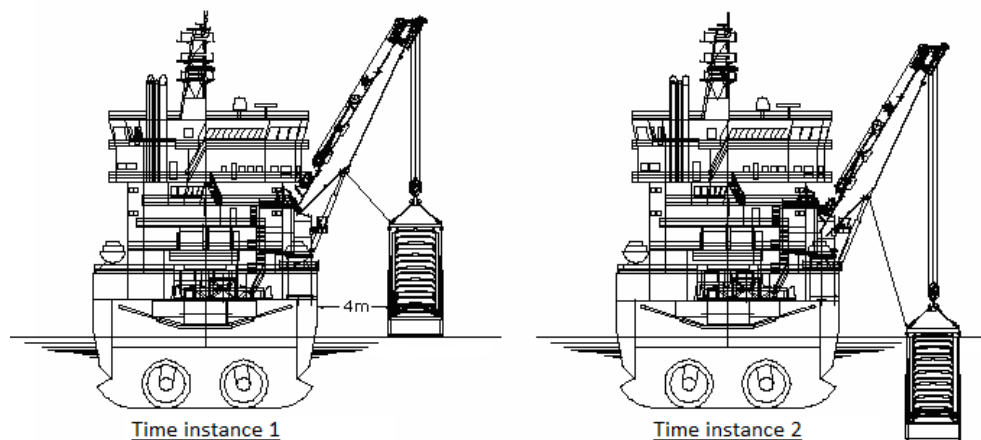
Figure 1: Graphic description of the two time instances during deployment being analyzed for installation over the side using crane [33]. Note that the module is a bit too high in the water column at time instance 2.

For time instance 1 slamming is to be analyzed using DNV recommended practice [10]. The calculation itself is carried out in the computer program MATLAB for practical purposes. To analyze time instance 2 MACSI2 (MArine Crane Simulation) will be used, a time simulation program for marine crane and lifting operations. The reason for choosing these time instances is to cover the most critical positions for slamming and uplift. At time instance 1 slamming is critical. At time instance 2 the unit is fully submerged and fully exposed to wave actions which are largest at sea surface and reduces exponentially down in the water column [11]. MACASI2 results will be taken into MATLAB for prost-processing.

Motion specifics of the crane tip and main sheave in the moonpool handling tower (MHT) must be known for slamming analyses to be run. As MACSI2 estimates the crane tip/main sheave motion and velocity, which is necessary input into slamming analyses, time instance 2 will be analyzed before time instance 1. During the post-processing of time instance 2 in MATLAB also time instance 1 will be analyzed.

The analyses are run for different sea states to find the limiting weather criteria for installation, hence varying H_S, T_P and wave heading. Irregular waves are used. An operability rosette will then be given for the 4 different analyses; two time instances for both installation methods. An operability rosette example is given in Figure 2.
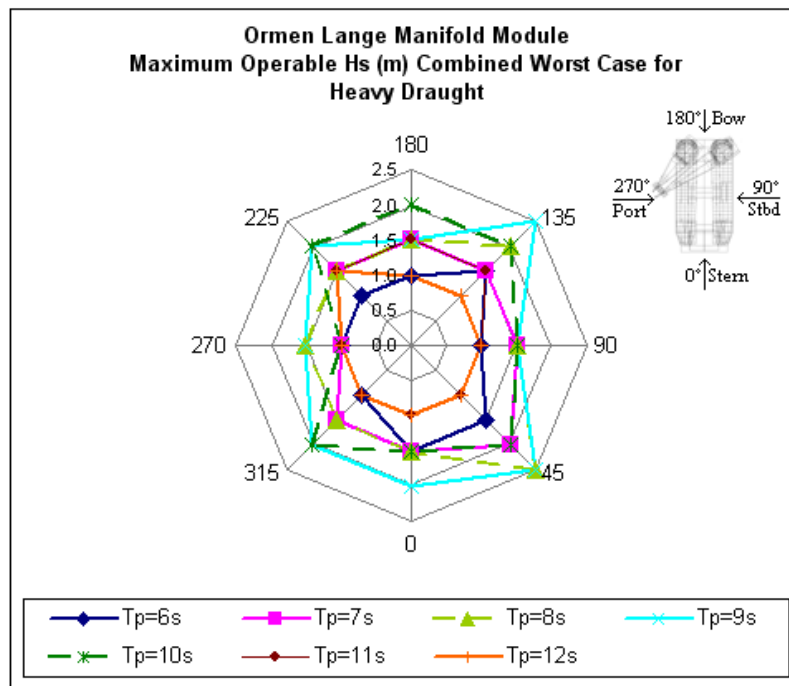
Figure 2: Operability rosette example [23].

During deployment DP will be used to hold wave heading 0⁰. Deviations can occur and to account for this also wave heading 30⁰ is analyzed. These wave headings are assumed to limit

the slack sling probability as optimal vessel motion specifics often are obtained for headings close to 0°. The limiting sea states for wave heading $0^\circ \pm 30^\circ$ will be taken into another computer program called Metocean Tool Box (MTB). Metocean Tool Box can calculate weather window statistics for given operation limits and installation times based on historical weather data. By using estimated operation limits of the two deployments method and a reference time for the installation the annual operability of the deployment methods can be computed and compared.

Vessel motions changes with loading condition as center of flotation moves. Here analyses are run for one loading condition only, fully loaded, as it is the comparison of operability between the two deployment methods that is of interest.

3. Main Assumptions

The main assumptions made in this report are listed below.

- As the module design is not yet decided, a box shaped module with outer dimensions 12x6x12 [m] is used. The weight is 250 [t]. Outer dimensions and module weight are set equal to the module requirements for future compression modules.
- Normand Subsea is taken as the installation vessel that is to be used for deployment of the largest compression module. Normand Subsea response amplitude operators (RAOs) are hence used as input for the analyses. The RAOs are provided by Subsea 7 and attached in Appendix 12.5.
- The main crane presently installed on Skandi Acergy is used instead of the main crane presently on Normand Subsea for deployment over the ship side. This is because the main crane on Normand Subsea can only take 140 [t] static weight, while the main crane on Skandi Acergy can take 400 [t] static load.
- Moonpool dimensions are assumed to be 14x7.5 [m] with moonpool center where the moonpool center presently is for the main moonpool at Normand Subsea.
- Hydrodynamic uplift, i.e. "slack slings", drives the operation limit.
- The two time instances used in the analyses are the most critical during splash zone lowering. Time instance 1 is when the lower end of the unit is at mean water level (MWL). Time instance 2 is when the unit is fully submerged with its top end 0.5 [m] below MWL.

4. Background Information

4.1 Ormen Lange

Presently Ormen Lange (OL) is Europe's third largest gas field and the gas wells are the largest in the world, see reference [42]. The field was discovered in 1997 and developed by Norsk Hydro which was operator during the development phase. The companies that share the license are Shell, Statoil, Petoro, Dong and ExxonMobil. Norske Shell operates the production phase which started in September 2007.

Ormen Lange is the first truly deepwater project on the Norwegian Continental Shelf with templates and wells located at water depths 850-1100 m, see illustration in Figure 3. The reservoir itself is approximately 2800 m below sea surface and covers ca. 350 km^2. The length is roughly 40 km while the width varies between 8 and 10 km. It is sited 120 km north-west of Kristiansund in the Norwegian Sea. In addition to the sand layers containing gas, some condensate is present. At site the weather conditions can be quite severe, and at the sea bottom the water temperature is minus 1.2 ⁰C. Because of the low temperature there is a risk of hydrate formation and hence potential blockage of the export pipelines to shore. Mono-ethylene glycol (MEG), which works as anti-freeze, is injected into the well stream to prevent formation of hydrates.
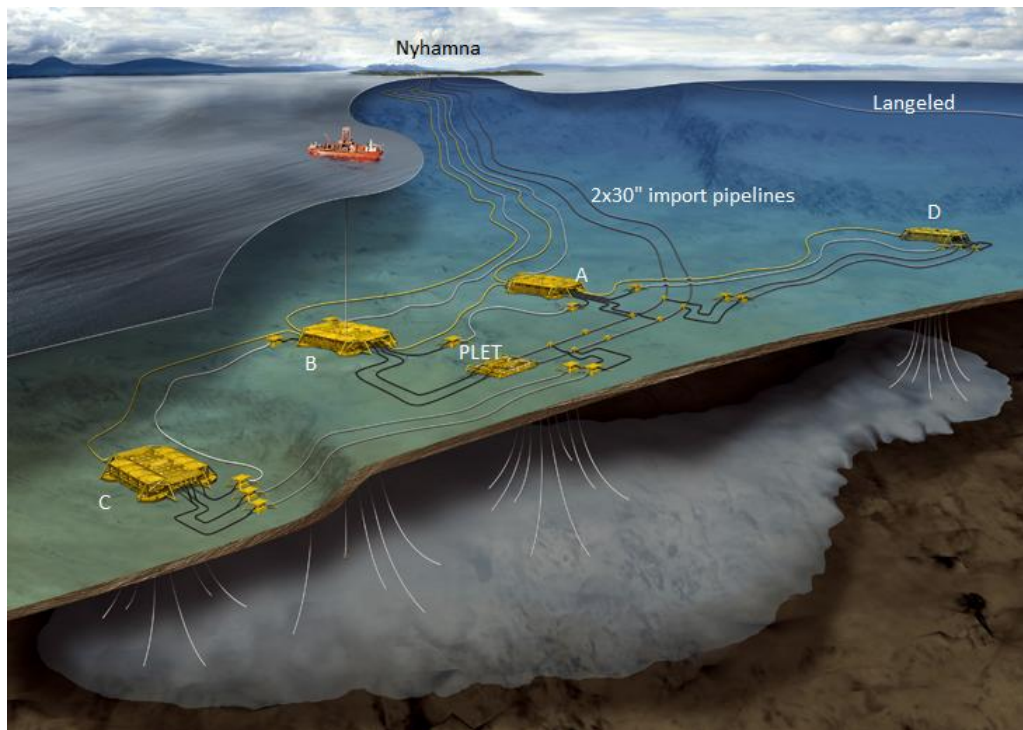
Figure 3: The Ormen Lange field [42].

Due to the Storegga slide about 8100 years ago the seabed is rough with peaks of heights between 30 and 60 meters. Soil conditions ranges from soft clay to very stiff clay with boulders. The

Storegga slide was a huge mudslide and Ormen Lange is located near the center of the depression created by the slide. There is a sharp land rise in bathymetry from the Ormen Lange field up to the continental shelf. An important concern has therefore been the probability for new slides. However after extensive research it was concluded that a new mudslide is at this point unlikely.

Gas, condensate, water and MEG are transported through two 120 km long multiphase import pipelines from the field to the onshore processing plant at Nyhamna in Aukra Municipality. According to [43] the well stream arriving Nyhamna is untreated and must therefore be routed to a facility for removal of liquid slugs. This is to prevent slugs from damaging the processing plant. Then gas, condensate, water and MEG are separated. MEG is recycled, the produced water is cleaned and released into the sea while the condensate is stabilized and stored before it is loaded on to tankers and exported. The gas itself is dried and compressed before it is exported. Export happens through the world's presently longest offshore gas export pipeline called Langeled which is about 1200 km long. The gas is routed via the platform Sleipner in the North Sea to Easington, England. Pipeline diameter is 42 inches upstream of Sleipner and 44 inches from Sleipner to Easington. At plateau gas production Ormen Lange produces about 20 billion standard cubic meters annually which is approximately equal to the annual energy demand in Norway. At maximum it can deliver up to 20 % of the gas demand in the UK.

4.2 Ormen Lange field layout

The field architecture is designed to maintain plateau production as the years pass and the field depletes. Four templates were planned to be installed, template A-D.   Templates A and B were installed first, approximately 4 km apart in the main production area [5]. They were installed between late summer 2005 and summer 2006 while production officially started during October 2007. In 2009 template D was installed. Installation of template C commenced in summer 2011 and the fist wells will come on stream by October 2012. For an overview of the field architecture see Figure 4.

All templates are similar 8 slot templates and connected to both the 30" multiphase export pipelines to Nyhamna [7]. In these multiphase pipelines gas, condensate, water and MEG are transported. For redundancy the two multiphase pipelines are internally connected via a pipeline end termination structure (PLET) close to template B. As stated in [19] the interconnection is made by a pig loop. In addition to the pig loop the PLET also includes a bottom structure, pipeline terminations, PLET modules and protection against dropped objects and trawling. In general references [5] and [19] are used to describe the field layout.

4.2.1 MEG and umbilical layout

Continuous injection of MEG in the wellheads is needed to prevent hydrate formation due to the low seabed temperature. MEG is supplied by two 6" pipelines from Nyhamna, one connected to

template A and the other to template B. From templates A and B there is an infield 6" pipeline to template D and C respectively, supplying template D and C with MEG. There is also a crossover pipeline from template A to B for flexibility. The system is illustrated in Figure 4. Umbilicals are needed for control and the umbilical layout is consistent with the MEG supply layout. In each umbilical there are power cables, fiber optic lines, hydraulic supply and return lines, corrosion/inhibitor and annulus bleed lines. For redundancy the crossover umbilical must be able to transfer chemicals, hydraulics, electric power and communication.
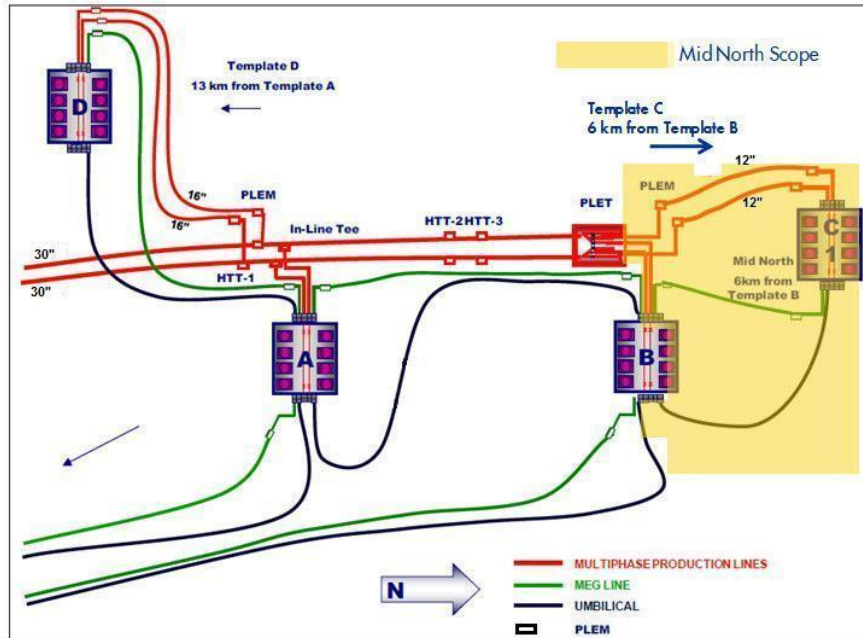
Figure 4: Overall field layout [7]. Red lines represent multiphase production lines, green lines are MEG lines and black lines are umbilicals.

4.2.2 Template systems

Each production template comprises a foundation bottom structure (FBS) and a manifold module with as-built weight of approximately 675 and 430 [t] respectively. See Figure 5. The FBS has suction anchors and skirts, and is protected against dropped objects and trawling. The suction anchors are used for leveling. Simultaneous drilling and production is possible, and the design assures safe installation and retrieval of production and drilling equipment due to bumpers and guide arrangements. The manifold module installed on the FBS co-mingles the gas production from the Xmas trees. In addition it distributes MEG, hydraulic supply, electrical power and optical communication. There are as few 3D bends in the manifold as possible to minimize pressure drop in the produced gas and piping erosion. The design also includes dual production headers and valves that can be operated by hydraulics and/or ROVs.

Figure 5: The foundation bottom structure to the left and the manifold module to the right [19].

4.2.3 Xmas tree systems

Eight Xmas trees are placed in specific slots at each template. A Xmas tree system is the wellhead component that completes the well and consists of a horizontal production tree, subsea control module (SCM) and choke module (CM) as presented in Figure 6. Both the SCM and the CM are separately retrievable. A SCM is used to control a Xmas tree, so the SCM controls all the sensors in the Xmas tree, its hydraulic functions and interface with down hole functions. When a command is sent from shore it is handled by the SCM which contains electro hydraulic controls. There are many sensors in the Xmas tree which the SCM monitors to assure safe production. The following can be listed:

- Temperature and pressure sensors.
- Wet gas meter. Controls/ monitors the water in the gas.
- Water fraction meter.
- Sand detection sensors.
- Communication/ power.

There are also important instrumentation and valves on the CM. The CM serves as a flow loop and controls the well stream into the manifold. A multibore vertical hub connects the CM and the manifold, hence connects produced gas flow, MEG, annulus test and control lines. Specific components in the CM are:

- Production choke valve. Adjusts the pipeline flow.
- MEG dosage valve (MDV). Allows continuous injection of MEG into the flow loop, either in the Xmas tree or choke module.
- Instrumentation.
- MEG injection point.
- Scale injection point.
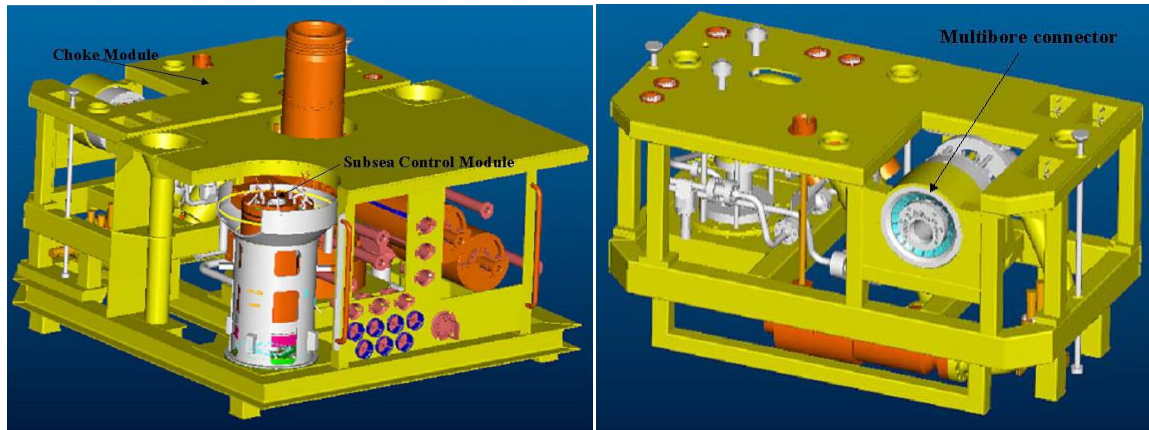
Figure 6: The left picture shows the whole Xmas tree system with the Xmas tree, subsea control module and choke module. The right picture shows the choke module only [5].

4.3 Future compression project

Gas and condensate is extracted by pressure depletion in the reservoir, hence utilizing the reservoir's natural pressure [29]. This leads to decreasing pressure in the reservoir. At some point the pressure is too low to maintain production due to low flow rates and increasing possibility of severe slug production in the multiphase pipelines to Nyhamna. Offshore compression is then needed to maintain plateau production and increase the recovery. Estimates show that for Ormen Lange compression is needed around 2016 but this can be postponed by 2 [years] if onshore pre-compression is used [6].

Presently there are two compression alternatives for the Ormen Lange field, either platform or subsea compression. Platform compression is a known technology and a safe choice compared to subsea compression which never has been done in this way before. But subsea compression has many advantages. The compression station can be placed closer to the wells which gives increased recovery due to reduced back-pressure on the wells. Also it is more cost efficient with regards to capital expenditure (CAPEX) and operating expenditure (OPEX). Capital expenditure is in [6] illustrated by comparing the weight estimates for the platform and the subsea compression station where the platform weight is about 4 times higher. And for a subsea compression station additional operation manning at Nyhamna is unnecessary, logistics and offshore operations are reduced and safety is increased. Final decision on offshore compression system is planned for 2012. In the rest of this report only subsea compression will be considered. The location of the subsea compression station is shown in Figure 7.
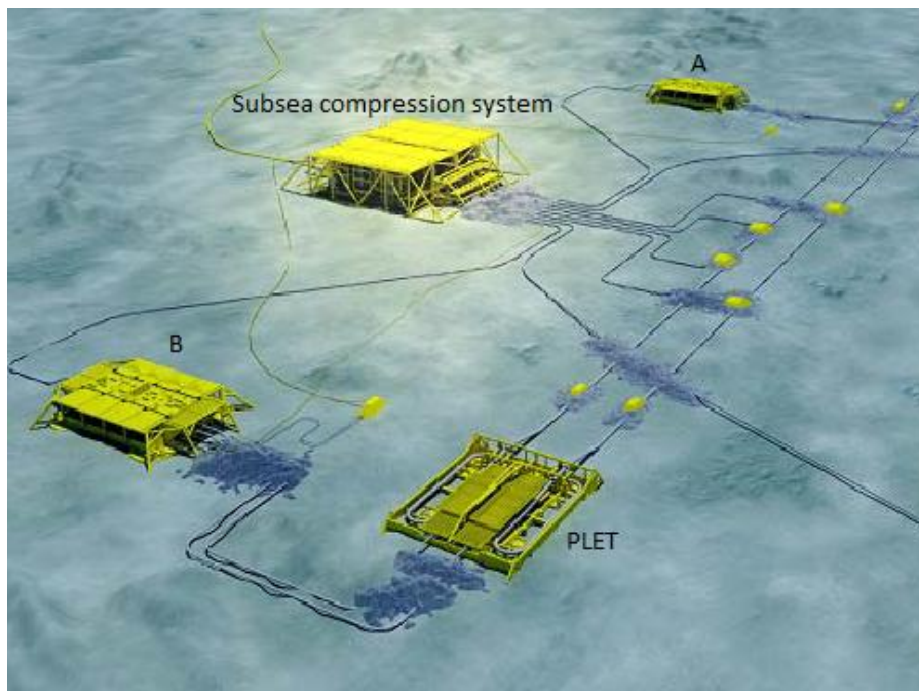
Figure 7: Ormen Lange future compression without templates C and D [6].

An engineering, procurement and construction (EPC) contract has not been signed yet. Therefore the subsea compression train designed by Aker Solution, from which a full scale test pilot is built, is described here. It will give a rough description of the system even though changes will be made. The full scale test pilot which includes one compressor train and its high voltage power supply system is now located in a flooded test pit at Nyhamna for two years of testing. This is to qualify and increase the confidence in the equipment. System descriptions are found in [29] and [6].

The subsea compression station is intended to have two compressor trains located on the same FBS, initially it was 4 trains but this has been changed. Before this change the whole station would be about 70 [m] long, 54 [m] wide, 14 [m] high and with a weight of 6500 [t]. The design case is to have a production capacity of 60 [Msm^3/sd] and an availability of 97.6 %. Limiting requirements for the compression modules are dimensions of 12x6x12 [m] in length, width and height and a weight of 250 [t].

In Figure 8 the pilot system design can be seen. The untreated well flow is taken in so the system must be able to handle varying compositions of gas, condensate, water, sand and MEG. Gas is separated from the rest of the well stream in a separator and routed to a compressor. Liquids and sand are removed from the separator and boosted by a centrifugal pump. Gas, liquids and sand are then mixed in the discharge pipelines and transported to Nyhamna. Liquids and sand cannot be taken into the compressor to avoid wearing and reduced availability. This is mainly prevented by the separator. In addition piping is arranged to slope any liquid condensation in the gas pipes

back to the separator. The piping is also arranged to prevent pockets and build-up of solids in the liquid piping.
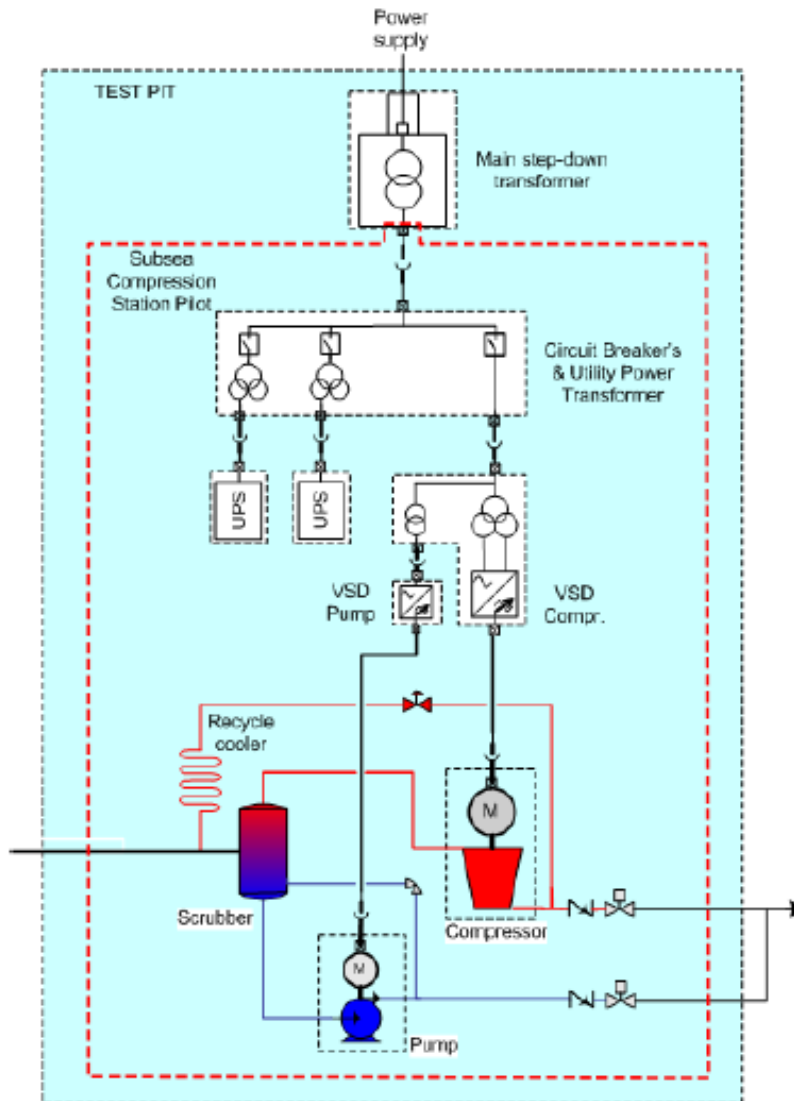
Figure 8: System design for the subsea compression system pilot [29].

The power to run the subsea compressor system is supplied via an umbilical containing a high voltage electrical cable. At the end of the umbilical the power is transformed down to 22 [kV] before it is distributed to the compressor system. The same umbilical also contains fiber optic cables for communication from shore to the compression system. Both normal operation and emergency monitoring and control are needed.

The modules that form a subsea compressor train can be divided into process and power modules. Process modules:

- Separator module. Separates liquids and sand from gas in the incoming untreated well flow.
- Anti-surge cooler module. If the pressure and/or flow is too low in the compressor a valve opens and the gas will be recycled through the anti-surge cooler. This module prevents the compressor train from going into surge. Surge means gas back-flow.
- Compressor module. Compresses the produce gas and includes a motor-compressor designed for about 12.5 [MW].
- Pump module. Boosts the liquids and sand by using a liquid filled motor centrifugal pump and has a design duty of 400 [kW].

Power modules:

- Circuit breaker module. Distributes 22 [kV] AC power from the transformer to the main components and protects the rest of the system in case one of the downstream modules fails.
- Compressor variable speed drive (VSD). Dives the compressor at the right frequency and torque.
- Pump VSD. Dives the pump at the right frequency and torque.
- Uninterruptible power supply (UPS). Distributes power to the low voltage systems like the subsea control system. It also has a back-up battery to perform a controlled emergency shutdown in case there is loss of main power supply.

5. Normand Subsea

Normand Subsea is the vessel intended to be used as a base case for analyses of future compression modules installation and/ or retrieval. At present the vessel is not suitable for the task so improvements must be assumed and included in the analyses. Even though the vessel's motions are less optimal for installation and retrieval in the required weather conditions logic is that if installation and retrieval with this vessel is feasible certainly installation with a purpose built vessel is feasible. It is therefore interesting to compare different deployment methods of the future compression units using Normand Subsea since it is assumed that the same trend will yield for a new vessel.

The Normand Subsea is an IMR and survey vessel customized for conducting work in regards to inspection, maintenance and repair [44]. In Figure 9 a picture of Normand Subsea is given. Vessel main dimensions:

- Length over all: 113.50 [m]
- Breadth: 24.00 [m]
- Depth: 11.00 [m]
- Draught fully loaded: 7.81 [m]
- Deadweight: 6300.00 [t]

Figure 9: Normand Subsea [44].

Dynamic Positioning (DP) is used for positioning and the system is equivalent with a DP class 2. Normand Subsea also has a helideck and 6 ROV handling systems with active heave compensation. There are 4 eyeball handing systems where ROVs are deployed/ retrieved through

moonpools in an enclosed hanger and 2 work class systems where the ROVs are deployed/ retrieved over the port side cursor guided.

Main moonpool dimensions are 7.2x7.2 [m]. The module handling tower (MHT) over the main moonpool can take 35 [t] in $H_s = 5$ [m], and module handling with ROV support is feasible down to 1200 [m] water depth (MWD). For heavier structures the main cargo crane can be used, it has a maximum capacity of 140 [t].

For power, propulsion and maneuvering there are 4 diesel electric main engines with generators, 2 azipull propellers and 4 thrusters. There are 2 tunnel thrusters, 1 forward and 1 aft, and 2 retractable azimuth thrusters. The whole system taken into account makes the economical speed approximately 12 [knots], hence 6.17 [m/s].

Since module requirements for the future compression station are 12x6x12 [m] in length, width and height and a weight of 250 [t], obviously Normand Subsea cannot be used as is. To install the modules through moonpool a new module handling tower system must be installed. Also the hangar that now contains 5 moonpools must be changed and a new, large moonpool constructed. The alternative is installing a new crane. Modifying the vessel can be demanding as changes may interfere with the ships main structure. It is also possible that the hull must be reinforced to take the extra loads.

These facts are neglected in this report, hence it is assumed that Normand Subsea has capacity to deploy and retrieve units both by crane and via moonpool without any significant structural changes of the hull. But since the cargo crane only can take 140 [t] the main crane installed on Skandi Acergy is used instead. This crane can take 400 [t] static loading and has a suiting working radius. And as the main moonpool of 7.2x7.2 [m] is too small it is assumed to be 14x7.5 [m] to take the structures [28]. Both crane pedestal and moonpool center are assumed to be as present on Normand Subsea.

6. Module Intervention and Handling

6.1 Ship motions

The motion at any point of the ship can be written as [11]:

$$s = (\eta_1 + z\eta_5 - y\eta_6)i + (\eta_2 - z\eta_4 + x\eta_6)j + (\eta_3 + y\eta_4 - x\eta_5)k \quad \text{Equation 1}$$
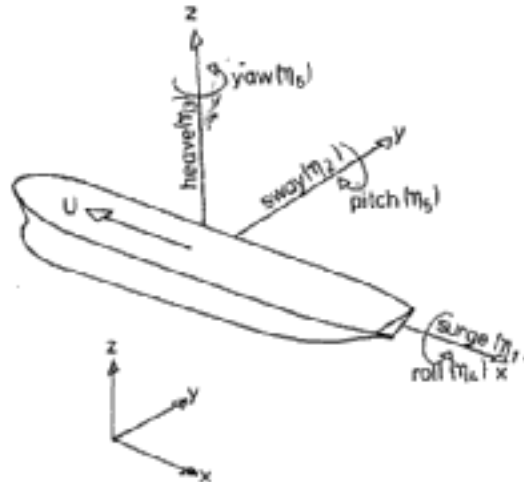
Figure 10: Ship modes of motion [11].

The coordinate system is fixed with z pointing upwards through the center of gravity of the ship. The origin is located in the plane of undisturbed free-surface. There are three translatory modes of motion where η_1 is surge, η_2 is sway and η_3 is heave. In addition three modes of rotational motion exist; η_4 is roll, η_5 is pitch and η_6 is yaw. These modes of motion can be seen in Figure 10 above together with the coordinate system. Note that the translatory motions are not necessarily the translatory motions of the center of gravity.

6.2 Installation alternatives

There are several ways to deploy and retrieve modules. In this report installation has main focus since the objective of the thesis is to compare annual availability of deployment by two different methods. Note that heavy lift installation is not considered. The preferred installation choice cannot only be technically favorable, it must also be economically feasible. Safe installation concerning personnel and equipment, optimized availability and overall costs are main factors. Lowering alternatives for modules of such dimensions and weight as the future compression modules are listed in [2]. In [2] also different installation vessels are considered. This is not taken into account here since Normand Subsea is chosen as the base case. Lowering alternatives:

- Crane installation over the side

- Crane or winch installation with A-frame over the stern
- Crane or winch installation with a module handling system (MHS) over the side
- Central located module handling tower over a moonpool on a construction vessel
- Wet tow where the module is directly connected to the ship
- Wet towing and installation by pencil buoy method
- Wet towing and installation by buoyancy tank assemblies (BTA), but mainly for heavier lifts.

6.2.1 Pre deployment

To protect module equipment at all times the equipment is placed inside a module frame [1]. This frame must be constructed to withstand the maximum forces the module is expected to experience, hence the design loads. In this case these forces may be the retrieval forces of the module in flooded condition. Module frames can be designed for lifting or specific lifting frames can be applied. The location of the lift points must be carefully considered. Also equipment for guide wires must be installed if guide wires are to be used during deployment.

During transit from shore to offshore site structures should be properly sea fastened and hence prevented from moving independent of sea condition. They can for example be placed on pallets with small guideposts that fit the module lift frames' guide funnels [1]. Modules are hence aligned. Structures with a high center of gravity (COG) can be fitted with chains between the corners of the module frames to strong points in the vessel deck. Each unit will have a dedicated parking slot on deck determined on beforehand to ensure safe transit and installation with consideration to ship stability and easy module handling. When at site modules are brought in position for either crane or winch deployment over the side or moonpool deployment by a deck skidding system. To secure the modules and pallets on the skidding rails during transportation they are bolted at each corner against the skids and fitted with "uplift-constrains". "Stoppers" are used to prevent horizontal movements.

6.2.2 Crane installation

A knuckle box boom crane is recommended for crane installation over the side without A-frame or MHS in [1], and example is displayed in Figure 11. Compared to a traditional crane a knuckle box boom crane is designed to minimize the pendulum motion of the load. This is achieved by keeping the tip of the boom as close as possible to the module lifted during pick-up and lowering. Reducing the pendulum motions of the load also reduces the safety hazard for people, equipment and structures on deck. This will again lead to increased availability in rough weather conditions compared to a traditional crane. In addition it has increased maneuverability and a wider reach due to its crane boom design. Knuckle box boom cranes typically have a working range of $8 - 55$ [m] with a safe working load (SWL) of $15 - 500$ [t] [41].

The crane must be able to handle the dynamic amplification factor (DAF) of the load during lowering, and it should have enough wire for working at the whole Ormen Lange field. Also the possibility of retrieving flooded modules should be considered when determining necessary crane capacity. In addition the crane must have an active heave compensation (AHC) system to safely land the module onto the seabed FBS. These requirements also yields for cranes and winches used for deploying modules in interaction with A-frames or other MHSs over the side and/or stern.

For safe handling and over boarding tugger winches and tugger wires can be used to control the module being deployed. This is specifically for lowering without guide rails. Constant tension tugger winches are then located on deck and wires are fastened onto the module, often there is one wire in each of the module's corners to prevent horizontal motions and rotations. These wires are taken off by ROVs roughly 30 [m] below sea surface. If necessary the cargo rail on the ship deck can be made detachable to make deployment easier.

SECTION #27
DECK CRANE
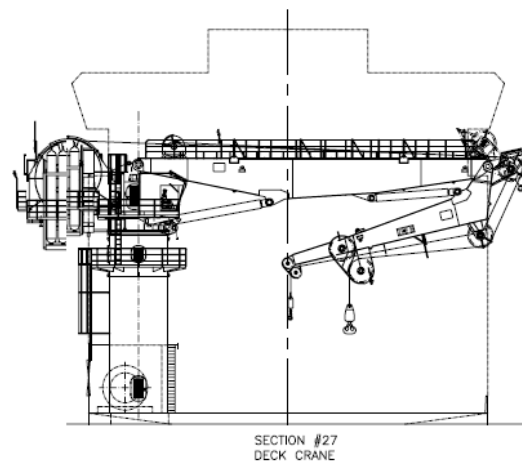
Figure 11: Knuckle box boom crane example [30].

A crane or a winch can also be used to lower modules over the stern or over the side using an A-frame or a MHS. Over the side MHS are not commonly used if properly designed at all. Currently a conceptual design from a contractor involves a MHS with guide rails and a cursor system attached to the ship side [34]. This conceptual design is illustrated in Figure 12. One advantage of such a system is that it can probably be adapted to the main vessel structure without significant hull changes, compared to for example changing the size of an existing moonpool. The availability will also be better than the availability for crane operations over the side since modules will be locked during lowering through the splash zone. Then degrees of freedom are reduced and the module is no longer free to rotate or move. But an important fact is that availability is probably less than for installation through a moonpool. Hence compared to crane deployment over the side availability is increased but the system is more costly, and compared to moonpool deployment the availability is reduced. In one way the solution therefore falls between two chairs.
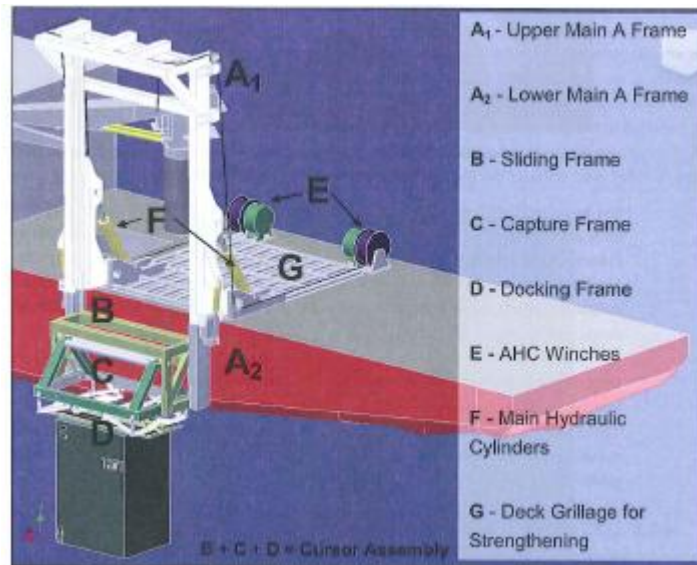
Figure 12: Conceptual design for MHS with guide rails and a cursor system attached to the ship side [34].

Anyways it may still be a good solution when it comes to installation of the future compression modules, at least if the only way to deploy modules through a moonpool is by building a new purpose built vessel. Building a purpose built vessel will be both time consuming and costly. So if an over the side MHS is feasible within rational economical and technical frames, and the increase in annual availability is significant compared to deployment over the side with a crane, it might be a good way forward.

6.2.3 Moonpool installation

A moonpool is a vertical opening in the ship hull extending through the air-water interface. It therefore provides a protected environment for module deployment since waves cannot directly impact the structure being lowered through the splash zone anymore. Above the moonpool opening there is a module handling tower (MHT) to help lower modules. One side of the MHT is open so modules can enter, often on skidding rails placed on the moonpool top door. There is also a cursor in the MHT, a horizontal oriented steel frame [1]. See Figure 13. The height of the MHT must be tall enough to take the module height, height of the pallet the module is stored on during transportation, skidding rails, lift frame and cursor.

The cursor is skidding on guiding rails through the moonpool to restrain the module from moving during deployment. It varies how many moonpool sides that have guiding rails. To assure safe module deployment when the module is fixed to the cursor loads imposed on the module are transferred to the cursor. The cursor must therefore be able to withstand high forces. Forces are transferred from the module through the locking mechanism to the cursor, via the guide rails to the moonpool walls and MHT and further on to the vessel main structure. Skew loads must also

be tackled in case the module's CoG is different from the module's volume center. The cursor is often designed as an open structure to minimize wave effects.
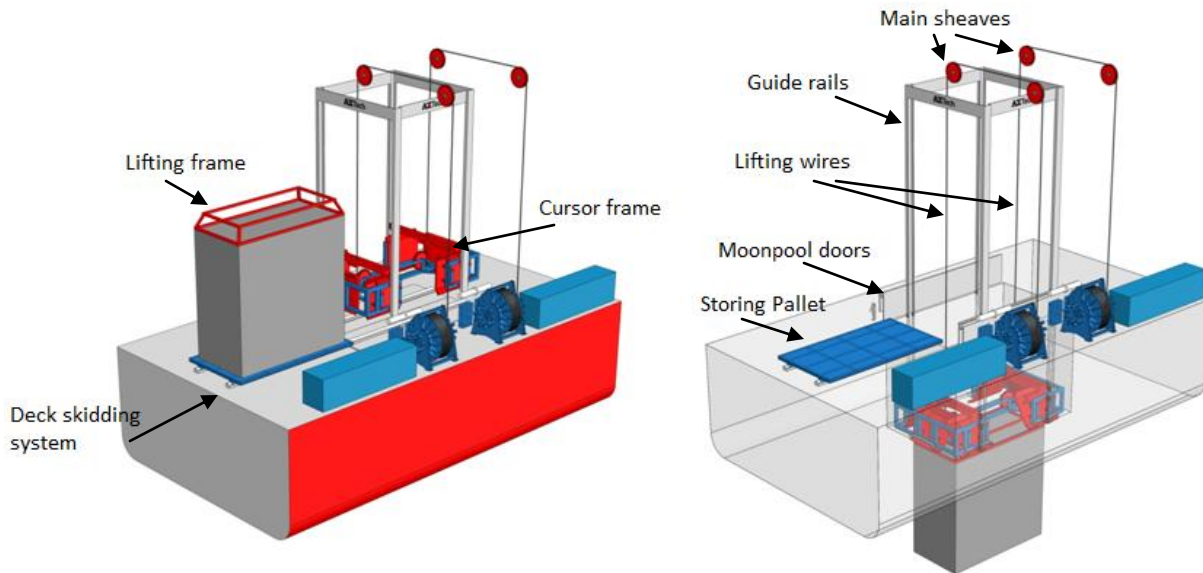
Figure 13: Illustrated moonpool features [35] (modified). A double fall wire system is used.

Lowering of the cursor frame is controlled by cursor winches. To secure the cursor in extreme conditions the system should be fitted with upper and lower parking stops. Also some kind of damping mechanism is often added to the system to absorb shock loads. As wave impacts reduce with increasing water depth the guiding rails should extend below the vessel hull, which in addition reduces vessel hull impacts. But during transit these guiding rails must be detached as they would cause unfortunate hydrodynamic properties to the vessel.

For lowering of the module a main lift wire is used. The main lift wire is routed from the main winch via the AHC over the main sheave. The main sheave is normally located in the top of the MHT at center location of the cursor frame. Also for the moonpool the winch must have enough wire capacity to be used in the whole Ormen Lange area. The lifting arrangement has to be constructed to handle the dynamic loads on the module during deployment (and retrieval) with a suiting safe working load (SWL). Guide wires are used to route the module from the vessel and down to the seabed and its position on the FBS. They are therefore connected at the top of the MHS and suspended down to the FBS, and prevent modules from rotating as structures are lowered down the water column. Between 2 and 4 guide wires are common. During retrieval guide wires assist in catching the module with lift frame onto the cursor. Guide wires can also possibly be used in combination with crane installation.

Moonpools are located as close as possible to the vessels center of flotation (CoF) to minimize motions of units being lowered through the moonpool. This can be seen from Equation 1. If the coordinate system in Figure 10 is taken to be in CoF one can see that rotations will be minimized. This will hence normally optimize availability. The availability by installing via a module handling tower (MHT) through a moonpool will in most cases be better than the availability by installing with crane either over the side with or without A-frame or MHS. This is partly due to larger ship motions at the lowering position when deploying with a crane over the side because of an offset from center of flotation.

Moonpools are favorable as long as the water plug in the moonpool does not enter resonance condition, which can lead to an oscillation amplitude up to 3 and even 4 times the wave height [12]. Resonance can be seen as large vertical motions referred to as piston mode resonance and internal sloshing leading to transverse breaking waves. The piston mode is often the most troublesome [4] and therefore the one considered here. The dynamic amplification of the water motions can have severe consequences. It can initiate slamming on structures being lowered and cause green water on deck which is a significant safety hazard for deck crew. Green water on deck can also lead to loss of or damage on equipment close to the moonpool deck opening. Resonance is caused by excitation at the same frequency as the natural frequency of the water plug. The excitation is a result of local vertical accelerations and pressure differences at the bottom of the moonpool. See Appendix 11 for equations. The oscillations can be reduced by several means [12]:

- Flanges. They reduce the oscillation by increasing the damping. Short flanges a little below the water surface are very effective.
- Closing the top of the moonpool. By closing the top air is no longer free to flow in and out of the moonpool top. Damping is hence increased by the air above the water surface.
- Damping chambers. Perforated bulkheads are then mounted on the moonpool walls. Vertical wave motion is converted into horizontal wave motion and much wave energy is dissipated as heat energy by reflecting and conflicting currents due to the perforation in the perforated bulkheads.
- Changing the draught. Water plug natural frequency is dependent on the ship draught. It is therefore assumed that a change in draft leads to reduction in oscillation.
- Aerate the moonpool. By aerating the moonpool water density is reduced which also reduced the impact loads on structures being lowered.

Note that sufficient moonpool cross-sectional area must be open for the lowering of the equipment considered which again affects the selection of means for oscillation reduction. In addition resonance can happen during transit. Then vortex shedding can be a problem caused by flow separation at the leading bottom edge of the moonpool. This case is not considered further as ship transit is outside the scope of this report.

6.2.4 Wet tow

Lifting through the splash zone is critical, especially offshore in harsh weather conditions. But instead of transporting the module on deck of an installation vessel, or on a barge, before lowering it through the splash zone it can be submerged inshore in more controlled environments and then towed out to site. This is called wet tow. When at site it can be winced down from an already submerged position. It is therefore argued that wet tow will in many cases increase the deployment availability. Safety can also be better since the risk of people or equipment being hurt or damaged by the pendulum motion of module during a crane lift is reduced. But if wet tow is considered challenges connected to vortex induced vibration (VIV) and fatigue may arise. Module design must therefore be ensured to withstand the VIV and fatigue experienced during the planned tow out. These factors are naturally depending on towing distance. Towing distance should generally be as short as possible for best project economy [22].

Wet tow can be performed in different ways, see Figure 14. The module can be attached directly to the installation vessel for example at the stern or through a moonpool, or it can be connected to a buoyancy element towed by the vessel [3]. Each towing method will give different loads during the tow. Stern connection has for example showed to often result in loads significantly larger than loads experienced when using a buoyancy element method.
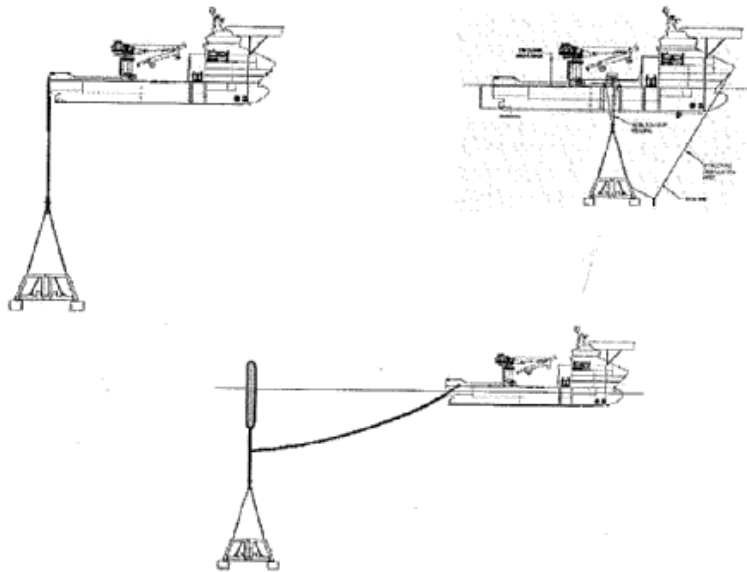
Figure 14: Examples of wet towing methods [3].

One or several buoyancy elements can be used. AMC has patented a single buoyancy element method where the buoyancy element is shaped like a pencil. The Pencil Buoy is a steel structure which contains internal ring stiffeners [22]. Internally it is subdivided into watertight compartments making it capable of handling a one-compartment damage. When using the Pencil

Buoy method the module is taken to the inshore transfer location either by barge or on deck of the installation vessel. It is then lowered in a winch wire connected to the vessel, but also to the Pencil Buoy lying on vessel deck. The tubular buoyancy tank is launched from deck by paying out wire while moving the vessel slowly forward. During wet tow the weight of both towed structure and rigging is carried by the Buoy and an illustration is given in Figure 15. Towing speed is limited to about 3-3.5 [knots]. At installation site the towing wire is winched in and loads again transferred to the winch wire before the Pencil Buoy is disconnected. Winch down can then start.
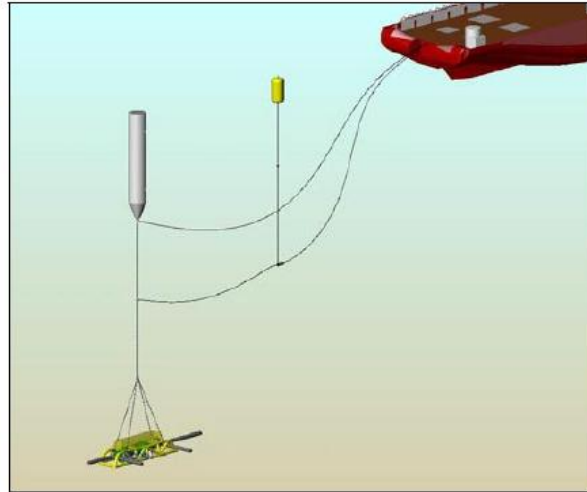
Figure 15: Pencil Buoy illustration [22].

There are other buoyancy element methods. Several buoyancy tanks can for example be used, called Buoyancy Tank Assembly (BTA). Then number and size of the tanks are dependent on the module which is to be towed. The main focus is to control the buoyancy.

6.3 Installation criteria

The limiting stage of the operation is believed to be the splash zone lowering, but the sea bed hover stage must also be looked into [23]. As this report considers deployment of a large unit through the splash zone the hover stage is not taken into account. Slack slings in the lower rigging is taken as the limiting condition. Slack slings can be a problem in the splash zone due to excessive hydrodynamic forces which generate uplift larger than the weight of the module being deployed. According to [10] hydrodynamic loads should not exceed 90 % of the minimum static weight of the object to ensure slack slings and hence snap loads are avoided. It must be noted that the minimum static weight of the object varies as the module is submerged. Here it relates to the mean water level and does not take into account the changing buoyancy force due to waves.

$$F_{hyd} \leq 0.9 \cdot F_{static-min}$$
<div style="text-align:right">Equation 2</div>

where

$$F_{static-min} = M_{min}g - \rho_w V_m g \qquad \text{Equation 3}$$

M$_{min}$ is the mass of the object in air before flooding of for example tubular has started. ρ_w is the sea water density, g is the acceleration due to gravity and V_m is the volume of the structure.

Equation 2 can be redefined into the following which is applied in this report as limiting:

$$F_{hyd} \leq (1 - 0.1) \cdot F_{static-min} \qquad \text{Equation 4}$$

$$F_{static-min} - F_{hyd} > 0.1 \cdot F_{static-min} \qquad \text{Equation 5}$$

In addition other criteria can be critical [23]; the roll/pitch motion of the vessel and the module, the surge/sway motion of the vessel, the forces on the main sheave and lifting points for lifting or lowering of the module and the wire's minimum breakage load (MBL), hence the wire's failing load. As final module design and installation vessel are not yet decided it would be hard to set any of these additional criteria as limiting.

6.4 Design rules and regulations

[1] is a study report on the functional requirements of module intervention and handling from a dedicated mono hull intervention vessel. The study assumes all compressor modules to be installed on the FBS. The scenario is then replacement of a single module for each intervention operation. Here module intervention and handling comprises;

- Operational methods and equipment needed for module storage and skidding on deck
- Module handling tower above moonpool
- Deployment via moonpool/over the side with crane trough splash zone
- Landing on seabed foundation
- Retrieval from seabed foundation
- Catching and guiding trough splash zone via moonpool/ over the side with crane
- Lift onto deck and skid into storage location for sea fastening

The list below gives the most relevant rules and regulations for such module intervention and handling.

- DNV Rules for Planning and Execution of Marine Operations, Jan. 2000
- Norwegian Marine Directorate, "Grønnbok"
- NS 3472: Steel Structures, Design Rules
- NS 5514: Dimensjonering av krankonstruksjoner
- NS 5820: Suppliers Documentation of Equipment
- DNV 1994: Rules for Certification of Lifting Appliances

- DNV 2.7.1: Offshore Containers, 1995
- Federation Europeenne de la Manutention (FEM) "Rules for the design of Hoisting Appliances" (1.001 3rd Edition 1987).
- Third Party Certification by ICP accepted by NMD
- Certificate of Testing of Lifting Appliances. ILO Form no. 2.
- Makers' Certificate for loose gear, ILO.
- DNV Recommended Practice, DNV-RP-H103, Risk Management in Marine- and Sub Sea Operations
- NORSOK Z-013 Risk and emergency preparedness analysis

6.5 Design parameters

The Future Compression module's design parameters given in [1] are listed below.

- Water depth: 860 [m]
- Design life: 30 years
- DAF (splash-zone lift): 1.75
- DAF (submerged lift): 2.00
- Target max Hs, moonpool installation: 4-5 [m]
- Target max Hs, crane installation: 2.5 [m]
- Lowering speed: 0.5 [m]

In addition the modules dimensions and weight requirements are as already mentioned 12x6x12 [m] and 250 [t].

7. Sea State Specifics

7.1 Wave spectra

Potential flow theory is based on some essential assumptions and boundary conditions. The main assumptions are incompressible and inviscid sea water with irrotational fluid motion. From potential theory linear wave theory for propagating waves can be derived as in [11] by assuming a horizontal sea bottom and a free-surface of infinite horizontal extent. Waves can then be seen as long crested sinusoidal waves with wave specifics as in Table 1:

	Infinite water depth
Velocity potential	$\varphi = \dfrac{g\zeta_a}{\omega} e^{kz} \cos(\omega t - kx)$
Connection between wave number k and circular frequency ω	$\dfrac{\omega^2}{g} = k$
Connection between wavelength λ and wave period T	$\lambda = \dfrac{g}{2\pi} T^2$
Wave profile	$\zeta = \zeta_a \sin(\omega t - kx)$
Dynamic pressure	$p_d = \rho g \zeta_a e^{kz} \sin(\omega t - kx)$
x-component of velocity	$v_x = \omega \zeta_a e^{kz} \sin(\omega t - kx)$
z-component of velocity	$v_z = \omega \zeta_a e^{kz} \cos(\omega t - kx)$
x-component of acceleration	$a_x = \omega^2 \zeta_a e^{kz} \cos(\omega t - kx)$
z-component of acceleration	$a_z = -\omega^2 \zeta_a e^{kz} \sin(\omega t - kx)$

$\omega = \dfrac{2\pi}{T}$, $k = \dfrac{2\pi}{\lambda}$, $T = Wave\ period$, $\lambda = Wavelength$, $\zeta_a = Wave\ amplitude$, $g = Acceleraiton\ of\ gravity$, $t = Time\ variable$, $x = Direction\ of\ wave\ propagation$, $z = Vertical\ coordinate\ positive\ upwards$, $z = 0\ mean\ water\ level$, $h = Average\ waterdepth$.
$Total\ pressure\ in\ the\ fluid$: $p_d - \rho g z + p_o$ ($p_o = atmospheric\ pressure$)

Table 1: Velocity potential, dispersion relationship, wave profile, pressure, velocity and acceleration for regular sinusoidal long crested waves on infinite water depth according to linear theory [11].

Short crested waves are not considered in this report.

Regular long crested waves are based on linear theory. Ocean waves are irregular and a method for describing irregular waves must therefore be developed. Due to the linearity it has been found that superposition of regular waves can be used to simulate irregular seas, hence can linear theory be used to formulate irregular seas and find statistical estimates for these irregular seas [11]. The sum of many regular wave components can for example be used to describe the wave elevation ζ of a long-crested irregular sea propagating in positive x-direction:

$$\zeta(x,t) = \sum_{j=1}^{N} \zeta_{a\,j} \sin(\omega_j t - k_j x + \epsilon_j) \qquad \text{Equation 6}$$

ζ_{a_j}, ω_j, k_j and ϵ_j are wave amplitude, circular frequency, wave number and random phase angle for wave j respectively. N is the total number of regular waves making up the irregular sea state.

A wave spectrum S(ω), which can be seen as a graph of how wave energy is distributed on frequencies, can be derived from wave amplitudes and the other way around.

$$\frac{1}{2}\zeta_{a_j}^2 = S(\omega_j)\Delta\omega \qquad\qquad \text{Equation 7}$$

$S(\omega_j)$ is the wave spectrum value at frequency ω_j and $\Delta\omega$ is a constant frequency difference between successive frequencies. Long-crested waves can hence be represented in both the time- and frequency-domain as seen in Figure 16. But to represent a sea state by a wave spectrum the sea must be seen as a stationary stochastic process.
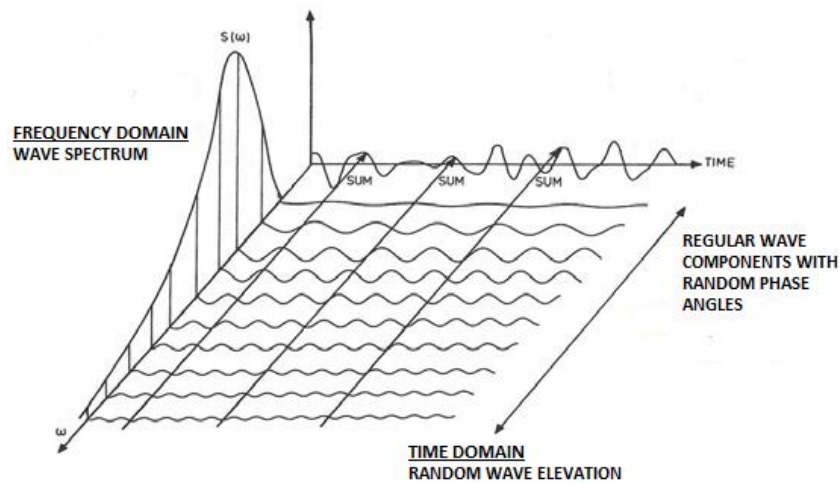
Figure 16: Waves represented both in the time- and frequency domain [11].

Many different spectral formulations have been developed with different input parameters. The spectra are generally generated based on measurements form a certain offshore field with its specific wind fetch area, water depth, wind, current and swell conditions. Torsethaugen and JONWAP wave spectra are two such wave spectra designed roughly to be used in the Norwegian Sea and the North Sea respectively.

7.1.1 JONSWAP wave spectrum
In the years 1968-1969 a multinational wave measurement project was executed in the south-east part of the North Sea [16]. This project resulted in the JONSWAP (Joint North Sea Wave Project) spectrum. The intention was to describe wind generated seas not yet fully developed. It is important to note that the measurements were taken at relatively shallow water depths and somewhat close to shore. Regardless of this the JONSWAP spectrum is often used for design purposes in the North Sea for constructions on deep water in fully developed sea.

The JONSWAP spectrum is a 5 parameter spectrum and is based on the Pierson-Moskowitz (PM) spectrum, a 1 parameter spectrum for the North-Atlantic only dependent on wind velocity. The PM spectrum:

$$S(\omega) = \frac{A}{\omega^5} e^{-\frac{B}{\omega^4}} \qquad \text{Equation 8}$$

$$A = 0.0081 g^2 \qquad \text{Equation 9}$$

$$B = 0.74 \left(\frac{g}{V_{wind}}\right)^4 \qquad \text{Equation 10}$$

V_{wind} is the wind velocity 19.5 [m] above MWL. But in the JONSWAP spectrum the wind velocity is replaced by the peak frequency $\omega_p = \frac{2\pi}{T_p}$ and parameters A and B are redefined:

$$A = \alpha g^2 \qquad \text{Equation 11}$$

$$B = \frac{5}{4}\omega_p^4 = \beta \omega_p^4 \qquad \text{Equation 12}$$

$$\rightarrow \omega_p = 0.87 \frac{g}{V_{wind}} \qquad \text{Equation 13}$$

Peak frequency ω_p is illustrated in Figure 20. In addition the mentioned changes the spectrum is peaked by multiplying an additional factor. This factor is added since the spectrum describes sea states not fully developed where the peak is sharper that for the PM spectrum. The equation for the JONSWAP spectrum is found by combining Equation 8 with Equations 11-12 and a peakendess factor:

$$S(\omega) = \alpha \frac{g^2}{\omega^5} e^{-\beta\left(\frac{\omega_p}{\omega}\right)^4} \gamma e^{-\frac{1}{2}\left(\frac{\omega-\omega_p}{\sigma\omega_p}\right)^2} \qquad \text{Equation 14}$$
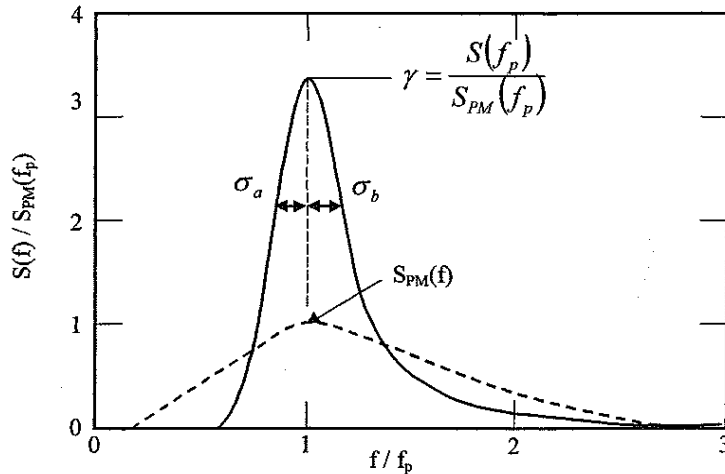
Figure 17: The JONSWAP and PM frequency spectra [16].

γ is the peakedness factor and varies between 1 and 7, and when $\gamma = 1$ the JONSWAP spectrum equals the PM spectrum. It is defined as the ratio between maximum energy in the JONSWAP and PM spectrum as shown in Figure 17 together with the two spectra. α is a spectral parameter that determines the shape of the spectrum in the high frequency part. σ is also a spectral parameter and equal to σ_a or σ_b depending on whether the frequency ω considered is lower than or equal to the peak frequency ω_p or above respectively. β is a form parameter.

7.1.2 Torsethaugen wave spectrum

At the Ormen Lange field the most suitable wave spectrum is the Torsethaugen double peaked spectrum [23]. An example of this wave spectrum is given in Figure 18. Low frequency waves, such as swell, travel faster than wind generated waves with higher wave frequency. Swell is waves entering an area from other locations. The reason why swell travel faster than wind generated waves is because low frequency waves on deep water have longer wave lengths than high frequency waves, see Equation 17, and the longer wave length the faster wave frequency velocity. Wave length and frequency is connected through the dispersion relationship, as seen in Table 1:

$$\omega^2 = kg \qquad \text{Equation 15}$$

and the wave number k equals [20]:

$$k = \frac{2\pi}{\lambda} \qquad \text{Equation 16}$$

By inserting the wave number into the dispersion relationship:

$$\lambda = \frac{2\pi}{\omega^2} g \qquad \text{Equation 17}$$

The wave frequency velocity can be found by combining the deepwater dispersion relationship and the following expression for wave frequency velocity c_w:

$$c_w = \frac{\omega}{k} \qquad \text{Equation 18}$$

$$\rightarrow c_w = \sqrt{\frac{g}{k}} = \sqrt{\frac{g\lambda}{2\pi}} \qquad \text{Equation 19}$$

Thus the longer wave length the higher wave frequency velocity.

Swell from remote areas can therefore enter local wind generated seas and create multiple peak wave spectra. The different spectra can have different peak frequency and direction of propagation, and the total spectra can therefore be quite complicated. In the Norwegian Sea swell from the Atlantic Ocean enters and the Torsethaugen spectrum is hence often used for design purposes here since it considers two sea states, wind seas and swell [36].

In fact the original Torsethaugen spectrum was developed based on measurements from the Norwegian Continental Shelf (Haltenbanken and Stadtfjord). Two JONSWAP spectra are fitted together. The two different sea states are divided by T_{PF} which is the spectral peak period for a fully developed sea at the location considered.

- Wind dominating sea: $T_P < T_{PF}$
- Swell dominated sea: $T_P > T_{PF}$

Necessary spectrum input is H_S and T_P, significant wave height and spectral peak period of the sea state respectively. Also residual parameters are needed and these parameters make the spectrum complex. To simplify the original Torsethaugen spectrum Torsethaugen and Haver developed a new spectral model which is summarized in [36]. A short version is given in Appendix 2. The purpose was to reduce the number of free parameters since many of the original parameters only had an effect at low sea states. And low sea states are not particularly interesting for design. In the simplified model all residual parameters needed to determine the spectrum are defined by H_S and T_P, and this parameterization has been made based on regression analyses and curve fitting.
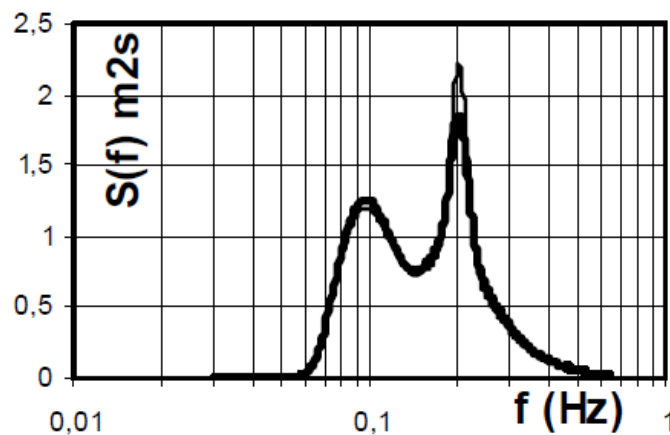
Figure 18: Example of a Torsethaugen spectrum, $H_S = 2$ [m] and $T_P = 5$ [s]. The thin line is the original spectrum while the solid line is the simplified spectrum [36].

7.2 Sea states analyzed

Sea state parameters H_S and T_P are chosen based on the Ormen Lange scatter diagram for H_s and T_p, see Appendix 1, and the target installation H_s values listed in Chapter 6.5 Design parameters. It will be of interest to analyze the lowering for a minimum range of H_S from 2.5 [m] to 4.5 [m] since both deployment over the side and through moonpool are considered. This range has been slightly enlarged and values in between included. The H_S values considered are as follows, and probable T_P values can hence be found by using the scatter diagram. When using the scatter diagram upper bound values have been utilized.

- $H_s = \{2.0, 2.5, 3.0, 3.5, 4.0, 4.5, 5.0, 5.5\}\,[m]$
- $T_p = \{7, 9, 11, 13, 15, 17\}[s]$

There are significant contributions to H$_S$ 2.0 – 3.0 [m] when T$_P$ = 7.0 [s], and this T$_P$ value also contributes to some H$_S$ values above 3.0 [m]. This is therefore the first wave period included. Then every second T$_P$ value up till 17 [s] is considered. T$_P$ > 17 [s] is neglected due to small probability of occurrence. Only every second value is used due to time limitations. It must be noted that all combinations of H_s and T_p values listed are analyzed.

Limiting sea states will change for changing wave headings since different wave headings will generate different vessel and module motions. The deployment analyses should therefore be run with different wave headings for the wave parameters of interest. Again, due to time limitations all wave headings cannot be analyzed. The following wave headings are chosen, where 0° equals bow waves. Wave headings change counter-clockwise.

- $Wave\ heading = \{0, 30, 60,\ 90,\ 120,\ 150,\ 180\}[degrees]$

Symmetry is assumed about the longitudinal center plain of the vessel. Representative results between 180° and 360° wave heading can hence be found based on the wave headings listed above. The module is in the analyses lowered on ship side for incoming waves. This is taken as conservative since waves will directly impact the module motions as well as indirectly affect its motions through the crane tip motions. If the module was lowered on the opposed side of the ship to the incoming waves the ship would act as a wave shield for the structure and hence less object motions would be generated. It would also reduce the risk of slamming since waves no longer would directly impact the structure to the same extent. It is intentional to obtain conservative results to account for uncertainties.

7.3 Wave spectrum discussion

Since irregular waves are considered a wave spectrum must be chosen. In this case both JONSWAP and Torsethaugen have their pros and cons. On one hand JONSWAP does not consider the incoming swell from the Atlantic at the Ormen Lange field, but Torsethaugen does. On the other hand not only T$_P$ but also T$_Z$ must be considered.

T$_P$ is the spectral peak period while T$_Z$ is the mean zero up-crossing period for successive waves [16]. Zero up-crossing equals the crossing of the zero level at positive derivative and can be found from the time history of the wave elevation, see Figure 19.
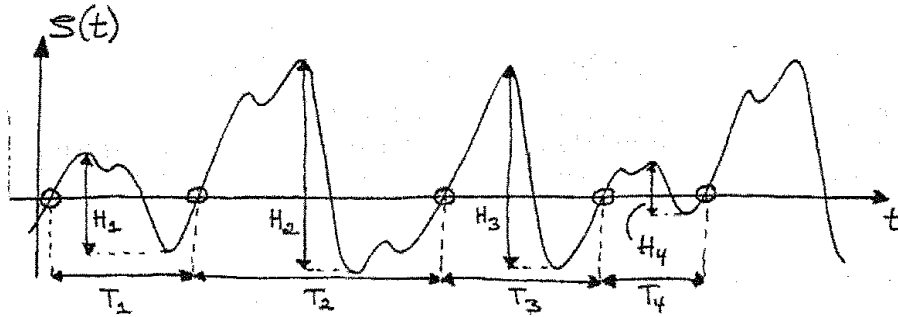
Figure 19: T_Z is the mean of the zero up-crossing periods, hence the mean of T_1, T_2, T_3, … [16].
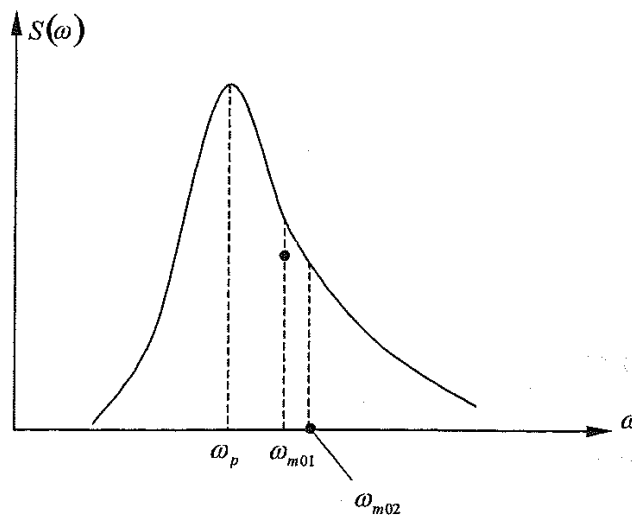
Figure 20: A wave spectrum. T_P, or ω_P, is shown. T_{m01} and T_{m02} are estimates of T_Z [16].

T_Z can be estimated by T_{m01} and T_{m02}, where T_{m01} is the center of gravity for the wave spectrum while T_{m02} is the spectrum's radius of inertia. They can be seen in Figure 20 above. From this figure it can also be seen that T_P and T_Z are unequal, which is normal for irregular sea states. In Appendix 1 an annual omnidirectional scatter diagram for H_S and T_Z is given. When using the two spectra with the H_S and T_P values given for the analyses specific T_Z values for given H_S and T_P combinations can be calculated. This can be seen from Equations 20-22.

$$T_Z = \frac{1}{N^+(0)}$$

Equation 20

where the expected zero up-crossing frequency $N^+(0)$ is [17]:

$$N^+(0) = \frac{1}{2\pi}\sqrt{\frac{m_2}{m_1}}$$

Equation 21

$$m_n = \int_0^\infty \omega^n S(\omega)d\omega \,; n = 0, 1, 2, …$$

Equation 22

The spectrum $S(\omega)$ is then what is needed to calculate T_z. In Torsethaugen only H_S and T_P is needed as spectrum input while 5 additional parameters must be defined for the JONSWAP spectrum. In [16] average values for γ and σ are listed while β already is given in the spectrum definition. Note that γ should be changed with changing H_S and T_P but for simplicity it is held constant in this report. To obtain α a formula in [25] is used and $T_p = \frac{2\pi}{\omega_p}$.

- $\bar{\gamma} = 3.3$
- $\sigma_a = 0.07$
- $\sigma_b = 0.09$
- $\beta = 1.25$
- $\alpha = \left(\frac{H_S}{4g}\right)^2 \omega_p^4 (0.065\gamma^{0.803} + 0.135)^{-1}$ Equation 23

The procedure described in Appendix 2 is applied for Torsethaugen to calculate the spectrum and then the resulting T_Z values. For the JONSWAP spectrum the parameters above are inserted into Equation 14 to obtain the spectrum. Also here T_Z values are computed.

For calculations the computer program MATLAB is utilized, and the scripts made are included in Appendix 13.2. See "Torsethaugen" and "JONSWAP". Note that in the MATLAB scripts the spectra are dependent on frequency f instead of ω. The JONSWAP spectrum has been reformulated from the expression in Equation 14 by assuming total wave energy, the area under the spectrum graph, to be independent of the denomination of the axes [16]:

$$\int_0^\infty S(f)df = \int_0^\infty S(\omega)d\omega = \int_0^\infty S(\omega)2\pi df$$ Equation 24

since $f = \frac{2\pi}{\omega}$. Hence:

$$S(f) = 2\pi S(\omega)$$ Equation 25

The JONSWAP spectrum written as S(f):

$$S(f) = 2\pi S(\omega = 2\pi f)$$ Equation 26

$$S(f) = 2\pi\alpha g^2 (2\pi f)^{-5} e^{-\beta\left(\frac{2\pi f_p}{2\pi f}\right)^4} \gamma^{e^{-\frac{1}{2}\left(\frac{2\pi f - 2\pi f_p}{\sigma 2\pi f_p}\right)^2}}$$ Equation 27

$$S(f) = \alpha \frac{g^2}{(2\pi)^4 f^5} e^{-\beta\left(\frac{f_p}{f}\right)^4} \gamma^{e^{-\frac{1}{2\sigma}\left(\frac{f}{f_p} - 1\right)^2}}$$ Equation 28

Resulting T_Z values considering the stated H_S and T_P input for both spectra are given in Tables 2-3. Table 2 represents Torsethaugen while Table 3 represents JONSWAP.

T_P/H_S	2.00	2.50	3.00	3.50	4.00	4.50	5.00	5.50
7.00	4.69	4.87	5.05	5.21	5.35	5.48	5.60	5.70
9.00	5.60	5.67	5.74	5.84	5.95	6.07	6.19	6.31
11.00	6.08	6.38	6.61	6.78	6.89	6.94	6.97	7.03
13.00	6.02	6.43	6.77	7.06	7.31	7.53	7.71	7.87
15.00	5.90	6.30	6.65	6.95	7.24	7.49	7.73	7.95
17.00	5.86	6.24	6.58	6.88	7.15	7.40	7.63	7.84

Table 2: T_Z values calculated by the Torsethaugen spectrum.

T_P/H_S	2.00	2.50	3.00	3.50	4.00	4.50	5.00	5.50
7.00	5.50	5.50	5.50	5.50	5.50	5.50	5.50	5.50
9.00	7.04	7.04	7.04	7.04	7.04	7.04	7.04	7.04
11.00	8.59	8.59	8.59	8.59	8.59	8.59	8.59	8.59
13.00	10.14	10.14	10.14	10.14	10.14	10.14	10.14	10.14
15.00	11.69	11.69	11.69	11.69	11.69	11.69	11.69	11.69
17.00	13.24	13.24	13.24	13.24	13.24	13.24	13.24	13.24

Table 3: T_Z values calculated by the JONSWAP spectrum.

It can clearly be seen that the JONSWAP spectrum covers a wider range of expected T_Z values for the listed H_S according to the H_S and T_Z scatter diagram in Appendix 1 than the Torsethaugen spectrum. The low T_Z for Torsethaugen at high H_S and T_P values is due to the fact that at high T_P values the spectrum is swell dominated. The swell generated peak is high and thin and the most of the energy is located around the secondary wind generated peak at a lower period. This is illustrated in Figure 21. More T_Z values are covered by the JONWAP spectrum since it is single peaked and the energy is centralized around this peak. So when T_P is large also T_Z is of a certain magnitude. Another fact important to remember for both spectra is that a spectrum is an average representation of a sea state. Less probable sea states are thus hard to represent using wave spectra.
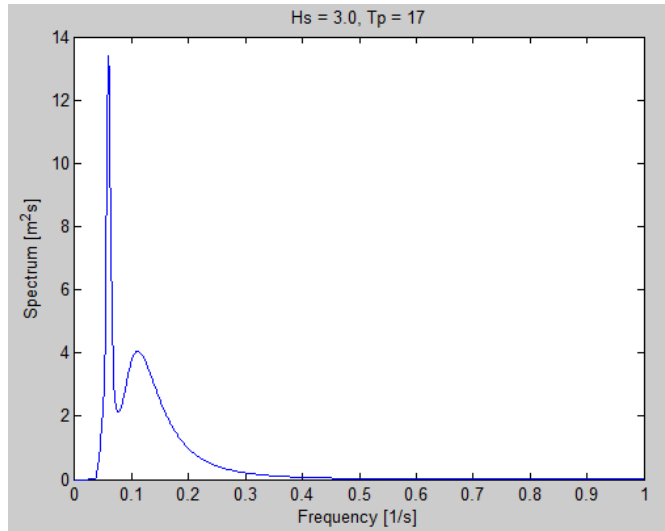
Figure 21: Torsethaugen wave spectrum S(f) for high T_P.

It is decided to run the analyses with both spectra since they are favorable in different ways. Torsethaugen since it considers the incoming swell at Ormen Lange and JONSWAP since it covers a wider range of expected T_Z values at site.

8. Wire and Crane Specifics

8.1 Wire data

For the analyses a double fall wire system will be used, see Figure 13. This is to get realistic wire data. The wire system is consistent in all analyses. No wire data is found on wires that have large enough minimum breakage load (MBL) when considering the module weight, dynamic amplification factor (DAF) and safety factor (SF) for installing the module in a single fall wire system.

From Certex online catalogue relevant wire data can be found [40]. The Big Hydra high performance wire rope is taken as appropriate, and to select required dimension and specifications MBL is used. In Figure 22 the cross section of a Big Hydra wire rope is outlined. The wire rope selection table is given in Appendix 3. Necessary MBL for the lowering of the largest OL subsea FC unit is computed by multiplying the module's weight in air with an estimated DAF and a nominal safety factor. γ_{SF} is the nominal safety factor which accounts for wearing, material used and the loading. In [26] a Shell standard minimum safety factor of 5.0 is required for wire rope.
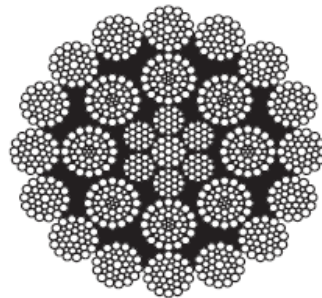
Figure 22: Big Hydra high performance wire rope [40].

A preliminary DAF must be found for the operation. In [26] a list of DAFs for offshore lifts to deploy equipment subsea is given. All rigging and lifting appliances shall be selected utilizing a minimum DAF of 2.0 unless additional analyses shows that conservative results can be obtained by a DAF less than 2.0.

Necessary safe working load (SWL) and MBL for the lifting wire is calculated in Appendix 3 based on the static weight of the object and the DAF and SF required.

- SWL: 250 [t]
- MBL: 1250 [t]

The wire rope from the selection in Appendix 3 with an MBL as close as possible but above MBL = 1250 [t] is chosen. This wire has MBL = 1259 [t] which means that it can also take the load when the weight of the wire rope extending from the crane tip to the module is considered.

Parameters of importance for the selected wire rope are listed in Appendix 3. The main parameters are also given below.

- Wire diameter, d_W: 0.127 [m]
- Mass per unit length: 73.10 [kg/m]
- MBL: 1259 [t]
- Circumscribed wire area, A_W: 0.007855 [m^2]
- Cross-sectional Young's modulus, E_W: 65.13 [GPa]
- Wire length, l_w: 36.81/ 30.69 [m]
- Wire drag coefficient: 1.2

Wire length is dependent on deployment method and calculations are given in Appendix 3, see Equations 78 and 79. 36.81 [m] is for crane deployment over the side while 30.69 [m] is for moonpool deployment. In Appendix 3 also the wire drag coefficient is found.

8.2 Crane and MHT specifics

8.2.1 Crane tip coordinates

Crane tip coordinates are needed for the analyses as the crane response is dominating for the module motion. Crane tip coordinates are input into MACSI2 while crane tip velocities are input into the slamming analyses. The crane will move with the vessel, so to get crane tip motions and velocities the vessel's RAOs are used together with the crane tip position. Crane tip location is given compared to the vessel's LCG for x- and y-direction and MWL for z-direction.

The crane tip coordinates for the analyses must be estimated from Norman Subsea drawings. Also the crane diagram for the main knuckle box boom crane presently at Skandi Acergy is used, a crane that can take a static load of 400 [t].This crane diagram is attached in Appendix 4, Figure 72.

Resulting crane tip coordinates calculated in Appendix 4:

- ct_x: 30.32 [m]
- ct_y: 20.00 [m]
- ct_z: 30.31 [m]

8.2.2 Coordinates for main sheave in moonpool MHT

Like crane tip coordinates are important for over the side analyses coordinates of the main sheave in the module handling tower are important for through moonpool analyses. These coordinates are also obtained using the Normand Subsea 1st deck drawing [31], but in addition pallet, skid rails, lift frame and cursor heights are taken from [1].

Resulting coordinates of the moonpool main sheave calculated in Appendix 5:

- ms_x: 6.92 [m]
- ms_y: 0.00 [m]
- ms_z: 24.19 [m]

8.2.3 Crane resilience

Longitudinal wire stiffness equals:

$$k_w = \frac{E_w A_w}{l_w} = \frac{E_w \pi d_w^2}{4 l_w}$$

Equation 29

See Chapter 8.1 Wire details for explanation of symbols. Notice that according to DNV [10] it is recommended to use the distance from block to crane tip as line length if multiple lines are used. For short wires, and especially wires with large Young's Modulus and wire cross-section area, the longitudinal wire stiffness can be over predicted compared to the combined stiffness of the crane and the wire length from the winch trough the block system and to the crane tip [25]. Too high stiffness K will again cause too low eigenperiod T_0 and hence resonance period of the system longitudinally:

$$T_0 = \frac{2\pi}{\omega_0} = \sqrt{\frac{M}{K}}$$

Equation 30

Here M is the total mass of the system being lowered (structure and lifting wire) including added mass and K is the longitudinal stiffness of the lifting system. If snap loads were to be predicted these would also imply too high tensions if an over predicted stiffness were applied, see Equation 31. From [10] characteristic snap load may be taken as the following where v_{snap} is the characteristic snap velocity.

$$F_{snap} = v_{snap}\sqrt{K \cdot M}$$

Equation 31

To get a more realistic longitudinal stiffness of the lifting system not only the wire stiffness is used. The total stiffness can be found as [10]:

$$\frac{1}{K} = \frac{1}{k_{rigging}} + \frac{1}{k_w} + \frac{1}{k_{soft}} + \frac{1}{k_{block}} + \frac{1}{k_{boom}} + \frac{1}{k_{other}} = \frac{1}{k_{crane}} + \frac{1}{k_w}$$

Equation 32

$k_{rigging}$ = stiffness of rigging [N/m]

k_w = stiffness of lifting wire(s) [N/m]

k_{soft} = stiffness of soft strop or passive heave compensation system if used [N/m]

k_{block} = stiffness of multiple lines in a block if used [N/m]

k_{boom} = stiffness of crane boom [N/m]

k_{other} = other stiffness contributions if any [N/m]

k_{crane} = the total crane system stiffness, which equals total stiffness minus wire stiffness [N/m]

In MACSI2 crane system resilience is asked for in addition to wire details where resilience is the reciprocal of stiffness. The formula can be seen in Equation 33. This additional stiffness helps preventing numerical convergence problems in MACSI2.

$$C_{resilience} = \frac{1}{k_{crane}}$$ Equation 33

No data for computing crane resilience of the main crane on Skandi Acergy is given. To compute crane resilience stiffnesses of crane pedestal, crane cylinder and crane boom are taken from [33] even though they yield for a 160 [t] crane on MVS Nordica. How these stiffnesses change with lifting capacity is not given, and since such data is hard to get hold of the values are assumed valid for the main crane on Skandi Acergy as well. The crane resilience of the main crane on Skandi Acergy:

$$C_{resilience} = \frac{1}{k_{pedestal}} + \frac{1}{k_{cylinder}} + \frac{1}{k_{boom}} = 2.9 \cdot 10^{-7} [\frac{m}{N}]$$ Equation 34

The crane resilience will change for lowering through the moonpool compared to lowering with a crane over the side. A module handling tower where the module is deployed by main winches and main sheaves in fixed positions is much stiffer than a knuckle boom box crane system. According to Shell in-house experience is the MHT with its deployment system seen as infinitely stiff and the crane resilience is hence equal to zero. Zero crane resilience may cause numerical problems in MACSI2 so a small number is used instead. $C_{resilience} = 1 \cdot 10^{-15} [\frac{m}{N}]$ is chosen.

9. Module Details

As mentioned no EPC contract has been signed for the future compression system. Therefore no final drawings and dimensions of the structures exists, only preliminary drafts without details. It has hence been decided to analyze a box structure with outer dimensions and weight equal to the limiting requirements for the compressor units.

Height = 12 [m]

Width = 6 [m]

Length = 12 [m]
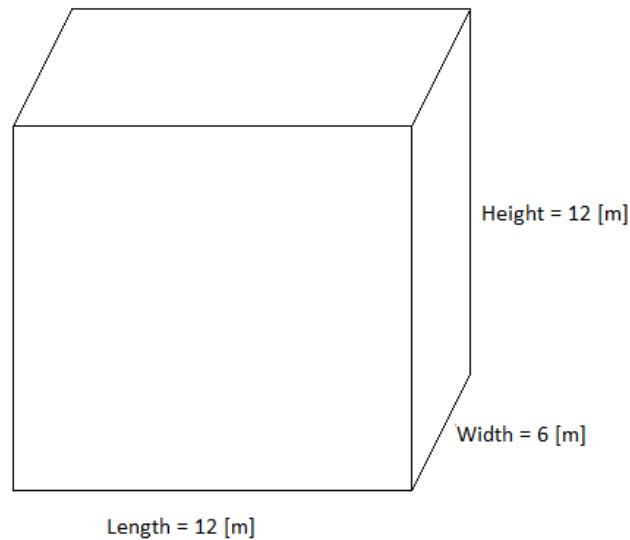
Figure 23: The unit being analyzed. Note that the drawing is not to scale and perforation is not included.

Necessary module features for the analyzes are calculated in Appendix 6.

- Dimensions in x-, y- and z-dir., l_m, w_m, h_m: 12 [m], 6 [m], 12 [m]
- Object mass, M_m: 250 [t]
- Object volume, V_m: 31.8 [m^3]
- Projected areas x-, y- and z-dir., A_{mx}, A_{my}, A_{mz}: 68.4 [m^2], 136.8 [m^2], 68.4 [m^2]
- Added mass coefficients in x-, y- and z-dir., C_{Ax}, C_{Ay}, C_{Az}: 13.2, 35.5, 13.2
- Linear drag coefficients in x-, y- and z-dir.: 0.2, 0.2, 0.2
- Quadratic drag coefficients in x-, y- and z-dir.,C_{Dx}, C_{Dy}, C_{Dz}: 2.7, 2.7, 2.7

The perforation rate is assumed to be 5 % in all directions. The hydrodynamic parameters are discussed in Chapter 9.1 Hydrodynamic coefficients.

9.1 Hydrodynamic coefficients

Hydrodynamic coefficients are needed in the analyses of time instance 2, when the module is fully submerged. But as the unit being lowered is taken as a box in this report, the methods used for finding added mass and drag are rather simple. If more structural details were know another

method could have been applied for calculating both added mass and drag. Then the contribution from each element in the real design could be estimated from simple geometrical shapes and the total added mass and drag found by adding the contributions together. Note that this method is not recommended if the structure has low perforation ratio [10] since interactional effects and oscillation amplitude dependency are excluded. It is in general hard to predict added mass and drag so if high accuracy is required CFD analyses or model tests should be performed.

9.1.1 Added mass

When a body moves in fluid it will accelerate the fluid particles around it. The fluid particles will be accelerated differently depending on their position relative to the moving body. To accelerate the fluid particles force is needed, and this force is called added mass. A body has 6 degrees of freedom if none are restricted. For each force and moment direction there are 6 added mass components, one for each mode of motion. As there are 6 excitation force and moment directions and 6 modes of motion there can be a total of 36 added mass coefficients [11]. Added mass A_{kj} is the added mass in direction k where k is the direction of the excitation force, while j is mode of motion. In this case rotations are neglected and coupling is not taken into account. In other words added mass A_{kj} only gets contribution from the added mass due to motion in the same direction as the force, hence when k = j. This is for simplicity.

Added mass and added mass coefficients are calculated based on [24] as shown in Appendix 7. Added mass coefficients are determined based on Equation 35 when added mass is known:

$$C_{Ai} = \frac{A_i}{\rho_w V_R} = \frac{A_i}{\rho_w V_m} \quad i = x, y, z \qquad \text{Equation 35}$$

The added mass and added mass coefficients calculations give following results:

- $A_x = 431.8 \, [t]$ and $C_{Ax} = 13.226$
- $A_y = 1160 \, [t]$ and $C_{Ay} = 35.531$
- $A_z = 431.8 \, [t]$ and $C_{Az} = 13.226$

The values in x- and z-direction are naturally equal as the projected areas, heights and perforation are equal. Figures for y-direction are as expected much higher than x- and z-direction as the projected area is 12x12 [m] as opposed to 12x6 [m].

9.1.2 Drag

Drag forces arises because of pressure differences upstream and downstream of an object in incoming flow due to flow separation. The pressure is lower downstream and a force in the direction of the water inflow will hence be generated. Also vortex shedding at the separation

points and surface friction contributes, but vortex shedding to a larger extent than surface friction. In Appendix 8 more details regarding drag in general can be found.

Also linear and quadratic drag coefficients for the object analyzed in this report are estimated in Appendix 8. Linear drag is almost neglectable since the flow is oscillating and quadratic drag is dominating, see Figure 2.1 in [37]. Linear drag coefficients are according to [15] therefore set equal to 0.2 in all directions. Quadratic drag coefficients are as mentioned dominating and quite high:

$$C_{Dx} = C_{Dy} = C_{Dz} = 2.7$$

9.1.3 Corrections to the hydrodynamic coefficients
The added mass and drag coefficients calculated represent the coefficients of a closed box placed in unrestricted and uniform incoming flow. For added mass calculations the inflow is also steady. In reality the module being lowered is perforated and it is placed both close to the ship hull/ moonpool walls and close to the water surface. And due to the waves incoming flow will be oscillating, which is already accounted for when estimating drag coefficients. All these factors will affect the hydrodynamic coefficients so corrections have to be applied. Note that ship bottom effects are neglected. So are also higher order effects from the free surface, except for quadratic drag. Detailed discussions are given in Appendix 9 and the main features are mentioned here.

- Perforation does not need to be considered due to low perforation rate of 5 %, neither for added mass nor drag coefficients.

- To be conservative added mass coefficients are not reduced due to oscillating flow.

- Free surface causes submergence to vary. This leads to varying added mass and drag coefficient with submergence, see Table 4. Here nondimensional depth equals submerged depth divided by module height.

Non.dim. depth	C_A correction			Quadratic drag coeff. corr.			Linear drag coeff. corr.		
	C_{Ax}	C_{Ay}	C_{Az}	C_{Dx}	C_{Dy}	C_{Dz}	x-dir	y-dir	z-dir
0	0	0	0	0	0	0	0	0	0
0.25	0.132	0.107	0.878	0.25	0.25	0.25	0.25	0.25	0.25
0.5	0.376	0.352	0.945	0.5	0.5	0.5	0.5	0.5	0.5
0.75	0.685	0.682	0.977	0.75	0.75	0.75	0.75	0.75	0.75
1	1	1	1	1	1	1	1	1	1

Table 4: Correction factors to hydrodynamic coefficients due to varying submergence.

- When considering crane deployment the module is lowered over the side with a distance from the ship hull large enough for added mass and drag coefficients not to be particularly affected by the fixed boundary. No correction is therefore applied.

- When considering moonpool deployment added mass and drag coefficients are corrected for restricting the flow. Resulting corrections:

$$\frac{C_{Az}}{C_{Az0}} = 1.72$$

$$\frac{C_{Dz}}{C_{Dz0}} = 5.55$$

In the equations coefficients indicated by 0 are coefficients for unrestricted flow.
The linear drag coefficient is corrected in the same way as the quadratic drag coefficient.

- Surface roughness corrections are not applied.

- Corrections for frequency of oscillation are not considered.

10. Moonpool Specifics

10.1 General analysis input

The footprint size of the module compared to the horizontal moonpool area is important. It is difficult to determine how much of the moonpool that has to be open and how large the clearance between module and moonpool walls has to be. To small clearance leads to blockage effects and excessive water particle velocities and accelerations. Model tests should be carried out find the necessary moonpool size.

No study has been performed on optimized moonpool dimensions based on the size of the module being lowered. From [28] moonpool dimensions are taken, a drawing made in connection with a study on purpose building an offshore installation vessel for installation of the Ormen Lange future compression modules. The draft is set equal to the draft of Normand Subsea. Dimensions are hence:

- Length: 14.0 [m]
- Width: 7.5 [m]
- Cross-sectional area: 105.0 [m^2]
- Draught: 7.81 [m]

In MACSI2 moonpool damping is needed as input, expressed by wave amplitude ratio at resonance. As no suiting monohull installation vessel with a large enough moonpool exists today it is hard to obtain such a ratio. But in MACSI2 the moonpool water motions are assumed unaffected by the module being lowered. This is a problem in this case where the module will cover most of the moonpool cross-sectional area and definitely affect the water velocities and accelerations. To account for the effect of the large module on fluid flow in the moonpool a large wave damping should be applied [15]. This damping is to be expressed by wave amplitude ratio at resonance, a ratio which is low when the damping is high. A highly damped system has damping ratio in the range 1.0-1.5. 1.5 was first chosen but then MACSI2 could not handle the analyses, probably due to numerical problems. 1.0 had to be applied for analyses to run.

High water particle velocities and accelerations are taken care of by a high drag coefficient in the moonpool, see Chapter 9.1.3 Corrections to the hydrodynamic coefficients.

The moonpool will most likely be aerated but this is not taken into account in this report.

10.2 Moonpool fluid flow

Moonpool vertical water particle velocities are needed in order to compute the slamming forces on the structure when lowered through the moonpool. See slamming force equation denoted Equation 44. In order to get approximate vertical water particle velocity values in the moonpool several assumptions are made. First of all only vertical motions of the ship and moonpool water

column are considered which is ok since slamming is most critical in the vertical direction, see Figure 24. Water particle velocity is set equal to the velocity of the water column, or water plug, in the moonpool as the cross-sectional area of the moonpool is constant along the ship draft. It is also assumed that the period of the water particle motion is similar to the zero up-crossing period of the sea state T_z. If water plug motion amplitude ζ_{wp_a} is found water plug velocity can be estimated since the time is known:

$$\dot{\zeta}_{wp\_a} = \frac{\zeta_{wp\_a}}{0.5 \cdot T_z}$$

Equation 36

Hence constant velocity for the water plug is assumed which is not really the case. One would imagine the oscillating water plug to have maximum velocity at mean level and reduced velocity with increased distance from the mean level. This maximum velocity should be applied since slamming is considered for the module bottom end located at the mean water level, but to find this velocity more detailed studied would have to be performed which there is no time for.
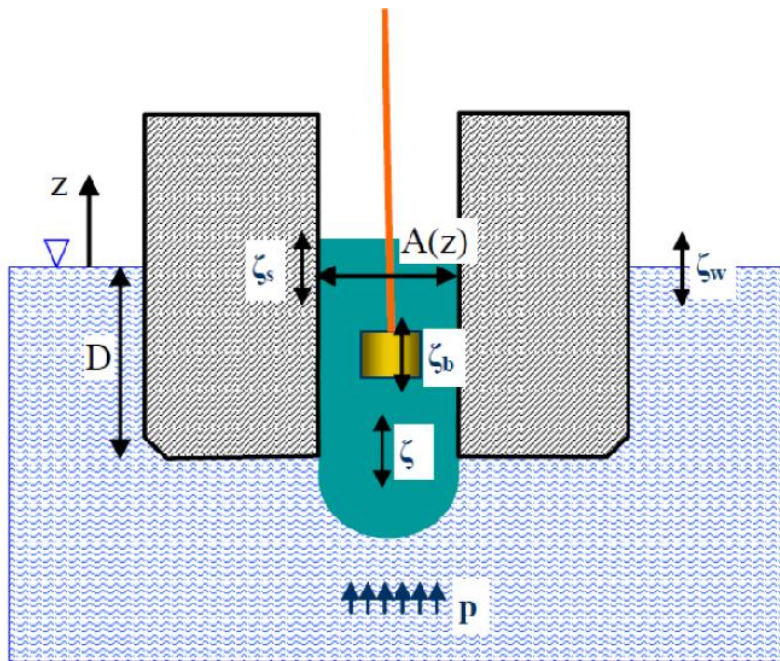
Figure 24: Moonpool specifics [10].

By using formulas provided in [10] the water plug motion amplitude can be estimated. The following assumptions are made in [10]:

- The moonpool dimensions are small compared to the breadth of the ship.
- Only motion of the water and object in vertical direction is considered.
- The blocking effect of the lifted object on the water in the moonpool is moderate.
- Cursors prevent impact into the moonpool walls. Only vertical forces parallel to the moonpool axis are considered.

These assumptions seems to fit the problem quite well, depending on the definition of having small dimensions compared to the breadth of the ship. The width of the moonpool is 7.5 [m] while the breadth of Normand Subsea is 24 [m]. On the other side the length of the moonpool is 14 [m] which is more than half the ship breadth. How this will affect the result in [10] is not known but the equations are still used. The definition of moderate blocking effect is also unknown.

In Appendix 11 the procedure for estimating the water plug motion amplitude is given.

When the water plug motion amplitudes are estimated water particle velocities for the moonpool can now be obtained by Equation 36. The T_z values obtained for the two wave spectra when all H_s and T_p values are used as input, see Tables 5 and 6. Resulting velocities are in Chapter 15.2 Vertical water particle velocities compared with characteristic vertical free surface wave particle velocities.

10.2.1 Moonpool fluid flow verification and results

In [10] a graph of relative water plug elevation divided by wave amplitude is given. Relative water plug elevation is the water plug elevation minus the elevation of the moonpool walls due to ship motion, see Equation 37. G_s represents the ship motion transfer function. The graph is shown in Figure 25 for varying relative damping ratios. Note that the graph yields for a 80 [m] long diving support vessel.

$$RAO = \left|\frac{\zeta_{wp} - \zeta_s}{\zeta}\right| = \left|\frac{\zeta_{wp}}{\zeta} - G_s\right|$$

Equation 37
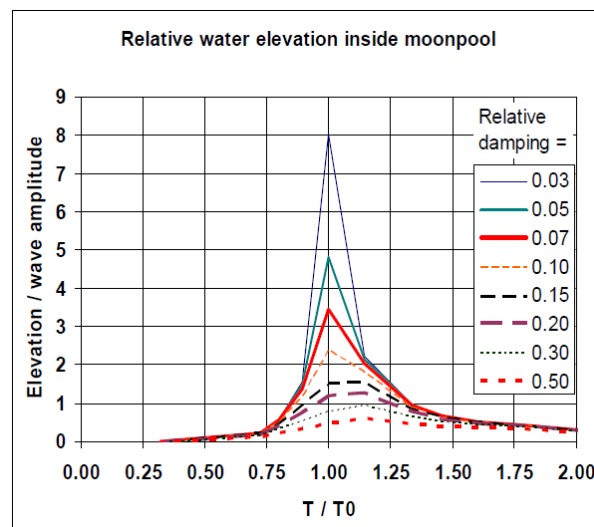
Figure 25: Relative water elevation in a moonpool calculated by DNV [10].

A similar plot is produced for relative damping $\eta = 0.19$, $T_p = \{7, 9, 11, 13, 15, 17\}[s]$ and wave heading 0° to check the calculations performed based on the Normand Subsea motion transfer function magnitudes and phase angles. $\eta = 0.19$ is in [10] given as appropriate for a moonpool with guidance structure which will be the case here. Wave heading 0° is chosen since it is the assumed wave heading for the DNV plot. The plot can be made since both the expressions for $\frac{\zeta_{wp}}{\zeta}$ and G_s are known, see Appendix 11. The plots are not expected to be exactly similar since different vessels with different lengths and heave transfer functions are used, but similarity should be obtained. In Figure 26 the result is presented and as expected the graph is comparable to the DNV graph for $\eta = 0.19$. The equations outlined in Appendix 11 are therefore assumed correct.

Note that the wave period is plotted against the natural period of the water plug. The basis for estimating the natural frequency is given by Faltinsen in [11]:

$$T_0 = 2\pi \sqrt{\frac{D}{g}}$$

Equation 38

D is the draught, 7.8 [m]. In both [12] and [10] an extended formula is given where "added draught" is accounted for.

$$T_0 = 2\pi \sqrt{\frac{D+d'}{g}} = 2\pi \sqrt{\frac{D+\kappa\sqrt{A_{moonpool}}}{g}} = 7.1 \, [s]$$

Equation 39

Equation 39 will be used since it is of newer date than the Equation 38. The κ value of 0.46 recommended in [10] is applied instead of $\kappa = 0.41$ as in [12]. This is because the value of 0.41 is taken from a paper written in 1977.
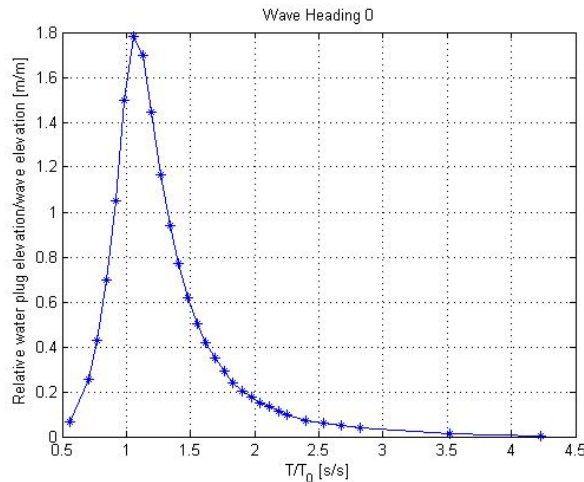
Figure 26: Relative water plug elevation computed from the given Normand Subsea heave transfer function magnitudes and phase angles.

The RAO for the water plug elevation to the wave elevation is also given, see Figure 27.
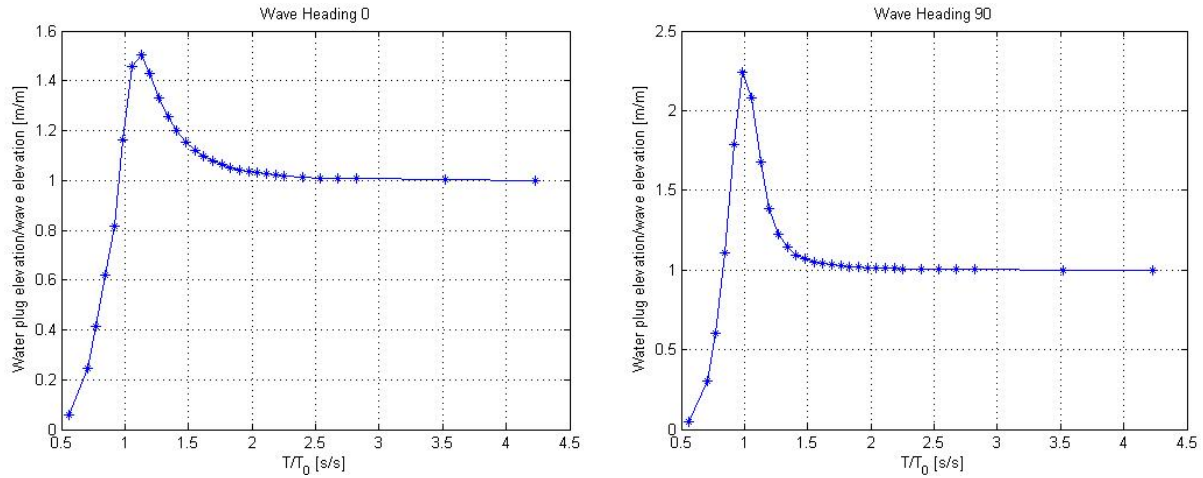
Figure 27: Water plug elevation to wave elevation for wave headings 0⁰ and 90⁰.

From Figure 27 can it be seen that the water plug amplitude equals the wave motion amplitude for long wave lengths. This can be explained by the excitation force of the water plug. The water plug is mainly excited by the undisturbed Froude-Krylov pressure under the moonpool. The equation for the FK excitation force is taken from [10]:

$$\frac{F_1(t)}{\zeta} = \rho_{mp} A_{moonpool} \cdot g e^{-kD} = \rho_{mp} A_{moonpool} \cdot g e^{-\frac{g}{T^2}D} \qquad \text{Equation 40}$$

Long wave lengths are equal to long wave periods as the deepwater dispersion relationship can be reformulated to $\lambda = \frac{2\pi}{g}T^2$. T will not impact the excitation force much when it has reached a certain threshold level according to Equation 40. But for small wave lengths T influences the FK excitation force significantly and reduces it. This reduction can be seen in Figure 27. Also the motion of the moonpool walls contributes to the water plug excitation force, see Appendix 11. But from Figure 26 it can be seen that for both short and long wave periods is the relative motion between the water plug and the ship moonpool walls quite small. The motion of the ship moonpool walls will hence have neglectable effect at these wave periods.

For excitation period equal to the natural period of the water plug resonance is obtained. The peak for water plug elevation divided by wave elevation has a small offset for wave heading 0⁰ but the offset is too small to be investigated further.

The reason why resonance ratio at wave heading 90⁰ is larger than at wave heading 0⁰ in Figure 27 is probably because of the difference in heave transfer function magnitude for Normand Subsea. For wave heading 90⁰ is the magnitude of the heave transfer function at T = 7.0 [s] 1.2 while it is 0.42 for wave heading 0⁰.

11.   MACSI2

MACSI2 is a dedicated marine crane simulation program developed by Peter Christian Sandvik. He works at MARINTEK in Trondheim in the offshore hydrodynamics department. MACSI2 version 1.2 was launched in 1998 and is based on DOS. It is a time domain analysis program that can include the dynamics in the splash zone and at the seabed [25] by using position dependent hydrodynamic coefficients. Also the wave field and dynamics inside a moonpool can be simulated. It therefore seems like a suiting program for the analyses to be conducted here. The following inputs are needed in the program:

- A definition of lifting system components and configurations
- Hydrodynamic description of the lifted body
- Environmental conditions (sea state, current)
- Vessel motion specifics (response amplitude operators (RAOs))

Obtained output consists of:

- Motion of the lifted body in three directions. Body rotations are not included.
- Lift line tension
- Motion of the ship and crane point, force components and distances.

This will be a direct winch-down operation both through moonpool and over the side. Since slack slings is the limiting condition the lift line tension has main focus. Note that no explanations of formulas used in the MACSI2 analyses will be given as the program is commercial and few equations are therefore listed in the program theory manual [25].

11.1 MACSI2 coordinate system

For correct input and hence also results the coordinate system used in the program is of great importance. It is a right handed coordinate system with origin at the mean water level (MWL) CoG. Positive x-direction is pointing to the ship stern, y-direction is to starboard and z-direction is upwards. Wave heading is taken counter-clockwise with zero degrees wave heading when the waves travel in positive x-directions. Hence head waves have a wave heading equal to zero. See Figure 28.
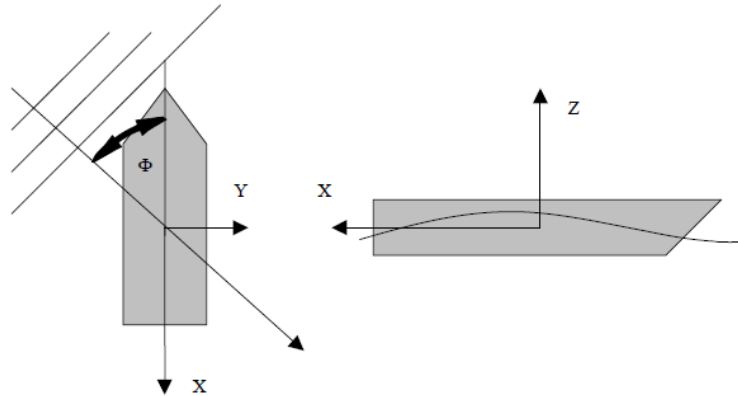
Figure 28: MACSI2 coordinate system [33].

11.2 MACSI2 important assumptions

- Body rotations are not taken as important and hence not included in the analyses. What is considered are roughly the load being lowered, the lift wire and the crane tip.
- It is not taken into account that the load may change the vessel motions. The unit is hence assumed to be light and with a small footprint compared to the wave length. Even though the unit is heavy and the footprint of the module being lowered is of a certain size is the program taken as applicable.
- The moonpool fluid flow is assumed unaffected by the module being lowered. This is a problem in this case where the module will cover most of the moonpool cross-sectional area and definitely affect the water velocities and accelerations. Peter Christian Sandvik meant that MACSI2 might even be useless for this purpose and that results might be unrealistic [15]. This problem was discovered at a stage where it was too late to change analyses program so MACSI2 will still be used.

11.3 MACSI2 analyses

The equation of motion used in the analyses [25]:

$$(M_m - A_i)\ddot{x}_i = F_{Wi} + F_{hydi} - W \qquad \text{Equation 41}$$

M_m : Module dry mass

$A_i = \rho_w V_m C_{Ai} C_{Ai_{corr}}$: Added mass in direction i (i = x, y, z)

C_{Ai} : Added mass coefficient in undisturbed fluid

$C_{Ai_{corr}}$: Position correction factor for the added mass coefficient

$\ddot{x}_i$: Object acceleration

F_{Wi} : Winch wire forces including drag

F_{hydi}: Hydrodynamic forces

$W = M_m g - B' = M_m g - \rho_w V_m' g$: Object weight

V_m' : Position dependent submerged volume

The hydrodynamic forces are dependent on total module mass, damping and stiffness and computed according to Equation 42:

$$F_{hydi} = (\rho_w V_m' + A_i)a_i + (B_{1i} + B_{2i}|u_r|)u_{ri} + \rho_w V_m \frac{\delta(C_{Ai}C_{Aicorr})}{\delta h}(\dot{x}_z - \dot{\zeta})u_{ri}$$

Equation 42

a_i : Wave particle acceleration

$B_{1i} = \frac{2\rho_w}{3\pi^2}\sqrt{2gX_i}A_i \cdot Linear\ drag\ coeff$: Linear drag when velocity = 1

$B_{2i} = \frac{1}{2}\rho_w A_i C_{Di}$: Quadratic drag when velocity = 1

X_i: Typical dimension

u_r : Relative water velocity

$\dot{x}_z$: Object velocity in z-direction

$\dot{\zeta}$: Surface elevation velocity in z-direction

The flow chart of the MACSI2 analyses is given in Figure 29. The input files, hydrodynamic correction files, vessel transfer function file and macro files are made according to descriptions in [25]. Input files, hydrodynamic correction files, RAO file and an example of each macro file type are given in Appendix 12. Note that explanations must be removed from input files before they can be used, but the first line must be left as is.
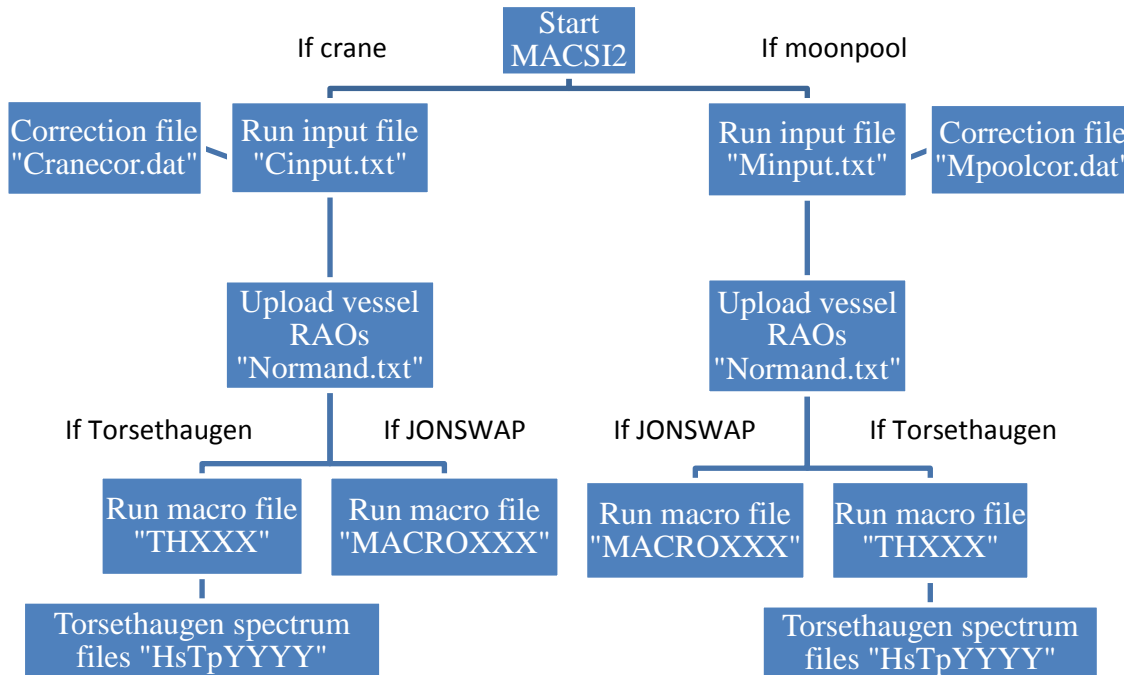
Figure 29: MACSI2 flow chart.

Note that neither guidelines, tugger lines nor heave compensation are used in these analyses. Rigging layout is not considered.

To run the analyses as quick as possible macro files for changing the sea states are created. In the macro file titles XXX indicates the wave heading (000, 030, …, 120, …). The macro files for the two wave spectra are roughly equal but the main difference is that JONSWAP is already programmed in MACSI2 and ready to use. Torsethaugen spectrum files on the other hand must be created by the user and called in the macro file. These files are stored as "HsTpYYYY" files where YYYY equals the significant wave height multiplied by 10 and the wave peak period. "HsTp4011" (H_s = 4.0 [m], T_p = 11.0 [s]) is given in Appendix 12 together with "MACRO000.mac" and "TH000.mac".

By preliminary testing simulation time was set to 600 [s] as recommended [14]. The tests were performed with the input ready at the time and a best guess for the variables not yet determined. Scatter of the results should be checked to verify the simulation time used. The duration of smooth start is set equal to 20 [s] which exceeds all the input wave periods. This is to be sure that the waves are built up and that no sudden wave impact will affect the analyses. Also numerical transients are avoided.

The resulting .OUT files produced by MACSI2 are post-processed using MATLAB. There functions with loops for checking all results can be programmed. The post-processing is then simplified as there are 48 different output files for each wave heading due to different

combinations of H_S and T_P. An .OUT file is provided in Appendix 12 while the MALAB script is explained in Chapter 14 MATLAB Scripts.

Based on the 600 [s] time history analyzed in MACSI2 a 2 hours maximum wire tension amplitude is estimated. In order to use a 600 [s] simulation of an irregular sea state to estimate response values of the same irregular sea state lasting for 2 hours certain assumptions must be made. The wave elevation and hence also the response are seen as stationary normally distributed stochastic processes [16]. This equals zero mean value as the values in the time history will be distributed evenly about zero over time. The variance is constant. A random process is seen as stationary when the probability distribution of the process is independent on absolute time [18]. If an additional assumption is made the single maxima in the wave elevation and response time histories can be seen as Rayleigh distributed; the process must be narrow-banded. A narrow-banded process is a process where the frequency interval is narrow. The energy in the process is then very concentrated around the mid value of the frequency interval. See reference [16] for further details.

The 2 hours maximum amplitude value of wire tension given a certain sea state is taken from the Rayleigh distribution of wire tension single maxima. It must be noted that this maximum value is not always usable. The system has to be mass dominated, not drag dominated since drag is a second order effect [15]. And if the wire has gone slack only a few times during the time history of the analyses it might not show on the estimated 2 hours max amplitude value. A few low tension values will not affect the overall estimated 2 hours max amplitude. Attention must hence also be paid to the minimum tension during the time history. To account for this the lower value of minimum wire tension from time history and static wire tension minus the 2 hours estimated max is used to check the slack sing criterion, see Equation 5. These values are marked with a red arrow in the output file, Appendix 12.8 MACSI2 -.OUT file.

In Chapter 14 MATLAB Scripts the MATLAB functions used for interpreting the .OUT files are included. They are also shortly described. It can be mentioned that the following variables are extracted from the output and used for calculations:

- The static wire tension before the dynamic analyses are run.
- T_z from the wave spectrum used in the analyses. It will deviate slightly from the computed values in Tables 2 and 3 since the spectrum used in MACSI2 for Torsethaugen is generated form 39 frequency values while JONSWAP is generated from 30.
- The minimum wire tension from the time history.
- The largest absolute value of the maximum and minimum crane motion vertical velocity.
- The maximum 2 hours crane tip vertical displacement amplitude.
- The maximum 2 hours wire tension amplitude.

12. Slamming Analyses

The DNV methodology outlined in [10] is applied for the slamming analyses, both for over the side with crane and through moonpool lowering. In [10] lifting through wave zone analysis guidelines are given in order to get simple conservative estimates of the forces acting on the object. Since many analyses will be run and several assumptions are made this is good enough at this level of detail within the time frames given.

Following main assumptions are made by DNV for using the equations given. Their validity is also discussed.

- The horizontal extent of the lifted object in the wave propagation direction is relatively small compared to the wave length. The vessel is assumed to hold $0° \pm 30°$ wave heading and the horizontal extent of the structure is 12 [m] in x-direction. Rearranging the deepwater dispersion relationship gives wavelength as a function of wave period;

$$\lambda = \frac{2\pi}{g} T^2 \qquad\qquad \text{Equation 43}$$

  Minimum wave period T_p in the analyses is 7 [s] which gives a wave length of 31.4 [m]. Then the horizontal extent is relatively small compared to the wave length. On the other side, minimum T_z for Torsethaugen wave spectrum is 4.7 [s] for $H_s = 2.0$ [m] and $T_p = 7.0$ [s], see Table 2. If this value is inserted into Equation 43 the wave length is barely longer than the length of the object. One can hence argue that the assumption is invalid for shorter T_p values for both Torsethaugen and JONSWAP wave spectra depending on whether T_p or T_z are used.
- The vertical motion of the object follows the crane tip motion. To some extent will the module probably affect the crane tip motion as well, but this is assumed neglectable. The assumption also implies no resonance. For crane over the side lowering the natural period was estimated to $T_0 = 2.9$ [s] in Chapter 15 Results. Moonpool eigenperiod will be even lower as crane resilience is decreased for the module handing system compared to the crane system. The guideline given in [10] is that $T_p > 1.6T_0$ where the larger value of $1.6T_0$ is 4.6 [s] for the installation methods. This is hence ok. Note that the natural period of the water plug in the moonpool is 7.1 [s] without the lowered object, see Equation 39.
- The load case is dominated by the vertical relative motion between object and water – other modes of motions can be disregarded. As the module is just above MWL this assumption is ok. When waves pass parts of the module will be submerged. Horizontal forces will arise, but compared to the vertical force from slamming these forces are probably low and less important. Especially since the whole sale area is assumed affected by slamming at the same time instance to ensure conservatism.

Only slamming and static forces are regarded to assess whether slack slings is a problem as the module is above the MWL. Minimum wire tension = static wire tension – slamming impact

force. The varying buoyancy force, mass force correcting for added mass and drag force are disregarded due to the position of the unit. Slamming impact force:

$$F_{slam} = 0.5\rho_w C_s A_s v_s^2$$
Equation 44

C_s is a slamming coefficient set equal to 5.0, the minimum value recommended if no specific theoretical or experimental methods are used to determine it. A_s is the sail area, the area exposed to slamming loads. A_s is here assumed equal to the projected area of the unit in z-direction, $A_{mz} = 68.4 \, [m^2]$. The slamming impact velocity v_s must be calculated for each sea state as it varies with hook lowering velocity v_c, characteristic single amplitude vertical velocity of the crane tip v_{ct} and characteristic vertical water particle velocity v_w:

$$v_s = v_c + \sqrt{v_{ct}^2 + v_w^2}$$
Equation 45

From the design parameters given in [1] a hook lowering velocity of 0.5 [m/s] is targeted. This is therefore the hook lowering velocity used in the analyses. Crane tip velocities for the different sea states are extracted from the MACSI2 output files by using MATLAB. MATLAB is also the program where the slamming analyses are performed, see Chapter 14 MATLAB Scripts for details. The last value needed for computing slamming impact velocity and thus slamming force is vertical water particle motion.

For crane deployment vertical water particle velocity is computed from Equation 94, hence there is one value for each H_s and T_p. The T_z values to be used are the ones extracted from MACSI2 given in Tables 5 and 6. Note also that d in Equation 94, the distance form water plane to center of gravity of submerged part of object, is zero. For moonpool deployment the same formula cannot be used as the vertical moonpool water particle velocities naturally differ from those of the free surface. The method described in Chapter 10.2 Moonpool fluid flow is therefore used instead.

13.   Metocean Tool Box (MTB)

MTB is a computer program used by Shell to find metocean information, forecasts, statistics and criteria for design and operational planning considering areas of interest. Metocean is a contraction of the words meteorological and oceanographic and does hence not only include weather forecasts but also wave and current forecasts. The program is scripted in MATLAB but has a simple interface so the user sees dialog boxes only.

The part of the program where weather windows are treated is chosen. There MTB uploads a time history, a numerically modeled hindcast from 01.09.1957 to 31.12.2009 with a three hour time step. Data gathered at site is normally measured over a relatively short period, a period too short to generate long-term probabilities, threshold levels and accurate probability distributions of wind and wave parameters [21]. Therefore a hindcast is created which is the opposite of a forecast.

 The creation of the hindcast used in MTB was a joint industry project where the Norwegian Meteorological Institute reanalyzed meteorological and oceanographic observations from 01.09.1957 to 31.12.2009. A reanalyze is a rerun of the past using a subset of available observations and a fixed model setup and data assimilation scheme to minimize the drift in error statistics over the period [21]. Note that the hindcast has been extended after the publication of [21]. Past conditions are hence tried recreated as accurate as possible based on assimilation of observations. The hindcast used is a combined high-resolution atmospheric downscaling and wave hindcast based on an earlier reanalysis called ERA40.

Based on the hindcast and operation specifics like limiting H_s, T_p/T_z and operation reference period weather window statistics can be found. The wanted statistics are obtained from time histories like the one shown in Figure 30. In Figure 30 the time history covers January to March 2001 with operation limits $H_s = 2.8$ [m], $T_p = all$ and operation time 6 hours. The time history itself is the thin blue line while the weather windows where installation is possible are marked with a thicker line.
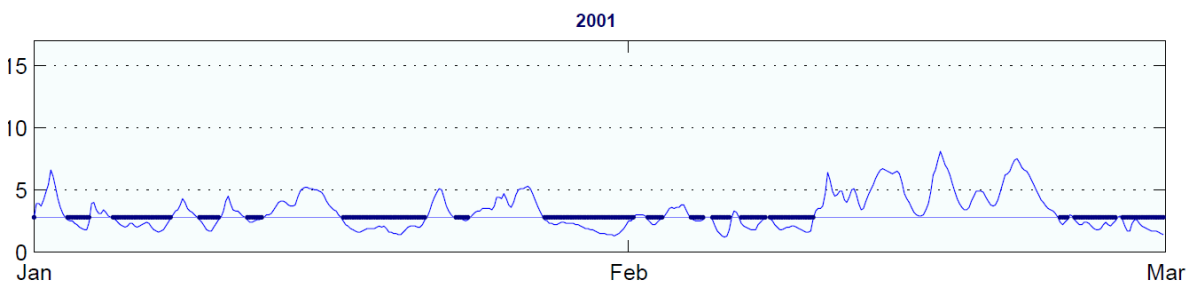
Figure 30: Time history example used to compute weather window statistics in MTB.

14. MATLAB Scripts

MATLAB scripts are programmed and used to:

- Generate sea state spectra JONSWAP or Torsethaugen. If Torsethaugen wave spectrum is chosen MACSI2 wave spectrum input files "HsTpYYYY" are generated.
- Gather and post-process analyses results from the MACSI2 output files for time instance 2, when the module is just submerged, both for over the side and moonpool deployment.
- Run slamming analyses. See Chapter 12. Slamming analyses for details.
- Plot resulting values for the following parameters as a function of H_s where each line represent a certain T_p. There is one figure for each wave heading.
  - Minimum wire tension for time instance 1: The lower value of
    - Static wire tension – maximum dynamic wire tension 2 hours amplitude.
    - Minimum wire tension from the time history.
  - Minimum wire tension for time instance 2: Static tension – slamming force
  - Vertical water particle velocity
  - Crane tip vertical velocity

An overview of how the different functions are connected through the main script "Main_file" is given in the flow chart in Figure 31. The diagram is to be read downwards and the rows are read from left to right. The MATLAB scripts are attached in Appendix 13 where also brief explanations of the functions are given.
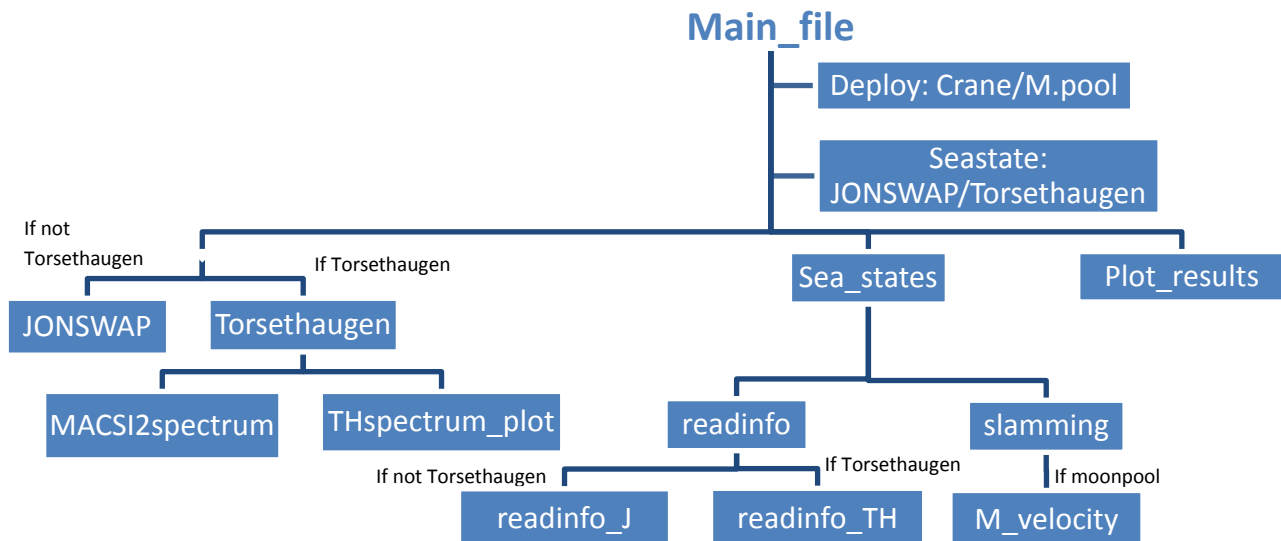
Figure 31: The system of the overall MATLAB script.

15.   Results

It must be noted that MACSI2 moonpool analyses cannot be run for all decided sea states. It is seen from Equation 39 that moonpool motion natural period is about $T_0 \approx 7.0$ [s]. The graphs given in Figure 27 is considering T, a single wave period or regular wave period. From MACSI2 results it seems like T is consistent with T_p because MACSI2 crashes for analyses with $T_p = 7$ [s]. No error message is given in the program but it is believed that it is due to numerical difficulties when resonance occurs which leads to large responses of the huge module. Also some high wave height makes the program crash. High wave heights leads to larger response even though T_p is further away from T_0.

JONSWAP wave spectrum can be run with most sea states at all wave headings except for $T_p = 7.0$ [s] and $H_s \geq 5.0$ [m]. Torsethaugen on the other hand can barely be run at all for wave headings 0° and 30° because all sea states are in the resonance region. A T_p value of 7.0 [s] equals a T_z value around 5.7 [s] considering both spectra, see Tables 5 and 6 below. T_z values for all Torstehaugen sea state are relatively close to 5.7 [s] compared to JONSWAP T_z values, and responses do therefore get much worse. It is therefore decided to use JONSWAP wave spectrum for moonpool analyses only, but it is compared with Torsethaugen results for 0° and 30° wave heading.

Natural periods of the lowered systems, module and wire rope, for both installation alternatives are calculated in Appendix 8, see Equations 103 and 104. Resulting values are:

- $T_{0_{crane}} = 2.9$ [s]
- $T_{0_{moonpool}} = 0.7$ [s]

15.1 T_z values for the wave spectra used in MACSI2

In MACSI2 a limited number of wave frequencies ω and wave spectrum values S(ω) are used to represent both wave spectra JONSWAP and Torsethaugen. The difference in T_z for the entire spectra based on a large amount of frequencies and the spectra for the limited number of frequencies are hence of interest to see how well the spectra are represented in MACSI2. Resulting T_z matrixes for the MACSI2 values are given in Tables 5 and 6 for Torsethaugen and JONSWAP wave spectra respectively. T_z values are not too far from the original T_z matrixes given in Tables 2 and 3. There is an increase for all T_z values in the MASCSI2 representation but taken into account that only 30 and 39 frequencies are used to represent the JONSWAP and Torsethaugen spectrum respectively the increase is not significant.

As the MACSI2 output is based on T_z values from the limited spectra in MACSI2 will MACSI2 T_z values also be used in the residual calculations for consistency.

T_p/H_s	2.00	2.50	3.00	3.50	4.00	4.50	5.00	5.50
7.00	5.32	5.43	5.53	5.63	5.72	5.79	5.91	5.97
9.00	6.36	6.26	6.25	6.29	6.34	6.47	6.53	6.65
11.00	6.97	7.23	7.30	7.33	7.43	7.38	7.41	7.40
13.00	6.98	7.20	7.52	7.70	7.94	8.14	8.23	8.38
15.00	6.90	7.08	7.43	7.53	7.82	7.93	8.15	8.36
17.00	6.84	7.00	7.29	7.50	7.76	8.09	8.25	8.53

Table 5: Tz values for the MACSI2 limited Torsethaugen wave spectrum.

T_p/H_s	2.00	2.50	3.00	3.50	4.00	4.50	5.00	5.50
7.00	5.71	5.71	5.71	5.71	5.71	5.71	5.71	5.71
9.00	7.34	7.34	7.34	7.34	7.34	7.34	7.34	7.34
11.00	8.97	8.97	8.97	8.97	8.97	8.97	8.97	8.97
13.00	10.60	10.60	10.60	10.60	10.60	10.60	10.60	10.60
15.00	12.23	12.23	12.23	12.23	12.23	12.23	12.23	12.23
17.00	13.87	13.87	13.87	13.87	13.87	13.87	13.87	13.87

Table 6: Tz values for the MACSI2 limited JONSWAP wave spectrum.

15.2 Vertical water particle velocities

Vertical water particle velocities are computed for both the free surface and in the moonpool. For the free surface Equation 94 is used while the method outlined in Chapter 10.2 Moonpool fluid flow is used for finding vertical water particle velocity in the moonpool. Vertical water particle velocities are given below in Figures 32-34 plotted against H_s where each graph represents a certain T_p. The free surface vertical water particle velocities do not change with heading such as the velocities in the moonpool. Therefore moonpool vertical water particle velocity is given for both heading 0⁰ and 90⁰. First free surface vertical water particle velocity figures are given for both spectra, then moonpool results are shown for two wave headings.

Note that moonpool water particle velocity is calculated based on the RAOs of the water plug elevation to the wave elevation. Results for 0⁰ and 90⁰ wave headings can be seen in Figure 27. An error source to the computed water particle velocities is that the graphs used are as shown in Figure 27 T_p dependent as T_p is taken as T. Instead graphs should be transformed into T_z dependent graphs. T_z is more representative for an irregular sea state than T_p, especially for Torsethaugen wave spectrum. If the graphs had been transformed and RAOs extracted based on T_z water particle velocities for Torsethaugen would be much higher as all T_z values are quite close to the resonance T_z. This is therefore an error source in calculations where moonpool water particle vertical velocity is used, as for example in the moonpool slamming analyses.

In the following figures water particle velocities calculated based on JONSWAP are given to the left while Torsethaugen results are given to the right. If only one plot is given in a figure the results are based on the JONSWAP wave spectrum.
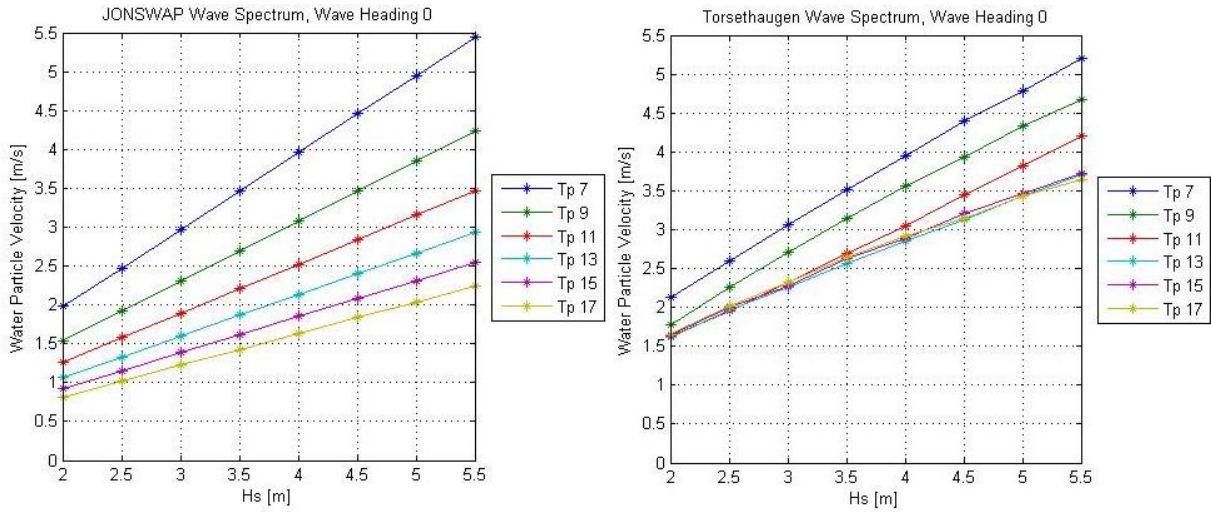
Figure 32: Free surface vertical water particle velocity. Wave heading is irrelevant.
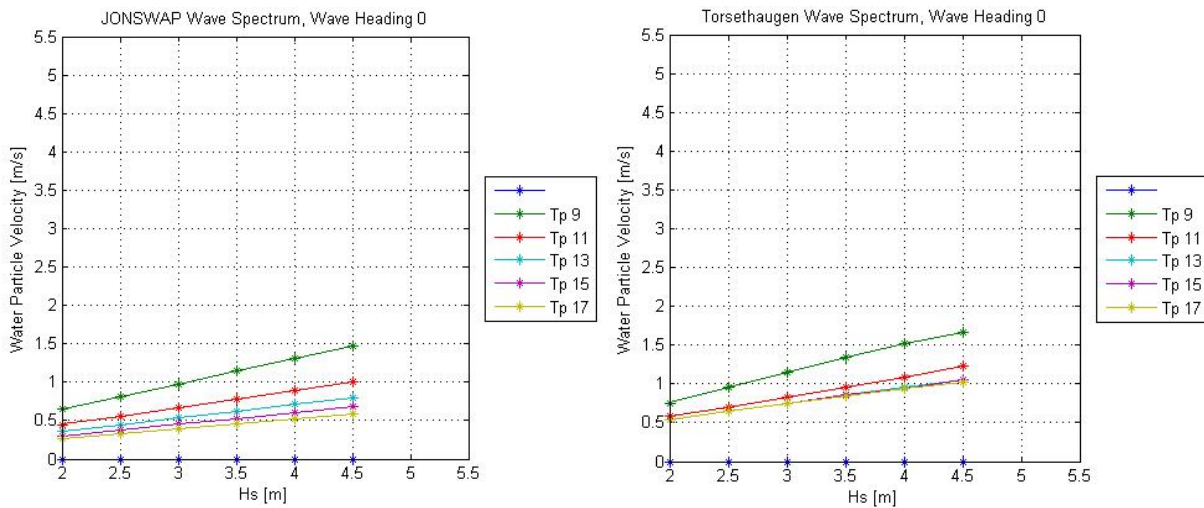
Figure 33: Moonpool vertical water particle velocity, wave heading 0°.
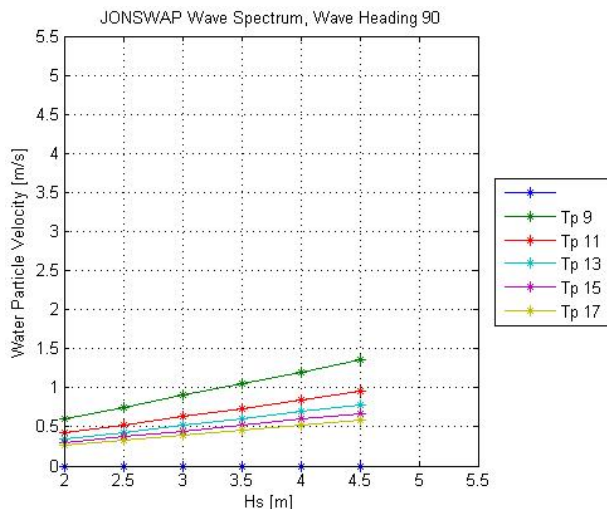
Figure 34: Moonpool vertical water particle velocity, wave heading 90⁰.

15.3 Vertical crane tip motion amplitude

Some of the estimated 2 hours vertical crane tip motion amplitudes are extracted from the MACSI2 output files. They can to a certain degree tell something about the ship transfer functions. Note that crane tip motion is also used when talking about the vertical motion of the sheave in the top of the MHT. Crane tip motions are extracted to see how the ship responds at different locations to different sea states. The response is of interest as the body lowered is set to follow the crane tip motion. There will be a phase angle between these motions. This will hence only give an indication of whether the results seem correct or not. It must also be remembered that hydrodynamic forces are driving as well, and they are dependent on water particle velocity.

In Table 7 results are given for the 2 hours estimated crane tip motion amplitude in meters.

Wave heading	Crane over the side		Crane over the side		Moonpool	
	JONSWAP		**Torsethaugen**		**JONSWAP**	
	$H_s = 2.5$ [m] $T_p = 9$ [s]	$H_s = 2.5$ [m] $T_p = 13$ [s]	$H_s = 2.5$ [m] $T_p = 9$ [s]	$H_s = 2.5$ [m] $T_p = 13$ [s]	$H_s = 2.5$ [m] $T_p = 9$ [s]	$H_s = 2.5$ [m] $T_p = 13$ [s]
0⁰	1.78	2.28	1.52	1.88	0.78	1.67
30⁰	1.65	2.93	1.51	2.34	0.95	1.79
60⁰	2.10	3.61	2.00	2.93	1.80	2.16
90⁰	2.54	3.92	2.34	3.15	2.62	2.48
120⁰	2.80	4.11	2.53	3.21	1.78	2.16
150⁰	2.25	3.48	2.03	2.57	0.96	1.80
180⁰	1.53	2.21	1.31	1.77	0.75	1.67

Table 7: 2 hours estimated crane tip motion amplitude in meters extracted from MACSI2 output files.

15.4 Vertical crane tip velocity

As crane tip velocity is of importance for the slamming impact velocity v_s, see Equation 45, crane tip velocity plots are given below in Figures 35 to 38. Note that crane tip velocity is also used when talking about the vertical velocity of the sheave at the top of the MHT. Each figure is given for a specific wave heading where crane tip vertical velocity is plotted against H_s for the different T_p values. Maximum crane tip vertical velocities for over the side deployment are obtained at wave heading 120⁰ for both JONSWAP and Torsethaugen spectra for all T_p values except from $T_p = 7$ [s], Torsethaugen. For moonpool deployment largest velocities are obtained at wave heading 90⁰ for all T_p values. Below maximum crane tip vertical velocity plots are given for both deployment methods. Crane deployment over the side results are given for wave headings 30⁰ and 120⁰ which are the most critical headings for weather window statistics and overall. Moonpool results are given for wave headings 30⁰ and 90⁰ for the same reasons.

Vertical crane velocity plots based on JONSWAP are given to the left while Torsethaugen plots are given to the right in the following figures. If only one plot is given in a figure the results are based on the JONSWAP wave spectrum.
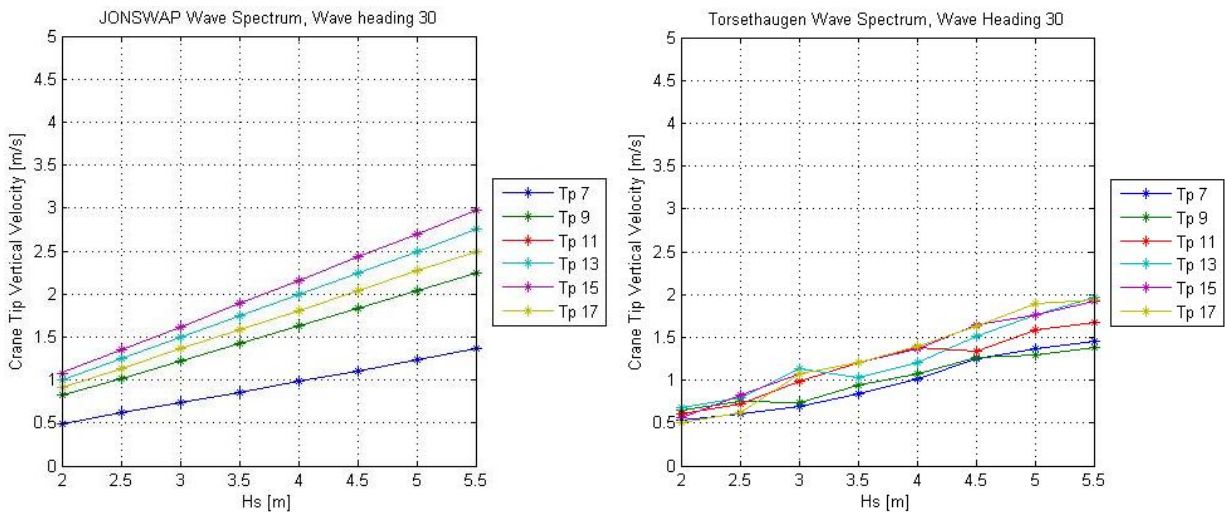
Figure 35: Crane tip vertical velocity considering crane installation over the side, wave heading 30⁰.
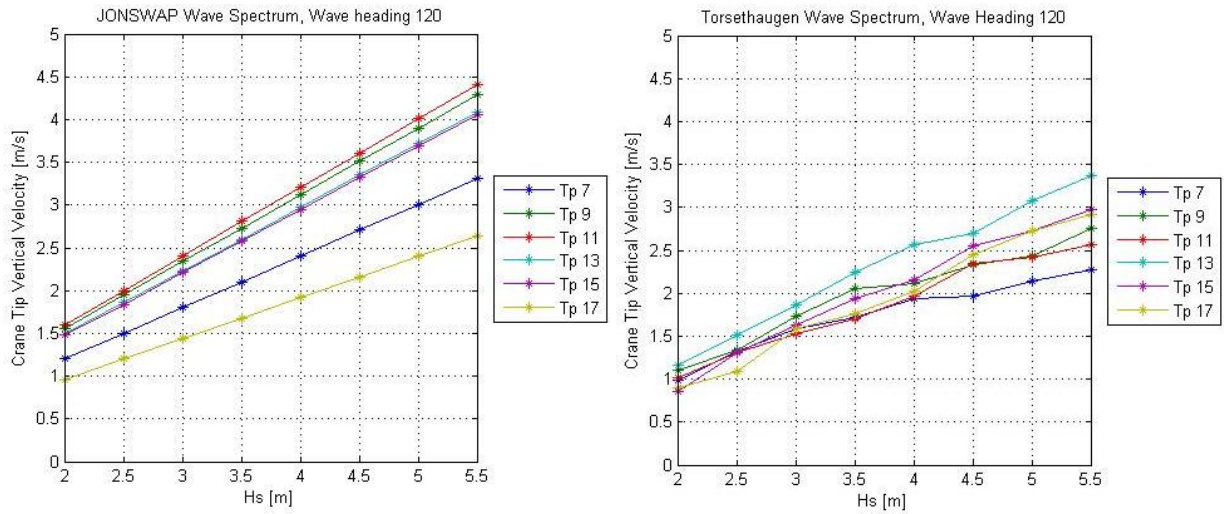
Figure 36: Crane tip vertical velocity considering crane installation over the side, wave heading 120º.
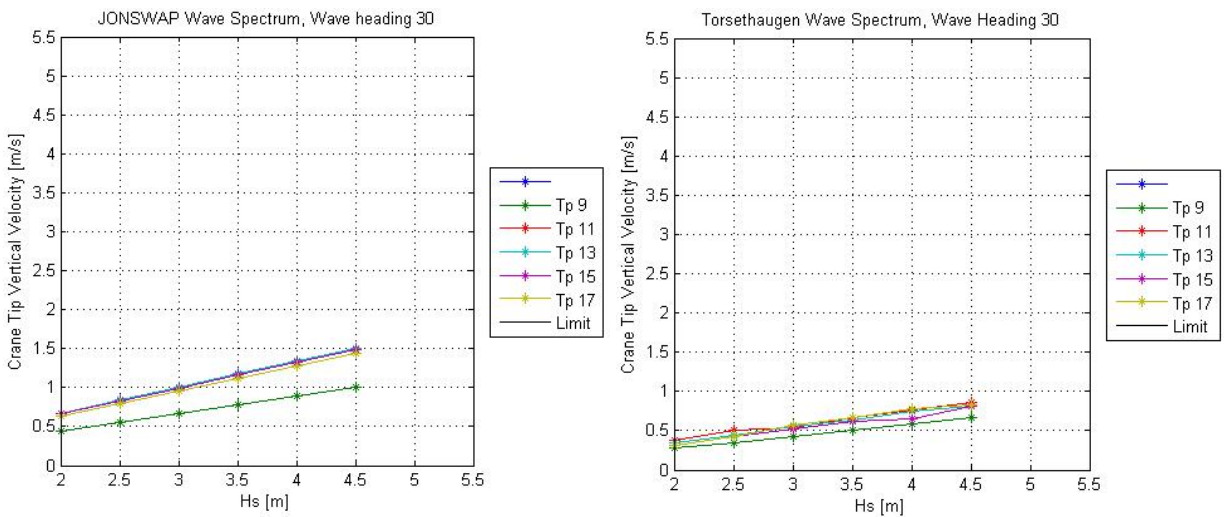
Figure 37: Crane tip vertical velocity considering through moonpool installation, wave heading 30º.
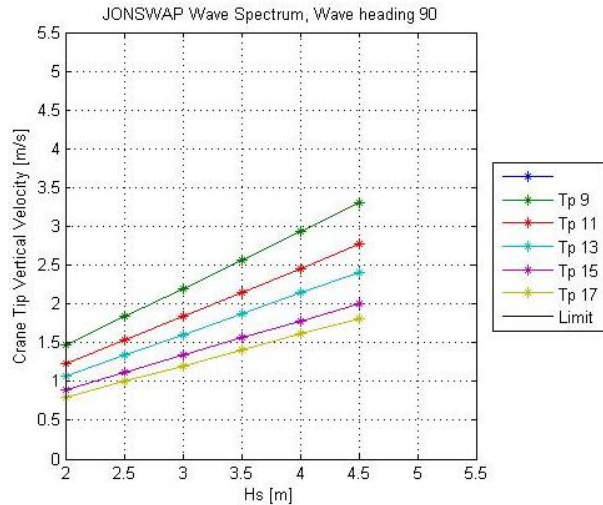
Figure 38: Crane tip vertical velocity considering through moonpool installation, wave heading 90⁰.

15.5 Minimum wire tension

Below results of minimum wire tension are given for both deployment methods and time instances. For time instance 1 the minimum wire tension equals the static tension in the wire minus the slamming force. For time instance 2 the minimum wire tension equals the minimum value of:

- Static tension in wire minus dynamic tension. Dynamic tension equals the 2 hours wire tension amplitude calculated in MACSI2.
- Minimum wire tension directly from the time history of the MACSI2 analyses.

Time instance 1 is when the module is just at the MWL and slamming is critical. Time instance 2 is when the module is statically placed with its top end 0.5 [m] below MWL. First results considering deployment over the side with crane are given. See Figures 39-46. Then the outcome of through moonpool deployment are listed in Figures 47-52. Minimum wire tension is plotted against H_s in seven graphs where each graph represents a T_p value. Results for wave headings 0⁰ and 30⁰ are given here as ships normally do such installations with head seas, hence 0⁰ wave heading. Then DP is used, but in case some drift is experienced also 30⁰ wave heading is accounted for. In addition minimum wire tension for wave headings 90⁰ and 120⁰ are given for crane deployment over the side. For moonpool deployment minimum wire tension for wave heading 90⁰ is given. That is because these headings are found to be the overall most critical wave headings when it comes to reducing design H_s for the specific deployment methods.

Critical H_s for the installation considering each T_p and wave heading is taken as the lower H_s value for which the T_p curves cross the slack slings limit given as the black solid line in the

figures. The critical H_s is called design H_s. In some of the figures the T_p lines are above the slack sling limit for all H_s, hence slack slings is not a problem. Then design H_s is set equal to 5.5 [m] which is the upper H_s value for which analyses are run, or 4.5 [m] for moonpool analyses. In other graphs some of the T_p lines are below the slack sling limit for all H_s. Then design H_s is set equal to 2.0 [m] which is the lower H_s value for which analyses are run.

Also here JONSWAP results are given to the left and Torsethaugen to the right. Note that plots for the residual wave headings considered in the report are given in Appendix 14.

- Crane lowering, time instance 1:
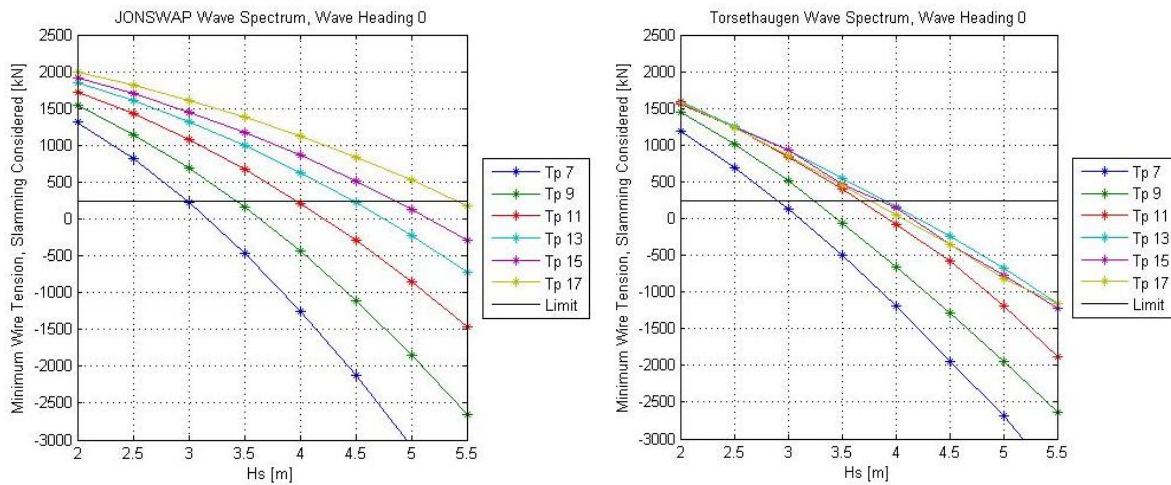
Figure 39: Crane deployment. Minimum wire tension [kN] for JONSWAP and Torsethaugen wave spectra, wave heading 0° at time instance 1.
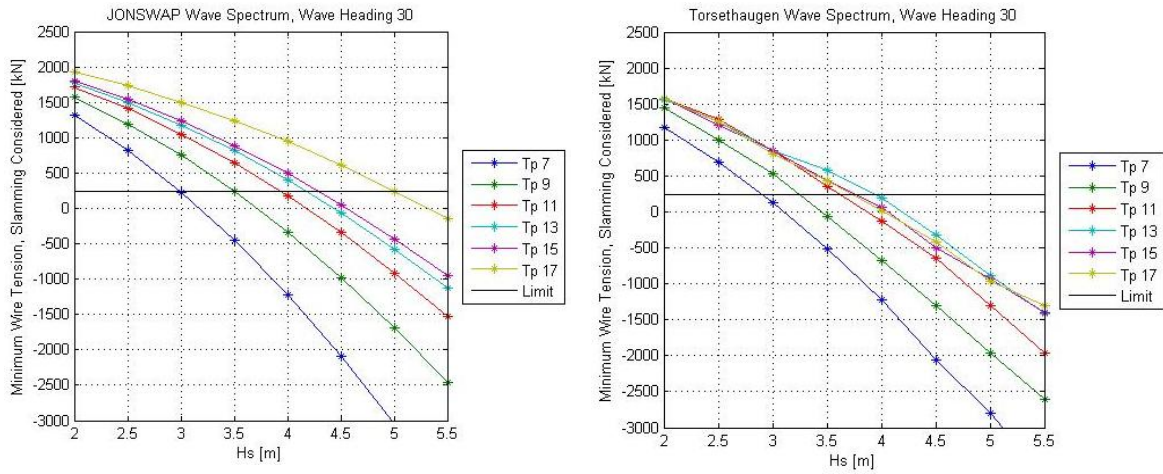
Figure 40: Crane deployment. Minimum wire tension [kN] for JONSWAP and Torsethaugen wave spectra, wave heading 30⁰ at time instance 1.

Figure 41: Crane deployment. Minimum wire tension [kN] for JONSWAP and Torsethaugen wave spectra, wave heading 90⁰ at time instance 1.
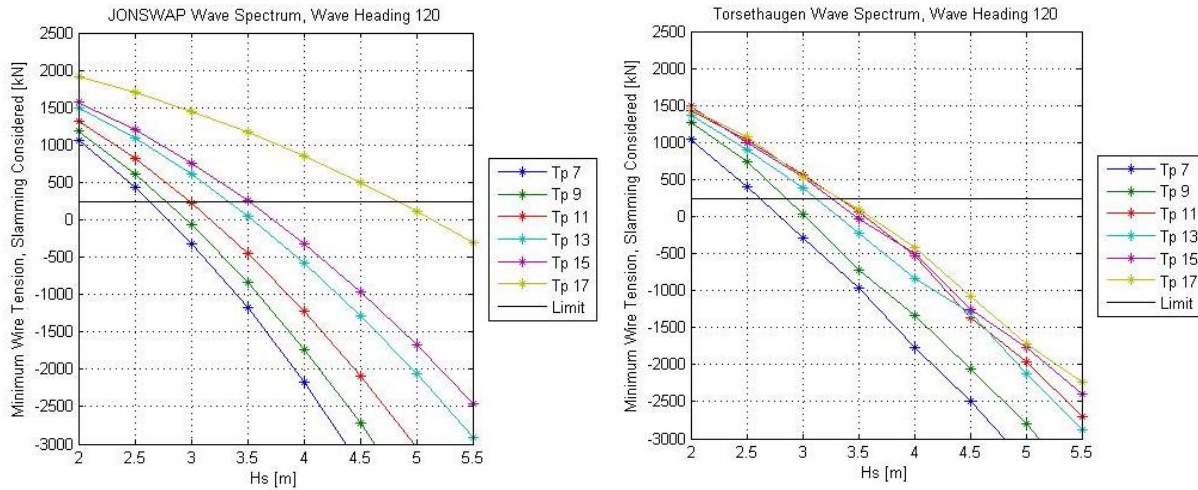
Figure 42: Crane deployment. Minimum wire tension [kN] for JONSWAP and Torsethaugen wave spectra, wave heading 120º at time instance 1.

- Crane lowering, time instance 2:
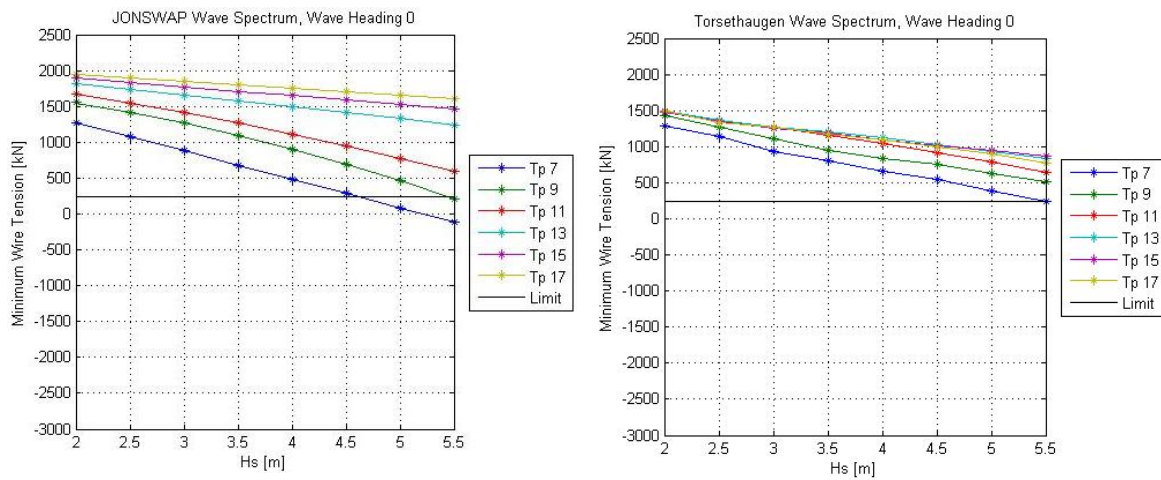
Figure 43: Crane deployment. Minimum wire tension [kN] for JONWAP and Torsethaugen wave spectra, wave heading 0º at time instance 2.
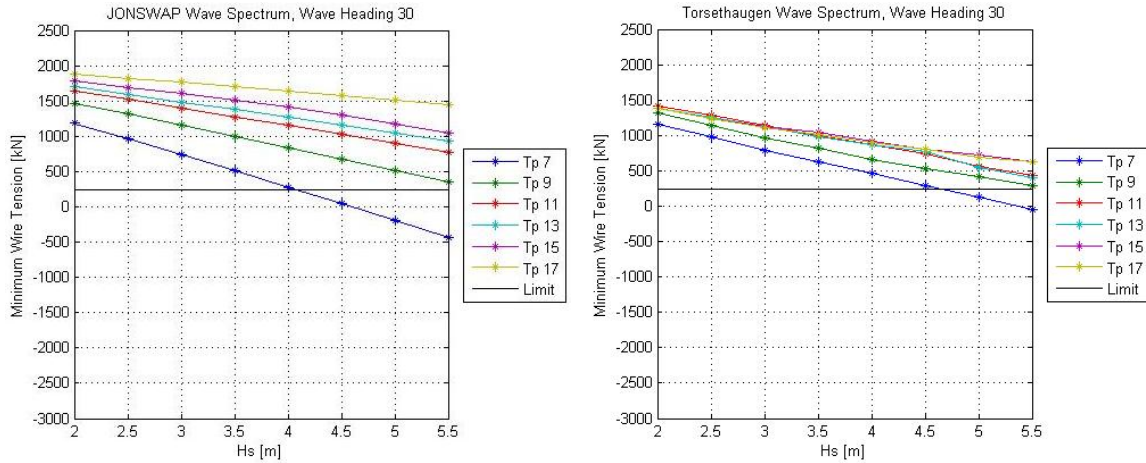
Figure 44: Crane deployment. Minimum wire tension [kN] for JONWAP and Torsethaugen wave spectra, wave heading 30⁰ at time instance 2.

Figure 45: Crane deployment. Minimum wire tension [kN] for JONWAP and Torsethaugen wave spectra, wave heading 90⁰ at time instance 2.
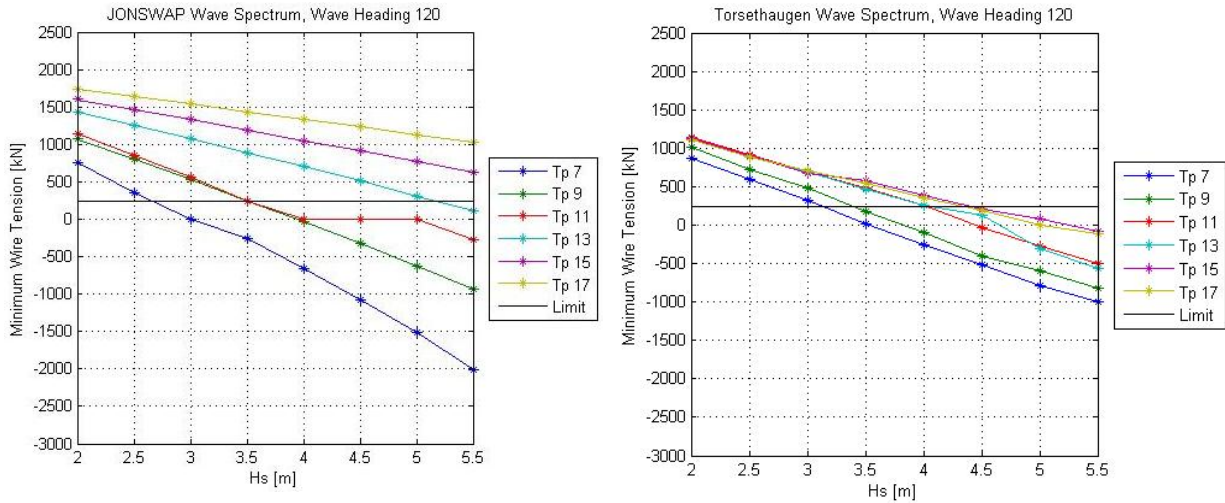
Figure 46: Crane deployment. Minimum wire tension [kN] for JONWAP and Torsethaugen wave spectra, wave heading 120° at time instance 2.

- Moonpool lowering, time instance 1:
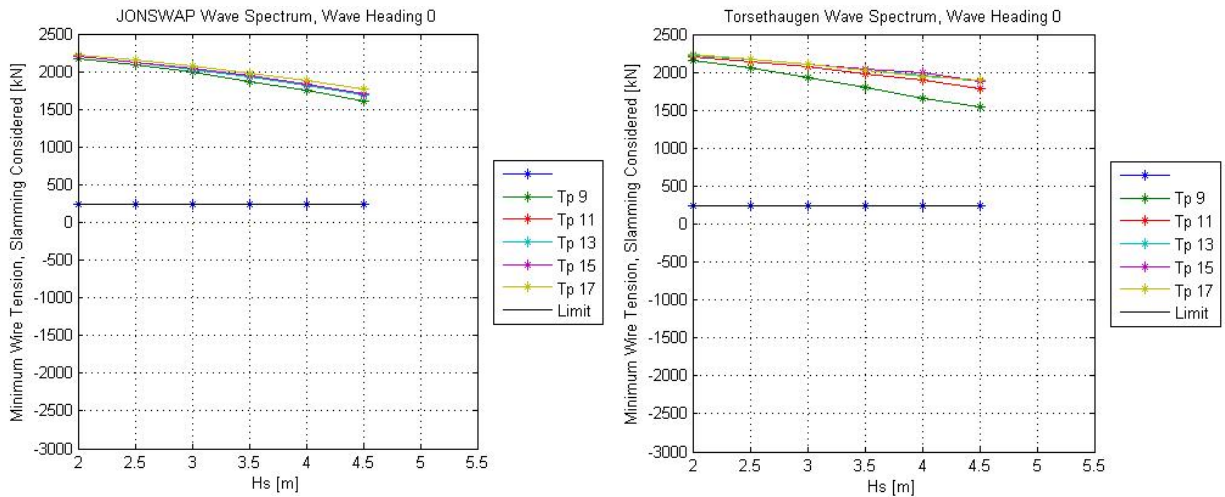
Figure 47: Moonpool deployment. Minimum wire tension [kN] for JONSWAP and Torsethaugen wave spectra, wave heading 0° at time instance 1.
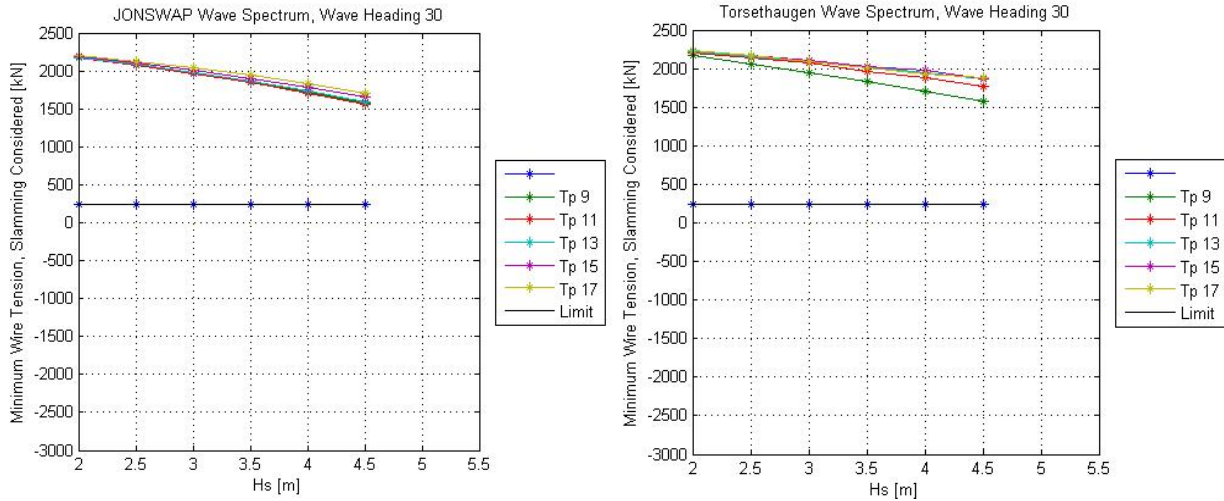
Figure 48: Moonpool deployment. Minimum wire tension [kN] for JONSWAP and Torsethaugen wave spectra, wave heading 30⁰ at time instance 1.

Figure 49: Moonpool deployment. Minimum wire tension [kN] for JONSWAP wave spectrum, wave heading 90⁰ at time instance 1.

- Moonpool lowering, time instance 2:
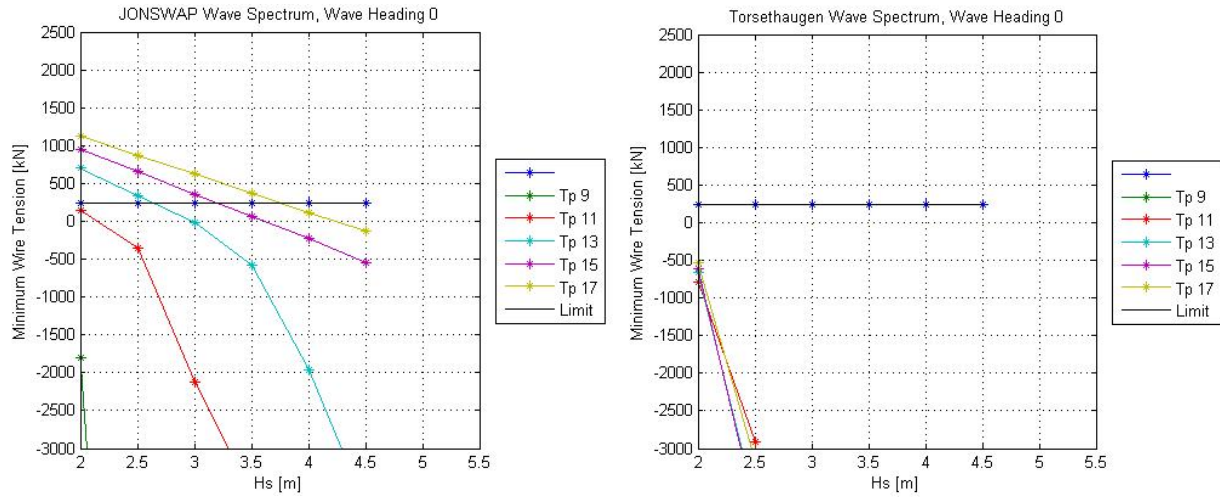
Figure 50: Moonpool deployment. Minimum wire tension [kN] for JONSWAP and Torsethaugen wave spectra, wave heading 0° at time instance 2.
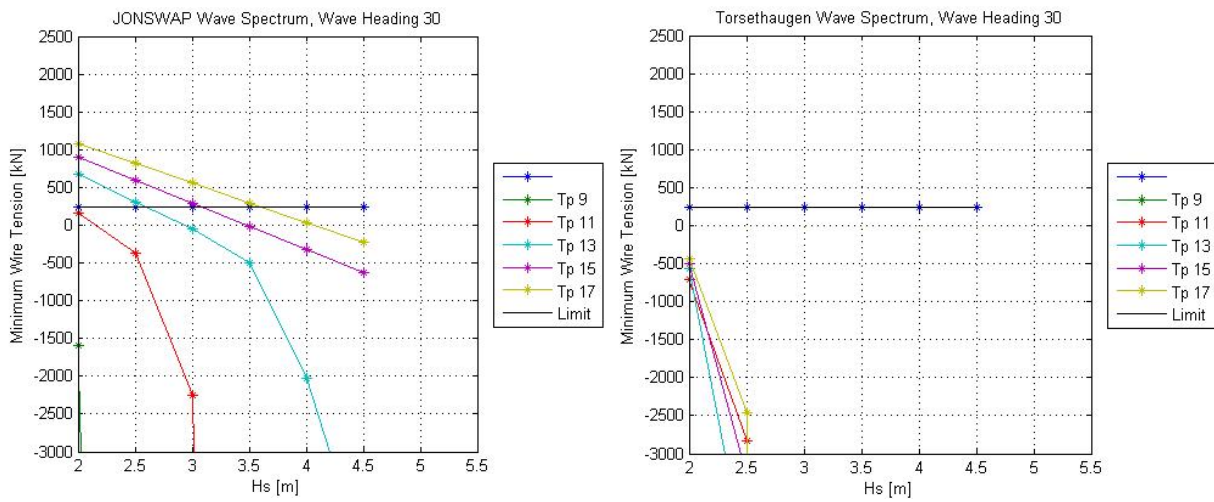
Figure 51: Moonpool deployment. Minimum wire tension [kN] for JONSWAP and Torsethaugen wave spectra, wave heading 30° at time instance 2.
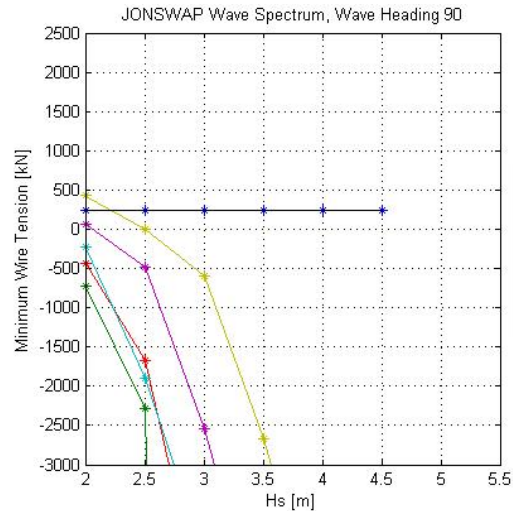
Figure 52: Moonpool deployment. Minimum wire tension [kN] for JONSWAP wave spectrum, wave heading 90⁰ at time instance 2.

15.6 Sensitivity checks

Sensitivity is checked for the hydrodynamic parameters and the total stiffness of the system. Note that only JONSWAP wave spectrum is used as the changes are assumed similar for Torsethaugen. Added mass and hence added mass coefficients, linear and quadratic drag coefficients and crane system stiffness are changed in the MACSI2 input file one at the time holding the other input variables as presented earlier in the report. The effect of change for each variable can hence be discovered.

The sensitivity checks will only affect time instance 2 results. When calculating the uplift at time instance 1 only crane tip velocity and water particle velocity changes with sea state. None of them are affected by changing added mass, drag nor crane stiffness. In addition checks are only performed for crane lowering as hydrodynamic parameters are more unaffected by boundaries here than in a moonpool. It will therefore be easier to see the effect of change. Besides moonpool results are already a bit uncertain due to MACSI2 assuming the water flow in the moonpool to be unaffected by the lowered object.

Wave headings 30⁰ and 120⁰ are used in the sensitivity analyses. That is because wave heading 30⁰ is most critical for the weather window analyses while wave heading 120⁰ is one of the overall most critical wave headings. The following changes are made to the MACSI2 input:

- Added mass, Figure 54:

Added mass values for the directions of translation are quite high, almost twice the module static weight in air in x- and z-direction and even higher in y-direction. See Chapter 9.1.1 Added mass. They are neither reduced for perforation nor oscillating flow. These factors might in reality

reduce the added mass and lower values are therefore used in the sensitivity check. Added mass values equal to the modules static weight in air is applied in x- and z-direction. Added mass in y-direction is found by using the same reduction factor as used in x- and z-direction. This factor equals $431.8\ [t]/250.0\ [t] = 1.73$. New values are then:

$$A_x = 250\ [t] \rightarrow C_{Ax} = \frac{A_x}{\rho_w V_m} = 7.66$$

$$A_y = 671\ [t] \rightarrow C_{Ay} = \frac{A_y}{\rho_w V_m} = 20.55$$

$$A_z = 250\ [t] \rightarrow C_{Az} = \frac{A_z}{\rho_w V_m} = 7.66$$

- Total crane system stiffness, Figure 55:

Total stiffness of the lifting system comprises of the wire stiffness and the total crane system stiffness. It will be time consuming to find a new lifting wire and hence wire stiffness for checking the sensitivity. The crane system stiffness on the other hand is uncertain and only based upon values given for a different crane than the crane considered in this report. See Equation 34. Crane pedestal, cylinder and boom stiffness are given but how they change with crane capacity is unknown. In addition other stiffness can be added, for example rigging stiffness. All together it is hard to say how correct the applied crane stiffness is. In worst case it is too high giving a smaller natural period than what actually will be the case. Reduced crane system stiffness is therefore applied to check the sensitivity. There are few values to base the sensitivity estimate on but instead of $k_{crane} = 3.46 \cdot 10^6$ [N/m] $k_{crane} = 2.0 \cdot 10^6$ [N/m] is used, which is almost half the original value.

- Linear and quadratic drag, Figures 56 and 57:

For the undisturbed fluid minimum and maximum KC numbers are calculated in Equations 99 and 100, $KC_{min} = 0.3$ and $KC_{max} = 4.4$. This makes linear drag insignificant according to Figure 2.1 in [37] since quadratic drag will dominate due to the oscillating flow. Linear drag will therefore be set equal to zero to see whether that affects the results obtained by fixing it to 0.2 as recommended [15].

In the analyses relatively high quadratic drag coefficients are used for all three directions of translation. Even if preliminary analyses were run for wave heading 0° with quadratic drag coefficients equal to 2.0 and 2.9 with almost no effect on the results new analyses are run to check sensitivity. Also here the quadratic drag coefficients will be set equal to 2.0. This is a smaller value than the one originally used. It is also in the mid-range between the minimum C_d value of 1.78 estimated by using the KC-C_d graph in Figure 78 and by DNV methods setting the KC correction factor equal to 2, $C_d = 2.32$. See Appendix 8.

Minimum wire tension figures from the sensitivity analyses considering wave headings 30° and 120° are given below in the same order as changes are discussed. Results for wave heading 30° are to the left while results for wave heading 120° are to the right. The original results are given first in Figure 53 to ease the comparison.
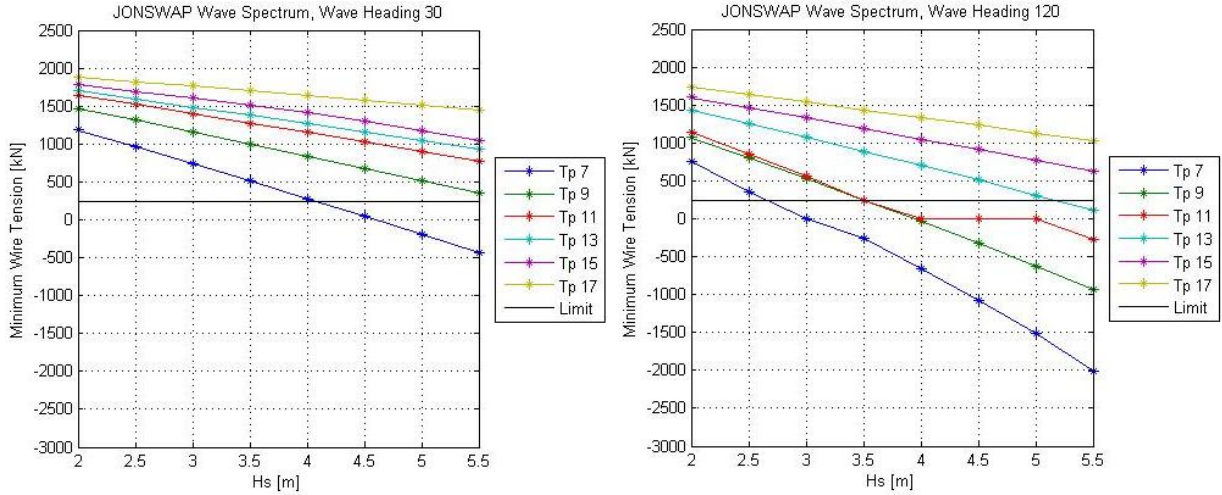
Figure 53: Original results for minimum wire tension, crane deployment at time instance 2.
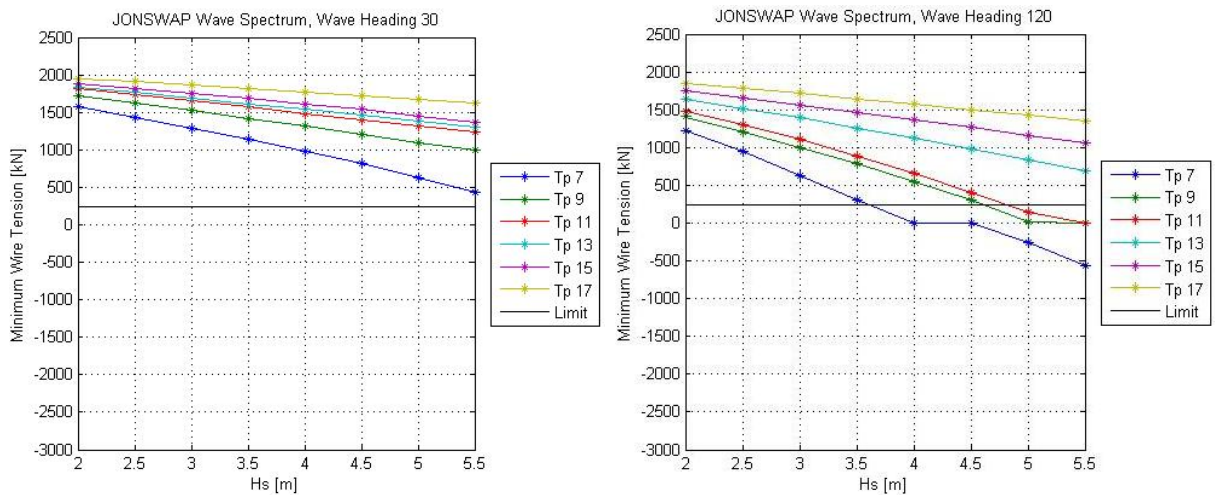
Figure 54: Added mass sensitivity check, crane deployment at time instance 2.
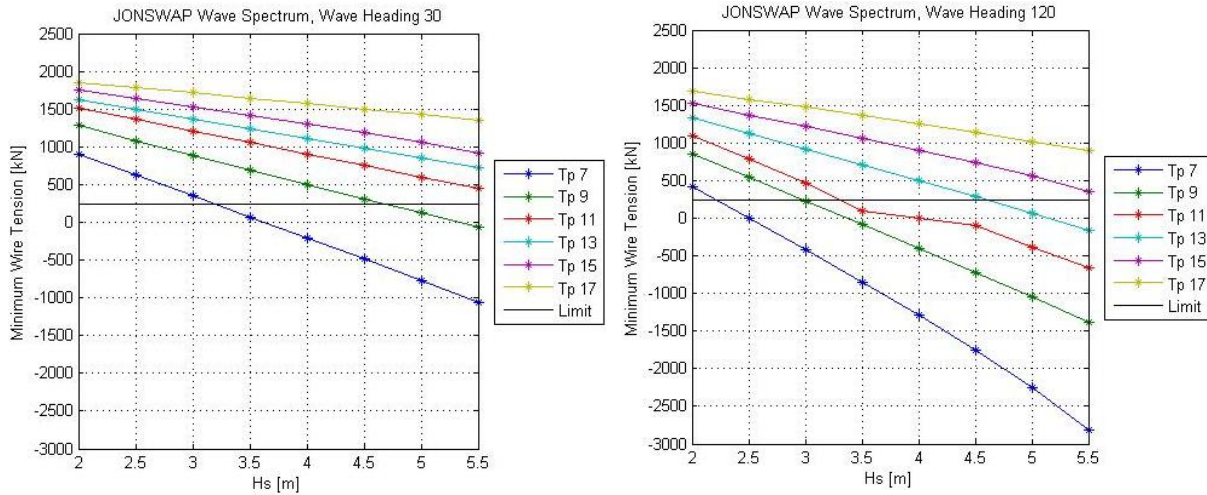
Figure 55: Stiffness sensitivity check, crane deployment at time instance 2.
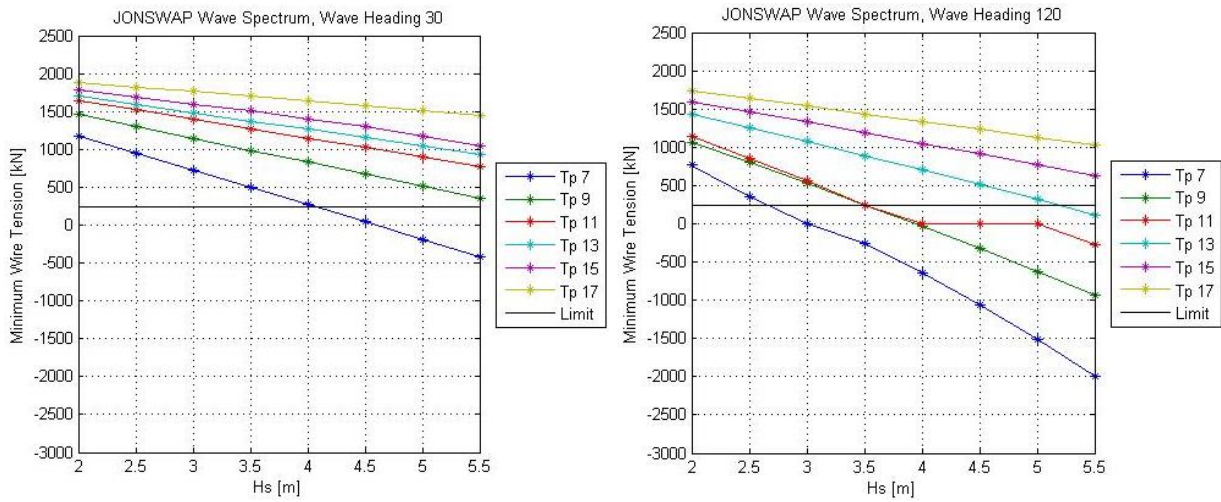
Figure 56: Neglecting linear drag to check sensitivity, crane deployment at time instance 2.
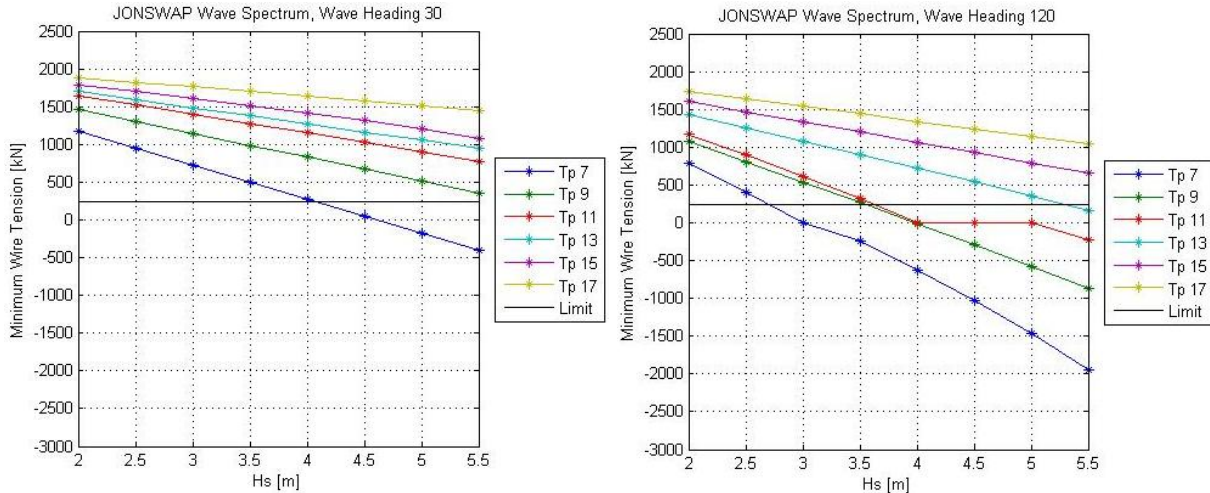
Figure 57: Quadratic drag sensitivity check, crane deployment at time instance 2.

15.7 Operability rosettes

In this report design H_s is taken as the limiting operational environmental criterion since that is the only factor listed in [9] which is looked into in this report. Operational limiting criterion is in [9] defined as less than or equal to the minimum value of:

- The environmental design criteria.
- Maximum wind and waves for safe working or transfer conditions of personnel.
- Equipment (for example ROVs or cranes) specified weather conditions.
- Limiting weather conditions for diving system, if any.
- Limiting weather conditions for position keeping systems.
- Any limitations identified based on operational experience with involved vessel, equipment, etc.
- Weather limitations for carrying out indentified contingency plans.

It is of interest to see the change in operation limit, hence design H_s, for the different T_p values used. Operability rosettes are therefore created. The circles represent H_s, colored lines T_p and wave headings are marked by straight lines. In the operability rosettes design H_s is plotted for all wave headings and T_p figures used in the analyses. Operability rosettes are given in Figures 58-61. Tables 8-11 contain the design H_s for each T_p and wave heading where slack slings become a problem and are the tables from which the operability rosettes are plotted. There are four operability rosettes, one for each installation method and time instance. The design H_s in the operability rosettes is the minimum value of JONSWAP and Torsethaugen wave spectra. Separate operability rosettes for JONSWAP and Torsethaugen for deployment with crane at time instance 2 can be seen in Appendix 15.

It should be noted that the overall design H_s, hence the overall lowest H_s for which deployment is safe irrelevant of T_p value, for wave headings $0^o \pm 30^o$ is used in the weather window analyses for conservatism.

Crane over the side, time instance 1.

Heading [°]/ Tp [s]	7	9	11	13	15	17
0	2,9	3,2	3,7	3,9	3,8	3,8
30	2,9	3,2	3,6	3,9	3,7	3,7
60	2,7	3	3,4	3,4	3,4	3,4
90	2,7	2,9	3,3	3,2	3,2	3,2
120	2,6	2,8	3	3,1	3,2	3,2
150	2,8	3,1	3,2	3,4	3,5	3,5
180	2,9	3,2	3,7	3,9	3,9	3,9
210	2,8	3,1	3,2	3,4	3,5	3,5
240	2,6	2,8	3	3,1	3,2	3,2
270	2,7	2,9	3,3	3,2	3,2	3,2
310	2,7	3	3,4	3,4	3,4	3,4
330	2,9	3,2	3,6	3,9	3,7	3,7

Table 8: Design H_s [m] for crane installation. Time instance 1 is considered and results are based on JONSWAP and Torsethaugen wave spectra.
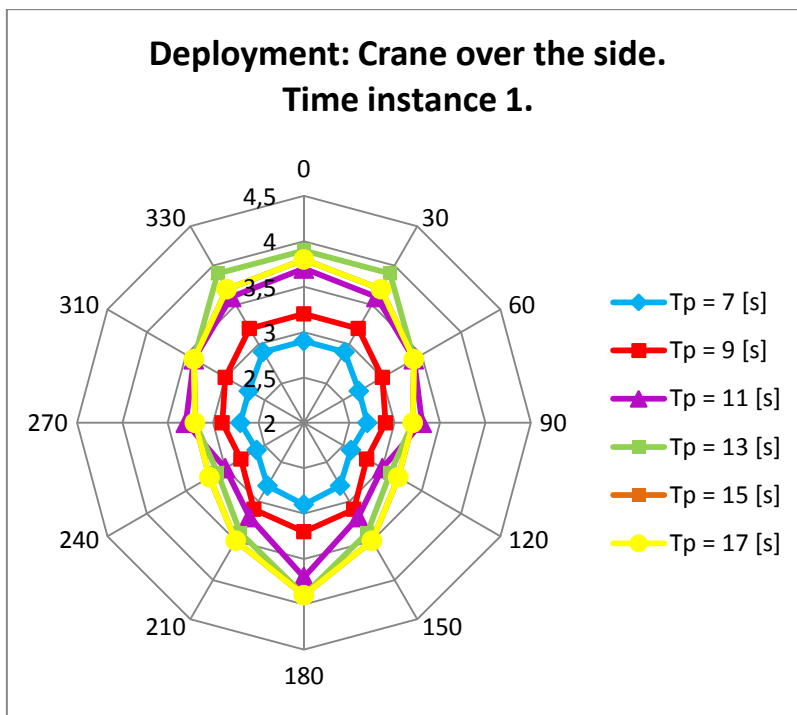
Figure 58: Operability rosette for crane deployment at time instance 1. Plot of design H_s given in Table 8. The circles represent design H_s from 2.0 – 4.5 [m].

Crane over the side, time instance 2.

Heading [º]/ Tp [s]	7	9	11	13	15	17
0	4,6	5,4	5,5	5,5	5,5	5,5
30	4,1	5,5	5,5	5,5	5,5	5,5
60	2,5	3	3,9	4,2	4,2	4,2
90	2,5	2,7	3,8	3,8	4,1	4,2
120	2,7	3,4	3,5	4	4,4	4,4
150	4,4	5,2	5,5	5,5	5,5	5,5
180	5,5	5,5	5,5	5,5	5,5	5,5
210	4,4	5,2	5,5	5,5	5,5	5,5
240	2,7	3,4	3,5	4	4,4	4,4
270	2,5	2,7	3,8	3,8	4,1	4,2
310	2,5	3	3,9	4,2	4,2	4,2
330	4,1	5,5	5,5	5,5	5,5	5,5

Table 9: Design H_s [m] for crane installation. Time instance 2 is considered and results based on JONSWAP and Torsethaugen wave spectra are used.
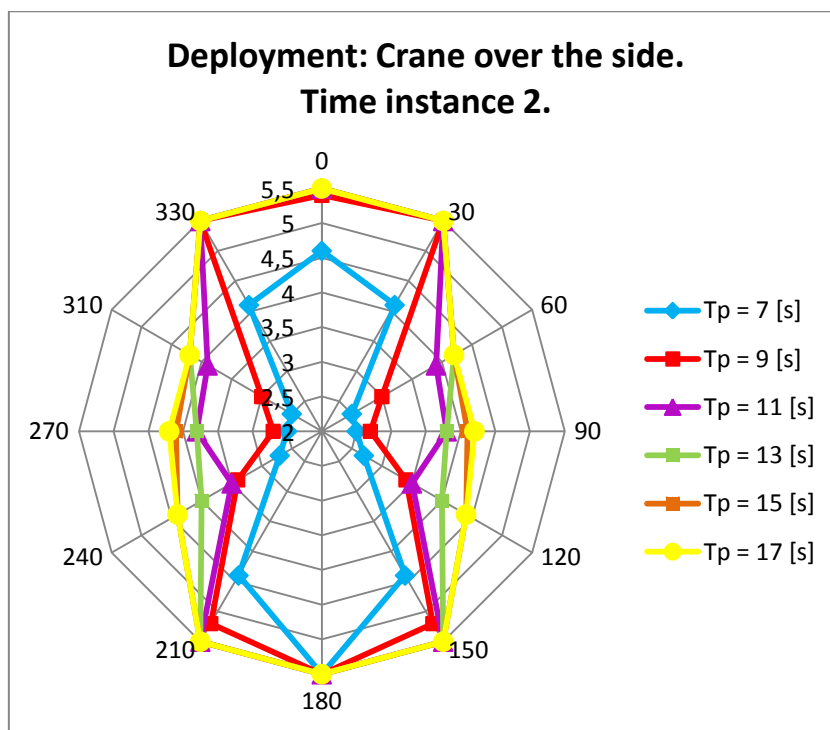
Figure 59: Operability rosette for crane deployment at time instance 2. Plot of design H_s given in Table 9. The circles represent design H_s from $2.0 - 5.5$ [m].

Through moonpool, time instance 1.

Heading [º]/ Tp [s]	9	11	13	15	17
0	4,5	4,5	4,5	4,5	4,5
30	4,5	4,5	4,5	4,5	4,5
60	4,5	4,5	4,5	4,5	4,5
90	3,8	4,5	4,5	4,5	4,5
120	4,5	4,5	4,5	4,5	4,5
150	4,5	4,5	4,5	4,5	4,5
180	4,5	4,5	4,5	4,5	4,5
210	4,5	4,5	4,5	4,5	4,5
240	4,5	4,5	4,5	4,5	4,5
270	3,8	4,5	4,5	4,5	4,5
310	4,5	4,5	4,5	4,5	4,5
330	4,5	4,5	4,5	4,5	4,5

Table 10: Design H_S [m] for moonpool installation. Time instance 1 is considered and results based on JONSWAP and Torsethaugen wave spectra are used.
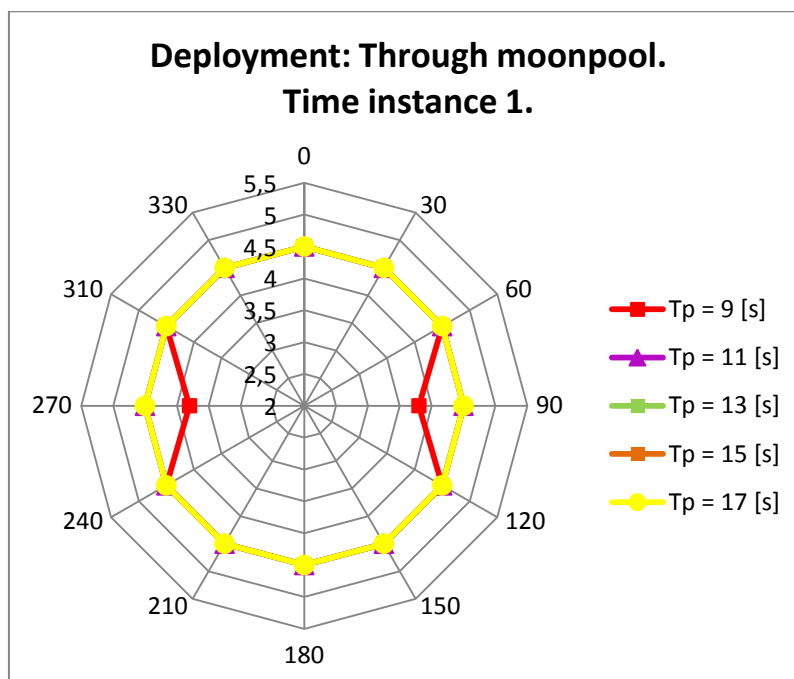
Figure 60: Operability rosette for moonpool deployment at time instance 1. Plot of design H_S given in Table 10. The circles represent design H_S from 2.0 – 5.5 [m].

Trough moonpool, time instance 2.

Heading [º]/ Tp [s]	9	11	13	15	17
0	2	2	2,6	3,2	3,7
30	2	2	2,6	3,1	3,5
60	2	2	2,1	2,4	2,9
90	2	2	2	2	2,2
120	2	2	2,4	2,6	3,1
150	2	2	2,5	3	3,5
180	2	2	2,5	3	3,6
210	2	2	2,5	3	3,5
240	2	2	2,4	2,6	3,1
270	2	2	2	2	2,2
310	2	2	2,1	2,4	2,9
330	2	2	2,6	3,1	3,5

Table 11: Design H_s [m] for moonpool installation. Time instance 2 is considered and results based on JONSWAP and Torsethaugen wave spectra are used.
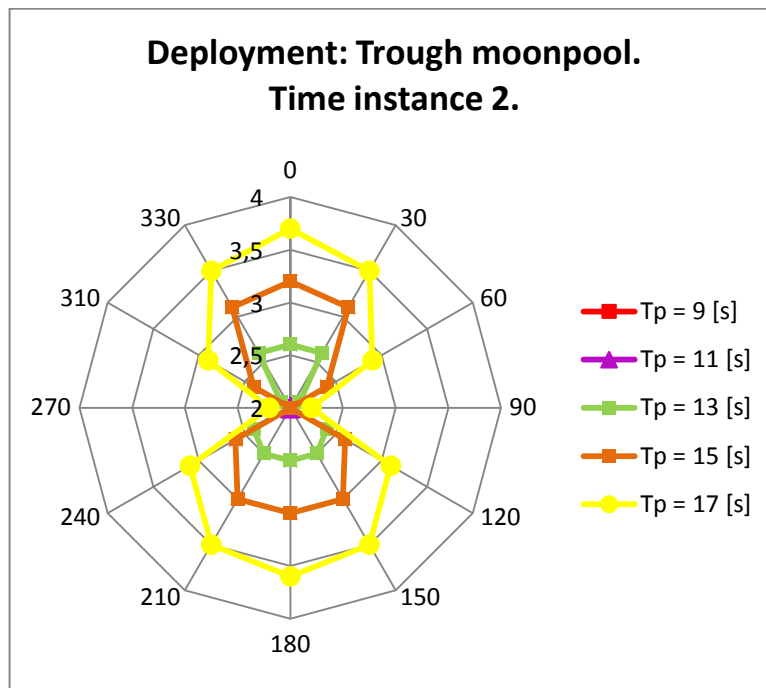
Figure 61: Operability rosette for moonpool deployment at time instance 2. Plot of design H_s given in Table 11. The circles represent design H_s from 2.0 – 4.0 [m].

15.8 Weather windows

From the operability rosettes in Figures 58-61 overall design H_s values are found. It is the lowest H_s value marked in each rosette considering wave headings $0° \pm 30°$. It can also be found by looking at Tables 8-11 where design H_s are given for all T_p values and wave headings. The lowest design H_s for wave headings $0° \pm 30°$ is hence used, independent of T_p. Note that for moonpool deployment at time instance 2 an additional operability demand is set, $T_p \geq 13.0$ [s]. Reason is that for $T_p < 13.0$ [s] T_p curves are never above the slack sling limit, see Figures 50-52. Hence is slack slings a problem for all H_s values considered at these T_ps. A summary of the resulting overall design H_s values are given in Table 12.

Uncertainties in weather forecasts and monitoring must be accounted for. This correction is performed by multiplying the operational limiting criterion, which here equals the overall design H_s for wave headings $0° \pm 30°$, with an alpha factor. The outcome is called a forecasted weather operational criterion OL_{WF}. Alpha factors are given in several tables in [9] and which table to use is dependent on how certain the weather forecasts and measurements are. Table 4-4 is used. That is based on [8] which states that during production at Ormen Lange with subsea infrastructure only waves and wind must be measured in real time at the location of the subsea compression station. Weather forecasts will hence be properly calibrated against monitored data. For selecting an alpha factor T_{POP} must be known.

T_{POP} is the planned operation time from issuance of the weather forecast to the module is landed on the seabed. T_{POP} should be based on a detailed time schedule for the operation. Presently such a comprehensive time schedule of the installation is impossible to make since final design and lifting design are far from ready. T_{POP} is hence found based on Shell in house experience and logic. To minimize forces on the module and the probability of slack slings the module will be lowered trough the splash zone as fast as possible, preferably within a couple of minutes. Below the splash zone wave forces are less as they decrease exponentially with the distance from MWL. Lowering is therefore not as critical anymore. Within half an hour the module can be lowered from below the splash zone to the seabed. Then some additional time is needed for safe landing. It will hence take less than 4 hours, 2-3 hours are reasonable, from the weather forecast is issued to the module is landed on the seabed. Note that design H_s for lowering through the splash zone is taken as the operation limit for the whole lifting sequence as it is assumed the most critical phase during the lift.

Based on $T_{POP} \leq 4$ and the overall design H_s values for the two deployment methods and time instances alpha factors can be found. In Table 12 design H_s, alpha factors and forecasted operational criteria are given for all four cases considered.

Deployment method	Time instance	Design H_s [m]	Alpha factor	OL_{WF} [m]	Additional operability demand
Crane	1	2.9	0.972	2.8	-
Crane	2	4.1	1.0	4.1	-
Moonpool	1	4.5	1.0	4.5	-
Moonpool	2	2.6	0.965	2.5	$T_p \geq 13.0[s]$

Table 12: Design Hs, alpha factors and OL$_{WF}$ for all four cases analyzed.

OL_{WF} values are then used to estimate annual weather window statistics given for six periods of the year. T_{POP} cannot be used directly as input into Metocean Tool Box (MTB) together with OL_{WF} values. In addition to the planned operation period a contingency period T_C must be added. T_C is added to cover general uncertainties in the planned operation time and possible contingency situations that requires additional time [9]. The contingency time can for conservatism be assumed equal to the planned operation time, say 3 hours. The operation reference period, which shall be used as input into MTB to find annual weather window statistics, is then $T_R = T_C + T_{POP} = 6\ hours$.

By inserting the operational criteria OL_{WF} and T_R into MTB the following weather window statistics are computed:

- The probability of arriving the offshore site and being able to deploy the module directly without any waiting, called "Completion operation %".
- How many days during the considered time period that installation can be performed, called "Time for operations days".
- "Mean operation length" in hours, hence the reference period T_R plus mean waiting time on weather when arrived at offshore site.
- "Mean waiting time" on weather when arriving at site in hours.
- How many times during the considered time period that the same installation can be performed. This number equals "Time for operations" divided by mean operation length.

Crane deployment at time instance 1 has operation limit $H_s = 2.8$ [m], $T_p = all$, wave heading = $0^o \pm 30^o$ and reference period = 6 hours. Based on these limitations weather windows statistics are calculated and given in Table 13.

Start of Period	21. Jun	21. Aug	21. Oct	21. Dec	21. Feb	21. Apr
End of Period	20. Aug	20. Oct	20. Dec	20. Feb	20. Apr	20. Jun
Completion operation (%)	91.05	63.65	36.20	29.78	45.98	83.72
Time for operation (days)	55.54	38.83	22.08	18.46	27.24	51.07
Mean operation length (hours)	7.87	22.49	65.32	88.60	45.08	10.68
Mean waiting time (hours)	1.87	16.49	59.32	82.57	39.08	4.68
Possible nr. of seq. operations	150.18	37.55	11.74	8.69	16.90	95.33

Table 13: Weather window statistics for crane deployment at time instance 1.

Crane deployment at time instance 2 has operation limit $H_s = 4.1$ [m], $T_p = all$, wave heading = $0^o \pm 30^o$ and reference period = 6 hours. Weather window statistics based on these limitations are given in Table 14.

Start of Period	21. Jun	21. Aug	21. Oct	21. Dec	21. Feb	21. Apr
End of Period	20. Aug	20. Oct	20. Dec	20. Feb	20. Apr	20. Jun
Completion operation (%)	98.60	85.80	66.80	59.13	73.38	95.50
Time for operation (days)	60.14	52.34	40.75	36.66	43.47	58.25
Mean operation length (hours)	6.17	9.06	16.98	24.32	14.92	6.83
Mean waiting time (hours)	0.17	3.06	10.98	18.32	8.92	0.83
Possible nr. of seq. operations	230.78	120.77	52.37	34.89	59.62	191.15

Table 14: Weather window statistics for crane deployment at time instance 2.

For moonpool deployment at time instance 1 slack slings is not a problem for wave heading = 0° $\pm 30^o$. Operation limit is hence set at the upper H_s value analyzed, $H_s = 4.5$ [m] for all T_p values. The reference period is also here 6 hours and resulting weather window statistics are listed in Table 15.

Start of Period	21. Jun	21. Aug	21. Oct	21. Dec	21. Feb	21. Apr
End of Period	20. Aug	20. Oct	20. Dec	20. Feb	20. Apr	20. Jun
Completion operation (%)	99.20	89.59	73.69	66.05	78.94	96.90
Time for operation (days)	60.51	54.65	44.95	40.95	46.77	59.11
Mean operation length (hours)	6.09	8.03	13.15	18.52	11.93	6.51
Mean waiting time (hours)	0.09	2.03	7.15	12.52	5.93	0.51
Possible nr. of seq. operations	236.67	145.55	72.09	47.93	79.64	208.53

Table 15: Weather window statistics for moonpool deployment at time instance 1.

Moonpool deployment at time instance 2 has operation limit $H_s < 2.5$ [m], $T_p \geq 13.0$ [s] wave heading = $0^o \pm 30^o$ and reference period = 6 hours. Resulting weather window statistics computed from the hindcast and operation limits are given in Table 16.

Start of Period	21. Jun	21. Aug	21. Oct	21. Dec	21. Feb	21. Apr
End of Period	20. Aug	20. Oct	20. Dec	20. Feb	20. Apr	20. Jun
Completion operation (%)	0.34	1.28	2.28	2.93	3.72	1.47
Time for operation (days)	0.21	0.78	1.39	1.81	2.20	0.90
Mean operation length (hours)	1242.14	736.00	633.40	547.43	534.13	1255.75
Mean waiting time (hours)	1236.14	730.00	626.75	540.05	528.13	1249.75
Possible nr. of seq. operations	0.59	1.00	1.16	1.37	1.34	0.58

Table 16: Weather window statistics for moonpool deployment at time instance 2.

16.   Discussion of Results

16.1 Duration of MACSI2 analyses

The duration of the MACSI2 analyses is of great importance since an irregular sea is modeled. The results will then vary depending on which time interval from the irregular sea that is extracted for different analyses, see Figure 62. If a short time interval is used the risk is that resulting output values will be unreasonably low if now extensive wave elevation peaks are included. But a long time interval ΔT is not a good solution in this case either as both time and computer capacity is limited. As time steps to avoid numerical instabilities in MACSI2 are small due to low natural periods of the lowered systems moonpool simulation time must be limited. From [25]:

$$\Delta T \leq \frac{T_0}{10} \qquad\qquad \text{Equation 46}$$

The natural periods are listed in Chapter 15 Results. The largest natural period of the deployed system for the two lowering methods is 2.9 [s] considering crane installation. If the scatter of the results is small a suiting simulation time of 10 [min] is recommended [14].
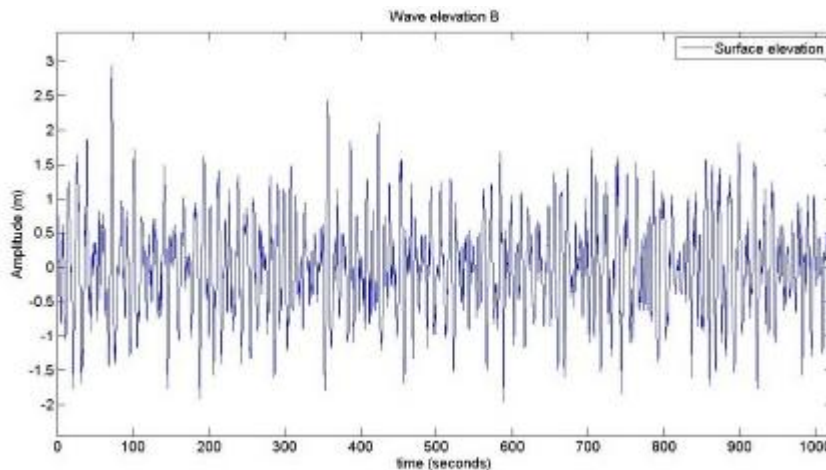
Figure 62: Irregular wave elevation example taken from [38].

The scatter of the 2 hours maximum wire tension amplitude is tested for different sea states and for both installation methods and wave spectra. The tests are performed by changing the random wave phase angle for each run but keeping the other input variables constant. Resulting values can be seen in Table 17 where the 2 hours maximum wire tension amplitude in [kN] and the largest scatter for the listed deployment conditions are given. Maximum and minimum wire tension amplitude values are bold.

| Simulation nr | Crane | | Crane | | Crane | | Moonpool | |
	Wave heading 0, $H_s = 2.5\,[m]$, $T_p = 7.0\,[s]$		Wave heading 0, $H_s = 4.5\,[m]$, $T_p = 11.0\,[s]$		Wave heading 90, $H_s = 2.5\,[m]$, $T_p = 7.0\,[s]$		Wave heading 0, $H_s = 2.5\,[m]$, $T_p = 15.0\,[s]$	
	JONS.	Torset.	JONS.	Torset.	JONS.	Torset.	JONS.	Torset.
1	1056.4	**994.2**	956.6	1206.9	1883.0	1717.2	1644.0	5350.1
2	1062.5	994.4	961.5	1206.6	1836.6	1750.1	**1647.8**	4925.6
3	1062.5	1016.4	963.5	**1252.8**	1821.8	1741.8	1627.0	7615.7
4	1048.4	1004.6	967.8	**1196.9**	1848.6	1760.8	**1618.7**	4302.5
5	**1047.2**	1022.8	957.5	1232.6	1825.0	1773.5	1632.6	**12361.8**
6	1050.5	1006.2	**951.8**	1239.1	1854.8	1738.9	1643.8	4126.4
7	1058.5	1017.2	**969.6**	1208.8	1812.7	1771.4	1636.5	**4074.1**
8	1060.2	1016.7	955.4	1222.7	**1889.0**	**1795.7**	1644.3	5539.7
9	**1064.8**	**1044.9**	967.0	1207.4	**1796.0**	**1705.4**	1626.0	11306.6
10	1047.7	1001.5	958.1	1221.8	1810.3	1775.5	1619.2	5177.0
Delta tension [kN]	17.6	50.7	17.8	55.9	93.0	90.3	25.3	8287.7

Table 17: Scatter test for MACSI2 analyses with duration 10 [min].

Considering crane deployment the largest scatter is obtained for small wave parameters $H_s = 2.5$ [m] and $T_p = 7.0$ [s], wave heading 90°. There the scatter is about 100 [kN]. It must be remembered that 100 [kN] is only 5 % of the submerged static weight of the object which is not that considerable. Besides, for actual deployment DP will be used to hold wave heading 0° ± 30° where the scatter is less. Looking at moonpool deployment JONSWAP wave spectrum will not give a significant scatter, and JONSWAP is the wave spectrum usable for moonpool analyses. The scatter is at least low for this T_p. The scatter for Torsethaugen on the other hand is huge. That is because Torsethaugen T_z values are very close to peak resonance T_z which will amplify any scatter significantly. But since MACSI2 cannot handle Torsethaugen analyses for all wave headings and JONSWAP results are used for moonpool deployment a simulation time of 10 [min] is accepted.

16.2 Water particle velocity

In Figures 32-34 plots of vertical water particle velocity are given. Water particle velocity is direct input into the slamming analyses since it is used to find slamming impact velocity, see Equation 45, and is hence of importance. Here Figures 32-34 will be discussed starting with the free surface water particle velocity before moonpool vertical water particle velocity is looked into.

It can be seen from Figure 32 that free surface vertical water particle velocities calculated based on Torsethaugen wave spectrum are generally larger than for the JONSWAP wave spectrum. This is a result of how the spectra are modeled, which leads to different T_z for the same H_s and T_p

spectrum input. See Tables 5 and 6 for T_z comparison of the numbers used in the calculations. Torsethaugen T_z values are normally found to be less than JONSWAP values. Free surface vertical water particle velocity is a function of the inverse of T_z, see Equation 94, so Torsethaugen results are generally larger than JONSWAP results. The difference between the two spectra is larger at high T_p values as the difference in T_z increases with increasing T_p, see the free surface vertical water particle velocity graphs for $T_p \geq 11$ [s]. The reason why Torsethaugen lines so gathered in Figure 32 is due to the small T_z range which is covered relative to the range covered by JONSWAP.

JONSWAP lines are linear and increases with increasing H_s as Equations 94 and 95 state. $v_w \propto \zeta_a = 0.9H_s$ since T_z in independent on H_s. For Torsethaugen on the other hand T_z is H_s dependent and free surface water particle velocity is hence not linearly increasing with H_s. The lines have a decreasing gradient since T_z generally increases with increasing H_s.

The moonpool vertical water particle velocities computed are less than for the free surface, see Figures 33 and 34. This is intentional for a moonpool since it shall provide a deployment area sheltered from the external environmental conditions. Torsethaugen values are a bit larger than JONSWAP values, also here due to the T_z difference between the two and the formula for vertical water particle velocity in the moonpool, Equation 36. But the differences between the two spectra are less than for the free surface as the moonpool velocity is proportional to $0.5T_z^{-1}$ which reduces the velocity difference between the two spectra caused by T_z. Otherwise the same trends as mentioned for the free surface can be seen; spectral differences increases with increasing T_p and Torsethaugen results are nonlinear as T_z is H_s dependent.

But as stated in Chapter 15.2 Vertical water particle velocity the moonpool velocities are probably not correctly estimated. The RAO values of water plug elevation in the moonpool to wave elevation are not transformed from T_p to T_z dependency. It means Torsethaugen water particle velocities in reality should be higher.

How the moonpool water particle velocity changes with wave heading and T_p is related to the water plug amplitude compared to the wave elevation, see RAO plots in Figure 27. The RAO plots are independent of wave spectrum. The ratio between the water plug amplitude and wave elevation is dependent on the ship transfer function which changes with wave heading and wave period.

The natural period of the water plug is $T = 7.1$ [s], so at $T_p = 9.0$ [s] resonance will have an effect. Then the magnitude of the water plug motion amplitude is increased which leads to increased vertical water particle velocity. Moonpool velocities for $T_p = 9.0$ [s] are larger for wave heading 0⁰ than 90⁰ because of the RAO graphs. For wave heading 0⁰ the RAO graph has a peak slightly shifted to the right of $T/T_0 = 1$ and the decrease after the RAO peak is less steep than for wave heading 90⁰.

16.3 Crane tip vertical displacement amplitude

From the transfer functions it is clear that wave heading 120° gives the largest crane tip motions when lowering over the side and that the amplitude increases with increasing T_P, see Table 7. But the increase do only continue until resonance T_p is reached for the given wave heading and H_s. Then the vertical displacement amplitude decreases again. This can be seen if crane tip motions are extracted from more of the sea states analyzed. Surprisingly enough wave heading 180° is better than 0°. This yields both wave spectra. Torsethaugen motion amplitudes are less than for JONSWAP. That must be due to the T_z values being lower for Torsethaugen, see Tables 5 and 6, which will cause less ship motions.

For the moonpool crane tip location crane tip motions are only obtained by JONSWAP wave spectrum as MACSI2 do not manage to run analyses for all wave headings with Torsethaugen. Here motions are less than for the crane tip position during over the side deployment and wave heading 90° is most critical. The motions decrease symmetrically about 90° degrees with increasing angle deviation. Strangely the peak amplitude at 90° has decreased for $T_p = 13$ [s] compared to $T_p = 9$ [s] while for the other wave headings the amplitude increases.

16.4 Crane tip vertical velocity

Crane tip vertical velocity plots both for over the side and moonpool deployment are given in Figures 35-38 for selected wave headings of interest. Crane tip vertical velocity enters directly into the equation of slamming velocity in the same way as water particle velocity does. This can be seen in Equation 45. The crane tip and water particle velocities are hence of equal importance.

Torsethaugen values are generally smaller than JONSWAP values for crane lowering over the side. The transfer function of the ship displacement in z-direction is a product of the transfer functions in heave, roll and pitch given for single wave periods T, see Equation 1. In MACSI2 these periods seems to be set equal to T_p before they are rearranged to T_z dependency since irregular waves are considered. T_z is then the period around which the wave energy is located. $T_p = 7$ [s] is the only T_p for which the two spectra have the same T_z except for that Torsethaugen T_z values change with H_s. The transfer functions should hence be quite similar, and if the two spectra create the same wave elevation resulting crane tip vertical velocity should be similar. And from Figure 35 this is seen. Only at high H_s do the two spectra differ which might imply that for higher H_s JONSWAP creates a larger wave elevation than Torsethaugen. It must also be noted that crane tip vertical velocities are taken directly from the MACSI2 analyses time histories. Some scatter must therefore be expected but the overall trend should give a realistic representation.

Which T_p that gives the largest crane tip velocities changes with changing wave heading. This is due to changing ship motion transfer function with wave heading, see Table 7. The transfer functions are also highly T_p dependent. Most of the times $T_p \geq 11$ [s] are dominant for the JONSWAP crane tip velocities but also $T_p = 9$ [s] results in large velocities. For $T_p \geq 11$ [s] JONSWAP wave spectrum results in T_z values larger than any of the T_z values obtained by Torstehaugen. $T_p \geq 13$ [s] give for Torstehaugen the T_z values closest to the T_z values obtained by JONSWAP when $T_p \geq 11$ [s]. $T_p \geq 13$ [s] are therefore the values causing largest crane tip velocities for Torsethaugen, but the velocities are not as large as for JONSWAP.

From the resulting MATLAB plots of crane tip vertical velocity for crane lowering over the side it is clear that wave heading 120° is the overall most critical wave heading for both wave spectra. That is also the case for crane tip vertical displacement amplitude as can be seen in Table 7. This is hence due to the ship motion transfer functions.

For moonpool lowering wave heading 90° gives the largest crane tip vertical velocities. The velocities are almost in the same range as velocities for over the side deployment at the same wave heading. For wave headings 0° and 30° crane tip velocities are much less than for over the side installation. In Chapter 10.2.1 Moonpool fluid flow verification and results are two magnitude values of the heave transfer function listed. The magnitude is 1.2 for wave heading 90^0 while it is 0.42 for wave heading 0^0. In both cases is $T_p = 7.0$ [s]. The crane tip response is hence large for heave which might explain why crane tip velocities at 90° wave heading are large, see Figure 38. Roll should not have much effect since the crane tip is located at the longitudinal centerline of the vessel. The reduction in crane tip velocity for wave headings 0^0 and 30^0 is probably due to reduced pitch compared to crane installation. $ms_x = 6.92$ [m] while $ct_x = 30.32$ [m].

Torsethaugen results are less than JONSWAP results for moonpool deployment also. In addition the Torsethaugen crane tip velocity lines for different T_p are very gathered, a result that has to be seen in connection with the narrow range of T_z values obtained by Torsethaugen.

16.5 Minimum wire tension

16.5.1 Time instance 1
Slamming results can be seen in Figures 39-42 and 47-49. The wire tension obtained when considering slamming is taken as the static wire tension minus the slamming impact force on the object. Equation 44 gives the slamming impact force where only slamming impact velocity, hence crane tip vertical velocity and water particle vertical velocity (Equation 45), changes with changing sea state. Figures giving crane tip vertical velocity and water particle velocity are therefore used to explain Figures 39-42 and 47-49.

First crane lowering over the side is considered. From Figure 32 giving vertical water particle velocities and Figures 35-36 giving crane tip vertical velocities it can be seen that velocities are significant and uplift due to slamming will arise. It should be noted that for H_s values in the range around 3 [m] where slamming uplift becomes a problem Torsethaugen will be more conservative than JONSWAP. The reason is that Torsethaugen water particle velocities are quite high for all T_p values. They are so high that they cause slamming uplift even though the crane tip vertical velocities for Torsethaugen are smaller than for JONSWAP. When calculating slamming impact velocity both crane tip vertical velocity and water particle velocity enter as squared. Hence will one high value, here the water particle velocity, contribute greatly to the outcome. At higher H_s and low T_p JONSWAP gives larger slamming forces on the module than Torsethaugen. That is because water particle velocities are quite similar for the two wave spectra while crane tip velocities are much larger for JONSWAP.

Resulting minimum wire tension changes with shifting wave heading. Water particle velocities are constant for all wave headings so how minimum wire tension change is all due to changing crane tip vertical velocities with wave heading.

During moonpool lowering both crane tip and water particle vertical velocities are less compared to crane installation, see Figures 33-34 and 37-38. Minimum wire tension results are hence also less than for crane installation. Water particle velocities are quite equal for both spectra at the lower T_p values which cause larger water particle velocites, Torsethaugen results are slightly higher. So as crane tip vertical velocities are larger for JONSWAP than Torsethaugen JONSWAP minimum wire tension results are conservative and hence used. It must be noted that both water particle velocities and crane tip velocities for wave headings 0⁰ and 30⁰ are very similar and one might represent the other. Slamming uplift is only a concern for wave heading 90⁰ where crane tip velocities are largest, see operability rosette in Figure 60.

Resulting minimum wire tension values change with wave heading also for moonpool lowering. Now both water particle and crane tip velocities change with wave heading. The shift in minimum wire tension values with wave heading for the considered combinations of H_s and T_p must thus be seen in the light of how both water particle and crane tip velocities change.

16.5.2 Time instance 2
Minimum wire tension values for both crane and moonpool deployment at time instance 2, when the module if fully submerged, are functions of crane tip motions and hydrodynamic forces on the module. The module is set to follow the crane tip motion, but there will be a phase angle between them. Crane tip transfer functions do therefore not give all the necessary information and transfer functions of module motion relative to wave elevation should have been created. As time is limited such transfer functions for the two crane tip locations have not been computed and

discussions are hence based upon the results given in Figures 32-34, Table 7 and Figures 43-46 and 50-52.

Torsethaugen gives lower minimum wire tension values than JONSWAP considering crane deployment at high T_p values, see Figures 43-46. The dynamic wire tension amplitudes are hence higher for Torsethaugen. This is a bit strange since JONSWAP wave spectrum causes higher crane tip motions in z-direction than Torsethaugen, see Table 7. But it might be because Torsethaugen T_z values are lower than JONSWAP T_z values for $T_p \geq 9$ [s] which gives higher water particle velocities and hence higher hydrodynamic forces. Water particle velocities are given in Figure 32. The difference in T_z for the spectra increases with increasing T_p, see Tables 5 and 6. From the minimum wire tension plots in Figures 43-46 it seems like the difference in water particle velocity is more important for the results than the difference in crane tip displacement. Torsethaugen is hence more and more conservative compared to JONSWAP. For $T_p = 7.0$ [s] T_z values for the two spectra are quite similar. Thus water particle velocities are similar. But JONSWAP gives higher crane tip motions and will therefore obtain lower minimum wire tensions due to larger responses and be conservative.

There is no clear trend on whether $T_p = 9$ [s] is conservative for JONSWAP or Torsethaugen considering crane deployment. The T_z values for Torsethaugen are less than for JONSWAP which means higher water particle velocities, but on the other hand JONSWAP gives higher crane tip motions. It therefore varies with wave heading which spectrum value that is conservative for $T_p = 9.0$ [s].

Minimum wire tension based on static wire tension minus the 2 hours wire tension amplitude is used for most cases. The only occurrences where minimum wire tension taken directly from the time history influences the results are for JONSWAP wave spectrum when $T_p = 9.0$ [s] at wave heading 90° and $T_p = 11$ [s] for wave headings 90° and 120°. Figure 63 shows the effect.
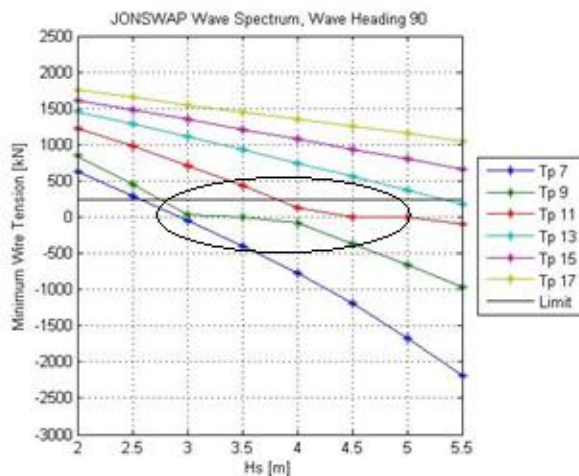
Figure 63: Minimum wire tension from time history affects the crane over boarding results.

Moonpool results given in Figures 50-52 are now discussed. The natural period of the lowering system in the moonpool is 0.7 [s] as computed in Equation 104, less the natural period of the lowered system when installed over the ship side. That is due to the change in crane resilience. Changing wire length will have less effect since it both reduces added mass and decreases wire stiffness. None of the T_p values analyzed are close to the natural period of the lowered system. But the resonance period of the moonpool water plug is $T_p = 7.0$ [s] which equals a T_z value around 5.7 [s] considering both spectra, see Tables 5 and 6. T_z values for all Torstehaugen sea state are relatively close to this T_z value compared to JONSWAP T_z values. Resonance is thus obtained with large responses and dynamic wire tension amplitude. This is the reason why Torsethaugen minimum wire tensions are much less than for JONSWAP in Figures 50 and 51.

For Torsethaugen wave spectrum there is in Table 7 found to be a large scatter in the results considering wave heading $0°$, $H_s = 2.5$ [m] and $T_p = 15$ [s]. This is believed caused by scatter magnification since T_z is relatively close to resonance T_z. Huge scatter can also be a problem for JONSWAP wave spectrum when JONSWAP T_z values are close to resonance. That is only the case for $T_p = 9.0$ [s].

A strange break in the curves can be seen for minimum wire tension less than about -500 [kN]. It is hard to tell why since few equations are given in the MACSI2 theory manual, but it might be due to numerical problems in the analyses. Anyways it is not of great importance as slack slings already has become a problem when the curves break. Design H_s and hence the probability of slack slings are absolutely worst at $90°$ wave heading. That might be due to that fact that crane tip velocities are largest at $90°$ wave heading.

16.6 Sensitivity checks

How sensitive minimum wire tension results considering crane deployment at time instance 2 are to changes in added mass, total crane system stiffness and linear and quadratic drag coefficients have been checked. Only JONSWAP results are tested. Resulting plots of minimum wire tension from the checks are given in Figures 54-57. The effect on minimum wire tension is more visible for wave heading $120°$ than $30°$. That is because minimum wire tension in general is more critical at wave heading $120°$ due to larger crane tip velocities.

The effect of added mass and stiffness changes can be understood by looking at the expression for natural period of the lowered system:

$$T_0 = 2\pi\sqrt{\frac{M}{K}} = 2\pi\sqrt{\frac{M_m + A_z + mass\ of\ wire}{\left(\frac{1}{k_w} + C_{resilience}\right)^{-1}}} \qquad \text{Equation 47}$$

So when added mass is reduced from 431.8 [t] to 250 [t] in z-direction total mass is reduced which leads to a reduced natural period, $T_0 = 2.5$ [s]. The original natural period in z-direction is

2.9 [s]. Then excitation wave periods, which for JONSWAP equals T_z values equal to or higher than 5.71 [s], are further from the resonance period and responses reduce. This is also the resulting outcome given in Figure 54. Minimum wire tension is hence increased and the possibility of the lifting wire going into compression reduced. The hydrodynamic forces are also reduced according to Equation 42, another reason why minimum wire tension is critical at higher H_s values.

Then total crane system stiffness is changed while added mass coefficients are reset. k_{crane} is reduced, hence will the crane resilience $C_{resilience}$ increase since it is the inverse of crane system stiffness. Increased crane resilience will again increase the natural period of the system, see the Equation 47. New values are as follows; $k_{crane} = 2.0 \cdot 10^6$ [N/m], $C_{resilience} = 5.0 \cdot 10^{-7}$ [m/N], $K_{TOT} = 1.91 \cdot 10^6$ [N/m] and hence $T_0 \approx 3.7$ [s]. This value is relatively close to 5.71 [s], the lowest T_z for the JONSWAP wave spectrum, compared to the old natural period of 2.9 [s]. Responses are therefore expected to be larger than for the original analyses, which is also the case as can be seen in Figure 55.

It must be remembered that no study is taken on to find realistic added mass and crane resilience parameters to be used in the sensitivity analyses. The probability of added mass and crane resilience values being realistic is therefore unknown and further work has to be done in order to ensure whether the order of magnitude is reasonable.

Both the modification of linear and quadratic drag coefficients gave close to no change in the minimum wire tension plots, Figures 56 and 57. This was as expected for the linear drag coefficient since its contribution is small compared to the quadratic drag coefficient at the Keulegan-Carpenter numbers considered. There are at least two explanations of why varying the quadratic drag coefficients do not affect the minimum wire tension results. One is that excitation periods are far enough away from resonance so that changing the drag coefficients within a certain range have limited effect on the response. At the same time coefficients within the same range have limited effect on the hydrodynamic force, see Equation 42. Another explanation is that these effects on response and hydrodynamic force might counteract each other; lower drag would lead to larger response but also lower hydrodynamic force and hence excitation force. The effect of changing quadratic drag coefficient is illustrated in Figure 64 for an object in deep water. Here the object is close to the surface which might affect the curves.
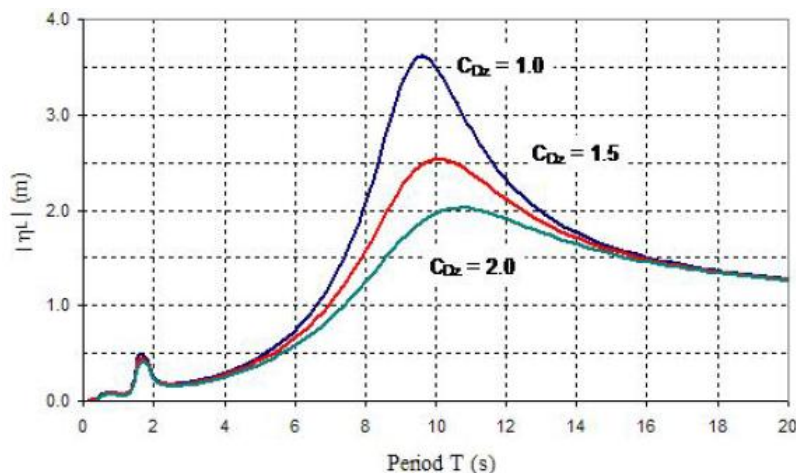
Figure 64: Example response amplitude of a lifted object in deep water due to a forced motion of 1 [m] at top end of cable [10].

16.7 Operability rosettes

The operability rosettes are summaries of the design H_s for each deployment method and time instance considering the sea states analyzed in this report. But as MACSI2 analyses are run for wave headings from 0° to 180° symmetry is assumed about the ship's longitudinal center plain. Design H_s values are therefore mirrored about 180° to obtain results for all 360°.

The operability rosette for crane lowering at time instance 1 given in Figure 58 looks as expected. 120° is the most critical wave heading as for crane tip vertical velocity since water particle velocity is constant with wave heading. Torsethaugen results are mainly used since Torsethaugen free surface water particle vertical velocities are larger than for JONSWAP, see Figure 32. $T_p = 11$ [s] for wave headings 120° and 150° are the only JONSWAP values used and the reason why the shape of this T_p curve is a little different from the others. Also free surface water particle velocities are largest for $T_p = 7$ [s] and decreases with increasing T_p, as long as T_z increases, and $T_p = 7.0$ [s] is the T_p value for which design H_s is lowest. This is correct as water particle velocity is dominating to crane tip vertical velocity and crane tip vertical velocity is quite similar for all T_p values. Crane tip vertical velocities are given in Figures 35-36.

For crane lowering over the side at time instance 2 the operability rosette in Figure 59 is a summary of both Torsethaugen and JONSWAP results. In Appendix 15 separate Torsethaugen and JONSWAP operability rosettes are given. From the separate rosettes 60° and 90° wave headings are more critical for Torsethaugen than 120° considering all T_p values. For JOSNWAP wave heading 90° is more critical than 120° for $T_p < 11$ [s]. This is illustrated in Figure 65 below by the arrows for the JONSWAP only operability rosette. Note that 120° is most critical for $T_p \geq 11$ [s]. This must be due to the contribution from hydrodynamic forces as crane tip motion

is worst for wave heading 120⁰, see Table 7. It must be remembered that the results are depending on both the motion of the crane tip and the hydrodynamic parameters acting on the module. Also head sea seems to be worse than following sea which is a little strange since most ships behave better in head seas. The same pattern is detected in Table 7 and it must therefore be due to the ship transfer functions.
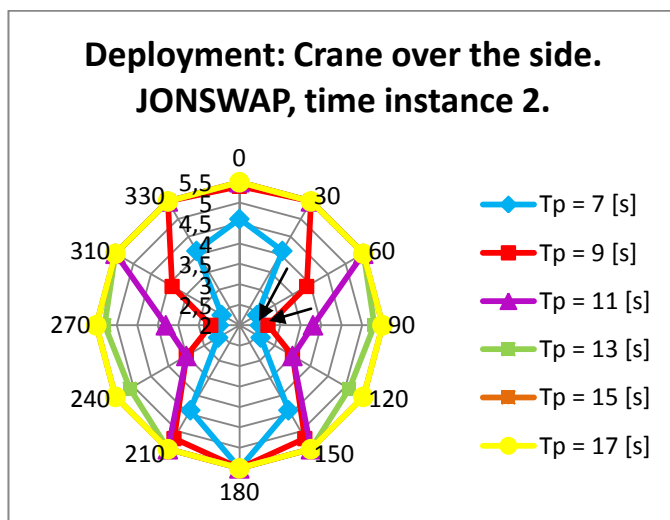
Figure 65: JONSWAP only operability rosette for crane installation at time instance 2.

In Figures 60 and 61 the operability rosettes for moonpool lowering at time instance 1 and 2 are given. It is obvious that uplift is not a significant problem for moonpool deployment at time instance 1, but at time instance 2 it certainly is. When slamming is considered, at time instance 1, water particle velocity and crane tip velocity are the changing input parameters. Slamming forces are not that significant due to overall low water particle velocities and crane tip vertical velocities. See Figures 33-34 and 37-38. But as shown in Figure 38 crane tip velocities are magnified at wave heading 90⁰. For $T_p = 9.0$ [s] largest crane tip velocities are obtained and uplift due to slamming is an issue. Water particle velocities do not change much with wave heading, see Figures 33-34.

From comparing Figures 59 and 61 it is clear that moonpool results are worse than crane results for over the side deployment considering time instance 2, module fully submerged. For $T_p \leq$ 11.0 [s] the module cannot be lowered through the moonpool at any of the H_s values analyzed. That is mainly due to the natural period of the water plug and hence large hydrodynamic forces. From Equation 39 $T_0 = 7.1$ [s] (corresponding to $T_z \approx 5.7$ [s]). The natural period of the lowered system has low effect. Low effect has also the crane tip motions as the motions in most cases are less than for crane deployment, see Table 7. Increasing operability with increasing T_p is due to decreasing hydrodynamic forces because of decreasing water particle velocity with increasing T_p.

Hydrodynamic forces are hence dominating over crane tip motions as crane tip motions tend to increase for increasing T_p values.

Remember that moonpool damping is very high in the MACSI2 analyses; wave height ratio in the moonpool at moonpool resonance is 1. But with such a large structure in the moonpool water particle velocities and accelerations between the lowered module and the moonpool walls are large. That is due to the assumption about constant mass flow rate:

$$\rho A V = constant \qquad\qquad \text{Equation 48}$$

ρ: density of the fluid [kg/m^3]
A: Free stream area [m^2]
V: Fluid velocity [m/s]

So when the open area for the flow to travel through decreases velocity will increase. This is taken care of in MACSI2 analyses by amplification of added mass and drag coefficients in z-direction, see Chapter 9.1.3 Corrections to hydrodynamic coefficients.

How design H_s changes with wave heading in Figure 61 is dependent on the ship transfer functions. As can be seen in Table 7 crane tip motion amplitude is largest for wave heading 90º and decreases symmetrically with increasing distance from 90º degrees, both counter-clockwise towards 0º and clockwise towards 180º. Also the moonpool water plug amplitude ratio to wave elevation calculated in Figure 27 can be used to explain the change in limiting H_s with wave heading. From Figure 27 it can be seen that the response is much larger for wave heading 90º than for wave heading 0º. This is therefore most likely the case in the MACSI2 analyses as well even though the damping is different. So since both crane tip motion and water particle velocities are largest at wave heading 90º this is naturally the heading where the operable H_s is lowest.

But as Peter Sandvik said, the results might be all wrong since the cross-section of the object lowered in the moonpool is quite large compared to the moonpool cross-section [15]. The presence of the object is disregarded when MACSI2 calculates the fluid flow in the moonpool. With a large structure like the one considered in this report the fluid flow will definitely be affected. To correct for the assumption Sandvik suggested setting the damping of the moonpool quite high, hence use a small wave amplitude ratio at resonance. Uncertainties in the results are therefore introduced and another program better suited for analyzing deployment of large modules in moonpools should perhaps have been used, at least to verify the results.

16.8 Weather window statistics

From Tables 13-16 it is clear that time instance 1 is most critical for crane deployment over the side while time instance 2 is most critical for moonpool lowering. The operation limits are

$OL_{WF} = 2.8$ [m] for crane lowering and $OL_{WF} = 2.5$ [m] with an addition requirement of $T_p \geq 13.0$ [s] for moonpool installation. A new table is made where the weather window statistics for what normally is taken as the best and worst yearly periods are listed for each deployment method's critical time instance. Values are taken from Tables 13 and 16. Mean operation length is not included because it equals mean waiting time plus operation reference period. Nor possible number of sequence operations is listed as it equals the time for operation divided by mean operation length.

Case considered	OL_{WF}	Best Period: 21. Jun. – 20. Aug.			Worst period: 21. Dec. – 20. Feb.		
		Completion operation %	Time for operation days	Mean waiting time hours	Completion operation %	Time for operation days	Mean waiting time hours
Crane, instance 1	H_s<2.8 [m]	91.05	55.54	1.87	29.78	18.46	82.57
Moonpool, instance 2	H_s<2.5 [m], $T_p \geq 13.0$ [s]	0.34	0.21	1236.14	2.39	1.81	540.05

Table 18: Summary of weather window statistics.

Annual time for operation is calculated for the two deployment methods based on their critical time instance. This is done by summing up time for operation over the periods given.

- Crane annual time for operation: 213.22 days → 58.4 % of the year
- Moonpool annual time for operation: 7.24 days →   2.0 % of the year

Weather window statistics vary greatly over the year. During summer the sea is calmer which is clearly seen in Table 18 for crane installation. Even for a sea state limitation of $H_s = 2.8$ [m] there is a 91.05 % probability that the module can be installed with crane over the side immediately after Normand Subsea arrives field location. Installation can be done in 55.54 days out of 64 and the mean waiting time at site before the sea state is within operability limit is only 1.87 hours. During winter storms come in from the Atlantic and the weather is generally rougher. Then operability is significantly reduced, also here considering crane installation. Completion operation, the probability of immediate deployment when arriving at site, reduces from 91.05 % to 29.78 %. This is a significant drop. Installation can now only be performed in 18.46 out of 64 days and the mean waiting time before staring installation after arriving at site is 82.57 hours. 82.57 hours equals 3.44 days. If one of the compression modules at the Ormen Lange future compression station gets damaged during winter so production cannot be maintained from Ormen Lange a 3.44 days waiting on weather is very expensive and should be avoided if possible. It also means increased ship costs which should be avoided.

But moonpool results are much worse than crane results, see Table 18. During winter completion operation is 2.93 % and 1.81 days out of 64 can be used for installing a new module. 540 hours, hence 22.5 days, are the mean waiting time compared to 3.44 days for crane installation. That is a significant reduction and results are so bad that moonpool deployments simply should not be used. The fact that moonpool deployment only can be performed in 2.0 % of the year confirms this.

It must also be stressed that winter results actually are better than summer results for moonpool lowering. Probability of completion reduces from 2.93 % to incredible low 0.34 % with a mean waiting time of 51.5 days. That is due to the additional operability demand of $T_p \geq 13.0$ [s]. Sea states with high wave periods are more probable during winter than summer.

For crane installation deployment is possible 58.4 % of the year. This is not good either even if it is much better than for moonpool deployment. If Shell is not able to install a new module in more than about 60 % of the year it means that in 40 % of the year nothing can be done if the compression station stops working and a new module is needed. In the end this means money lost. But is must be remembered that DNV slamming results obtained by the methodology outlined in [10] are stated as simple and conservative. If more thorough slamming analyses were performed the weather forecasted operation limit could be increased to a higher H_s. From comparing weather window statistics for $OL_{WF} = 4.1$ [m] and 4.5 [m] in Tables 14 and 15 it is clear that even a small increase in OL_{WF} will most probably give an important improvement in weather window statistics. Wave elevation is assumed normally distributed [16], so it is less probable with high wave heights than smaller wave heights close to zero. The improvement in weather window statistics should therefore be better for small wave heights like 2.8 [m] than height wave heights around 4.1-4.5 [m].

The conclusion can also be that Normand Subsea is not the vessel to use. Analyses with a more suiting vessel might give better results when it comes to operability.

Moonpool results are also uncertain due to the simplifications and assumptions made for both time instance 1 and 2. But slamming should not be a problem since the intention of having a moonpool is that both motions and moonpool fluid flow velocities are to be reduced to increase operability. This is seen here. On the other hand, trying to put a huge module with sail area 12x6 [m] in a moonpool with cross-section 14x7.5 [m] does not sound like a good idea. it will hence cover about 70 % of the moonpool area. Moonpool dimensions should therefore be reconsidered and the size optimized with regards to high water particle velocities between the module and moonpool side walls and hence large hydrodynamic forces.

17. Conclusion and Further Work

17.1 Conclusion

During deployment of the module wave heading $0^0 \pm 30^0$ will be held by DP. These wave headings are therefore used when annual weather window statistics are estimated. Time instance 1, the module bottom end at mean water level, is worst for crane deployment over the side. It therefore drives the operation limit which equals $H_s = 2.8$ [m], $T_p = all$. For moonpool deployment time instance 2 is worst and gives the moonpool lowering operation limit of $H_s = 2.5$ [m], $T_p \geq 13.0$ [s]. Time instance 2 is when the module is submerged with its top end 0.5 [m] below mean water level. Based on these operation limits and an installation reference period of 6 hours, which covers the time needed from the weather forecast is issued to the module is landed on the seabed, weather window statistics are computed.

Moonpool deployment is clearly worse than crane deployment with a very low annual weather window. A module like the one considered in this report can only be lowered in 7.24 days, hence 2.0 % of the year. This is a very bad result and deployment of such a structure in a moonpool with dimensions 14x7.5 [m] should not be done. It also means that if something happens to a future compression module so production at Ormen Lange cannot be maintained Shell will not be able to replace it with a new module at any time of the year. It will hence cost them a lot of money. But it must be stressed that the size of the module's sail area is almost the same as the cross-section of the moonpool. By redesign the moonpool dimensions better results should be possible to obtain, but the size is limited by the main dimensions of Normand Subsea. Results are also highly uncertain because the analysis program used does not account for the effect a large module in the moonpool will have on the moonpool flow field.

Crane deployment is the preferred choice since deployment is possible in 213.22 days out of 365 days, hence 58.4 % of the year. This is not good either even if it is much better than for moonpool deployment. If Shell is not able to install a new module in more than about 60 % of the year it means that in 40 % of the year nothing can be done if the compression station stops working and a new module is needed. In the end this means money lost. But is must be remembered that DNV slamming results obtained by their methodology are stated as simple and conservative. So by improving the accuracy improved operability should be obtained. Another conclusion is that Normand Subsea is not a good vessel to use for deployment considering both crane and moonpool results.

17.2 Future work

For many of the elements in the methodology used can more work be conducted to verify the results and to reduce the uncertainty. Examples of further work that should be done are:

- Run CFD analyses or model tests to get more accurate hydrodynamic coefficients. As can be seen from the sensitivity checks in Chapter 16.2 Sensitivity checks the added mass is of importance because a change will affect the natural period of the system lowered.

- Run sensitivity checks where the parameters studied (added mass, stiffness and drag) are changed within their most probable range to see how this change will affect the minimum wire tension.

- Sensitivity checks for moonpool minimum wire tension should be run for the same parameters as for crane lowering over the side; added mass, stiffness and drag. Changing drag is expected to have a more significant impact on the result than for crane deployment because:
  - Moonpool water plug resonance period is in the wave excitation period range.
  - The drag coefficient in z-direction is increased in the moonpool to account for the increased water particle velocities between lowered module and moonpool walls. The correction factor used is 5.55 so drag coefficient estimated for the module in infinite unrestricted flow is hence quite important for the moonpool drag.

- Find a better way to estimate moonpool fluid flow velocities by "hand calculations". CFD analyses should be run at least to verify the results. The fluid flow will impact the slamming force and hence the probability of getting slack slings.

- A more accurate method for estimating slamming forces should be used. It is noted in DNV [10] that the methodology will give easy and conservative results and the method is pretty simplified. CFD analyses or model tests might be used instead.

- Compute local forces on the module lowered to make sure the module itself is designed to withstand the impact loads from the sea states within the operability limits.

- Look into the operability limits. Other criteria that might result in even lower operability limits are for example limiting weather conditions for position keeping, safe working on deck and to use the equipment.

- Estimate the time needed for module deployment more thoroughly. Now it is only a rough estimate based on in-house experience since few design/module intervention details have been decided or are known at all. This time estimate is important for the weather window analyses.

- The real crane resilience of the main cargo crane on Skandi Acergy should be computed.

- Current and wind should be included in the analyses. Presently only waves are accounted for.

- Another lifting wire might be used if the Shell safety factor can be challenged and lowered.

- Moonpool dimensions should be optimized and analyses run over again to see whether the results get any better for moonpool lowering at time instance 2.

18. References

- [1] Aker Solutions, "Functional requirements for module intervention and handling from vessel". Ormen Lange Subsea Compression Conceptual Studies. Document no.:37-1Y-AKS-O15-20003, 17.04.2009.
- [2] Aker Solutions, "Installation Review of Ormen Lange Subsea Compression Station Concept". Ormen Lange Subsea Compression Conceptual Studies. Document no.: 37-1Y-AKS-O15-20001, 26.02.2009.
- [3] Aker Solutions, "OL Subsea Compression Maturation Studies, Submerged tow feasibility, CRT 240". Document no.: 37-1Y-AKS-X15-20018. 15.12.2010.
- [4] Alsgaard, J., "Numerical Investigation of Piston Mode Resonance in a Moonpool using OpenFOAM". M. Sc. Thesis, Norwegian University of Science and Technology, Department of Marine Technology. 14.06.2012.
- [5] Bernt, T., "Subsea Facililties". Offshore Technology Conference, OTC 16553. Huston, Texas, U.S.A, 3-6 May 2004.
- [6] Bjerkreim, B., Fydenlund, S., Lie, J. A., Staver, K. O., Haram, K. O., Nystad, B., Skofteland, H., Gedde, H., Tesei, A., Postic, M., "Ormen Lange Subsea Compression Pilot System". Offshore Technology Conference, OTC 20028. Huston, Texas, USA, 4-7 May 2009.
- [7] Conversation with Marie Sandøy 03.02.12, Shell graduate Hardware engineer.
- [8] Det Kongelige Olje- og Energidepartement, "Utbygging og drift av Ormen Lange og anlegg og drift av Langeled m.v.". St.prp. nr. 41, 2003-2004.
- [9] DNV, "Marine Operations, General". DNV-OS-H101, October 2011.
- [10] DNV, "MODELLING AND ANALYSISS OF MARINE OPERATIONS". DNV-RP-H103, April 2011.
- [11] Faltinsen, O. M., "Sea Loads on Ships and Offshore Structures". Cambridge University Press, 1998.
- [12] Gaillarde, G., Cotteleer, A., "Water Motion in Moonpools Empirical and Theoretical Approach". Proceedings of the Association Technique Maritime et Aeronautique, Paris, France. 2004.
- [13] Gansel, L. C., McClimans, T. A., Myrhaug, D., "The Effects of Fish Cages on Ambient Currents". Journal of Offshore Mechanics and Arctic Enginerering, February 2012, Vol. 134/ 011303-1.
- [14] Meeting with NTNU Marine Technology supervisors D. Myrhaug and B. J. Leira, Trondheim 22.03.12.
- [15] Meeting with P. C. Sandivik, MARINTEK A/S, Trondheim, 22.03.12.
- [16] Myrhaug, D., "Kompendium i TMR4180 Marin Dynamikk Uregelmessig sjø". Department of marine technology, Marine technology centre, Torndheim, Norway. January 2007.

- [17] Myrhaug, D., "Kompendium i TMR4235 Stochasitc Theory of Sealoads, Statistics of Narrow Band Processes and Equivalent Linearization". Department of marine technology, Marine technology centre, Trondheim, Norway.
- [18] Myrhaug, D., "TMR4235 Stochastic Theory of Sealoads. Copies from: D.E. Newland "An introduction to random vibrations, spectral and wavelet analysis", 1993, 3rd Edition". Department of Marine Technology, NTNU. August 2005.
- [19] Nordvik, B., Kilde, E., "Ormen Lange – Challenges in Offshore Project Execution". Offshore Technology Conference, OTC 18963. Huston, Texas, U.S.A, 30 April – 3 May 2007.
- [20] Pettersen, B., "Kompendium i TMR 4247 Marin Teknikk 3 Hydrodynamikk". Department of marine technology, Marine technology centre, Trondheim, Norway. January 2007.
- [21] Reistad, M., Breivik, Ø., Haakenstad, H., Aarnes, O. J., Furevik, B. R.,"A high-resolution hindcast of wind and waves for The North Sea, The Norwegian Sea and The Barents Sea". Norwegian Meteorological Institute, Report no. 2009/14, 22.12.2009.
- [22] Risoey, T., Mork, H., Johnsgard, H., Gramnaes, J., "The Pencil Buoy Method – A Subsurface Transportation and Installaion Method". Offshore Technology Conference, OTC 19040. Huston, Texas, U.S.A, 30 April – 3 May 2007.
- [23] Saipem, "Dynamic Lowering Analysis (MM Installation)". Ormen Lange Mid-North Development, Template C Installation. Document no.: 37-1B-SA2-O16-00008, 22.12.2011.
- [24] Sandvik, P. C., "Theory related to subsea lifting operations". Subsea Lifting Operations, Stavanger, November 27th -28th 2007.
- [25] Sandvik, P. C., "User's Manual MACSI-2". MARINTEK A/S , 15.02.1994
- [26] Shell, "Subsea Lifting and Rigging Analysis". Shell Deepwater Pipeline Systems, internal standard. Document no.: EPP-PS-77, 10.12.2009.
- [27] Shell, "Technical standard, Offshore Metocean Design and Operational Criteria (Vol. 3), General Criteria, Ormen Lange A, Block 6305/5". DEP 37.00.10.10-EPE, 29.09.2010.
- [28] Shell Shipping Technology, "General Arrangement Concept Design". Contractor drawing no.: 4853A00101R02, 07.02.2012.
- [29] Skofteland, H., Hilditch, M., Normann, T., Eriksson, K. G., Nyborg, K., Postic, M., Camatti, M., "Ormen Lange Subsea Compression Pilot – Subsea Comression Station". Offshore Technology Conference, OTC 20030. Huston, Texas, USA, 4-7 May 2009.
- [30] Solstad Shipping AS, "Arrangement on B-deck". Vik Sandvik project no.:3624, Drawing no.: 103-003.
- [31] Solstad Shipping AS, "Arrangement on 1st deck". Vik Sandvik project no.:3624, Drawing no.: 103-001.
- [32] Subsea 7, "NormandSubsea_EC1_RaoMACSI2.txt".
- [33] Subsea 7, "Protection Cover Installation Analysis Report, Garn West". Shell ISSC Project, Draugen Field – Norway. Document no.: DE3-25-JTU.T.2001, 31.08.2005.

- [34] Technip Norge AS, "Ormen Lange – Subsea Compression Installation and Intervention Study". Technical Study Report – Phase 1. Document no.: 37-1Y-NN-X15-00008, 25.03.2011.
- [35] Thurlow, J., "Normand Subsea Modification Study, Ormen Lange Gas Compression, Module Handling". Subsea 7, April 2012.
- [36] Torsethaugen, K., Haver, S., "Simplified double peak spectral model for ocean waves". ISOPE Touson, France. Paper no.: 2004-JSC-193, 2004.
- [37] Øritsland, O., "A Summary of Subsea Module Hydrodynamic Data". MARINTEK Report No. 511110.05, 1989.
- [38] http://emps.exeter.ac.uk/renewable-energy/research/research-interests/offshore/resource-assessment/facilities/floatingwavebuoys/
- [39] http://www.aerospaceweb.org/question/aerodynamics/q0215.shtml
- [40] http://www.certex.com/products/1.pdf
- [41] http://www.nov.com/Lifting_and_Handling/Cranes/Knuckle_Boom_Cranes.aspx
- [42] http://www.shell.no/home/content/nor/products_services/solutions_for_businesses/ep/ormenlange/no/facts/
- [43] http://sww.shell.com/ui/news/UIENews/AnIntroductiontoOrmenLangefromanEnvironmentalDesignperspective
- [44] http://www.subsea7.com/files/docs/Datasheets/Vessels/Normand_Subsea.pdf

Appendix 1: Ormen Lange Scatter Diagrams

Ormen Lange omnidirectional all year scatter diagram. Significant Wave Height H_S (m) vs. T_P (sec). Entries give the number of measured sea states in each H_S/T_P bin.

H_S Lower	H_S Upper	TP 1	2	3	4	5	6	7	8	9	10	11	12	13	14	15	16	17	18	19	20	21	22	23	24	25
14.5	15.0																									
14.0	14.5																									
13.5	14.0																2									
13.0	13.5																1									
12.5	13.0														4	1	2									
12.0	12.5														3	2	2									
11.5	12.0														8	4	4									
11.0	11.5													7	16	3	2									
10.5	11.0												1	5	15	13	3									
10.0	10.5												3	26	35	12	5									
9.5	10.0												21	34	39	16	8									
9.0	9.5											4	44	64	70	11	7									
8.5	9.0											19	82	135	101	27	18									
8.0	8.5											72	118	198	94	21	16						1			
7.5	8.0											190	275	318	170	28	26									
7.0	7.5										4	370	385	299	125	46	40									
6.5	7.0									2	11	577	488	284	168	61	26									
6.0	6.5									17	76	799	620	339	230	72	37	1								
5.5	6.0								4	71	201	982	671	387	259	99	42	2								
5.0	5.5								30	229	458	1436	713	464	342	112	72	3								
4.5	5.0							8	152	768	805	1239	1089	813	482	142	70	5								
4.0	4.5						4	64	449	1233	1346	1171	1139	969	530	229	100	9					4			
3.5	4.0						61	323	1106	1569	1418	1570	1512	1078	665	260	86	12					2			
3.0	3.5					5	290	957	1693	1642	1764	2010	1780	1183	779	264	77	16					6			
2.5	3.0					50	1054	1688	1875	1841	2391	2615	1962	1278	666	262	111	16					6			
2.0	2.5					298	2556	1948	2131	2753	3119	2625	2101	1388	605	260	92	24					10			
1.5	2.0				113	1408	3543	2448	3424	4071	3390	2720	2086	977	454	221	87	33					14			
1.0	1.5			15	638	2431	4264	3601	4354	3790	2947	2106	1108	545	252	212	96	30					6			
0.5	1.0		2	148	640	1643	3313	1865	1963	1664	1064	532	310	162	85	90	72	20								
0.0	0.5		1	9	3	28	32	37	25	19	15	6	2	1	1	37	16	8								
Sum		0	3	172	1394	5863	15117	12939	17206	19669	19009	21043	16510	10955	6198	2505	1120	179	0	0	0	0	49	0	0	0
Cumulative		0	3	175	1569	7432	22549	35488	52694	72363	91372	112415	128925	139880	146078	148583	149703	149882					149931			

Total number of measured waves: 149995. (Cumulative figures and some high-T_P/low-population cells are read from a dense rotated table and may contain minor transcription uncertainty.)

Figure 66: Ormen Lange omnidirectional all year scatter diagram, H_S and T_P [27]. In total 149995 waves are measured. High T_P values with no measurements are not included.
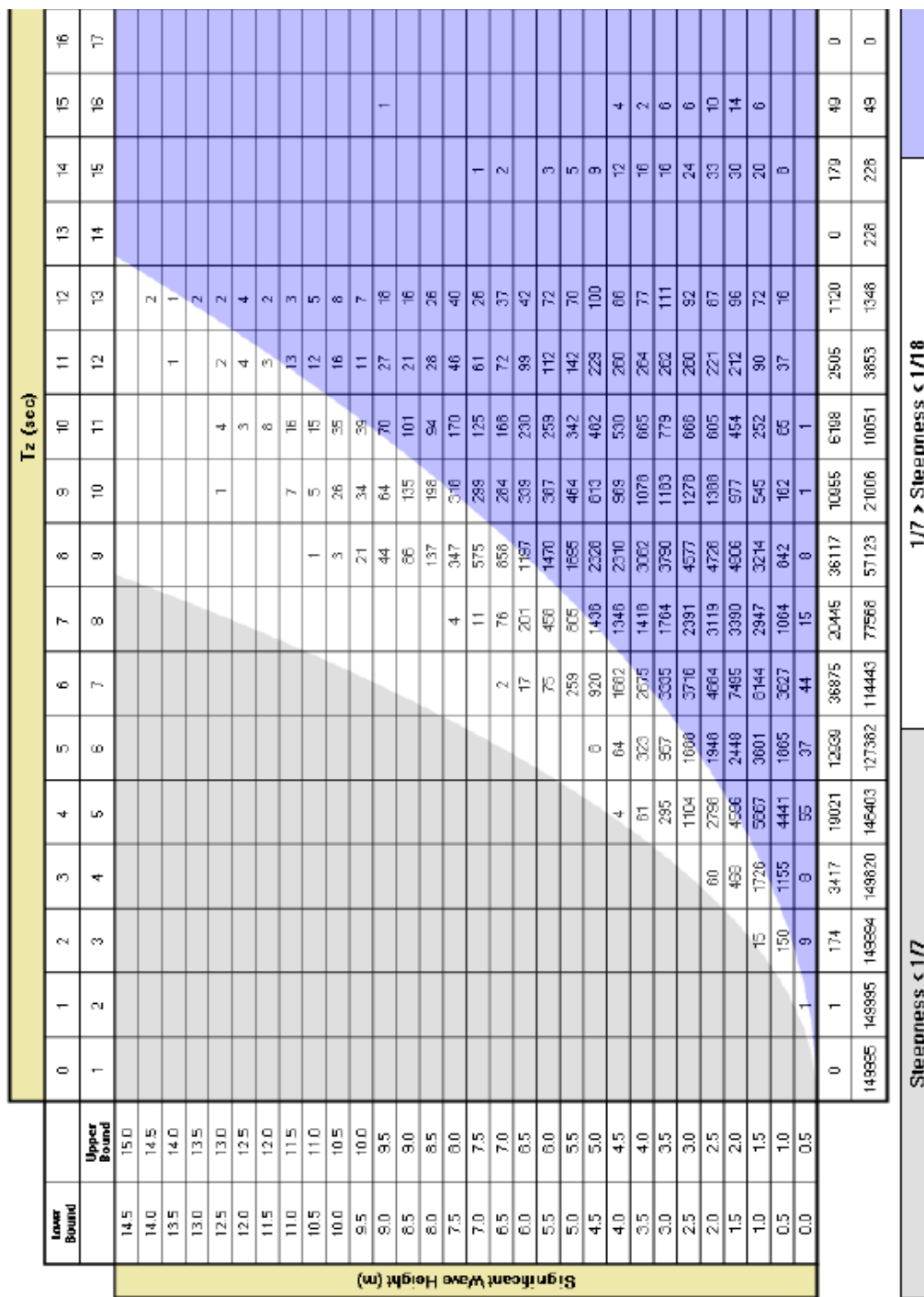
Figure 67: Ormen Lange omnidirectional all year scatter diagram, H_S and T_Z [27]. In total 149995 waves are measured. High T_Z values with no measurements are not included.

Appendix 2: Simplified Torsethaugen Wave Spectrum [36]

Note that the parameters used here are not included in the nomenclature.

Empirical parameters:

Parameter	Value
a_f	6.6 [sm$^{-1/3}$]
a_e	2.0 [sm$^{-1/3}$]
a_u	25 [s]
a_{10}	0.7
a_1	0.5
k_g	35.0
b_1	2.0 [s]
a_{20}	0.6
a_2	0.3
a_3	6.0

<u>Fully developed sea peak period for the location:</u>

$$T_{pf} = a_f H_s^{1/3}$$

Equation 49

If $T_p \leq T_{pf}$ the primary spectral peak corresponds to the local wind sea system, while if $T_p > T_{pf}$ the primary spectral peak corresponds to the swell sea system.

<u>Wave period scale factors:</u>

For each of the sea systems a non-dimensional period scale is introduced by using a lower an upper value of T_P. The two limits, lower and then upper respectively equals:

$$T_l = a_e H_s^{1/2}$$

Equation 50

$$T_u = a_u$$

Equation 51

Non-dimensional scales for the spectral peak period are defined as follows, wind sea then swell sea respectively:

$$\epsilon_l = \frac{T_{pf} - T_p}{T_{pf} - T_l}$$

Equation 52

$$\epsilon_u = \frac{T_p - T_{pf}}{T_u - T_{pf}}$$

Equation 53

Note that for values of T_p below T_l or above T_u $\epsilon = 1$.

<u>Spectral parameters for wind dominated sea $T_p \leq T_{pf}$:</u>

Primary peak:

- Significant wave height:

$$H_{w1} = R_w H_s \qquad \text{Equation 54}$$

$$R_w = (1 - a_{10})e^{-\left(\frac{\epsilon_l}{a_1}\right)^2} + a_{10} \qquad \text{Equation 55}$$

- Spectral peak period:

$$T_{pw1} = T_p \qquad \text{Equation 56}$$

- Peak enhancement factor:

$$\gamma = k_g s_p^{\frac{6}{7}} \qquad \text{Equation 57}$$

$$S_p = \frac{2\pi}{g} \frac{H_{w1}}{T_{pw1}^2} \qquad \text{Equation 58}$$

Secondary peak:

- Significant wave height:

$$H_{w2} = (1 - R_w^2)^{\frac{1}{2}} H_s \qquad \text{Equation 59}$$

- Spectral peak period:

$$T_{pw2} = T_{pf} + b_1 \qquad \text{Equation 60}$$

- Peak enhancement factor:

$$\gamma = 1 \qquad \text{Equation 61}$$

Spectral parameters for swell dominated sea $T_p > T_{pf}$:

Primary peak:

- Significant wave height:

$$H_{s1} = R_s H_s \qquad \text{Equation 62}$$

$$R_s = (1 - a_{20})e^{-\left(\frac{\epsilon_u}{a_2}\right)^2} + a_{20} \qquad \text{Equation 63}$$

- Spectral peak period:

$$T_{ps1} = T_p \qquad \text{Equation 64}$$

- Peak enhancement factor:

$$\gamma = \gamma_f(1 + a_3\epsilon_u) \qquad \text{Equation 65}$$

$$\gamma_f = k_g s_f^{\frac{6}{7}} \qquad \text{Equation 66}$$

$$s_f = \frac{2\pi}{g}\frac{H_s}{T_{pf}^2} \qquad \text{Equation 67}$$

Secondary peak:

- Significant wave height:

$$H_{s2} = (1 - R_s^2)^{\frac{1}{2}} H_s \qquad \text{Equation 68}$$

- Spectral peak period:

$$T_{ps2} = a_f H_{s2}^{1/3} \qquad \text{Equation 69}$$

- Peak enhancement factor:

$$\gamma = 1 \qquad \text{Equation 70}$$

Resulting spectral formula:

$$S(f_n) = \sum_{j=1}^{2} E_j S_{jn}(f_{jn}) \qquad \text{Equation 71}$$

j = 1 primary sea system, j = 2 secondary peak system

$$E_1 = \frac{1}{16}H_1^2 T_{p1} \qquad \text{Equation 72}$$

$$E_2 = \frac{1}{16}H_2^2 T_{p2} \qquad \text{Equation 73}$$

$$S_{1n}(f_{1n}) = G_0 A_\gamma f_{1n}^{-4} e^{-f_{1n}^{-4}} \gamma^{e^{-\frac{1}{2\sigma^2}(f_{1n}-1)^2}} \qquad \text{Equation 74}$$

$$S_{2n}(f_{2n}) = G_0 f_{2n}^{-4} e^{-f_{2n}^{-4}} \qquad \text{Equation 75}$$

$f_{1n} = fT_{p1}$, $f_{2n} = fT_{p2}$, $G_0 = 3.26$, $A_\gamma = \frac{1+1.1\ln(\gamma)^{1.19}}{\gamma}$ and $\sigma = 0.07$ for $f_n < 1$ and $\sigma = 0.09$ for $f_n > 1$

For wind dominated sea cases:

$H_1 = H_{w1}$ and $H_2 = H_{w2}$

$T_{p1} = T_{pw1}$ and $T_{p2} = T_{pw2}$

For swell dominated sea cases:

$H_1 = H_{s1}$ and $H_2 = H_{s2}$

$T_{p1} = T_{ps1}$ and $T_{p2} = T_{ps2}$

Appendix 3: Bid Hydra High Performance Wire Data

Necessary safe working load (SWL) and minimum breakage load (MBL) of the lifting wire:

$$SWL = 0.5 * Static\ weight\ of\ object\ in\ air * DAF = 0.5 * 250\ [t] * 2.0 = 250\ [t]$$

<div align="right">Equation 76</div>

The SWL is divided by two since a double fall wire system is applied. A nominal safety factor γ_{SF} of 5 gives the following MBL:

$$MBL = SWL \cdot \gamma_{SF} = 250\ [t] \cdot 5 = 1250\ [t] \qquad \text{Equation 77}$$

As MACSI2 analyses are run for the module being fully submerged with its top end 0.5 [m] below the MWL the wire length l_w is not long. It equals the length of wire from the crane tip/ main sheave in MHT to the volume center of the module in z-direction. Wire length is hence dependent on deployment method:

$$l_w = ct_z + top\ end\ submergence + 0.5 \cdot module\ height$$

$$= 30.31\ [m] + 0.5\ [m] + 0.5 \cdot 12\ [m] = 36.81\ [m] \qquad \text{Equation 78}$$

$$l_w = ms_z + top\ end\ submergence + 0.5 \cdot module\ height$$

$$= 24.19\ [m] + 0.5\ [m] + 0.5 \cdot 12\ [m] = 30.69\ [m] \qquad \text{Equation 79}$$
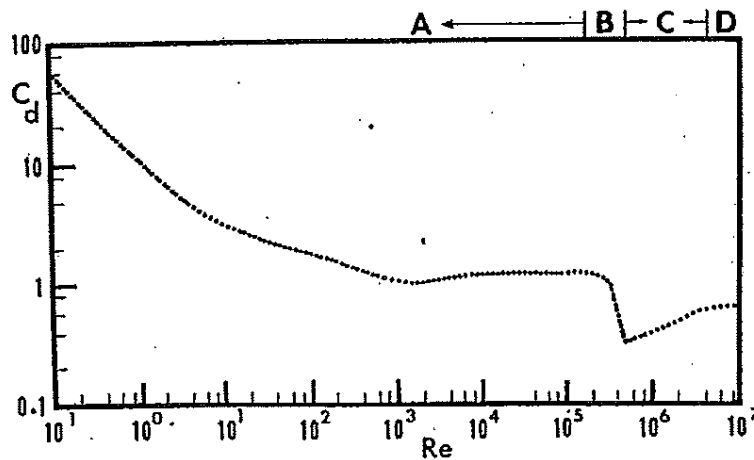
Figure 68: 2D drag coefficient for circular cylinder as function of Re number [37].

Also the wire rope drag coefficient must be estimated. The graph in Figure 78, Appendix 8 should not be used. That is because 3D shapes are given, and here the drag coefficient should be

the 2D drag coefficient since wire rope end effects will not be present. In Appendix 8 it is found that the DNV procedure seems reasonable. There it is corrected for oscillatory flow and hence KC by multiplying the steady flow coefficient by a factor of 2. This method is applied. Based on Figure 68 the steady flow drag coefficient is taken as 0.6 ($R_e = 4.3 \cdot 10^6 - 2.4 \cdot 10^7$), and corrected for KC the coefficient becomes $C_{Dw} = 1.2$.

Table 19 equals the Big Hydra wire rope selection table from which the wire rope is selected. The wire rope with MBL closes to 1259 [t] (but above) is used.

Rope diameter		Approximate mass				Minimum breaking force (Fmin)			Axial stiffness @20% load		Torque generated @20% load Lang's		Metallic cross section	
		In air		Submerged										
mm	in	kg/m	lb/ft	kg/m	lb/ft	kN	Tonnes	2000lbs	MN	Mlbs	kN.m	lbs.ft	mm²	in²
76	3	26.1	17.6	22.7	15.3	4747	484	533	295	66	3.68	2717	2813	4.36
76.2	3	26.3	17.7	22.9	15.4	4777	487	537	297	67	3.72	2742	2828	4.38
80		29.0	19.5	25.2	16.9	5249	535	590	327	74	4.18	3083	3117	4.83
82.6	3¼	30.9	20.8	26.9	18.1	5581	569	627	349	78	4.54	3351	3323	5.15
84		31.9	21.4	27.8	18.6	5778	589	649	361	81	4.84	3569	3436	5.33
88		35.0	23.5	30.5	20.5	6071	619	682	396	89	5.43	4004	3771	5.85
88.9	3½	35.7	24.0	31.1	20.9	6194	631	696	404	91	5.57	4106	3849	5.97
92		38.3	25.7	33.3	22.4	6634	676	745	433	97	6.36	4688	4122	6.39
95.3	3¾	41.0	27.6	35.7	24.0	7086	722	796	464	104	6.79	5009	4423	6.86
96		41.6	28.0	36.2	24.3	7198	734	809	471	106	6.99	5155	4488	6.96
100		45.2	30.4	39.3	26.4	7797	795	876	511	115	8.17	6021	4870	7.55
101.6	4	46.7	31.4	40.6	27.3	8103	826	910	528	119	8.31	6127	5027	7.79
108	4¼	52.9	35.5	46.0	30.9	9076	925	1020	596	134	9.84	7253	5680	8.80
114.3	4½	59.1	39.7	51.4	34.6	10121	1032	1137	668	150	11.68	8616	6362	9.86
120.7	4¾	66.1	44.4	57.5	38.6	11240	1146	1263	745	167	13.69	10091	7095	11.00
127	5	73.1	49.1	63.6	42.7	12355	1259	1388	825	185	15.81	11661	7855	12.18
133.4	5¼	80.9	54.4	70.4	47.3	13616	1388	1530	910	205	18.10	13346	8666	13.43
139.7	5½	88.5	59.5	77.0	51.7	14726	1501	1654	998	224	20.77	15316	9504	14.73

Table 19: Big Hydra wire rope selection table [40].

Wire diameter: $d_w := 0.127 m$

Mass per unit length: $m_w := 73.10 \dfrac{kg}{m}$

MBL: $MBL := 1259 t$

Axial stiffness at 20% load: $k := 825 MN$

Metallic cross section: $A_{metallic} := 0.007855 m^2$

Circumscribed rope area: $A_{outer} := \pi \cdot \dfrac{d_w^2}{4} = 0.013 m^2$

Wire fill factor: $c_f := \dfrac{A_{metallic}}{A_{outer}} = 0.62$

Apparent Young's modulus at 20% load: $E_{ap} := \dfrac{k}{A_{outer}} = 6.513 \times 10^{10} Pa$

Steel Young's modulus: $E_s := \dfrac{E_{ap}}{c_f} = 1.05 \times 10^{11} Pa$

Appendix 4: Crane Tip Coordinates

In [32] Normand Subsea's LCG is given for fully loaded condition, LCG = 46.52 [m] forward of AP. This LCG value is given for VCG = 9.99 [m] and is not the CoG at MWL, but it is assumed valid at MWL since no other information is provided. From the arrangement drawing of Normand Subsea's 1 deck displayed in Figure 69 can the longitudinal and lateral positions of the crane pedestal be measured. Frames are marked and the frame spacing given. The longitudinal distance between LCG and crane tip is assumed equal to the longitudinal distance between LCG and crane pedestal.
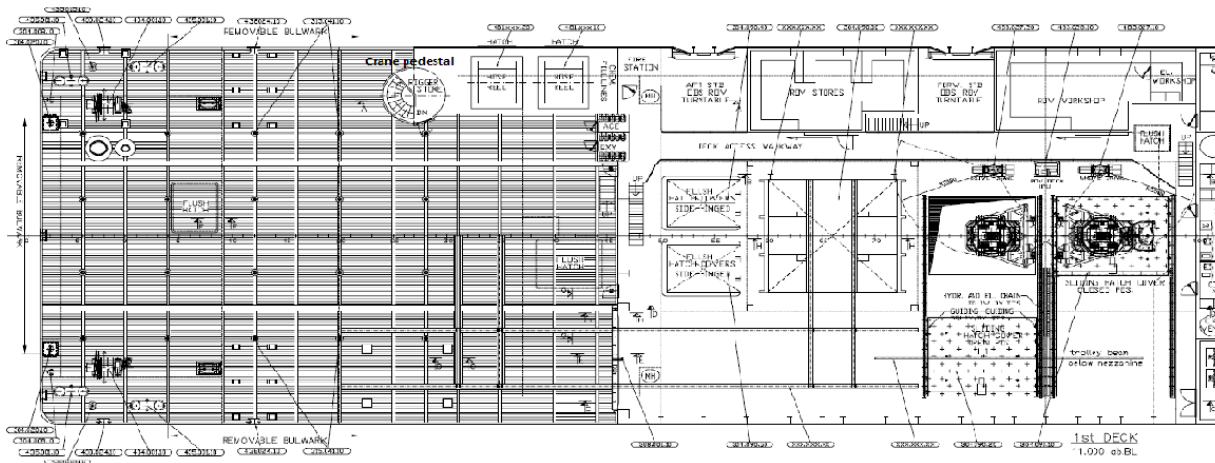
Figure 69: 1st deck arrangement drawing, Normand Subsea [31].

The lateral distance from the longitudinal centerline of Normand Subsea to the crane pedestal is also measured form the same arrangement drawing. This length is measured to equal about 9.3 [m]. As the width of the ship is 24 [m] the residual length from the crane pedestal to the ship side is 2.7 [m]. The length between the center of the crane pedestal and the crane tip, which is assumed located in the module center, is taken from the Skandi Acergy main crane curve, see Figure 72. It is important to remember that the distance between structure and hull must be optimized regarding safety of both the module and vessel side. But the further away out from the vessel side the unit is positioned during lowering the larger motions and hence less availability. Optimized distance is taken as 5 [m] to obtain conservative results based on Shell in-house experience. In Figure 71 the lateral lengths mentioned are illustrated. The crane tip is then placed in the area where the Skandi Acergy main crane has optimal capacity. Crane tip position is marked on the crane curve in Figure 72.

The z-coordinate of the crane tip is the distance between the crane tip and deck plus the deck freeboard. In Figure 70 is the minimum length between the crane tip and deck calculated. Note that minimum sling angle of 60° is taken from [33]. Deck freeboard on Normand Subsea can be found from the information in Chapter 5 Normand Subsea; vessel depth minus fully loaded draft.

Resulting crane tip coordinates:

$$ct_x = LCG\ location\ forward\ of\ AP - crane\ pedestal\ location\ forward\ of\ AP$$

$$= 46.52\ [m] - (27\ frames \cdot 0.6\ [m]) = 30.32\ [m] \qquad \text{Equation 80}$$

$$ct_y = half\ width\ of\ ship + load\ overboarding\ distance + half\ width\ of\ module$$

$$= (9.3\ [m] + 2.7[m]) + 5[m] + 3[m] = 20.00\ [m] \qquad \text{Equation 81}$$

$$ct_z = crane\ tip\ height\ above\ deck + vessel\ depth - fully\ loaded\ draft$$

$$= 27.12\ [m] + 11\ [m] - 7.81\ [m] = 30.31\ [m] \qquad \text{Equation 82}$$

Figure 70: Minimum crane tip height above deck
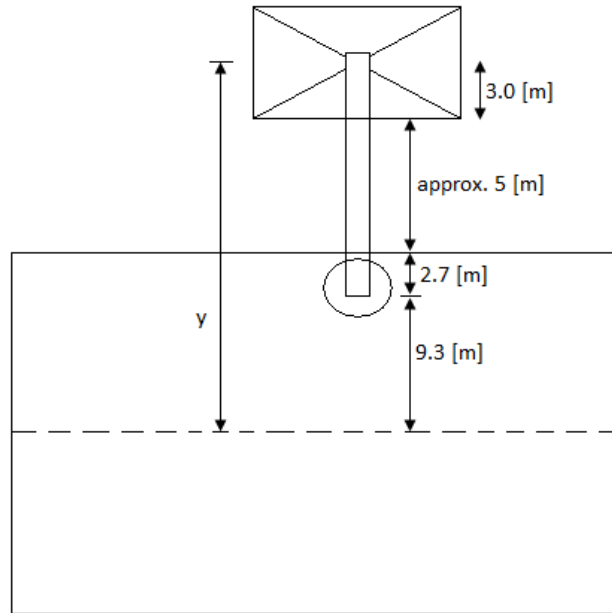
Figure 71: Lateral distances considered during lowering.
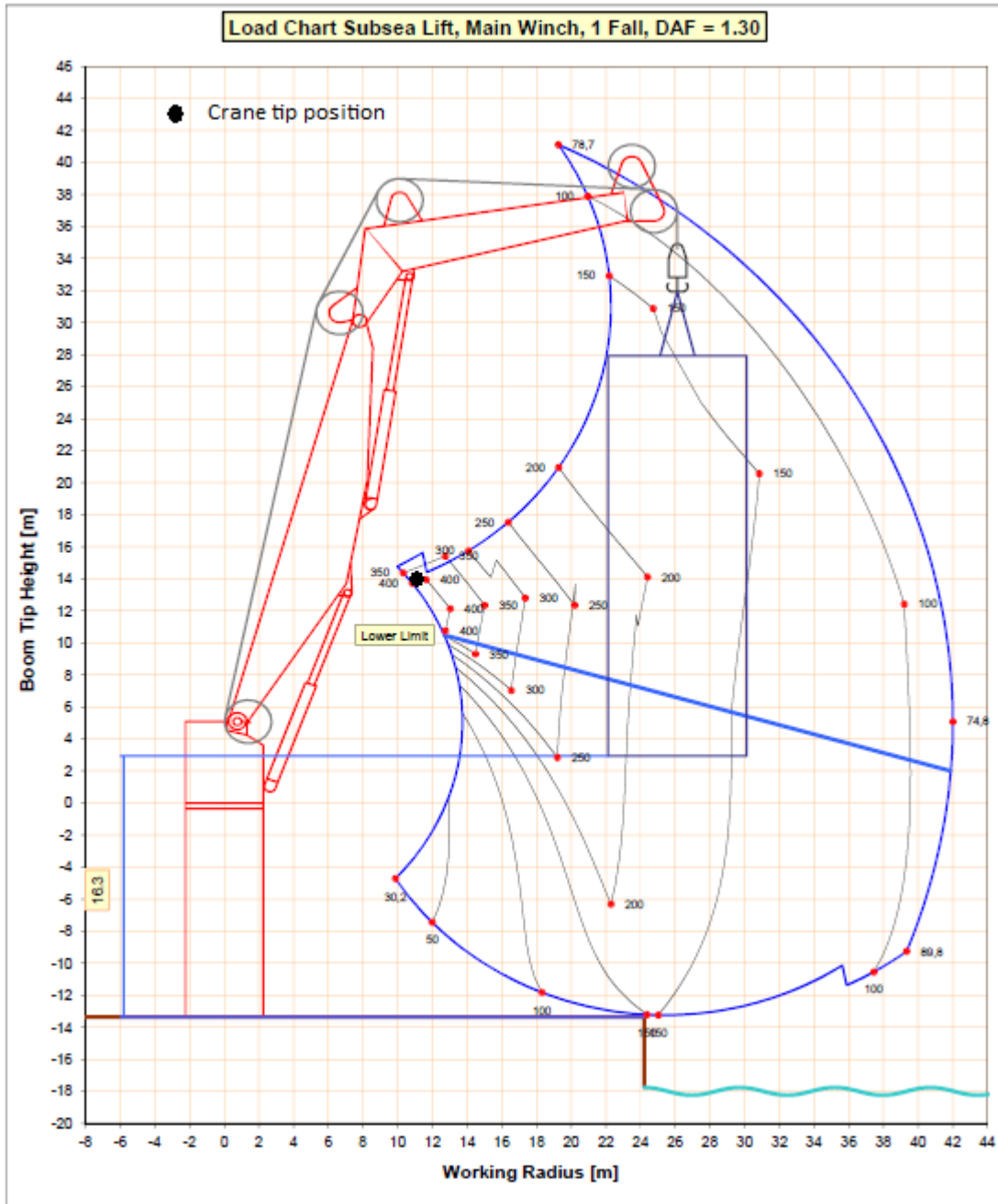
Figure 72: Skandi Acergy main crane curve.

Appendix 5: Moonpool Main Sheave Coordinates

As previously stated moonpool center is as is on Normand Subsea, but dimensions are changed. It is assumed to be 14 [m] long and 7.5 [m] wide. But since the new cursor system is unknown it is assumed that the center of the module will be in the center of the moonpool during deployment. For optimized lowering the main sheave is assumed to be located in the top of the MHT above the lowered unit's CoG. The x-coordinate of the main sheave compared to the vessel's LCG at MWL is found by taking the vessel's LCG at MWL forward of AP and subtract the distance form AP to the center of the moonpool. Because the moonpool is located symmetrically about the longitudinal vessel centerline the main sheave y-coordinate is taken as 0.

Tower lift height must include the height of storing pallet plus skid rails, module, lift frame and cursor. In addition is has to lift the module of the deck. The main sheave, assumed located in the top of the module handling tower, z-coordinate is hence found by adding tower lift height and deck freeboard.

Resulting coordinates for the moonpool main sheave:

$$ms_x = LCG\ location\ forward\ of\ AP - moonpool\ center\ location\ forward\ of\ AP$$

$$= 46.52\ [m] - (66\ \text{frames} \cdot 0.6\ [m]) = 6.92\ [m] \qquad \text{Equation 83}$$

$$ms_y = 0\ [m] \qquad \text{Equation 84}$$

$$ms_z = pallet\ and\ skidd\ rails + module\ height + lift\ frame + cursor + lift$$
$$+ vessel\ depth - fully\ loaded\ vessel\ draft$$

$$= 1.0\ [m] + 12\ [m] + 2\ [m] + 5\ [m] + 1\ [m] + 11\ [m] - 7.81\ [m] = 24.19\ [m]$$

$$\text{Equation 85}$$

Appendix 6: Module Details

- Perforation rate:

  It is hard to set a perforation rate on such a structure without any drawings. Perforation is taken as where water can flow freely through the unit without disturbance. What is known is that structures for the future compression system are expected to be quite complex containing much tubing and equipment. Perforation is hence assumed to be low in all directions. Somewhere in the range 0-5 % is assumed and $p_x = p_y = p_z = 5$ % will be applied. This is a conservative assumption as perforation will reduce added mass. Low perforation means higher added mass and increased hydrodynamic forces, see Equation 42.

- The structure's CoG:

  The structure's CoG is assumed to be located in the volume center since nothing else is known.

- Object volume V_m:

  The object mass is 250 [t] in air including rigging. To find the submerged mass it is assumed that all volumes inside the structure are water filled before submergence. This additional weight of water is assumed comprised in the object mass. As the structure is made of steel the submerged weight can be found by:

$$F_S = F_G - B \qquad \text{Equation 86}$$

  F_S is the submerged weight, F_G is the weight in air and B is the buoyancy. The buoyancy equals the weight of the water displaced by the structure:

$$B = g\rho_w V_m = g\rho_w \frac{M_m}{\rho_{steel}} = \rho_w \frac{F_G}{\rho_{steel}} \qquad \text{Equation 87}$$

  Insert Equation 87 into Equation 86:

$$F_S = F_G - \rho_w \frac{F_G}{\rho_{steel}} = F_G\left(1 - \frac{\rho_{steel}}{\rho_w}\right) = F_G\left(\frac{\rho_{steel}-\rho_w}{\rho_{steel}}\right) \qquad \text{Equation 88}$$

  Module volume can now be computed by using Equations 86-88:

$$V_m = \frac{F_G - F_S}{g\rho_{water}} = \frac{250[t] - 250[t]\left(\frac{7.850 - 1.025\left[\frac{t}{m^3}\right]}{7.850}\right)}{9.81\left[\frac{m}{s^2}\right] \cdot 1.025\left[\frac{t}{m^3}\right]} = 31.8\ [m^3] \qquad \text{Equation 89}$$

- Projected areas x-, y- and z-direction A_{mx}, A_{my} and A_{mz}:

  Solid projected areas for the three directions are found by multiplying the projected side lengths and correct for perforation:

$$A_{mx} = w_m h_m (1 - p_x) = 6 \cdot 12 \,[m^2](1 - 0.05) = 68.4 \,[m^2] \qquad \text{Equation 90}$$

$$A_{my} = l_m h_m (1 - p_y) = 12 \cdot 12 \,[m^2](1 - 0.05) = 136.8 \,[m^2] \qquad \text{Equation 91}$$

$$A_{mz} = l_m w_m (1 - p_z) = 12 \cdot 6 \,[m^2](1 - 0.05) = 68.4 \,[m^2] \qquad \text{Equation 92}$$

Appendix 7: Added Mass Calculations from MatCad

Macsi2 input:

Defining constants.

$$t := 1000 kg$$

$$\rho_{swater} := 1025 \frac{kg}{m^3}$$

$$\rho_{steel} := 7850 \frac{kg}{m^3}$$

Water depth: $\quad d := 850 m$

Module details:

Note:CoG and CoB are assumed located in the module center.

Module dimensions: $\quad l_m := 12m \qquad w_m := 6m \qquad h_m := 12m$

Assumed perforation: $\quad p_x := 5\% \qquad p_y := 5\% \qquad p_z := 5\%$

Projected area: $\quad A_{m\_x} := w_m \cdot h_m \cdot (1 - p_x) \qquad\qquad A_{m\_x} = 68.4 m^2$

$$A_{m\_y} := l_m \cdot h_m \cdot (1 - p_y) \qquad\qquad A_{m\_y} = 136.8 m^2$$

$$A_{m\_z} := l_m \cdot w_m \cdot (1 - p_z) \qquad\qquad A_{m\_z} = 68.4 m^2$$

Module mass inc. rigging: $\quad M_m := 250 t$

Module dry weight inc. rigging: $\quad F_G := M_m \cdot g \qquad\qquad F_G = 2.452 \times 10^6 N$

Module submerged weight: $\quad F_S := F_G \cdot \dfrac{(\rho_{steel} - \rho_{swater})}{\rho_{steel}} \qquad F_S = 2.132 \times 10^6 N$

Module volume: $\quad V_B := \dfrac{F_G - F_S}{g \cdot \rho_{swater}} = 3.185 \times 10^4 L$

Added mass for the module
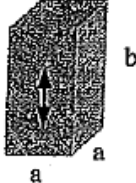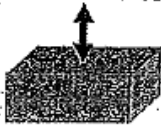
Geometry		Formula	b/a	α	β
{1} Rectangular block with quadratic base Ref. [1]	b a a a = base edge	$m_a = \alpha \rho V$ $= \beta \rho V_p$ Block volume: $V = a^2 b$ Volume related to m_a of quadratic plate: $V_p = 0.579 \cdot \dfrac{\pi a^3}{4}$	0 0.1 0.3 0.50 0.75 1.00 1.25 1.60 2.00 2.40 2.80 3.60	- 5.139 2.016 1.310 0.916 0.705 0.575 0.458 0.373 0.316 0.274 0.217	1.00 1.13 1.33 1.44 1.51 1.55 1.58 1.61 1.64 1.67 1.69 1.72
{2} Rectangular block with rectangular base		Approximation: $m_a = \alpha \beta \rho V_c$ Cylinder volume, V_c	α and V_c from rectangular plate, {1}, Table 1. β from {1}, this table.		

Figure 73: Table 2 in [24] used to compute added mass.
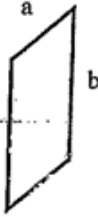
Geometry		Formula	b/a	α	β
{1} Rectangular Ref. [1]	a b a = shortest edge	$m_a = \alpha \rho V_c$ Cylinder volume: $V_c = \dfrac{\pi a^2}{4} b$	1.0 1.2 1.25 1.33 1.5 2.0 2.5 3.0 4.0 5.0 8.0 10.0	0.579 0.630 0.642 0.660 0.691 0.757 0.801 0.830 0.871 0.897 0.934 0.947	

Figure 74: Table 1 in [24] used to compute added mass.

$$\text{ratio}_2 := \begin{pmatrix} 1.0 \\ 1.2 \\ 1.25 \\ 1.33 \\ 1.5 \\ 2.0 \\ 2.5 \\ 3.0 \\ 4.0 \\ 5.0 \\ 8.0 \\ 10.0 \end{pmatrix} \qquad \alpha_2 := \begin{pmatrix} 0.570 \\ 0.630 \\ 0.642 \\ 0.680 \\ 0.691 \\ 0.757 \\ 0.801 \\ 0.830 \\ 0.871 \\ 0.897 \\ 0.934 \\ 0.947 \end{pmatrix}$$

$$\text{ratio}_1 := \begin{pmatrix} 0.00 \\ 0.10 \\ 0.30 \\ 0.50 \\ 0.75 \\ 1.00 \\ 1.25 \\ 1.60 \\ 2.00 \\ 2.40 \\ 2.80 \\ 3.60 \end{pmatrix} \qquad \beta_1 := \begin{pmatrix} 1.00 \\ 1.13 \\ 1.33 \\ 1.44 \\ 1.51 \\ 1.55 \\ 1.58 \\ 1.61 \\ 1.64 \\ 1.67 \\ 1.69 \\ 1.72 \end{pmatrix} \qquad \alpha_1 := \begin{pmatrix} 0 \\ 5.139 \\ 2.016 \\ 1.310 \\ 0.916 \\ 0.705 \\ 0.575 \\ 0.453 \\ 0.373 \\ 0.318 \\ 0.274 \\ 0.217 \end{pmatrix}$$

Perforation coeff.:

$$C_{px} := e^{\left(\frac{-p_x \cdot 100}{28} \right)} \qquad C_{px} = 0.836$$

$$C_{py} := e^{\left(\frac{-p_y \cdot 100}{28} \right)} \qquad C_{py} = 0.836$$

$$C_{pz} := e^{\left(\frac{-p_z \cdot 100}{28} \right)} \qquad C_{pz} = 0.836$$

X-direction:

Length: $a := w_m$ $a = 6m$

Width: $b := h_m$ $b = 12m$

Ratio b/a: $ratio_{ba} := \dfrac{b}{a}$ $ratio_{ba} = 2$

Alfa: $\alpha_{ba} := linterp(ratio_2, \alpha_2, ratio_{ba})$ $\alpha_{ba} = 0.757$

Length: $a := w_m$ $a = 6m$

Width: $b := l_m$ $b = 12m$

Ratio b/a: $ratio_{ba} := \dfrac{b}{a}$ $ratio_{ba} = 2$

Betta: $\beta_{ba} := linterp(ratio_1, \beta_1, ratio_{ba})$ $\beta_{ba} = 1.64$

Added mass: $M_{added\_x} := \alpha_{ba} \cdot \beta_{ba} \cdot \rho_{swater} \cdot \pi \cdot w_m^2 \cdot \dfrac{h_m}{4}$

$M_{added\_x} = 4.318 \times 10^5 \, kg$

Mass coefficient: $C_{Ax} := \dfrac{M_{added\_x}}{\rho_{swater} \cdot V_B}$ $C_{Ax} = 13.226$

Y-direction:

Length: $a := l_m$ $a = 12m$

Width: $b := w_m$ $b = 6m$

Ratio b/a: $ratio_{ba} := \dfrac{b}{a}$ $ratio_{ba} = 0.5$

Alfa: $\alpha_{ba} := linterp(ratio_1, \alpha_1, ratio_{ba})$ $\alpha_{ba} = 1.31$

Betta: $\beta_{ba} := linterp(ratio_1, \beta_1, ratio_{ba})$ $\beta_{ba} = 1.44$

Added mass:

$$M_{added\_y} := \beta_{ba} \cdot \rho_{swater} \cdot 0.579\pi \cdot \frac{a^3}{4}$$

$$M_{added\_y} = 1.16 \times 10^6 \, kg$$

Mass coefficient:

$$C_{Ay} := \frac{M_{added\_y}}{\rho_{swater} \cdot V_B} \qquad\qquad C_{Ay} = 35.531$$

Z-direction:

Length:
$$a := w_m \qquad\qquad a = 6m$$

Width:
$$b := l_m \qquad\qquad b = 12m$$

Ratio b/a:
$$ratio_{ba} := \frac{b}{a} \qquad\qquad ratio_{ba} = 2$$

Alfa:
$$\alpha_{ba} := linterp(ratio_2, \alpha_2, ratio_{ba}) \qquad\qquad \alpha_{ba} = 0.757$$

Length:
$$a := w_m \qquad\qquad a = 6m$$

Width:
$$b := h_m \qquad\qquad b = 12m$$

Ratio b/a:
$$ratio_{ba} := \frac{b}{a} \qquad\qquad ratio_{ba} = 2$$

Betta:
$$\beta_{ba} := linterp(ratio_1, \beta_1, ratio_{ba}) \qquad\qquad \beta_{ba} = 1.64$$

Added mass:
$$M_{added\_z} := \alpha_{ba} \cdot \beta_{ba} \cdot \rho_{swater} \cdot \pi \cdot w_m^2 \cdot \frac{l_m}{4}$$

$$M_{added\_z} = 4.318 \times 10^5 \, kg$$

Mass coefficient:
$$C_{Az} := \frac{M_{added\_z}}{\rho_{swater} \cdot V_B} \qquad\qquad C_{Az} = 13.226$$

Appendix 8: Drag Coefficients

Assume a two dimensional circular cylinder completely surrounded by water as in Figure 75 a). If the fluid flow around the cylinder is potential, irrotational and incompressible, the fluid will have tangential velocity at the cylinder surface. This tangential velocity U_e is expressed by the following relation; $U_e = 2U_\infty \sin \theta$. U_∞ is the incident fluid velocity and θ is an angular coordinate. The pressure forces on the cylinder under these conditions will cancel each other [11]. The pressure from $\theta = 0°\text{-}\pm90°$ is equal to the pressure from $\theta = \pm90°\text{-}\pm180°$, as shown in Figure 75 b), making the total net forces in lift and drag direction zero. The total zero drag force described here is known as D'Alemberts paradox.

In reality there is no tangential velocity on the cylinder surface. Due to the no-slip condition, claiming the velocity of the fluid to equal the surface velocity of the cylinder, the fluid velocity has to be zero. In a small region from the body surface the fluid velocity will increase from zero to the tangential velocity obtained by assuming ideal fluid. This region is called the boundary layer. Its thickness depends strongly on the Reynolds number R_e. R_e is defined as $R_e = \frac{U_\infty D}{v}$ where D is the characteristic length of the body, here the diameter, and v is the kinematic viscosity of water. Increasing R_e results in the development of vortices shed from separation points.
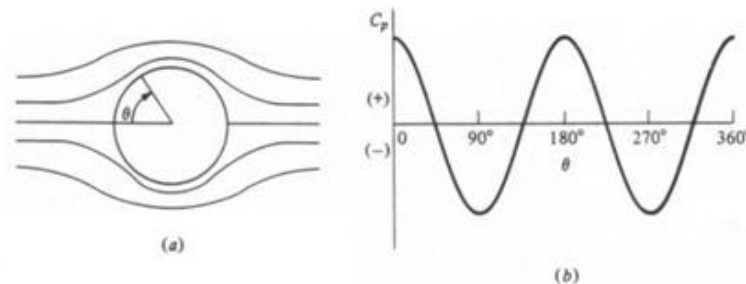
Figure 75: a) Potential flow around a cylinder. b) The resulting pressure coefficient C$_P$. [39].

Separation points are where the fluid detaches from the body surface. What happens when a fluid particle moves from $\theta = 0°$ to $\theta = \pm90°$ is that it experiences decreasing pressure from the stagnation point, $\theta = 0°$. After $\theta = \pm90°$ the pressure starts to increase, causing an ambient pressure gradient on the particle. The particle will be slowed down until it has zero forward speed as the pressure increases, and then it separates from the surface. Vortices will then tend to form.

It is assumed that the pressure can be found from potential theory for θ between - 90° and +90° [11]. On the lee side of the cylinder, between the separation points, it is seen that the pressure is almost constant but strongly dependent on Reynolds number. See Figure 76. The pressure is therefore taken as constant for other θ values then values between - 90° and +90°. As a result of the pressure difference upstream and downstream of the cylinder a drag force is created in the direction of the inflow. An error is introduced by the way pressure is modeled at $\theta = \pm90°$ but

this is neglected since the contribution to the drag force is low. Shear forces due to surface friction will also contribute to the drag force but the contribution is only 1-3 % of the pressure contribution. Here drag force is taken as F_d and the drag coefficient is then defined:

$$C_d = \frac{F_d}{\frac{1}{2}\rho_w U_\infty^2 A_m}$$

Equation 93
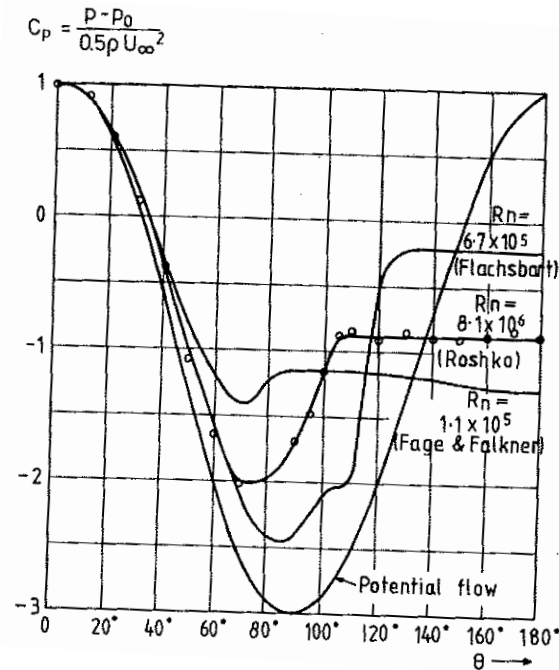
Figure 76: Average pressure distribution p around a smooth circular cylinder in steady incident flow [11].

This is in reality the quadratic drag coefficient since it is dependent on velocity squared. In addition linear drag coefficients are requested in MACSI2, but after consulting Peter Christian Sandvik, the creator of MACSI2, he said to ignore it or at most set the linear drag coefficient equal to 0.2 in all directions for the case considered in this report [15].

Drag force is naturally dependent on geometrical shape and will exist as long as there is pressure difference upstream and downstream of a body and/or surface friction. To estimate the drag coefficients Reynolds numbers are needed. The values are found based on inflow velocity, characteristic dimension and water kinematic viscosity. The inflow velocity is estimated based on a formula in [10] for characteristic wave particle velocity in the vertical direction:

$$v_z = \zeta_a \left(\frac{2\pi}{T_z}\right) e^{-\frac{4\pi^2 d}{T_z^2 g}}$$

Equation 94

$$\zeta_a = 0.9 H_s$$

Equation 95

ζ_a is then characteristic wave amplitude. Sea state values are in the range $H_s = 2.0$ - 5.5 [m] and $T_z = 4.7$ - 13.2 [s]. These T_z values are taken from Tables 2 and 3 and are here used to get the largest range in vertical velocities. d is the distance from MWL to center of gravity of the submerged part of the objet, which here equals 6 [m] + 0.5 [m] since CoG is located in the volume centre of the unit and the top end is fixed 0.5 [m] below MWL. Inserting upper and lower H_s and T_z values together with d in Equations 94 and 95 gives following range of vertical free surface water particle velocity; $v_z = 0.72 - 2.0$ [m/s]. Note that as wave particle motions are circular at deep water the characteristic velocity in x- and y- directions equal the characteristic velocity in z- direction. The characteristic length of the object ranges from 6 [m] in y – direction to 12 [m] in x- and z- directions while water kinematic viscosity equals 10^{-6} [m²/s]. Resulting range of Re numbers are therefore:

$$R_{e\_min} = \frac{v_{ymin}D_y}{\nu} = \frac{0.72\left[\frac{m}{s}\right]\cdot 6\,[m]}{10^{-6}\,[\frac{m2}{s}]} = 4.3 \cdot 10^6 \qquad \text{Equation 96}$$

$$R_{e\_max} = \frac{v_{xmax}D_x}{\nu} = \frac{v_{zmax}D_z}{\nu} = \frac{2.0\left[\frac{m}{s}\right]\cdot 12\,[m]}{10^{-6}\,[\frac{m2}{s}]} = 2.4 \cdot 10^7 \qquad \text{Equation 97}$$

The flow is hence turbulent.

It must be remembered that the flow is not steady, it oscillates due to the wave motions. Then the Keulegan-Carpenter (KC) number is of great importance. The KC number is a measure of how far the oscillating flow particles travel during one oscillation compared to the characteristic length of the object in the flow [20]:

$$KC = \frac{v_{i0}T}{D_i} \; ; i = x, y, z \qquad \text{Equation 98}$$

v_{i0} is then the particle velocity amplitude in direction i. Characteristic wave particle velocity estimated in Equation 94 is assumed to yields as particle velocity amplitude since the particles travel in circular orbits with velocity in direction i fluctuating about zero. T is taken as T_z. Minimum and maximum KC numbers can then be found:

$$KC_{min} = \frac{v_{xmin}T_{zmin}}{D_x} = \frac{v_{zmin}T_{zmin}}{D_z} = \frac{0.72\left[\frac{m}{s}\right]\cdot 4.7\,[s]}{12\,[m]} = 0.3 \qquad \text{Equation 99}$$

$$KC_{max} = \frac{v_{ymax}T_{zmax}}{D_y} = \frac{2.0\left[\frac{m}{s}\right]\cdot 13.2\,[s]}{6\,[m]} = 4.4 \qquad \text{Equation 100}$$

Low KC numbers like 0.3 indicates that the flow oscillates quite rapidly. KC = 0.3 means that the flow particles only travel 0.3 times the characteristic length of the body during one oscillation. The oscillation might therefore be too rapid for vortices to form on a blunt body. But here sharp edges are present and vortex shedding is assumed to happen even at quite low KC numbers. Figures 2.39 and 2.40 in [20] give drag and mass coefficients plotted against Re and KC numbers

for a cylinder. At high Re numbers, typically about $Re = 6 \cdot 10^5$ the coefficients starts to get unaffected by Re and only dependent on KC.

Whether a box structure also is unaffected by Re for values above $Re \approx 6 \cdot 10^5$ is not given. Two methods are therefore used to estimate the drag coefficient; one that computes the quadratic drag coefficient C_D based on Re and corrects for KC according to [10], the other by using a graph in [37] where $C_{DD} \cdot KC$ is plotted against KC. C_{DD} is the total drag force, the sum of linear and quadratic drag.

Table B-2, Appendix B in [10] is used and the quadratic drag coefficients of interesting geometries are extracted and given below in Figure 77. Either rectangular plate normal to flow direction or square rod parallel to flow should be applied. For the rectangular plate B/H ratio will be 1 or 2 which basically results in the same quadratic drag coefficient of 1.16. The effect of the plate having a thickness can be seen by the square rod. When B/H = 1 and the length of the rod L equals 1, hence a cube shape, $C_D = 1.15$. This in only a small reduction compared to the plate. For further increase of L C_D has a more rapid decrease before it again increases slightly. As L/D never has a value larger than 1 (D taken as the largest value of the rectangular plate) is the reduction of the drag coefficient computed by the rectangular plate due to extension in the direction of incoming flow insignificant. $C_D = 1.16$ is therefore used. This value must then be corrected for the KC number. In [10] it is stated that C_D in oscillatory flow is typically two to three times the C_D value in steady flow. A factor of two is hence used to find the corrected C_D. The final quadratic drag value $C_D = 2.32$. If adding a linear drag coefficient of 0.2 then $C_{DD} = 2.52$.
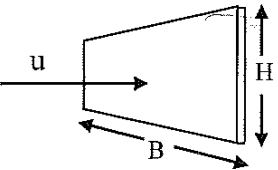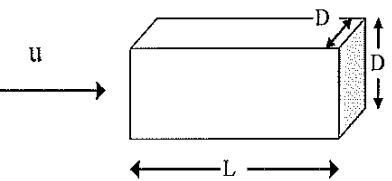
Geometry	Dimensions	C_{DS}
Rectangular plate normal to flow direction	B/H	
	1	1.16
	5	1.20
	10	1.50
	∞	1.90
		$R_e > 10^3$
Square rod parallel to flow	L/D	
	1.0	1.15
	1.5	0.97
	2.0	0.87
	2.5	0.90
	3.0	0.93
	4.0	0.95
	5.0	0.95
		$R_e = 1.7 \cdot 10^5$

Figure 77: Table B-2, Appendix B in [10] used to find quadratic drag coefficient.

The other method is by using Figure 78. Here total drag coefficients are plotted for different shapes against KC values. Note that the values yield for a specific frequency range but they will

here be used generally. The shape most similar to the box considered in this report is shape 5, a cube. When KC = 14, which is the highest KC value where $C_{DD} \cdot KC$ is given for shape 5, $C_{DD} = \frac{C_{DD} \cdot KC}{KC} = \frac{13.8}{13.8} = 1$. This is consistent with the figure given on page 4.2 in [37] for different shapes in steady flow where the drag coefficient is between 0.9 and 1. For a further decrease of KC in Figure 78 C_{DD} increases. For $KC_{max} = 4.4$ $C_{DD} \approx \frac{7.8}{4.4} = 1.78$. It is hard to say from the graph but it is anticipated that the graph continues down to where $KC \approx 0.85$ and $C_{DD} \cdot KC \approx 2$. Then $C_{DD} \approx 2.35$. The factor between C_{DD} for KC = 0.85 and KC = 13.8 is hence about 2.3.

The minimum KC value in the analyses is about 0.3 which is not included in the Figure 78. By extrapolating the lower part of the graph using the two points KC = 0.85 and 2 a C_{DD} value of 2.87 is obtained. Extrapolation should be used with care and does not necessarily give the correct value but linearity seems reasonable based on the lower graph in figure 2.1, [37]. Now the factor between C_{DD} for KC = 0.3 and KC = 13.8 is approximately 2.9. As the linear drag coefficient must be subtracted from both C_{DD} values, it does not affect the ratio. The statement made in [10] about C_D in oscillatory flow being typically two to three times the C_D value for steady flow seems therefore reasonable. With KC = 0.3 and $C_{DD} = 2.87$ the quadratic drag coefficient C_D becomes 2.67 if the linear coefficient is taken as 0.2.
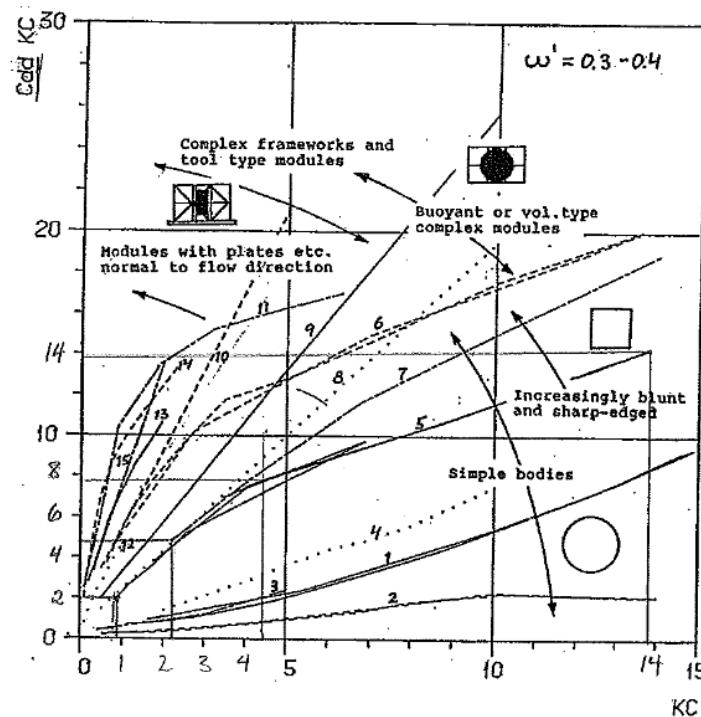
Figure 78: Shape number 5, a box, is used to estimate the total drag coefficients for different KC values [37].

By extrapolation of the graph given in Figure 78 a higher quadratic drag coefficient is obtained compared to the coefficient from formulas in [10]. But for the method given in [10] only a factor

of two was applied to correct for KC. It is hard to say whether it is conservative to use a high C_D or not. The argument for a high C_D being conservative is that the higher C_D the higher drag force and the higher hydrodynamic forces [10]:

$$F_{hyd} = \sqrt{(F_D - F_{slam})^2 + (F_M - F_\rho)^2}$$

Equation 101

See also Equation 42. The higher hydrodynamic forces the higher possibility of slack slings, see Equation 41. But close to resonance a low C_D will be conservative. Then high drag leads to excessive damping and hence less response, which will decrease the probability of slack slings. The natural periods of the lowered systems:

$$T_0 = 2\pi\sqrt{\frac{M}{K}} = 2\pi\sqrt{\frac{M_m + A_z + mass\ of\ wire}{\left(\frac{1}{k_w} + C_{resilience}\right)^{-1}}} = 2\pi\sqrt{\frac{M_m + A_z + mass\ of\ wire}{\left(\frac{1}{\frac{nE_w\pi d_w^2}{4l_w}} + C_{resilience}\right)^{-1}}}$$

Equation 102

$$T_{0_{crane}} = 2\pi\sqrt{\frac{250\cdot10^3\,[kg] + 4.32\cdot10^5\,[kg] + 2\cdot73.1\left[\frac{kg}{m}\right]\cdot36.8\,[m]}{\left(\frac{1}{\frac{2\cdot65\cdot10^9\,[Pa]\cdot\pi\cdot(0.127\,[m])^2}{4\cdot36.8\,[m]}} + 2.89\cdot10^{-7}\left[\frac{m}{N}\right]\right)^{-1}}} = 2.9\,[s]$$

Equation 103

This is in z-direction for crane deployment. Note that the eigenperiod for lowering through moonpool will be even lower as the crane system stiffness is increased. Wire length has less influence.

$$T_{0_{moonpool}} = 2\pi\sqrt{\frac{250\cdot10^3\,[kg] + 4.32\cdot10^5\,[kg] + 2\cdot73.1\left[\frac{kg}{m}\right]\cdot30.69\,[m]}{\left(\frac{1}{\frac{2\cdot65\cdot10^9\,[Pa]\cdot\pi\cdot(0.127\,[m])^2}{4\cdot30.69\,[m]}} + 1\cdot10^{-15}\left[\frac{m}{N}\right]\right)^{-1}}} = 0.71\,[s]$$

Equation 104

Wave periods will be above the natural period of the module. To help deciding which drag coefficient to use preliminary analyses are performed with quadratic drag coefficients equal to 2.0 and 2.9 in all directions for wave heading 0°. All other analysis input parameters are unchanged. Results are surprisingly similar, so similar that differences might result from changed random wave phase angles and hence different irregular sea state sections. It is therefore decided

to use the higher drag coefficient estimated from Figure 78 since this is based on KC directly and because the natural period is quite low compared to wave periods. Hence $C_D = 2.7$. This value is used in all analyses independent of KC and Re numbers due to time limitations. Uncertainty is introduced since extrapolation of a cube box graph is used. But the uncertainty is assumed less than if DNV results were to be used since a random number between 2 and 3 has to be picked to correct for oscillating flow.

Appendix 9: Correction of Hydrodynamic Coefficients

Perforation does not need to be considered due to the low perforation rate, 5 %. The effect of perforation on added mass is neglected if the ratio is lower or equal to 5 % according to [10]. This is also shown in Figure 79. See [10] for modifications if the perforation rate is larger.

The effect of perforation on drag is given in [13]. Towing tests of cylinders with perforation rates 0, 30, 60, 75, 82 and 90 % are performed. The perforation is made by a metal mesh with different opening sizes between the individual strings. Normalized drag is plotted against perforation as shown in Figure 80. Note that perforation rates 30 and 60 % are not included. Drag is found to decrease with increasing porosity but not significantly before the porosity reaches 75 % or higher. It is also found that for the two models with porosity above 75 % the vortex street is no longer distinct but several separate vortex streets are shown. The reason for reduced drag with increased porosity is that the throughflow of water increases. And increased throughflow leads to narrower wake. The wake gets narrower due to decreased velocity defect (wake velocity – water inflow velocity) in the wake and blockage of water by the model. But as the perforation in this case is low the effect is not accounted for.
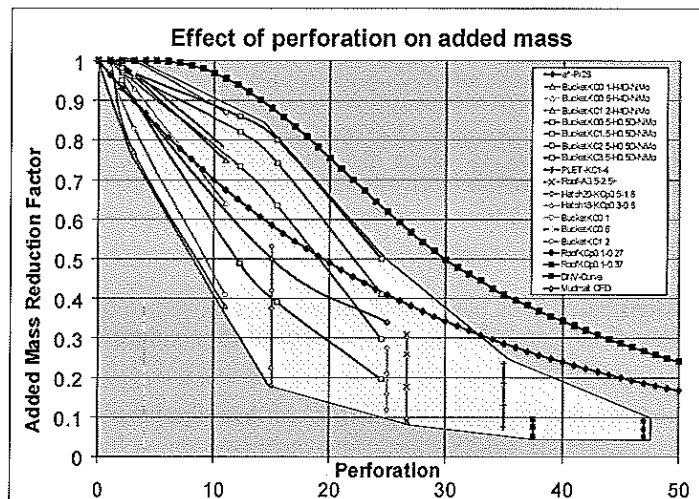
Figure 4-7
Added mass reduction factor A_{33}/A_{33S} as function of the perforation rate (percentage)

Figure 79: How added mass is affected by perforation [10]. DNV correction is represented by the upper line.
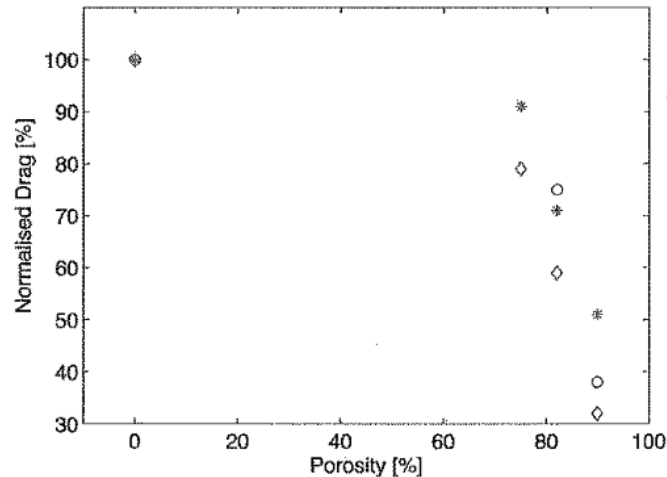
Fig. 4   Drag forces in percent of the drag force acting on the
solid cylinder; ○: towing speed of 0.01 m/s and ★ and ◇: tow-
ing speeds of 0.05 m/s and 0.2 m/s, respectively

Figure 80: How drag is affected by perforation [13].

Not only the drag coefficient but also the added mass coefficient is KC dependent. In Figure 79 the light grey area gives added mass reduction coefficients with constant perforation rates for different KC numbers. These lines are vertical. It may seem like the lower the KC number the lower the reduction factor and hence the lower the added mass and added mass coefficient. In these analyses a high added mass coefficient is conservative as a high mass force leads to a high hydrodynamic force, see Equation 42. High hydrodynamic force implies high possibility of excessive uplift and hence slack slings, see Equation 41. But as the reduction ratio is low at low perforation rates, no method for KC corrections is given. For conservativeness the added mass and hence added mass coefficients are not modified for KC.

As the module is close to the surface at time instance 2 waves will cause the submergence to vary. Depending on the incoming waves the module, which top end is fixed 0.5 [m] below MWL, can have a submerged height of for example 3 [m] instead of 12 [m]. It is assumed that the vertical cross-section is equally submerged even though this is not exactly the case when waves pass. This will not only lead to changing buoyancy but also changing hydrodynamic coefficients. Note that higher order effects, except for quadratic drag, are neglected.

Added mass coefficients are initially calculated as shown in Appendix 7, based on tables for rectangular boxes. To correct for the varying submerged unit height, ranging from $0 - 12$ [m], added mass coefficients are calculated for submerged box heights 0, 3, 6 and 9 [m]. The ratios between estimated added mass coefficients of the changing submerged height and the original added mass coefficients for the fully submerged unit are calculated. How this is done can be seen for submerged height = 3 [m] in Appendix 10. The correction ratios are taken into MACSI2 correction files for hydrodynamic coefficients.

Also drag coefficients are modified for surface closeness but in a simpler way than the added mass coefficients. It is known that hydrodynamic forces are zero when the module is above MWL and the drag coefficients are known for the fully submerged structure. Then drag coefficients for the partly submerged unit is simply found by using linearity. The ratio between the estimated drag coefficient for the partly submerged height and the original drag coefficients for full submergence is 0 above MWL. It is 1 when the unit is submerged. Hence when the structure is 25 % submerged the ratio is 25 % since linearity is used.

When lowering over the side with crane the module will be adjacent to the ship side. It is known that added mass and drag increases with proximity to fixed boundaries as shown in Figure 81. Based on Shell in-house experience it is assumed in Appendix 4 that the module will have a distance of about 5 [m] to the ship side during installation. If the width of the unit, 6 [m], is taken as the diameter of the cylinder in Figure 81 e/D = 5 [m]/6 [m] = 0.83. For a square cylinder it can be seen that the increase in added mass and drag coefficients is insignificant and will hence be disregarded. There is therefore no added mass and drag coefficients correction for being near the ship side.
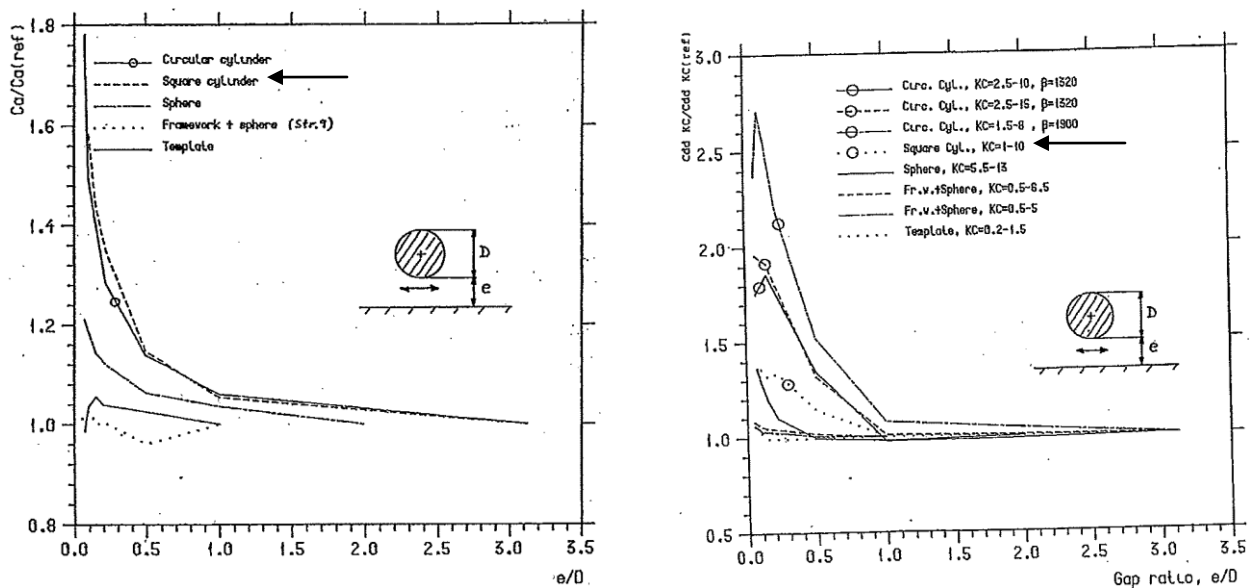
Figure 81: Added mass coefficient increase to the left and drag coefficient increase to the right with proximity to the fixed boundary [37]. The line for square cylinder is indicated by an arrow.

For moonpool deployment added mass and drag coefficient are corrected. Added mass and drag coefficients will increase inside the moonpool since the flow is restricted, especially when there object is lowered. To account for this flow restriction a modification is applied to the added mass coefficient in the calculations. The correction [10]:

$$\frac{C_{Az}}{C_{Az0}} = 1 + 1.9\left(\frac{A_{mz}}{A_{moonpool}}\right)^{\frac{9}{4}} = 1 + 1.9\left(\frac{68.4\,[m^2]}{105\,[m^2]}\right)^{\frac{9}{4}} = 1.72\,;\ \ for\ \frac{A_{mz}}{A_{moonpool}} < 0.8$$

<div align="right">Equation 105</div>

C_{Az0} is the added mass coefficient in unrestricted flow while C_{Az} is the increased added mass coefficient. A_{mz} is the projected solid area in z-direction of the object and $A_{moonpool}$ is the projected area of the moonpool. Also the drag coefficients, linear and quadratic, must be corrected for the restricted flow around the object in the moonpool. In [10] it does not say whether the correction shall be applied to both linear and quadratic drag coefficients both it is assumed valid for them both:

$$\frac{C_{Dz}}{C_{Dz0}} = \frac{1-\frac{0.5 A_{mz}}{A_{moonpool}}}{\left(1-\frac{A_{mz}}{A_{moonpool}}\right)^2} = \frac{1-\frac{0.5 \cdot 68.4\,[m^2]}{105\,[m^2]}}{\left(1-\frac{68.4\,[m^2]}{105\,[m^2]}\right)^2} = 5.55\,; \quad for\,\frac{A_{mz}}{A_{moonpool}} < 0.8$$

<div align="right">Equation 106</div>

C_{Dz0} is the drag coefficient in unrestricted flow while C_{Dz} is the increased drag coefficient.

Surface roughness of the module is another factor of importance for added mass and drag coefficients. Roughness on the structural surface of the unit being lowered will be present due to welds, machining and painting [20]. Marine growth is not a problem as installation of a new structure is considered. Surface roughness will affect whether the flow around the object is laminar or turbulent which affects the hydrodynamic coefficients. Roughness is commonly measured by $k_{roughness}/D$. $k_{roughness}$ is a measure of the surface roughness and D is the original dimension without roughness, for example the diameter of a cylinder. Curves showing how added mass and drag coefficients as functions of Reynolds number are affected by surface roughness are given in Figures 82 and 83. KC numbers are fixed. Note that curves given here are for straight oscillating flow. How well the curves represent the oscillating flow of waves where particle motions are circular or elliptical dependent on water depth is unknown. It is assumed that values will decrease for oscillating flow generated by waves [20].
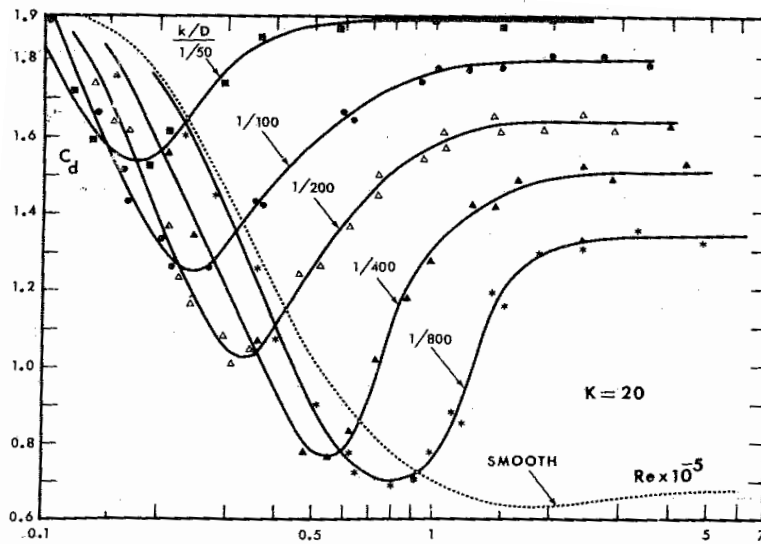
Figure 82: C$_D$ as function of Re and surface roughness [20].
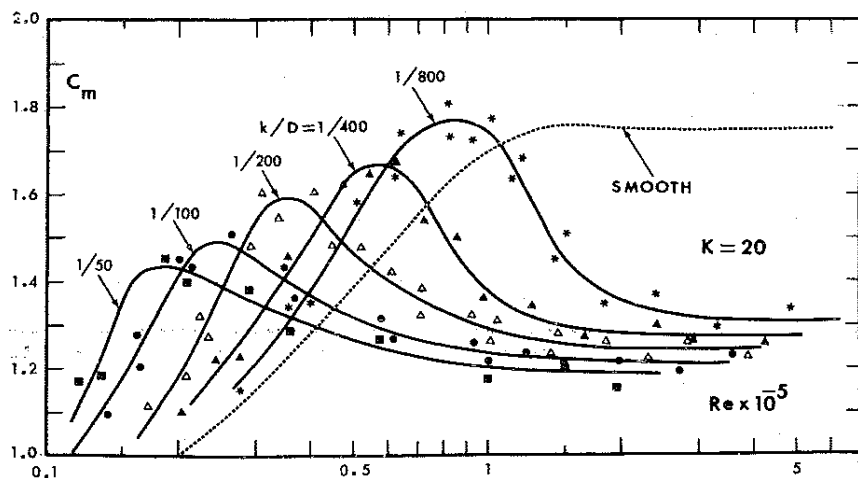
Figure 83: C_m, mass coefficient, as function of Re and surface roughness [20].

The surface roughness of the module is unknown and both KC and Reynolds numbers must be estimated. The resulting correction will hence add extra uncertainty to the computed hydrodynamic coefficients and is therefore not considered.

Note that added mass and damping are in general quite dependent on frequency of oscillation as shown in [20]. But as procedures for computing added mass given in [24] do not consider the frequency of oscillation, nor does the method for computing quadratic drag, it is not accounted for in this report.

Appendix 10: Surface Correction of Added Mass Coefficients

MathCad is used. Module submerged height = 3 [m] instead of 12 [m] as when the structure is fully submerged. See Figures 73 and 74 for ratios, $\alpha -$ and $\beta -$parameters.

Module details:

Note:CoG and CoB are assumed located in the module center.

Module dimensions: $l_m := 12m$ $w_m := 6m$ $h_m := 3m$

Assumed perforation: $p_x := 5\%$ $p_y := 5\%$ $p_z := 5\%$

Projected area: $A_{m\_x} := w_m \cdot h_m \cdot (1 - p_x)$ $A_{m\_x} = 17.1m^2$

$A_{m\_y} := l_m \cdot h_m \cdot (1 - p_y)$ $A_{m\_y} = 34.2m^2$

$A_{m\_z} := l_m \cdot w_m \cdot (1 - p_z)$ $A_{m\_z} = 68.4m^2$

Module mass inc. rigging: $M_m := 250t$

Module dry weight inc. rigging: $F_G := M_m \cdot g$ $F_G = 2.452 \times 10^6 N$

Module submerged weight: $F_S := F_G \dfrac{(\rho_{steel} - \rho_{swater})}{\rho_{steel}}$ $F_S = 2.132 \times 10^6 N$

Module volume: $V_B := \dfrac{F_G - F_S}{g \cdot \rho_{swater}} = 3.185 \times 10^4 L$

$$\text{ratio}_2 := \begin{pmatrix} 1.0 \\ 1.2 \\ 1.25 \\ 1.33 \\ 1.5 \\ 2.0 \\ 2.5 \\ 3.0 \\ 4.0 \\ 5.0 \\ 8.0 \\ 10.0 \end{pmatrix} \qquad \alpha_2 := \begin{pmatrix} 0.570 \\ 0.630 \\ 0.642 \\ 0.680 \\ 0.691 \\ 0.757 \\ 0.801 \\ 0.830 \\ 0.871 \\ 0.897 \\ 0.934 \\ 0.947 \end{pmatrix}$$

$$\text{ratio}_1 := \begin{pmatrix} 0.00 \\ 0.10 \\ 0.30 \\ 0.50 \\ 0.75 \\ 1.00 \\ 1.25 \\ 1.60 \\ 2.00 \\ 2.40 \\ 2.80 \\ 3.60 \end{pmatrix} \qquad \beta_1 := \begin{pmatrix} 1.00 \\ 1.13 \\ 1.33 \\ 1.44 \\ 1.51 \\ 1.55 \\ 1.58 \\ 1.61 \\ 1.64 \\ 1.67 \\ 1.69 \\ 1.72 \end{pmatrix} \qquad \alpha_1 := \begin{pmatrix} 0 \\ 5.139 \\ 2.016 \\ 1.310 \\ 0.916 \\ 0.705 \\ 0.575 \\ 0.453 \\ 0.373 \\ 0.318 \\ 0.274 \\ 0.217 \end{pmatrix}$$

Perforation coeff.:

$$C_{px} := e^{\left(\frac{-p_x \cdot 100}{28}\right)} \qquad C_{px} = 0.836$$

$$C_{py} := e^{\left(\frac{-p_y \cdot 100}{28}\right)} \qquad C_{py} = 0.836$$

$$C_{pz} := e^{\left(\frac{-p_z \cdot 100}{28}\right)} \qquad C_{pz} = 0.836$$

X-direction:

136

Length: $\qquad a := h_m \qquad\qquad a = 3\,m$

Width: $\qquad b := w_m \qquad\qquad b = 6\,m$

Ratio b/a: $\qquad ratio_{ba} := \dfrac{b}{a} \qquad\qquad ratio_{ba} = 2$

Alfa: $\qquad \alpha_{ba} := linterp\left(ratio_2, \alpha_2, ratio_{ba}\right) \qquad\qquad \alpha_{ba} = 0.757$

Length: $\qquad a := h_m \qquad\qquad a = 3\,m$

Width: $\qquad b := l_m \qquad\qquad b = 12\,m$

Ratio b/a: $\qquad ratio_{ba} := \dfrac{b}{a} \qquad\qquad ratio_{ba} = 4$

Betta: $\qquad \beta_{ba} := linterp\left(ratio_1, \beta_1, ratio_{ba}\right) \qquad\qquad \beta_{ba} = 1.735$

Added mass: $\qquad M_{added\_x} := \alpha_{ba} \cdot \beta_{ba} \cdot \rho_{swater} \cdot \pi \cdot h_m^2 \cdot \dfrac{w_m}{4}$

$$M_{added\_x} = 5.71 \times 10^4\,kg$$

Mass coefficient: $\qquad C_{Ax} := \dfrac{M_{added\_x}}{\rho_{swater} \cdot V_B} \qquad\qquad C_{Ax} = 1.749$

Original coeff: $\qquad Prior_{cax} := 13.226$

Correction: $\qquad CMx := \dfrac{C_{Ax}}{Prior_{cax}} = 0.132$

Y-direction:

Length: $\qquad a := h_m \qquad\qquad a = 3\,m$

Width: $\qquad b := l_m \qquad\qquad b = 12\,m$

Ratio b/a: $\qquad ratio_{ba} := \dfrac{b}{a} \qquad\qquad ratio_{ba} = 4$

Alfa: $\qquad \alpha_{ba} := linterp\left(ratio_2, \alpha_2, ratio_{ba}\right) \qquad\qquad \alpha_{ba} = 0.871$

Length: $\qquad a := h_m \qquad\qquad a = 3\,m$

Width:	$b := w_m$	$b = 6\,m$

Ratio b/a: $\quad ratio_{ba} := \dfrac{b}{a}$ $\qquad ratio_{ba} = 2$

Betta: $\quad \beta_{ba} := linterp\left(ratio_1, \beta_1, ratio_{ba}\right)$ $\qquad \beta_{ba} = 1.64$

Added mass: $\quad M_{added\_y} := \alpha_{ba} \cdot \beta_{ba} \cdot \rho_{swater} \cdot \pi \cdot h_m^2 \cdot \dfrac{l_m}{4}$

$$M_{added\_y} = 1.242 \times 10^5\,kg$$

Mass coefficient: $\quad C_{Ay} := \dfrac{M_{added\_y}}{\rho_{swater} \cdot V_B}$ $\qquad C_{Ay} = 3.805$

Original coeff: $\quad Prior_{cay} := 35.531$

Correction: $\quad CMy := \dfrac{C_{Ay}}{Prior_{cay}} = 0.107$

Z-direction:

Length: $\quad a := w_m$ $\qquad a = 6\,m$

Width: $\quad b := l_m$ $\qquad b = 12\,m$

Ratio b/a: $\quad ratio_{ba} := \dfrac{b}{a}$ $\qquad ratio_{ba} = 2$

Alfa: $\quad \alpha_{ba} := linterp\left(ratio_2, \alpha_2, ratio_{ba}\right)$ $\qquad \alpha_{ba} = 0.757$

Length: $\quad a := w_m$ $\qquad a = 6\,m$

Width: $\quad b := h_m$ $\qquad b = 3\,m$

Ratio b/a: $\quad ratio_{ba} := \dfrac{b}{a}$ $\qquad ratio_{ba} = 0.5$

Betta: $\quad \beta_{ba} := linterp\left(ratio_1, \beta_1, ratio_{ba}\right)$ $\qquad \beta_{ba} = 1.64$

Added mass: $\quad M_{added\_z} := \alpha_{ba} \cdot \beta_{ba} \cdot \rho_{swater} \cdot \pi \cdot w_m^2 \cdot \dfrac{l_m}{4}$

$$M_{added\_z} = 3.791 \times 10^5\,kg$$

Mass coefficient: $\quad C_{Az} := \dfrac{M_{added\_z}}{\rho_{swater} \cdot V_B}$ $\qquad C_{Az} = 11.613$

Original coeff: $\text{Prior}_{caz} := 13.226$

Correction: $\text{MCz} := \dfrac{C_{Az}}{\text{Prior}_{caz}} = 0.878$

Appendix 11: Moonpool Water Plug Motion Amplitude

The equation of motion for the moonpool water plug:

$$\left(M_{wp} + A_{33wp}\right)\ddot{\zeta}_{wp} + C_{ps}|\dot{\zeta}_{wp} - \dot{\zeta}_s|(\dot{\zeta}_{wp} - \dot{\zeta}_s) + C_b|\dot{\zeta}_{wp} - \dot{\zeta}_b|(\dot{\zeta}_{wp} - \dot{\zeta}_b) +$$
$$K_{moonpool}\zeta_{wp} = F(t) \qquad\qquad\qquad\qquad\qquad \text{Equation 107}$$

M_{wp}: Mass of water plug equal to $\rho_{mp}A_{moonpool}D$ [kg]

A_{33wp}: Added mass of water plug in heave. $A_{33wp} = \rho_{mp}\kappa A_{moonpool}\sqrt{A_{moonpool}}$ where κ is found to be 0.46 for a rectangular moonpool

ζ_{wp} : Motion of water plug [m]

ζ_b : Motion of body in moonpool [m]

ζ_s : Heave motion of ship [m]

C_{ps} : Damping of relative motion between water plug and ship moonpool walls [kg/m]

C_b : Damping of relative motion between water plug and body in moonpool [kg/m]

$K_{moonpool}$: Water plane stiffness in moonpool, $K_{moonpool} = \rho_{mp}gA_{moonpool}$ [N/m]

$F(t)$: Excitation force on water plug [N]

See also Figure 24. For the slamming analyses no unit is lowered down into the moonpool so the damping effect of the body in the previous equation is removed. The residual damping of relative motion between the moonpool and water plug is linearized to simplify the calculations.

$$M_{wp_{TOT}}\ddot{\zeta}_{wp} + C_{ps1}(\dot{\zeta}_{wp} - \dot{\zeta}_s) + K_{moonpool}\zeta_{wp} = F(t) \qquad \text{Equation 108}$$

$M_{wp_{TOT}}$ is the total mass of the water plug including added mass while $C_{ps1} = 2\eta\sqrt{K_{moonpool}M_{wp_{TOT}}}$ is the linearized damping coefficient. η is the relative damping ratio to critical damping and in [10] a list of η for different moonpool cases is given. The value for a moonpool including guidance structure is used. Guidance structure must be present in the moonpool to lower the cursor system which will be used during module moonpool installation. Hence $\eta = 0.19$.

The motion of the water plug is complex:

$$\zeta_{wp} = \zeta_{wp}(t) = \zeta_{wp\_a}e^{i\omega t} \qquad\qquad\qquad \text{Equation 109}$$

The derivative and double derivative of ζ_{wp} with respect to time hence becomes:

$$\dot{\zeta}_{wp} = \frac{d}{dt}\zeta_{wp}(t) = i\omega\zeta_{wp\_a}e^{i\omega t}$$ Equation 110

$$\ddot{\zeta}_{wp} = \frac{d}{dt}\dot{\zeta}_{wp} = -\omega^2\zeta_{wp\_a}e^{i\omega t}$$ Equation 111

Also the ship heave motion ζ_s and the water plug excitation force F(t) are rewritten and transfer functions applied.

$$\zeta_s = G_s\zeta$$ Equation 112

$$F(t) = G_w\zeta$$ Equation 113

G_s is the transfer function of the wave elevation and the ship elevation at the moonpool location. It contains information about the magnitude ratio between the two elevations. It also holds information regarding the phase lag from the wave elevation to the response which here is considered the ship elevation at the moonpool. G_w is the transfer function of the moonpool excitation force and the wave elevation.

Insert Equations 110-113 into Equation 108:

$$-\omega^2 M_{wp_{TOT}}\zeta_{wp} + i\omega C_{ps1}(\zeta_{wp} - G_s\zeta) + K_{moonpool}\zeta_{wp} = G_w\zeta$$ Equation 114

The ratio between the motion of the water plug and the wave motion can hence be found.

$$-\omega^2 M_{wp_{TOT}}\zeta_{wp} + i\omega C_{ps1}\zeta_{wp} + K_{moonpool}\zeta_{wp} = i\omega C_{ps1}G_s\zeta + G_w\zeta$$

Equation 115

$$\frac{\zeta_{wp}}{\zeta} = \frac{(i\omega C_{ps1}G_s + G_w)}{-\omega^2 M_{wp_{TOT}} + i\omega C_{ps1} + K_{moonpool}} \quad \Big| \cdot \frac{\frac{1}{K_{moonpool}}}{\frac{1}{K_{moonpool}}}$$ Equation 116

$$\frac{\zeta_{wp}}{\zeta} = \frac{i\omega\frac{2\eta\sqrt{K_{moonpool}M_{wp_{TOT}}}}{K_{moonpool}}G_s + \frac{G_w}{K_{moonpool}}}{-\frac{\omega^2 M_{wp_{TOT}}}{K_{moonpool}} + i\omega\frac{2\eta\sqrt{K_{moonpool}M_{wp_{TOT}}}}{K_{moonpool}} + \frac{K_{moonpool}}{K_{moonpool}}}$$ Equation 117

$$\frac{\zeta_{wp}}{\zeta} = \frac{\frac{G_w}{\rho_{mp}gA_{moonpool}} + i2\eta G_s\frac{\omega}{\omega_0}}{1 - \left(\frac{\omega}{\omega_0}\right)^2 + i2\eta\frac{\omega}{\omega_0}}$$ Equation 118

A complex denominator is not ideal if the magnitude of the ratio between the response and the excitation is of interest. A trick is therefore applied. Now x represents the nominator.

$$a = 1 - \left(\frac{\omega}{\omega_0}\right)^2$$ Equation 119

$$b = 2\eta \frac{\omega}{\omega_0} \qquad \text{Equation 120}$$

$$\frac{\zeta_{wp}}{\zeta} = \frac{x}{a+ib} \cdot \frac{a-ib}{a-ib} = \frac{x(a-ib)}{a^2+b^2} \qquad \text{Equation 121}$$

Inserting for x and Equations 119 and 120:

$$\frac{\zeta_{wp}}{\zeta} = \frac{\left(\frac{G_W}{\rho_{mp}gA_{moonpool}}+i2\eta G_s\frac{\omega}{\omega_0}\right)\cdot\left(1-\left(\frac{\omega}{\omega_0}\right)^2-i2\eta\frac{\omega}{\omega_0}\right)}{1-2\left(\frac{\omega}{\omega_0}\right)^2+\left(\frac{\omega}{\omega_0}\right)^4+4\eta^2\left(\frac{\omega}{\omega_0}\right)^2} \qquad \text{Equation 122}$$

$$\frac{\zeta_{wp}}{\zeta} = \frac{\frac{G_W}{\rho_{mp}gA_{moonpool}}\left(1-\left(\frac{\omega}{\omega_0}\right)^2\right)+G_s4\eta^2\left(\frac{\omega}{\omega_0}\right)^2+i2\eta\frac{\omega}{\omega_0}\left(G_s\left(1-\left(\frac{\omega}{\omega_0}\right)^2\right)-\frac{G_W}{\rho_{mp}gA_{moonpool}}\right)}{1-2\left(\frac{\omega}{\omega_0}\right)^2+\left(\frac{\omega}{\omega_0}\right)^4+4\eta^2\left(\frac{\omega}{\omega_0}\right)^2}$$

$$\text{Equation 123}$$

The heave transfer function for the Normand Subsea is known, but just by magnitude and phase angle for certain wave periods and wave headings. Note that the heave transfer function is given for CoG but the center of the moonpool is located in close proximity to the Ship's LCG, the offset in y-direction is 0 while the offset in x-direction is 6.9 [m]. There will therefore be no contribution to heave from roll and neglectable contribution to heave from pitch at the moonpool. The heave transfer function is hence used as is.

In Appendix 11.1 is the procedure used for computing the complex expression of a general transfer function $H(\omega)$ based on magnitude and phase given. This method is used to estimate $G_s = A_{Gs}(\omega) + iB_{Gs}(\omega)$ for the wave periods T_p and wave headings of interest in this report. The calculations are carried out as a part of the programmed MATLAB function "M_velocity" (Moonpool velocity), see Appendix 13.2.11. In "M_Velocity" the text file G_s is taken in which in the first column contains T_p values. The residual 12 columns in G_s represents Normand Subsea's heave transfer function for wave headings 0°, 30°, 60°, 90°, 120°, 150° and 180°. Column 2 and 3 represents the magnitude and phase angle at wave heading 0° and so on for the wave headings considered.

To solve Equation 123 for ζ_{wp} a relationship between G_W and G_s is needed since only G_s is known. In [10] the following statements are made to find a usable relationship:

- Excitation force due to incoming waves, F_1, and due to ship motion, F_2, can be assessed as for a ship without moonpool. $F(t) = F_1(t) + F_2(t)$
- The fluid pressure expressions valid for long crested waves can be used.
- Deep water is assumed.

By a procedure given in [10] G_w can be expressed as:

$$G_w = \frac{F(t)}{\zeta} = \rho_{mp} A_{moonpool}(ge^{-kD} - \omega^2 \kappa \sqrt{A_{moonpool}} G_s) \qquad \text{Equation 124}$$

Insert for $G_s = A_{Gs}(\omega) + iB_{Gs}(\omega)$:

$$G_w = \rho_{mp} A_{moonpool}(ge^{-kD} - \omega^2 \kappa \sqrt{A_{moonpool}}(A_{Gs}(\omega) + iB_{Gs}(\omega)))$$

<div align="right">Equation 125</div>

$$G_w = \rho_{mp} A_{moonpool}\left(ge^{-kD} - \omega^2 \kappa A_{Gs}(\omega)\sqrt{A_{moonpool}}\right) + i\left(-\rho_{mp} A_{moonpool}\omega^2 \kappa B_{Gs}(\omega)\sqrt{A_{moonpool}}\right)$$

<div align="right">Equation 126</div>

Hence:

$$A_{Gw}(\omega) = \rho_{mp} A_{moonpool}\left(ge^{-kD} - \omega^2 \kappa A_{Gs}(\omega)\sqrt{A_{moonpool}}\right) \qquad \text{Equation 127}$$

$$B_{Gw}(\omega) = -\rho_{mp} A_{moonpool}\omega^2 \kappa B_{Gs}(\omega)\sqrt{A_{moonpool}} \qquad \text{Equation 128}$$

Now $G_w = A_{Gw}(\omega) + iB_{Gw}(\omega)$ where $A_{Gw}(\omega)$ and $B_{Gw}(\omega)$ are expressed by $A_{Gs}(\omega)$ and $B_{Gs}(\omega)$ in Equations 127 and 128. By inserting for G_w in Equation 123 the final equation for the water plug to wave elevation becomes:

$$\frac{\zeta_{wp}}{\zeta} = \frac{\frac{(A_{Gw}+iB_{Gw})}{\rho_{mp}gA_{moonpool}}\left(1-\left(\frac{\omega}{\omega_0}\right)^2\right)+(A_{Gs}+iB_{Gs})4\eta^2\left(\frac{\omega}{\omega_0}\right)^2 + i2\eta\frac{\omega}{\omega_0}\left((A_{Gs}+iB_{Gs})\left(1-\left(\frac{\omega}{\omega_0}\right)^2\right)-\frac{(A_{Gw}+iB_{Gw})}{\rho_{mp}gA_{moonpool}}\right)}{1-2\left(\frac{\omega}{\omega_0}\right)^2+\left(\frac{\omega}{\omega_0}\right)^4+4\eta^2\left(\frac{\omega}{\omega_0}\right)^2} \qquad \text{Equation 129}$$

$$\frac{\zeta_{wp}}{\zeta} = \frac{\left(\frac{A_{Gw}}{\rho_{mp}gA_{moonpool}}-B_{Gs}2\eta\frac{\omega}{\omega_0}\right)\cdot\left(1-\left(\frac{\omega}{\omega_0}\right)^2\right)+\left(A_{Gs}4\eta^2\frac{\omega}{\omega_0}+\frac{B_{Gw}}{\rho_{mp}gA_{moonpool}}2\eta\right)\cdot\left(\frac{\omega}{\omega_0}\right)+ i\left(\left(\frac{B_{Gw}}{\rho_{mp}gA_{moonpool}}+A_{Gs}2\eta\frac{\omega}{\omega_0}\right)\cdot\left(1-\left(\frac{\omega}{\omega_0}\right)^2\right)+\left(B_{Gs}4\eta^2\frac{\omega}{\omega_0}-\frac{A_{Gw}}{\rho_{mp}gA_{moonpool}}2\eta\right)\cdot\left(\frac{\omega}{\omega_0}\right)\right)}{1-2\left(\frac{\omega}{\omega_0}\right)^2+\left(\frac{\omega}{\omega_0}\right)^4+4\eta^2\left(\frac{\omega}{\omega_0}\right)^2}$$

<div align="right">Equation 130</div>

Now

$$A(\omega)_{ratio} = \frac{\left(\frac{A_{Gw}}{\rho_{mp}gA_{moonpool}}-B_{Gs}2\eta\frac{\omega}{\omega_0}\right)\left(1-\left(\frac{\omega}{\omega_0}\right)^2\right)+\left(A_{Gs}4\eta^2\frac{\omega}{\omega_0}+\frac{B_{Gw}}{\rho_{mp}gA_{moonpool}}-2\eta\right)\left(\frac{\omega}{\omega_0}\right)}{1-2\left(\frac{\omega}{\omega_0}\right)^2+\left(\frac{\omega}{\omega_0}\right)^4+4\eta^2\left(\frac{\omega}{\omega_0}\right)^2}$$

<div align="right">Equation 131</div>

$$B(\omega)_{ratio} = \frac{\left(\frac{B_{Gw}}{\rho_{mp}gA_{moonpool}}+A_{Gs}2\eta\frac{\omega}{\omega_0}\right)\left(1-\left(\frac{\omega}{\omega_0}\right)^2\right)+\left(B_{Gs}4\eta^2\frac{\omega}{\omega_0}-\frac{A_{Gw}}{\rho_{mp}gA_{moonpool}}-2\eta\right)\left(\frac{\omega}{\omega_0}\right)}{1-2\left(\frac{\omega}{\omega_0}\right)^2+\left(\frac{\omega}{\omega_0}\right)^4+4\eta^2\left(\frac{\omega}{\omega_0}\right)^2}$$

<div align="right">Equation 132</div>

The final expression for ζ_{wp} can be expressed by the complex ratio:

$$\zeta_{wp} = (A(\omega)_{ratio} + iB(\omega)_{ratio}) \cdot \zeta \qquad \text{Equation 133}$$

The motion amplitude for the water plug is therefore:

$$|\zeta_{wp}| = \zeta \cdot \sqrt{A(\omega)_{ratio}^2 + B(\omega)_{ratio}^2} \qquad \text{Equation 134}$$

Appendix 11.1 Transfer functions

The transfer functions G_s and G_w are complex and they therefore contain a real and an imaginary part. Generally a complex transfer function can be written:

$$H(\omega) = Real + iImaginary = A(\omega) + iB(\omega) \qquad \text{Equation 135}$$

$H(\omega)$ is hence a vector in the real and imaginary plane, see Figure 84. Note that the phase angle is here defined as positive when the response is prior to the wave top seen at the ship's CoG.
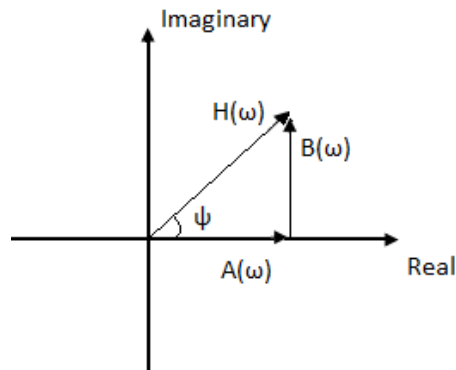
<div align="center">**Figure 84: General transfer function H(ω).**</div>

The magnitude of the transfer function and hence the length of the transfer function vector is defined as the square root of the real and the imaginary parts squared and added. See Equation 136. The tangent of the phase angle ψ equals the ratio between the imaginary part and the real part [18], see Equation 137.

$$|H(\omega)| = \sqrt{A(\omega)^2 + B(\omega)^2} \qquad \text{Equation 136}$$

$$\tan(\psi) = \frac{B(\omega)}{A(\omega)} \qquad \text{Equation 137}$$

Hence if the phase angle ψ and the magnitude of the transfer function $|H(\omega)|$ are known $A(\omega)$ and $B(\omega)$ can be computed since $A(\omega)$ and $B(\omega)$ are the two unknowns in Equations 136 and 137 above. Solve Equation 136 for $B(\omega)$ and Equation 137 for $A(\omega)$:

$$B(\omega) = \sqrt{|H(\omega)|^2 - A(\omega)^2} \qquad \text{Equation 138}$$

$$A(\omega) = \frac{B(\omega)}{\tan(\psi)} \qquad \text{Equation 139}$$

$A(\omega)$ can now be computed by inserting Equation 138 into Equation 139:

$$A(\omega) = \frac{\sqrt{|H(\omega)|^2 - A(\omega)^2}}{\tan(\psi)} \qquad \text{Equation 140}$$

$$A(\omega)^2 = \frac{|H(\omega)|^2 - A(\omega)^2}{\tan(\psi)^2} \qquad \text{Equation 141}$$

$$A(\omega)^2 \left(1 + \frac{1}{\tan(\psi)^2}\right) = \frac{|H(\omega)|^2}{\tan(\psi)^2} \qquad \text{Equation 142}$$

$$A(\omega) = \frac{|H(\omega)|}{\sqrt{(\tan(\psi)^2 + 1)}} \qquad \text{Equation 143}$$

The sign of $A(\omega)$ and $B(\omega)$ must be carefully decided. $\tan(\psi)$ is a periodic function as can be seen in Figure 85.
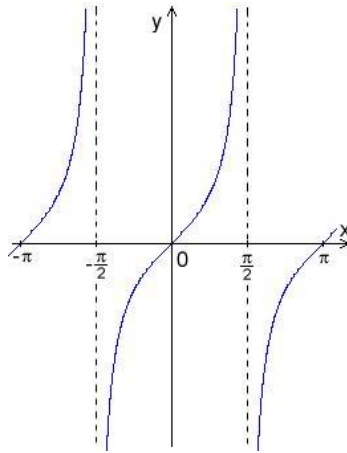
Figure 85: The periodic function of tan(ψ).

When inserting phase values into $\tan(\psi)$ $A(\omega)$ will always be positive if no attention is paid to which quadrant the phase values are located. The values of $A(\omega)$ and $B(\omega)$ are hence decided based on Equations 143 and 138 but the signs are determined based on quadrant location of ψ as given in Figure 86. With $A(\omega)$ and $B(\omega)$ determined the transfer function is known.
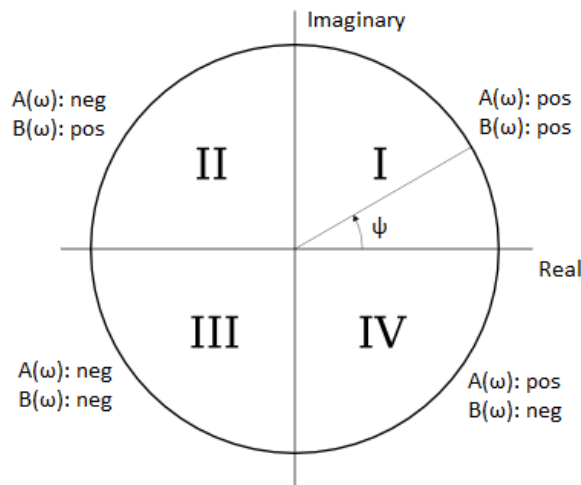
Figure 86: The signs of $A(\omega)$ and $B(\omega)$ are determined by ψ.

Appendix 12: MACSI2 Input Files, Hydrodynamic Correction Files, Normand Subsea RAO file, Macro Files for both Spectra, Torsethaugen Spectrum File and a MACSI2 Output File.

Appendix 12.1 Crane input file, "Cinput.txt"

```
MACSI-2 INPUT FILE
1 1 0 0 1                    '(Winch vel., wire, guideline, heave comp., motion param.)
1 0 0 0 0                    '(Varying hyd. coeff., bounday infl., guidance, static guidance, tugger)
1                           'WIRE DATA
2                             '(No. of wire parts)
65130000000 0.127 1.2         '(E-mod., diameter, drag coeff.)
73.1                          '(Nominal wire density)
0.0000028959                  '(Crane resilience)
5                           'WINCH OPERATION PARAMETERS
36.81 0  0                    '(Start length, velocity, stop time)
6                           'LOAD PARAMETERS
250000 31.85                  '(Mass, volume)
68.4 136.8 68.4               '(Proj. areas)
12 6 12                       '(Dimensions)
13.226 35.531 13.226          '(Mass. coeff.)
2.7 2.7 2.7 0.2 0.2 0.2       (Quad. and linear drag coeff.)
7                           'OVERALL DIMENSIONS
30.32 -20 30.31               '(Crane coordinates, x, y, z)
0 1000                        '(Offset if via sheave, water depth)
8                           'HULL AND MOONPOOL DATA
12 7.8 105 1.0                 '(Half breadth, draught, moonpool area, reson. moonpool amp. ratio)
10                          'FILE FOR CORRECTION COEFFS. FOR BEING CLOSE TO THE SURFACE
Cranecor.dat                  '(File name)
0                           'LAST LINE
```

Appendix 12.2 Correction file for hydrodynamic coefficients, "Cranecor.dat"

```
Corrections to hydrodynamic coeffs.
1 0
Depth corrections (Non.dim. depth, Sub. volume, CM xyz, b2 xyz, b1 xyz)
5
0 0 0 0 0 0 0 0 0 0 0
0.25 0.25 0.132 0.107 0.878 0.25 0.25 0.25 0.25 0.25 0.25
0.5 0.5 0.376 0.352 0.945 0.5 0.5 0.5 0.5 0.5 0.5
0.75 0.75 0.685 0.682 0.977 0.75 0.75 0.75 0.75 0.75 0.75
1 1 1 1 1 1 1 1 1 1 1
```

Appendix 12.3 Moonpool input file, "Minput.txt"

```
MACSI-2 INPUT FILE
1 1 0 0 1                    '(Winch vel., wire, guideline, heave comp., motion param.)
1 1 0 0 0                    '(Varying hyd. coeff., bounday infl., guidance, static guidance, tugger)
1                           'WIRE DATA
2                               '(No. of wire parts)
65130000000 0.127 1.2          '(E-mod., diameter, drag coeff.)
73.1                           '(Nominal wire density)
0.00000028959                  '(Crane resilience)
5                           'WINCH OPERATION PARAMETERS
30.69  0                        '(Start length, velocity, stop time)
6                           'LOAD PARAMETERS
250000 31.85                   '(Mass, volume)
68.4 136.8 68.4                '(Proj. areas)
12 6 12                        '(Dimensions)
13.226 35.531 13.226           '(Mass. coeff.)
2.7 2.7 2.7 0.2 0.2 0.2        '(Quad. and linear drag coeff.)
7                           'OVERALL DIMENSIONS
6.92 0 24.19                   '(Crane coordinates, x, y, z)
0 1000                         '(Offset if via sheave, water depth)
8                           'HULL AND MOONPOOL DATA
12 7.8 105 1                    '(Half breadth, draught, moonpool area, reson. moonpool amp. ratio)
10                          'FILE FOR CORRECTION COEFFS. FOR BEING CLOSE TO THE SURFACE
Mpoolcor.dat                   '(File name)
0                           'LAST LINE
```

Appendix 12.4 Correction file for hydrodynamic coefficients, "Mpoolcor.dat"

```
Corrections to hydrodynamic coeffs.
1 1
Depth corrections (Non.dim. depth, Sub. volume, CM, b2, b1)
5
0 0 0 0 0 0 0 0 0 0 0
0.25 0.25 0.132 0.107 0.878 0.25 0.25 0.25 0.25 0.25 0.25
0.5 0.5 0.376 0.352 0.945 0.5 0.5 0.5 0.5 0.5 0.5
0.75 0.75 0.685 0.682 0.977 0.75 0.75 0.75 0.75 0.75 0.75
1 1 1 1 1 1 1 1 1 1 1
Moonpool corrections (Cmz, b2z, b1z)
1.72 5.55 5.55
```

Appendix 12.5 Normand Subsea transfer function file "Normand.txt"

MSV Normand Subsea RAO. No roll reduction tank used.

"Original file name: EC1 - macsi2.mac, LPP = 103.240 m, B = 24.000 m, T = 7.810m. Motion ref. point:COG, LCG=46,52m fw AP, VCG=9.99m. "

30	7										
0	0	2.18									
0											
4.00	0.01	334.40	0.00	180.00	0.01	357.80	0.00	0.00	0.00	188.30	0.00	0.00
5.00	0.02	250.60	0.00	180.00	0.04	229.30	0.00	0.00	0.00	34.90	0.00	0.00
5.50	0.02	31.90	0.00	180.00	0.03	201.90	0.00	0.00	0.05	166.60	0.00	0.00
6.00	0.07	73.80	0.00	180.00	0.11	88.20	0.00	0.00	0.10	184.20	0.00	0.00
6.50	0.08	82.20	0.00	180.00	0.29	88.30	0.00	0.00	0.07	199.40	0.00	0.00
7.00	0.04	89.80	0.00	180.00	0.42	102.70	0.00	0.00	0.05	49.60	0.00	0.00
7.50	0.04	256.60	0.00	180.00	0.37	119.10	0.00	0.00	0.20	53.10	0.00	0.00
8.00	0.13	263.50	0.00	180.00	0.20	126.00	0.00	0.00	0.35	59.80	0.00	0.00
8.50	0.23	265.40	0.00	180.00	0.05	58.40	0.00	0.00	0.49	65.50	0.00	0.00
9.00	0.33	266.40	0.00	180.00	0.19	354.00	0.00	0.00	0.60	69.90	0.00	0.00
9.50	0.41	267.00	0.00	180.00	0.33	351.00	0.00	0.00	0.69	73.30	0.00	0.00
10.00	0.48	267.50	0.00	180.00	0.44	351.60	0.00	0.00	0.76	75.90	0.00	0.00
10.50	0.55	267.90	0.00	180.00	0.54	352.70	0.00	0.00	0.82	78.00	0.00	0.00
11.00	0.61	268.10	0.00	180.00	0.62	353.70	0.00	0.00	0.86	79.70	0.00	0.00
11.50	0.65	268.40	0.00	180.00	0.68	354.60	0.00	0.00	0.90	81.10	0.00	0.00
12.00	0.69	268.50	0.00	180.00	0.73	355.40	0.00	0.00	0.92	82.20	0.00	0.00
12.50	0.73	268.70	0.00	180.00	0.77	356.00	0.00	0.00	0.95	83.10	0.00	0.00
13.00	0.76	268.80	0.00	180.00	0.81	356.60	0.00	0.00	0.97	83.90	0.00	0.00
13.50	0.78	268.90	0.00	180.00	0.84	357.00	0.00	0.00	0.98	84.50	0.00	0.00
14.00	0.81	269.00	0.00	180.00	0.86	357.40	0.00	0.00	0.99	85.10	0.00	0.00
14.50	0.83	269.10	0.00	180.00	0.88	357.70	0.00	0.00	1.00	85.50	0.00	0.00
15.00	0.84	269.20	0.00	180.00	0.89	358.00	0.00	0.00	1.01	85.90	0.00	0.00
15.50	0.86	269.20	0.00	180.00	0.91	358.20	0.00	0.00	1.02	86.30	0.00	0.00
16.00	0.87	269.30	0.00	180.00	0.92	358.40	0.00	0.00	1.02	86.60	0.00	0.00
17.00	0.89	269.40	0.00	180.00	0.94	358.80	0.00	0.00	1.03	87.10	0.00	0.00
18.00	0.91	269.50	0.00	180.00	0.95	359.00	0.00	0.00	1.04	87.50	0.00	0.00
19.00	0.92	269.50	0.00	180.00	0.96	359.20	0.00	0.00	1.04	87.80	0.00	0.00
20.00	0.93	269.60	0.00	180.00	0.97	359.30	0.00	0.00	1.04	88.10	0.00	0.00
25.00	0.96	269.70	0.00	180.00	0.99	359.70	0.00	0.00	1.05	88.90	0.00	0.00
30.00	0.97	269.80	0.00	180.00	1.00	359.90	0.00	0.00	1.05	89.30	0.00	0.00
30											
4.00	0.01	91.10	0.01	134.30	0.01	95.00	0.00	221.40	0.00	327.20	0.00	311.20
5.00	0.01	306.00	0.01	317.70	0.03	222.50	0.00	85.20	0.02	174.10	0.01	57.10

5.50	0.04	73.50	0.02	128.60	0.06	97.70	0.03	206.60	0.06	179.50	0.02	46.30
6.00	0.07	82.70	0.05	133.10	0.19	83.00	0.06	216.60	0.05	185.00	0.00	70.70
6.50	0.04	89.40	0.05	145.90	0.32	85.90	0.09	225.80	0.05	47.00	0.03	202.70
7.00	0.03	256.10	0.04	188.10	0.35	97.60	0.11	236.40	0.19	50.20	0.06	201.20
7.50	0.11	263.90	0.06	238.80	0.22	104.00	0.12	248.50	0.33	57.90	0.10	198.30
8.00	0.20	265.70	0.10	256.70	0.09	45.20	0.13	261.80	0.45	64.20	0.14	195.70
8.50	0.29	266.60	0.14	263.30	0.23	356.00	0.14	275.50	0.55	69.10	0.17	193.40
9.00	0.36	267.20	0.18	266.20	0.37	351.90	0.16	289.30	0.63	72.90	0.20	191.50
9.50	0.43	267.70	0.22	267.60	0.49	352.30	0.18	302.80	0.69	75.80	0.23	189.90
10.00	0.49	268.00	0.25	268.40	0.59	353.30	0.21	316.00	0.74	78.00	0.25	188.50
10.50	0.54	268.30	0.28	268.70	0.66	354.30	0.26	328.60	0.77	79.80	0.27	187.40
11.00	0.58	268.50	0.31	268.80	0.72	355.20	0.34	340.70	0.80	81.20	0.28	186.40
11.50	0.61	268.60	0.33	268.70	0.77	355.90	0.46	352.40	0.82	82.40	0.29	185.40
12.00	0.64	268.80	0.35	268.30	0.80	356.50	0.70	4.20	0.84	83.30	0.30	184.30
12.50	0.67	268.90	0.37	267.40	0.84	357.00	1.31	18.70	0.85	84.10	0.29	181.90
13.00	0.69	269.00	0.42	267.80	0.86	357.40	3.64	68.70	0.86	84.70	0.31	165.00
13.50	0.71	269.10	0.39	275.20	0.88	357.80	2.70	178.60	0.87	85.30	0.42	181.70
14.00	0.72	269.20	0.39	272.30	0.90	358.00	1.30	202.50	0.88	85.70	0.39	184.20
14.50	0.74	269.20	0.40	271.40	0.91	358.30	0.89	211.30	0.88	86.10	0.38	184.00
15.00	0.75	269.30	0.41	271.00	0.92	358.50	0.70	217.40	0.89	86.50	0.38	183.70
15.50	0.76	269.30	0.42	270.70	0.93	358.70	0.60	222.30	0.89	86.80	0.38	183.40
16.00	0.77	269.40	0.43	270.60	0.94	358.80	0.53	226.40	0.90	87.00	0.39	183.10
17.00	0.78	269.50	0.44	270.40	0.96	359.10	0.45	233.00	0.90	87.50	0.39	182.70
18.00	0.80	269.50	0.45	270.30	0.97	359.30	0.41	238.20	0.90	87.80	0.40	182.40
19.00	0.81	269.60	0.45	270.20	0.97	359.40	0.38	242.30	0.91	88.10	0.40	182.10
20.00	0.81	269.60	0.46	270.20	0.98	359.50	0.36	245.60	0.91	88.30	0.40	181.90
25.00	0.84	269.80	0.48	270.10	0.99	359.80	0.32	255.60	0.91	89.00	0.41	181.30
30.00	0.85	269.80	0.49	270.00	1.00	359.90	0.30	260.40	0.91	89.30	0.42	181.00
60												
4.00	0.01	215.50	0.02	218.00	0.01	178.80	0.01	244.20	0.01	223.00	0.01	69.90
5.00	0.02	91.30	0.05	135.10	0.08	88.60	0.03	252.10	0.02	34.30	0.02	243.20
5.50	0.01	262.80	0.01	179.60	0.09	54.00	0.04	265.50	0.08	27.10	0.06	221.50
6.00	0.07	266.80	0.07	279.60	0.11	1.20	0.06	277.80	0.18	32.00	0.10	210.50
6.50	0.13	267.40	0.15	279.40	0.24	332.10	0.08	287.80	0.29	42.60	0.13	203.20
7.00	0.18	267.80	0.24	277.40	0.45	329.40	0.10	296.50	0.38	53.50	0.17	197.90
7.50	0.23	268.10	0.31	275.60	0.64	336.90	0.12	304.60	0.44	62.40	0.19	193.80
8.00	0.27	268.40	0.38	274.20	0.76	344.40	0.14	313.00	0.48	69.20	0.22	190.80
8.50	0.30	268.60	0.44	273.20	0.83	349.50	0.16	322.00	0.50	74.00	0.24	188.40
9.00	0.33	268.80	0.49	272.40	0.87	352.80	0.18	331.80	0.51	77.40	0.26	186.60
9.50	0.35	268.90	0.54	271.80	0.90	354.80	0.21	342.50	0.52	79.80	0.28	185.10
10.00	0.37	269.00	0.57	271.30	0.92	356.20	0.26	353.70	0.52	81.60	0.29	183.80
10.50	0.39	269.10	0.61	270.90	0.94	357.10	0.33	5.00	0.53	82.90	0.30	182.70

11.00	0.40	269.20	0.64	270.50	0.95	357.70	0.44	16.00	0.53	83.90	0.31	181.60
11.50	0.41	269.30	0.66	270.20	0.96	358.20	0.62	26.50	0.53	84.70	0.32	180.30
12.00	0.42	269.40	0.69	269.80	0.96	358.50	0.99	37.00	0.53	85.30	0.32	178.30
12.50	0.43	269.40	0.72	269.30	0.97	358.80	1.91	51.10	0.53	85.80	0.32	173.30
13.00	0.43	269.50	0.78	271.60	0.97	359.00	4.82	102.20	0.53	86.30	0.41	160.60
13.50	0.44	269.50	0.71	274.30	0.98	359.20	4.00	198.60	0.53	86.60	0.48	184.30
14.00	0.45	269.50	0.72	271.80	0.98	359.30	2.07	225.00	0.53	87.00	0.42	185.90
14.50	0.45	269.60	0.74	271.10	0.98	359.40	1.45	232.90	0.53	87.20	0.40	184.70
15.00	0.45	269.60	0.75	270.80	0.98	359.50	1.16	237.50	0.53	87.40	0.40	183.90
15.50	0.46	269.60	0.76	270.60	0.99	359.60	0.99	241.00	0.53	87.60	0.40	183.40
16.00	0.46	269.70	0.77	270.50	0.99	359.60	0.89	243.80	0.53	87.80	0.40	183.00
17.00	0.47	269.70	0.78	270.30	0.99	359.70	0.76	248.10	0.53	88.10	0.40	182.40
18.00	0.47	269.70	0.79	270.20	0.99	359.80	0.69	251.30	0.53	88.30	0.40	182.10
19.00	0.47	269.80	0.80	270.20	0.99	359.80	0.65	253.80	0.53	88.50	0.41	181.80
20.00	0.48	269.80	0.81	270.10	1.00	359.90	0.62	255.70	0.53	88.70	0.41	181.60
25.00	0.49	269.90	0.83	270.00	1.00	359.90	0.55	261.70	0.53	89.20	0.42	181.10
30.00	0.49	269.90	0.84	270.00	1.00	0.00	0.52	264.50	0.53	89.40	0.42	180.90

90

4.00	0.00	180.00	0.13	358.60	0.04	343.40	0.01	353.00	0.01	237.50	0.01	67.40
5.00	0.00	180.00	0.27	311.30	0.17	296.80	0.03	303.70	0.02	211.20	0.02	50.30
5.50	0.00	180.00	0.34	299.40	0.31	287.10	0.04	291.70	0.03	215.70	0.02	50.10
6.00	0.00	180.00	0.40	291.40	0.54	285.80	0.05	283.60	0.05	232.00	0.02	52.20
6.50	0.00	180.00	0.47	285.70	0.87	294.30	0.05	277.70	0.08	259.70	0.02	55.40
7.00	0.00	180.00	0.52	281.70	1.20	311.30	0.06	272.80	0.08	293.20	0.02	59.20
7.50	0.00	180.00	0.57	278.70	1.34	328.90	0.05	268.10	0.07	323.00	0.02	63.00
8.00	0.00	180.00	0.62	276.50	1.32	341.30	0.04	261.90	0.05	343.40	0.02	66.60
8.50	0.00	180.00	0.66	274.90	1.26	348.70	0.03	248.20	0.04	355.80	0.02	70.10
9.00	0.00	180.00	0.69	273.80	1.20	353.00	0.01	178.80	0.03	3.10	0.02	73.20
9.50	0.00	180.00	0.73	272.90	1.15	355.50	0.04	116.40	0.02	7.20	0.02	76.10
10.00	0.00	180.00	0.75	272.30	1.12	357.00	0.10	104.80	0.02	9.60	0.02	78.80
10.50	0.00	180.00	0.78	271.80	1.09	358.00	0.18	100.50	0.02	10.70	0.02	81.40
11.00	0.00	180.00	0.80	271.40	1.07	358.60	0.30	98.60	0.01	11.20	0.03	84.00
11.50	0.00	180.00	0.82	271.10	1.06	359.10	0.51	97.90	0.01	11.10	0.03	86.70
12.00	0.00	180.00	0.84	271.00	1.05	359.30	0.90	99.10	0.01	10.80	0.04	90.20
12.50	0.00	180.00	0.87	271.10	1.04	359.50	1.86	105.40	0.01	10.40	0.07	98.00
13.00	0.00	180.00	0.89	274.30	1.03	359.70	4.89	150.40	0.01	9.90	0.15	142.60
13.50	0.00	180.00	0.82	272.30	1.03	359.70	4.19	240.20	0.01	9.30	0.11	234.80
14.00	0.00	180.00	0.85	270.60	1.02	359.80	2.24	262.60	0.01	8.70	0.05	260.20
14.50	0.00	180.00	0.87	270.40	1.02	359.90	1.59	266.80	0.01	8.10	0.03	266.00
15.00	0.00	180.00	0.88	270.30	1.02	359.90	1.29	268.20	0.01	7.60	0.02	268.60
15.50	0.00	180.00	0.89	270.20	1.01	359.90	1.12	268.90	0.01	0.00	0.02	0.00
16.00	0.00	180.00	0.90	270.20	1.01	359.90	1.01	269.20	0.00	0.00	0.01	0.00

17.00	0.00	180.00	0.91	270.10	1.01	0.00	0.87	269.60	0.00	0.00	0.01	0.00
18.00	0.00	180.00	0.92	270.10	1.01	0.00	0.80	269.70	0.00	0.00	0.01	0.00
19.00	0.00	180.00	0.93	270.10	1.01	0.00	0.75	269.80	0.00	0.00	0.01	0.00
20.00	0.00	180.00	0.94	270.10	1.00	0.00	0.71	269.90	0.00	0.00	0.01	0.00
25.00	0.00	180.00	0.96	270.00	1.00	0.00	0.63	269.90	0.00	0.00	0.01	0.00
30.00	0.00	180.00	0.97	270.00	1.00	0.00	0.60	270.00	0.00	0.00	0.00	0.00
120												
4.00	0.01	144.50	0.01	253.10	0.01	275.10	0.00	173.40	0.00	125.90	0.00	16.40
5.00	0.02	268.70	0.02	48.80	0.04	114.60	0.04	320.70	0.02	332.30	0.00	92.50
5.50	0.01	97.20	0.03	353.70	0.06	94.10	0.06	297.60	0.03	257.20	0.02	0.60
6.00	0.07	93.20	0.07	298.50	0.03	100.50	0.09	276.90	0.11	233.00	0.06	354.90
6.50	0.13	92.60	0.14	282.90	0.13	278.50	0.12	260.50	0.23	237.50	0.10	354.50
7.00	0.18	92.20	0.22	277.50	0.40	301.10	0.15	248.10	0.33	248.60	0.15	355.10
7.50	0.23	91.90	0.30	275.00	0.64	321.80	0.17	238.30	0.39	257.30	0.18	355.80
8.00	0.27	91.60	0.37	273.70	0.78	335.90	0.20	229.80	0.42	262.00	0.21	356.60
8.50	0.30	91.40	0.43	272.90	0.85	344.40	0.23	221.80	0.44	264.50	0.24	357.30
9.00	0.33	91.20	0.49	272.40	0.89	349.50	0.26	213.60	0.46	266.00	0.26	357.80
9.50	0.35	91.10	0.53	272.10	0.91	352.60	0.29	204.90	0.47	266.90	0.28	358.30
10.00	0.37	91.00	0.57	271.80	0.93	354.60	0.34	195.70	0.49	267.60	0.29	358.80
10.50	0.39	90.90	0.61	271.70	0.94	355.90	0.40	186.00	0.49	268.10	0.31	359.40
11.00	0.40	90.80	0.63	271.60	0.95	356.80	0.51	176.50	0.50	268.40	0.31	359.90
11.50	0.41	90.70	0.66	271.60	0.96	357.50	0.70	167.80	0.50	268.70	0.32	0.70
12.00	0.42	90.60	0.68	271.80	0.96	358.00	1.08	161.10	0.51	268.90	0.32	2.00
12.50	0.43	90.60	0.71	272.60	0.97	358.30	2.02	160.40	0.51	269.10	0.30	4.20
13.00	0.43	90.50	0.69	275.60	0.97	358.60	4.95	198.90	0.51	269.30	0.23	349.50
13.50	0.44	90.50	0.68	269.20	0.98	358.80	4.09	283.60	0.52	269.40	0.41	343.60
14.00	0.45	90.50	0.72	269.20	0.98	359.00	2.11	301.20	0.52	269.50	0.41	352.70
14.50	0.45	90.40	0.73	269.50	0.98	359.10	1.47	301.30	0.52	269.50	0.40	355.10
15.00	0.45	90.40	0.75	269.70	0.99	359.30	1.17	299.30	0.52	269.60	0.40	356.10
15.50	0.46	90.40	0.76	269.80	0.99	359.40	1.00	297.10	0.52	269.70	0.40	356.70
16.00	0.46	90.30	0.77	269.80	0.99	359.40	0.89	295.00	0.52	269.70	0.40	357.10
17.00	0.47	90.30	0.78	269.90	0.99	359.60	0.77	291.30	0.52	269.80	0.40	357.70
18.00	0.47	90.30	0.79	269.90	0.99	359.60	0.70	288.30	0.52	269.80	0.40	358.00
19.00	0.47	90.20	0.80	270.00	0.99	359.70	0.65	286.00	0.53	269.90	0.41	358.20
20.00	0.48	90.20	0.81	270.00	1.00	359.80	0.62	284.00	0.53	269.90	0.41	358.40
25.00	0.49	90.10	0.83	270.00	1.00	359.90	0.55	278.20	0.53	270.00	0.42	358.90
30.00	0.49	90.10	0.84	270.00	1.00	359.90	0.52	275.50	0.53	0.00	0.42	359.10
150												
4.00	0.01	268.90	0.00	185.90	0.01	167.10	0.00	14.30	0.00	344.80	0.00	147.10
5.00	0.01	54.00	0.01	203.80	0.03	258.50	0.01	144.10	0.01	122.20	0.00	325.30
5.50	0.04	286.50	0.01	175.80	0.02	228.90	0.01	311.40	0.04	22.20	0.01	143.50
6.00	0.07	277.30	0.01	87.30	0.08	84.60	0.05	302.10	0.08	13.00	0.01	159.90

6.50	0.04	270.60	0.02	69.30	0.22	96.30	0.09	290.90	0.05	7.50	0.01	329.00
7.00	0.03	103.90	0.01	306.60	0.25	120.40	0.12	279.30	0.08	255.60	0.05	337.50
7.50	0.11	96.10	0.05	274.70	0.11	153.20	0.15	268.30	0.22	252.40	0.08	342.20
8.00	0.20	94.30	0.09	271.70	0.10	310.30	0.18	258.30	0.35	256.70	0.12	345.50
8.50	0.29	93.40	0.14	271.10	0.27	333.00	0.20	249.10	0.45	259.90	0.16	348.00
9.00	0.36	92.80	0.18	271.10	0.41	341.50	0.23	240.40	0.54	262.10	0.19	349.90
9.50	0.43	92.30	0.22	271.20	0.52	346.40	0.26	231.90	0.60	263.70	0.22	351.40
10.00	0.49	92.00	0.25	271.30	0.61	349.50	0.30	223.40	0.66	264.90	0.24	352.60
10.50	0.54	91.70	0.28	271.40	0.68	351.70	0.35	214.80	0.70	265.80	0.26	353.60
11.00	0.58	91.50	0.30	271.60	0.73	353.30	0.43	206.10	0.74	266.50	0.28	354.40
11.50	0.61	91.40	0.33	271.80	0.78	354.50	0.57	197.80	0.77	267.00	0.29	355.10
12.00	0.64	91.20	0.35	272.30	0.81	355.40	0.82	190.50	0.79	267.50	0.29	355.70
12.50	0.67	91.10	0.36	273.60	0.84	356.10	1.48	187.60	0.81	267.90	0.29	355.80
13.00	0.69	91.00	0.34	276.70	0.86	356.70	3.87	222.10	0.83	268.20	0.27	340.70
13.50	0.71	90.90	0.36	266.10	0.88	357.10	2.87	315.50	0.84	268.50	0.41	349.60
14.00	0.72	90.80	0.39	268.10	0.90	357.50	1.36	327.20	0.85	268.70	0.39	354.80
14.50	0.74	90.80	0.40	268.90	0.91	357.80	0.92	324.70	0.86	268.90	0.38	355.80
15.00	0.75	90.70	0.41	269.30	0.93	358.10	0.72	320.60	0.87	269.00	0.38	356.40
15.50	0.76	90.70	0.42	269.50	0.94	358.30	0.61	316.60	0.87	269.10	0.39	356.70
16.00	0.77	90.60	0.43	269.60	0.94	358.50	0.54	313.00	0.88	269.30	0.39	357.00
17.00	0.78	90.50	0.44	269.80	0.96	358.80	0.45	306.70	0.89	269.40	0.39	357.40
18.00	0.80	90.50	0.45	269.80	0.97	359.10	0.41	301.70	0.89	269.60	0.40	357.70
19.00	0.81	90.40	0.45	269.90	0.97	359.20	0.38	297.60	0.90	269.70	0.40	357.90
20.00	0.81	90.40	0.46	269.90	0.98	359.40	0.36	294.30	0.90	269.80	0.40	358.10
25.00	0.84	90.20	0.48	270.00	0.99	359.70	0.32	284.30	0.91	269.90	0.41	358.70
30.00	0.85	90.20	0.49	270.00	1.00	359.90	0.30	279.50	0.91	270.00	0.42	359.00
180												
4.00	0.01	25.60	0.00	180.00	0.01	225.80	0.00	0.00	0.00	82.40	0.00	0.00
5.00	0.02	109.40	0.00	180.00	0.02	283.60	0.00	0.00	0.02	169.20	0.00	0.00
5.50	0.02	328.10	0.00	180.00	0.05	254.90	0.00	0.00	0.02	65.80	0.00	0.00
6.00	0.07	286.20	0.00	180.00	0.01	41.70	0.00	0.00	0.08	20.30	0.00	0.00
6.50	0.08	277.80	0.00	180.00	0.18	88.40	0.00	0.00	0.11	28.10	0.00	0.00
7.00	0.04	270.20	0.00	180.00	0.32	114.40	0.00	0.00	0.04	26.90	0.00	0.00
7.50	0.04	103.40	0.00	180.00	0.27	140.50	0.00	0.00	0.11	252.40	0.00	0.00
8.00	0.13	96.50	0.00	180.00	0.12	170.10	0.00	0.00	0.25	254.60	0.00	0.00
8.50	0.23	94.60	0.00	180.00	0.08	305.70	0.00	0.00	0.39	257.90	0.00	0.00
9.00	0.33	93.60	0.00	180.00	0.23	333.50	0.00	0.00	0.50	260.40	0.00	0.00
9.50	0.41	93.00	0.00	180.00	0.37	341.70	0.00	0.00	0.59	262.20	0.00	0.00
10.00	0.48	92.50	0.00	180.00	0.47	346.30	0.00	0.00	0.67	263.60	0.00	0.00
10.50	0.55	92.10	0.00	180.00	0.56	349.20	0.00	0.00	0.74	264.70	0.00	0.00
11.00	0.61	91.90	0.00	180.00	0.63	351.30	0.00	0.00	0.79	265.60	0.00	0.00
11.50	0.65	91.60	0.00	180.00	0.69	352.90	0.00	0.00	0.83	266.30	0.00	0.00

12.00	0.69	91.50	0.00	180.00	0.74	354.00	0.00	0.00	0.87	266.90	0.00	0.00
12.50	0.73	91.30	0.00	180.00	0.78	355.00	0.00	0.00	0.90	267.30	0.00	0.00
13.00	0.76	91.20	0.00	180.00	0.81	355.70	0.00	0.00	0.92	267.70	0.00	0.00
13.50	0.78	91.10	0.00	180.00	0.84	356.30	0.00	0.00	0.94	268.00	0.00	0.00
14.00	0.81	91.00	0.00	180.00	0.86	356.80	0.00	0.00	0.96	268.30	0.00	0.00
14.50	0.83	90.90	0.00	180.00	0.88	357.20	0.00	0.00	0.97	268.60	0.00	0.00
15.00	0.84	90.80	0.00	180.00	0.90	357.50	0.00	0.00	0.98	268.70	0.00	0.00
15.50	0.86	90.80	0.00	180.00	0.91	357.80	0.00	0.00	0.99	268.90	0.00	0.00
16.00	0.87	90.70	0.00	180.00	0.92	358.10	0.00	0.00	1.00	269.10	0.00	0.00
17.00	0.89	90.60	0.00	180.00	0.94	358.50	0.00	0.00	1.01	269.30	0.00	0.00
18.00	0.91	90.50	0.00	180.00	0.95	358.80	0.00	0.00	1.02	269.50	0.00	0.00
19.00	0.92	90.50	0.00	180.00	0.96	359.00	0.00	0.00	1.03	269.60	0.00	0.00
20.00	0.93	90.40	0.00	180.00	0.97	359.20	0.00	0.00	1.03	269.70	0.00	0.00
25.00	0.96	90.30	0.00	180.00	0.99	359.60	0.00	0.00	1.05	269.90	0.00	0.00
30.00	0.97	90.20	0.00	180.00	1.00	359.80	0.00	0.00	1.05	270.00	0.00	0.00

Appendix 12.6 MACSI2 macro files for JONSWAP and Torsethaugen

Note that the following macro files will be used for crane installation. To use them for moonpool installation an additional line must be added after the first "Results from static analyses to file?" question. It should say "/   ' Display moonpool transfer functions? (N)". Also sea states with $T_p = 7.0$ [s] must be removed, and so must analyses for $H_s \geq 5.0$ [m].

Appendix 12.6.1 JONSWAP macro file "MACRO000"

Below is the Macro file "MACRO000.mac", hence the JONSWAP macro file for wave heading 0°. Only macros for H_S = 2 [m] are given (all T_P values are included), but to include all H_S values the given file will just be extended.

```
3              ' *** MACSI-2 MAIN MENU ***
2              ' *** MACSI-2 ENVIRONMENT ***
y              ' Shall irregular waves be included ? (Y)
 2             ' ENTER OPTION FOR WAVE SPECTRUM DEFINITION :
2                    ' SIGNIFICANT HEIGHT, m
7                    ' PEAK PERIOD, s
3.3                  ' GAMMA
/                    ' BETA
/                    ' SIGMA A
/                    ' SIGMA B
/                    ' NUMBER OF WAVE COMPONENTS TO BE MODELLED
0                    ' WAVE DIRECTION (deg.)
 0             ' *** MACSI-2 ENVIRONMENT ***
5              ' *** MACSI-2 MAIN MENU ***
1                    ' Enter simulation number
600                  ' Enter simulation time (sec.)
2              ' *** M A C S I - 2 -> SIMULATION PREPARATION ***
20                   ' Duration of smooth start :
/                    ' Omitted time (s) :
1              ' *** M A C S I - 2 -> SIMULATION PREPARATION ***
Y              ' Results from static analysis to file ? (N)
y              ' Results to file ? (Y)
3              ' *** MACSI-2 MAIN MENU ***
2              ' *** MACSI-2 ENVIRONMENT ***
/              ' Shall irregular waves be included ? (Y)
 2             ' ENTER OPTION FOR WAVE SPECTRUM DEFINITION :
2                    ' SIGNIFICANT HEIGHT, m
9                    ' PEAK PERIOD, s
3.3                  ' GAMMA
/                    ' BETA
/                    ' SIGMA A
```

```
/                    ' SIGMA B
/                    ' NUMBER OF WAVE COMPONENTS TO BE MODELLED
0                    ' WAVE DIRECTION (deg.)
 0          ' *** MACSI-2 ENVIRONMENT ***
5          ' *** MACSI-2 MAIN MENU ***
2                    ' Enter simulation number
600                  ' Enter simulation time (sec.)
2          ' *** M A C S I - 2 -> SIMULATION PREPARATION ***
20                   ' Duration of smooth start :
/                    ' Omitted time (s) :
1          ' *** M A C S I - 2 -> SIMULATION PREPARATION ***
Y          ' Results from static analysis to file ? (N)
y          ' Results to file ? (Y)
3          ' *** MACSI-2 MAIN MENU ***
2          ' *** MACSI-2 ENVIRONMENT ***
/          ' Shall irregular waves be included ? (Y)
 2         ' ENTER OPTION FOR WAVE SPECTRUM DEFINITION :
2                    ' SIGNIFICANT HEIGHT, m
11                   ' PEAK PERIOD, s
3.3                  ' GAMMA
/                    ' BETA
/                    ' SIGMA A
/                    ' SIGMA B
/                    ' NUMBER OF WAVE COMPONENTS TO BE MODELLED
0                    ' WAVE DIRECTION (deg.)
 0         ' *** MACSI-2 ENVIRONMENT ***
5          ' *** MACSI-2 MAIN MENU ***
3                    ' Enter simulation number
600                  ' Enter simulation time (sec.)
2          ' *** M A C S I - 2 -> SIMULATION PREPARATION ***
20                   ' Duration of smooth start :
/                    ' Omitted time (s) :
1          ' *** M A C S I - 2 -> SIMULATION PREPARATION ***
Y          ' Results from static analysis to file ? (N)
y          ' Results to file ? (Y)
3          ' *** MACSI-2 MAIN MENU ***
2          ' *** MACSI-2 ENVIRONMENT ***
/          ' Shall irregular waves be included ? (Y)
 2         ' ENTER OPTION FOR WAVE SPECTRUM DEFINITION :
2                    ' SIGNIFICANT HEIGHT, m
13                   ' PEAK PERIOD, s
3.3                  ' GAMMA
```

```
/                         ' BETA
/                         ' SIGMA A
/                         ' SIGMA B
/                         ' NUMBER OF WAVE COMPONENTS TO BE MODELLED
0                         ' WAVE DIRECTION (deg.)
 0              ' *** MACSI-2 ENVIRONMENT ***
5              ' *** MACSI-2 MAIN MENU ***
4                    ' Enter simulation number
600                  ' Enter simulation time (sec.)
2              ' *** M A C S I - 2 -> SIMULATION PREPARATION ***
20                    ' Duration of smooth start :
/                     ' Omitted time (s) :
1              ' *** M A C S I - 2 -> SIMULATION PREPARATION ***
Y              ' Results from static analysis to file ? (N)
y              ' Results to file ? (Y)
3              ' *** MACSI-2 MAIN MENU ***
2              ' *** MACSI-2 ENVIRONMENT ***
/              ' Shall irregular waves be included ? (Y)
 2             ' ENTER OPTION FOR WAVE SPECTRUM DEFINITION :
2                     ' SIGNIFICANT HEIGHT, m
15                    ' PEAK PERIOD, s
3.3                   ' GAMMA
/                     ' BETA
/                     ' SIGMA A
/                     ' SIGMA B
/                     ' NUMBER OF WAVE COMPONENTS TO BE MODELLED
0                     ' WAVE DIRECTION (deg.)
 0             ' *** MACSI-2 ENVIRONMENT ***
5              ' *** MACSI-2 MAIN MENU ***
5                    ' Enter simulation number
600                  ' Enter simulation time (sec.)
2              ' *** M A C S I - 2 -> SIMULATION PREPARATION ***
20                   ' Duration of smooth start :
/                    ' Omitted time (s) :
1              ' *** M A C S I - 2 -> SIMULATION PREPARATION ***
Y              ' Results from static analysis to file ? (N)
y              ' Results to file ? (Y)
3              ' *** MACSI-2 MAIN MENU ***
2              ' *** MACSI-2 ENVIRONMENT ***
/              ' Shall irregular waves be included ? (Y)
 2             ' ENTER OPTION FOR WAVE SPECTRUM DEFINITION :
2                    ' SIGNIFICANT HEIGHT, m
```

```
17                     ' PEAK PERIOD, s
3.3                    ' GAMMA
/                      ' BETA
/                      ' SIGMA A
/                      ' SIGMA B
/                      ' NUMBER OF WAVE COMPONENTS TO BE MODELLED
0                      ' WAVE DIRECTION (deg.)
 0          ' *** MACSI-2 ENVIRONMENT ***
5           ' *** MACSI-2 MAIN MENU ***
6                      ' Enter simulation number
600                    ' Enter simulation time (sec.)
2           ' *** M A C S I - 2 -> SIMULATION PREPARATION ***
20                     ' Duration of smooth start :
/                      ' Omitted time (s) :
1           ' *** M A C S I - 2 -> SIMULATION PREPARATION ***
Y           ' Results from static analysis to file ? (N)
y           ' Results to file ? (Y)
```

Appendix 12.6.2 Torsethaugen macro file "TH000"

Below is the Macro file "TH000.mac", hence the Torsethaugen macro file for wave heading $0°$.
Only macros for $H_S = 2$ [m] are given (all T_P values are included), but to include all H_S values the
given file will just be extended.

```
3           ' *** MACSI-2 MAIN MENU ***
2           ' *** MACSI-2 ENVIRONMENT ***
Y           ' Shall irregular waves be included ? (Y)
 3          ' ENTER OPTION FOR WAVE SPECTRUM DEFINITION :
39                     ' NUMBER OF WAVE COMPONENTS TO BE MODELLED
HsTp2007               ' ENTER NAME OF WAVE SPECTRUM FILE
0                      ' WAVE DIRECTION (deg.)
 0          ' *** MACSI-2 ENVIRONMENT ***
5           ' *** MACSI-2 MAIN MENU ***
1                      ' Enter simulation number
600                    ' Enter simulation time (sec.)
2           ' *** M A C S I - 2 -> SIMULATION PREPARATION ***
20                     ' Duration of smooth start :
/                      ' Omitted time (s) :
 1          ' *** M A C S I - 2 -> SIMULATION PREPARATION ***
Y           ' Results from static analysis to file ? (N)
Y           ' Results to file ? (Y)
3           ' *** MACSI-2 MAIN MENU ***
2           ' *** MACSI-2 ENVIRONMENT ***
```

```
/                ' Shall irregular waves be included ? (Y)
 3               ' ENTER OPTION FOR WAVE SPECTRUM DEFINITION :
39                   ' NUMBER OF WAVE COMPONENTS TO BE MODELLED
HsTp2009             ' ENTER NAME OF WAVE SPECTRUM FILE
/                    ' WAVE DIRECTION (deg.)
 0               ' *** MACSI-2 ENVIRONMENT ***
5               ' *** MACSI-2 MAIN MENU ***
2                   ' Enter simulation number
600                 ' Enter simulation time (sec.)
2               ' *** M A C S I - 2 -> SIMULATION PREPARATION ***
20                  ' Duration of smooth start :
/                   ' Omitted time (s) :
 1              ' *** M A C S I - 2 -> SIMULATION PREPARATION ***
Y               ' Results from static analysis to file ? (N)
Y               ' Results to file ? (Y)
3               ' *** MACSI-2 MAIN MENU ***
2               ' *** MACSI-2 ENVIRONMENT ***
/               ' Shall irregular waves be included ? (Y)
 3               ' ENTER OPTION FOR WAVE SPECTRUM DEFINITION :
39                   ' NUMBER OF WAVE COMPONENTS TO BE MODELLED
HsTp2011             ' ENTER NAME OF WAVE SPECTRUM FILE
/                    ' WAVE DIRECTION (deg.)
 0               ' *** MACSI-2 ENVIRONMENT ***
5               ' *** MACSI-2 MAIN MENU ***
3                   ' Enter simulation number
600                 ' Enter simulation time (sec.)
2               ' *** M A C S I - 2 -> SIMULATION PREPARATION ***
20                  ' Duration of smooth start :
/                   ' Omitted time (s) :
 1              ' *** M A C S I - 2 -> SIMULATION PREPARATION ***
Y               ' Results from static analysis to file ? (N)
Y               ' Results to file ? (Y)
3               ' *** MACSI-2 MAIN MENU ***
2               ' *** MACSI-2 ENVIRONMENT ***
/               ' Shall irregular waves be included ? (Y)
 3               ' ENTER OPTION FOR WAVE SPECTRUM DEFINITION :
39                   ' NUMBER OF WAVE COMPONENTS TO BE MODELLED
HsTp2013             ' ENTER NAME OF WAVE SPECTRUM FILE
/                    ' WAVE DIRECTION (deg.)
 0               ' *** MACSI-2 ENVIRONMENT ***
5               ' *** MACSI-2 MAIN MENU ***
4                   ' Enter simulation number
```

```
600                   ' Enter simulation time (sec.)
2              ' *** M A C S I - 2 -> SIMULATION PREPARATION ***
20                    ' Duration of smooth start :
/                     ' Omitted time (s) :
 1             ' *** M A C S I - 2 -> SIMULATION PREPARATION ***
Y              ' Results from static analysis to file ? (N)
Y              ' Results to file ? (Y)
3              ' *** MACSI-2 MAIN MENU ***
2              ' *** MACSI-2 ENVIRONMENT ***
/              ' Shall irregular waves be included ? (Y)
 3             ' ENTER OPTION FOR WAVE SPECTRUM DEFINITION :
39                    ' NUMBER OF WAVE COMPONENTS TO BE MODELLED
HsTp2015              ' ENTER NAME OF WAVE SPECTRUM FILE
/                     ' WAVE DIRECTION (deg.)
 0             ' *** MACSI-2 ENVIRONMENT ***
5              ' *** MACSI-2 MAIN MENU ***
5                     ' Enter simulation number
600                   ' Enter simulation time (sec.)
2              ' *** M A C S I - 2 -> SIMULATION PREPARATION ***
20                    ' Duration of smooth start :
/                     ' Omitted time (s) :
 1             ' *** M A C S I - 2 -> SIMULATION PREPARATION ***
Y              ' Results from static analysis to file ? (N)
Y              ' Results to file ? (Y)
3              ' *** MACSI-2 MAIN MENU ***
2              ' *** MACSI-2 ENVIRONMENT ***
/              ' Shall irregular waves be included ? (Y)
 3             ' ENTER OPTION FOR WAVE SPECTRUM DEFINITION :
39                    ' NUMBER OF WAVE COMPONENTS TO BE MODELLED
HsTp2017              ' ENTER NAME OF WAVE SPECTRUM FILE
/                     ' WAVE DIRECTION (deg.)
 0             ' *** MACSI-2 ENVIRONMENT ***
5              ' *** MACSI-2 MAIN MENU ***
6                     ' Enter simulation number
600                   ' Enter simulation time (sec.)
2              ' *** M A C S I - 2 -> SIMULATION PREPARATION ***
20                    ' Duration of smooth start :
/                     ' Omitted time (s) :
 1             ' *** M A C S I - 2 -> SIMULATION PREPARATION ***
Y              ' Results from static analysis to file ? (N)
Y              ' Results to file ? (Y)
```

Appendix 12.7 Torsethaugen spectrum input file "HsTp4011"

39 indicates number of components used to specify the spectrum. 0.062 is the frequency interval $\Delta\omega$ between each frequency ω_i at which $S(\omega_i)$ is given. The left column represents ω_i, the right $S(\omega_i)$. These files are created and stored by MATLAB.

```
Torsethaugen spectrum with Hs = 4.0 and Tp = 11
39      0.062832
0.339292      0.013137
0.402124      0.349823
0.464956      1.194535
0.527788      2.351823
0.590619      3.010023
0.653451      1.900726
0.716283      1.372887
0.779115      1.090376
0.841947      0.864238
0.904779      0.685063
0.967611      0.546374
1.030442      0.439653
1.093274      0.357178
1.156106      0.292856
1.218938      0.242156
1.281770      0.201776
1.344602      0.169309
1.407434      0.142983
1.470265      0.121472
1.533097      0.103775
1.595929      0.089123
1.658761      0.076919
1.721593      0.066698
1.784425      0.058092
1.847256      0.050811
1.910088      0.044620
1.972920      0.039332
2.035752      0.034796
2.098584      0.030889
2.161416      0.027510
2.224248      0.024577
2.287079      0.022022
2.349911      0.019788
2.412743      0.017829
2.475575      0.016105
2.538407      0.014583
2.601239      0.013236
2.664071      0.012040
2.726902      0.010976
```

Appendix 12.8 MACSI2 -.OUT File

Example of a MACSI2 output file for crane deployment over the side where the module is just submerged, time instance 2. The JONSWAP wave spectrum is generated by $H_s = 4.5$ [m] and $T_p = 11.0$ [s]. Wave heading equals 0°.

```
M A C S I - 2  MARINE CRANE SIMULATION   Input to simulation no. 33:
    =====================================================================

    MAIN CONFIGURATION AND SYSTEM DATA:
        Lift line directly from crane to load
                                   X        Y        Z
        Crane top coordinates, m :  30.32   -20.00   30.31
        Water depth         :            1000.00 m
        No Guidewires are used
        No Guideance stiffness applied
        No Static forces on the object applied
        No Tugger wires applied
        No Heave Compensator is used
    CRANE/LIFT LINE DATA:
        Crane system resilience  :          .2896E-06 m/N
        Liftline material     :        Wire rope
        Number of wire parts    :              2
        Wire diameter        :            .127 m
        Mass pr unit length    :            .926 kg/m
        Youngs modulus       :          .6513E+11 N/m2
        Drag coefficient      :          1.200 Ns2/m3
    OBJECT DESCRIPTION:
        Mass            :          .2500E+06 Kg
        Volume          :            31.850 m3
                              X        Y        Z
        Dimensions, m       :  12.000   6.000   12.000
        Section areas, m2     :  68.400 136.800  68.400
        Mass coefficients     :  13.226  35.531  13.226
        Linear drag coefficients :   .200    .200    .200
        Quadratic drag coeff.  :  2.700   2.700   2.700

        Included interaction effects:  SURFACE
        Coefficient corrections are read from file: Cranecor.dat
    WINCH OPERATION:
        Zero winch speed
```

Line length   :   36.8 m

CRANE TOP MOTIONS:
    Waves and vessel transfer functions
    Vessel transfer functions are read from file: Normand.txt

ENVIRONMENTAL DATA:
    Current velocity   :   .00 m/s
    Current direction   :   .00 deg
    Wave data: JONSWAP spectrum   , 30 components.
      Significant height :   HS =   4.50 m
      Zerocrossing period :   TZ =   8.97 s
      Wave direction   :   .0 deg.

  SIMULATION TIME INCREMENT: .170 s

! STATIC CONFIGURATION OF THE CRANE SYSTEM : !
===

  SYSTEM SPECIFICATION :

    DIRECT WINCH-DOWN SYSTEM

  STATIC POSITIONS :

                         X (m): Y (m): Z (m):
    LOAD COORDINATES   :   30.32 -20.00 -7.16

    CRANE TOP COORDINATES   : 30.32 -20.00 30.31

  FORCE EQILIBRIUM :

    TOTAL HORIZONTAL FORCE ON THE LOAD :   .0 N
    VERTICAL FORCE FROM THE LOAD   : -2132240.0 N
            WIRE   :   8708.7 N
    RESULTING WIRE TENSION AT WINCH   : 2123532.0 N

NUMBER OF ITERATIONS: 2

! * EIGENVALUE ANALYSIS - RESONANCE PERIODS * !
==

LIFTED OBJECT IN AIR:
   Vertical resonance period without compensator: 1.75 s
   Transverse pendulum resonance periods:
      Direction: X   Y

      (No guidance stiffness or guidewires used):   12.28 s 12.28 s

LIFTED OBJECT FULLY SUBMERGED:
   Vertical resonance period without compensator: 2.90 s
   Transverse pendulum resonance periods:
      Direction: X   Y

      (Excl. tugger wires):   21.77 s 31.31 s

   Largest recommended time increment in the simulation
      to avoid numerical problems will be :   .170 s

   SELECTED TIME INCREMENT   :   .170 s

MAXIMA AND MINIMA FOUND FROM SIMULATION NO. 33:
===

| | CRANE MOTION (m): | | | BODY MOTION (m) : | | | TENSION |
	X	Y	Z	X	Y	Z	(kN):
MAXIMUM	31.40	-20.00	33.72	33.93	-20.00	-3.75	2947.63
MINIMUM	29.23	-20.00	26.82	28.03	-20.00	-10.91	946.79
Max at (s)	336.94	20.06	350.38	352.93	20.06	350.38	345.10
Min at (s)	341.87	20.06	344.93	347.65	20.06	344.93	361.09
MAX. VELOCITY	.71	.00	1.98	1.82	.00	2.01	1322.72
MIN. VELOCITY	-.70	.00	-1.94	-1.64	.00	-2.15	-942.62
Max at (s)	344.25	20.06	347.48	350.72	20.06	347.14	362.11
Min at (s)	339.66	20.06	342.55	355.48	20.06	342.72	360.41

	X	Y	Z	X	Y	Z	TENSION
MAX. ACCEL.	.54	.00	1.26	.88	.00	1.64	2203.25
MIN. ACCEL.	-.50	.00	-1.08	-1.18	.00	-1.52	-1404.58
Max at (s)	503.73	20.06	345.10	48.62	20.06	345.27	361.43
Min at (s)	39.10	20.06	340.34	352.93	20.06	361.26	362.96

	CRANE MOTION (m):			BODY MOTION (m) :			TENSION
	X	Y	Z	X	Y	Z	(kN):
MEAN VALUE	30.32	-20.00	30.31	30.37	-20.00	-7.15	2134.33
ST.DEV.	.357	.000	1.024	.860	.000	1.070	246.17
MEAN VELOCITY	.00	.00	.00	.00	.00	.00	-.41
ST.DEV.	.246	.000	.606	.489	.000	.644	258.73
MEAN ACCEL.	.00	.00	.00	.00	.00	.00	-.29
ST.DEV.	.180	.000	.379	.314	.000	.424	340.66

Estimated:

	X	Y	Z	X	Y	Z	TENSION
MEAN PERIOD (s)	9.12	.00	10.62	11.06	.00	10.44	5.98
MAX AMPL (sim.)	1.10	.00	3.11	2.60	.00	3.25	791.60
MAX AMPL (1 hr)	1.30	.00	3.67	3.07	.00	3.84	920.49
MAX AMPL (2 hr)	1.36	.00	3.86	3.23	.00	4.04	964.97

NEGLIGIBLE RISK FOR WIRE SLACK

The last 3412 steps of the simulated time series
are used in the statistical analysis.

Appendix 13: MATLAB Scripts and Script Descriptions

Appendix 13.1 Script descriptions

- "Main_file"

  "Main_file" is the spinal cord of the MATLAB script used. It starts by defining important constants like the acceleration of gravity and all values of interest for significant wave height H_s, wave peak period T_p and wave heading. Two inputs are needed; whether it should be crane or moonpool deployment and whether the JONSWAP or Torsethaugen wave spectrum should be used. First installation method is chosen. If crane lowering is wanted type 1 and enter, if lowering trough moonpool is wanted type 2 and enter. Then spectrum is chosen. Type 1 for JONSWAP and 2 for Torsethaugen. Dependent on wave spectrum "Main_file" either calls the function "JONSWAP" or "Torsethaugen". These functions generate the desired wave spectrum. Torsethaugen also generates necessary MACSI2 spectrum input files. See the "JONSWAP" and "Torstehaugen" paragraph for further descriptions. After that the function "Sea_state" is run. The last part of "Main_file" is to activate the function "Plot_results".

- "JONSWAP"/ "Torsethaugen"
  - Input: H_s, T_p, wave headings
  - Output: T_z computed from the spectrum

  Generates the chosen spectrum based on H_s and T_p. Resulting spectrum estimated T_z values are computed for all combinations of H_s and T_p and written to a text file. If "Torsethaugen" is used "MACSI2spectrum" and "THspectrum_plot" are called.

- "MACSI2spectrum"
  - Input: H_s, T_p, frequencies f for which the spectrum is defined, $S(f)$
  - Output: The chosen frequencies and spectrum values for these specific frequencies to be used in MACSI2.

  Based on the total wave spectrum taken in as input a representative spectrum is generated based on 39 selected frequencies. These selected frequencies and their belonging spectrum values are redefined so that angular frequency ω is used instead of frequency f and then written to a certain MACSI2 wave spectrum input filed. The MACSI2 wave spectrum input file is named after the H_s and T_p for which the spectrum is generated.

- "THspectrum_plot"
  - Input: H_s, T_p, frequencies f for which the spectrum is defined, $S(f)$, the chosen frequencies and spectrum values for these specific frequencies to be used in MACSI2.

The function generates Torsethaugen spectrum plots against frequency for all H_s and T_p values. Also chosen MACSI2 frequencies and spectrum values are plotted so the accuracy of spectra input into MACSI2 can be assessed.

- "Sea_states"
  - Input: H_s, T_p, deployment method, which wave spectrum that is to be considered and wave headings.
  - Output: The static weight of the module, calculated T_z values from the MACSI2 spectra, minimum wire tension for time instance 2, slamming force acting upwards for time instance 1, vertical water particle velocities and vertical crane tip velocities for all combinations of H_s and T_p.

 "Sea_states" calls the functions "readinfo" and "slamming".

- "readinfo"
  - Input: H_s, T_p, wave headings, deployment method and which wave spectrum that is to be considered.
  - Output: Calculated T_z values from the MACSI2 spectra, minimum wire tension for time instance 2, maximum crane tip vertical motion matrix and maximum crane tip vertical velocity matrix.

The function defines matrixes for all the output parameters and calls either "readinfo_J" or "readinfo_TH" depending on which wave spectrum that is chosen.

- "readinfo_J"/ "readinfo_TH"
  - Input: H_s, T_p, wave headings, deployment method and the empty matrixes for the output variables to be filled into.
  - Output: As for "readinfo"

"readinfo_J" and "readinfo_TH" do both extract parameters of interest from the MACSI2 output files. They navigate into the directories where the files are stored and open the output files one by one. Each output file is generated from a certain wave spectrum considering a specific H_s, T_p and wave heading combination. The extracted parameters are:

- T_z
- Static wire tension
- Minimum wire tension from the time history
- Maximum vertical crane tip velocity from the time history
- Maximum vertical crane tip motion amplitude from the 2 hours estimate
- Maximum wire tension amplitude from the 2 hours estimate

Minimum wire tension values for time instance 2 are calculated according to what is stated in Chapter 14 MATLAB Scripts. Each output value is placed in a matrix where its matrix position is dependent on H_s and T_p. Every row represents a T_p value while every column represents a H_s value.

- "slamming"
  - Input: H_s, T_p, wave headings, deployment method, which wave spectrum to use, T_z from MACSI2 and maximum vertical crane tip velocity.
  - Output: Vertical water particle velocity and slamming force acting upwards.

  The methodology listen in Chapter 12 Slamming Analyses is followed in order to compute the slamming forces at time instance 1. Vertical water particle velocities are calculated differently for the two deployment methods. If the structure is lowered over the side vertical water particle velocities are estimated from Equation 94 while if moonpool is used estimates are computed according to Equation 36. Moonpool vertical water particle velocities are calculated by the function "M_velocity".

- "M_velocity"
  - Input: H_s, T_p, wave headings, T_z from MACSI2.
  - Output: Vertical water particle velocities in the moonpool.

  Calculates moonpool vertical water particle velocities according to Equations 36 by using Equation 134 combined with T_z values from the MACSI2 spectra given in Tables 5 and 6.

- "Plot_results"
  - Input: H_s, T_p, wave headings, static weight of module, deployment method, chosen wave spectrum, minimum wire tension for time instance 1, slamming force upwards at time instance 2, vertical water particle velocity and vertical crane tip velocity.

  Minimum wire tension values for time instance 2 are calculated by subtracting the slamming force from the static wire tension. Then 4 plots are created for each wave heading. Minimum wire tension values for time instance 1, minimum wire tension values for time instance 2, vertical water particle velocities and vertical crane tip velocities are plotted against H_s with different lines representing different T_p values.

Appendix 13.2 MATLAB scripts

Appendix 13.2.1 "Main_file.m"

```matlab
clear all

g = 9.81;

%Choose deployment method and wave spectrum
Deploy = input('By Crane or Moonpool? Crane = 1, Moonpool = 2: ');
Seastate = input('Use JONSWAP or Torsethaugen? JONSWAP = 1, Torsethaugen = 2:
');

%Sea states analyzed
if Deploy == 2
    Hs = [2 2.5 3 3.5 4 4.5];
    Tp = [9 11 13 15 17];
    if Seastate == 2
        headings = [0 30];
        [Tz, fidS] = Torsethaugen(Deploy, Hs, Tp, g);
    else
        headings = [0 30 60 90 120 150 180];
        [Tz, fidS] = JONSWAP(Deploy, Hs, Tp, g);
    end
else
    Hs = [2 2.5 3 3.5 4 4.5 5.0 5.5];
    Tp = [7 9 11 13 15 17];
    if Seastate == 2
        headings = [0 30 60 90 120 150 180];
        [Tz, fidS] = Torsethaugen(Deploy, Hs, Tp, g);
    else
        headings = [0 30 60 90 120 150 180];
        [Tz, fidS] = JONSWAP(Deploy, Hs, Tp, g);
    end
end

%Read MACSI2 output and perform calculations
[Static_weight, Tz_calc, MinWiretension, Vw, F_slam, Cranevel_max,
Cranemotion] = Sea_states(Hs, Tp, g, Deploy, Seastate, headings, fidS);

%Plot results
Plot_results(Seastate, Deploy, Hs, Tp, headings, Static_weight,
MinWiretension, F_slam, Vw, Cranevel_max);
```

Appendix 13.2.2 "JONSWAP.m"

```matlab
function [Tz, fidS] = JONSWAP(Deploy, Hs, Tp, g)
%% Defining parameters
fp = 1./Tp;
gamma = 3.3;
sigma_a = 0.07;
sigma_b = 0.09;
delta_f = 0.001;
delta_omega = 2*pi*delta_f;
f = [0.001:delta_f:1];
omega = 2.*pi.*f;
Tz = zeros(size(Tp,2)+1,size(Hs,2)+1);

%% Computing the spectrum
for j = 1:length(Tp)
    for k = 1:length(Hs)
        Sf = zeros(1,size(f,2));
        Sw = zeros(1,size(f,2));

        alpha(j,k) = (Hs(1,k)/(4*g))^2*(2*pi*fp(1,j))^4*(0.065*gamma^0.803 +
0.135)^-1;

        for i = 1:length(f)
            if f(1,i) <= fp(1,j)
                sigma = sigma_a;
            else
                sigma = sigma_b;
            end
            Sf(1,i) = alpha(j,k)*g^2*(2*pi)^-4*f(1,i)^-5*exp(-
5/4*(fp(1,j)/f(1,i))^4)*gamma^exp(-(f(1,i)/fp(1,j)-1)^2/(2*sigma^2));
            Sw(1,i) = Sf(1,i)/(2*pi);
        end
%% Possibility to plot spectrum. If desirable remove comment signs
%         figure(k+(j-1)*length(Hs)+100);
%         plot(f,Sf)
%         title(sprintf('Hs = %0.1f, Tp = %d', Hs(1,k), Tp(1,j)))
%         xlabel('Frequency [1/s]')
%         ylabel('Spectrum [m^2s]')

%% Estimate Tz
        m0 = sum(Sw,2)*delta_omega;
        m2 = sum((Sw.*omega.^2),2)*delta_omega;
        Tz(j+1,k+1) = 1/(1/(2*pi)*sqrt(m2/m0));
    end
end

Tz(1,2:size(Tz,2)) = Hs;
Tz(2:size(Tz,1),1) = Tp;

%% Write Tz results to text file Jonswap_Tz
fidS = fopen('Jonswap_Tz.txt', 'w');
fprintf(fidS, 'Tz values for the JONSWAP spectrum\n\n');
fprintf(fidS, 'Hs values are given in the top row, Tp values in the first
column\n');
fprintf(fidS, '-------------------------------------------------------------
--\n');
```

```
if Deploy == 2
    for i = 1:size(Tz,1)
        fprintf(fidS,'%5.2f %5.2f %5.2f %5.2f %5.2f %5.2f %5.2f\n', Tz(i,:));
    end
else
    for i = 1:size(Tz,1)
        fprintf(fidS,'%5.2f %5.2f %5.2f %5.2f %5.2f %5.2f %5.2f %5.2f
%5.2f\n', Tz(i,:));
    end
end
fprintf(fidS, '----------------------------------------------------------
--\n');
end
```

Appendix 13.2.3 "Torsethaugen.m"

```matlab
function [Tz, fidS] = Torsethaugen(Deploy, Hs, Tp, g)
%% Define parameters
delta_f = 0.001;
delta_omega = 2*pi*delta_f;
f = [0.001:delta_f:1];
omega = 2.*pi.*f;
Tz = zeros(size(Tp,2)+1,size(Hs,2)+1);
F = 1:(length(Hs)*length(Tp));

%% Compute the spectrum
for j = 1:length(Tp)
    for k = 1:length(Hs)

        S1 = zeros(1,size(f,2));
        S2 = zeros(1,size(f,2));
        Sf = zeros(1,size(f,2));
        Sw = zeros(1,size(f,2));

        %Define spectrum parameters
        af = 6.6;
        ae = 2.0;
        au = 25;
        a10 = 0.7;
        a1 = 0.5;
        kg = 35.0;
        b1 = 2.0;
        a20 = 0.6;
        a2 = 0.3;
        a3 = 6;

        %Calculating parameters
        Tpf = af*Hs(1,k)^(1/3);
        Tl = ae*Hs(1,k)^0.5;
        Tu = au;

        if Tp(1,j) > Tl || Tp(1,j) < Tu
            el = (Tpf-Tp(1,j))/(Tpf-Tl);
            eu = (Tp(1,j)-Tpf)/(Tu-Tpf);
        else
            el = 1;
            eu = 1;
        end

        %If Tp < Tpf the sea state is wind dominated and if Tp >= Tpf the sea
        %state is swell dominated.
        if Tp(1,j) < Tpf
            %Primary peak
            Rw = (1-a10)*exp(-(el/a1)^2) + a10;
            H1 = Rw*Hs(1,k);
            Tp1 = Tp(1,j);
            sp = (2*pi/g)*H1/(Tp1^2);
            gamma1 = kg*sp^(6/7);
            %Secondary peak
            H2 = ((1-Rw^2)^0.5)*Hs(1,k);
            Tp2 = Tpf + b1;
```

```matlab
                gamma2 = 1;
        else
            %Primary peak
            Rs = (1-a20)*exp(-(eu/a2)^2) + a20;
            H1 = Rs*Hs(1,k);
            Tp1 = Tp(1,j);
            sf = (2*pi/g)*Hs(1,k)/Tpf^2;
            gammaf = kg*sf^(6/7);
            gamma1 = gammaf*(1 + a3*eu);
            %Secondary peak
            H2 = ((1-Rs^2)^0.5)*Hs(1,k);
            Tp2 = af*H2^(1/3);
            gamma2 = 1;
        end


        E1 = (1/16)*H1^2*Tp1;
        E2 = (1/16)*H2^2*Tp2;
        G0 = 3.26;
        Agamma = (1 + 1.1*log(gamma1)^1.19)/gamma1;


        for i = 1:length(f)
            f1 = f(1,i)*Tp1;
            f2 = f(1,i)*Tp2;
            if f1 < 1
                sigma = 0.07;
            else
                sigma = 0.09;
            end


            S1(1,i) = G0*Agamma*(f1^-4)*exp(-(f1^-4))*gamma1^(exp((-
1/(2*sigma^2))*(f1-1)^2));
            S2(1,i) = G0*(f2^-4)*exp(-(f2^-4));
            Sf(1,i) = E1*S1(1,i) + E2*S2(1,i);
            Sw(1,i) = Sf(1,i)/(2*pi);
        end
%% Estimate Tz
        m0 = sum(Sw,2)*delta_omega;
        m2 = sum((Sw.*omega.^2),2)*delta_omega;
        Tz(j+1,k+1) = 1/(1/(2*pi)*sqrt(m2/m0));

%% Construct MACSI2 spectrum input file
        [Chosen_f, Chosen_Sf] = MACSI2spectrum(k, j, Hs, Tp, f, Sf);

%% Possibility to plot spectrum. If desirable remove comment sign.
%           THspectrum_plot(Hs, Tp, k, j, f, Sf, Chosen_f, Chosen_Sf)
    end
end

Tz(1,2:size(Tz,2)) = Hs;
Tz(2:size(Tz,1),1) = Tp;

%% Write Tz results to text file Torsethaugen_Tz
fidS = fopen('Torsethaugen_Tz.txt', 'w');
fprintf(fidS, 'Tz values for the Torsethaugen spectra\n\n');
fprintf(fidS, 'Hs values are given in the top row, Tp values in the first
column\n\n');
```

```matlab
fprintf(fidS, '---------------------------------------------------------------
--\n');
if Deploy == 2
    for i = 1:size(Tz,1)
        fprintf(fidS,'%5.2f %5.2f %5.2f %5.2f %5.2f %5.2f %5.2f\n', Tz(i,:));
    end
else
    for i = 1:size(Tz,1)
        fprintf(fidS,'%5.2f %5.2f %5.2f %5.2f %5.2f %5.2f %5.2f %5.2f
%5.2f\n', Tz(i,:));
    end
end
fprintf(fidS, '---------------------------------------------------------------
--\n');
end
```

Appendix 13.2.4 "MACSI2spectrum.m"

```matlab
function [Chosen_f, Chosen_Sf] = MACSI2spectrum(k, j, Hs, Tp, f, Sf)
%% Defining constants
Intervals = 39;
Chosen_f = zeros(1,Intervals);
Chosen_Sf = zeros(1,Intervals);
Chosen_omega = zeros(1,Intervals);
Chosen_Somega = zeros(1,Intervals);

%% Find Macsi2 spectrum input
%Interval length
[I,J] = find(Sf > 0.05);
delta = floor((J(1,length(J))-J(1,1))/Intervals);

%Extract chosen frequencies and spectrum values
for i = 1:Intervals
    Chosen_f(1,i) = f(1,J(1,1+(i-1)*delta));
    Chosen_Sf(1,i) = Sf(1,J(1,1+(i-1)*delta));
end

%Find delta f and omega for the extracted MACSI2 spectrum input values
Chosen_delta_f = (Chosen_f(1,2)-Chosen_f(1,1));
Chosen_delta_omega = (Chosen_delta_f*2*pi);
for i = 1:Intervals
    Chosen_omega(1,i) = Chosen_f(1,1)*2*pi+(i-1)*Chosen_delta_omega;
    Chosen_Somega(1,i) = Chosen_Sf(1,i)/(2*pi);
end

%% Wright chosen values to Macsi2 input text file
if Tp(1,j) < 10
   fid = fopen(sprintf('HsTp%d0%d',10*Hs(1,k),Tp(1,j)),'w');
else
   fid = fopen(sprintf('HsTp%d%d',10*Hs(1,k),Tp(1,j)),'w');
end
fprintf(fid, 'Torsethaugen spectrum with Hs = %0.1f and Tp = %0.1d\n',
Hs(1,k), Tp(1,j));
fprintf(fid, '%d     %f\n', Intervals, Chosen_delta_omega);
for i = 1:Intervals
    fprintf(fid, '%f      %f\n', Chosen_omega(1,i), Chosen_Somega(1,i))  ;
end
fclose(fid);
end
```

Appendix 13.2.5 "THspectrum_plot.m"

```matlab
function THspectrum_plot(Hs, Tp, k, j, f, Sf, Chosen_f, Chosen_Sf)

%Blue line is original spectrum, red line is MACSI2 spectrum
figure(k+(j-1)*length(Hs)+200);
plot(f,Sf)
title(sprintf('Hs = %0.1f, Tp = %d', Hs(1,k), Tp(1,j)))
xlabel('Frequency [1/s]')
ylabel('Spectrum [m^2s]')
grid on
hold on
plot(Chosen_f, Chosen_Sf,'r', 'Marker', 'x', 'MarkerSize', 4)

end
```

Appendix 13.2.6 "Sea_states.m"

```matlab
function [Static_weight, Tz_calc, MinWiretension, Vw, F_slam, Cranevel_max,
Cranemotion] = Sea_states(Hs, Tp, g, Deploy, Seastate, headings, fidS)

Static_weight = 250*g;

%% Read MACSI2 output
[Tz_calc, MinWiretension, Cranemotion, Cranevel_max] = readinfo(headings, Hs,
Tp, Deploy, Seastate, fidS);

%% Perform slamming analyses
[Vw, F_slam] = slamming(headings, Hs, Tp, g, Deploy, Tz_calc, Cranevel_max);

end
```

Appendix 13.2.7 "readinfo.m"

```matlab
function [Tz_calc, MinWiretension, Cranemotion, Cranevel_max] =
readinfo(headings, Hs, Tp, Deploy, Seastate, fidS)
%% Define parameters
Tz_calc = zeros(size(Tp,2)+1,size(Hs,2)+1);
MinWiretension = zeros(size(Tp,2)+1, size(Hs,2)+1, size(headings,2));
MaxWiretension = zeros(size(Tp,2)+1, size(Hs,2)+1, size(headings,2));
Cranemotion = zeros(size(Tp,2)+1, size(Hs,2)+1, size(headings,2));
Cranevel_max = zeros(size(Tp,2)+1, size(Hs,2)+1, size(headings,2));
Craneaccel_max = zeros(size(Tp,2)+1, size(Hs,2)+1, size(headings,2));
Tz_calc(1,2:size(Tz_calc,2)) = Hs;
Tz_calc(2:size(Tz_calc,1),1) = Tp;

%Parameter matrixes row and column headings
for i = 1:length(headings)
    MinWiretension(1,1,i) = headings(1,i);
    MaxWiretension(1,1,i) = headings(1,i);
    Cranemotion(1,1,i) = headings(1,i);
    Cranevel_max(1,1,i) = headings(1,i);
    Craneaccel_max(1,1,i) = headings(1,i);
    MinWiretension(1,2:size(MinWiretension,2),i) = Hs;
    MaxWiretension(1,2:size(MaxWiretension,2),i) = Hs;
    Cranemotion(1,2:size(MinWiretension,2),i) = Hs;
    Cranevel_max(1,2:size(MinWiretension,2),i) = Hs;
    Craneaccel_max(1,2:size(MinWiretension,2),i) = Hs;
    MinWiretension(2:size(MinWiretension,1),1,i) = Tp;
    MaxWiretension(2:size(MaxWiretension,1),1,i) = Tp;
    Cranemotion(2:size(MinWiretension,1),1,i) = Tp;
    Cranevel_max(2:size(MinWiretension,1),1,i) = Tp;
    Craneaccel_max(2:size(MinWiretension,1),1,i) = Tp;
end

%% Read MACSI2 output file
if Seastate == 2
    [Tz_calc, MinWiretension, Cranemotion, Cranevel_max] =
readinfo_TH(headings, Hs, Tp, Deploy, Tz_calc, MinWiretension, MaxWiretension,
Cranemotion, Cranevel_max, Craneaccel_max, fidS);
else
    [Tz_calc, MinWiretension, Cranemotion, Cranevel_max] =
readinfo_J(headings, Hs, Tp, Deploy, Tz_calc, MinWiretension, MaxWiretension,
Cranemotion, Cranevel_max, Craneaccel_max, fidS);
end


end
```

Appendix 13.2.8 "readinfo_J.m"

```matlab
function [Tz_calc, MinWiretension, Cranemotion, Cranevel_max] =
readinfo_J(headings, Hs, Tp, Deploy, Tz_calc, MinWiretension, MaxWiretension,
Cranemotion, Cranevel_max, Craneaccel_max, fidS)
%% Open folders where MACSI2 output files are stored
if Deploy == 2
    deploy = 'Moonpool';
else
    deploy = 'Crane';
end

for k = 1:size(headings,2)
    for l = 1:size(Hs,2)
        for i = 1:size(Tp,2)
            if i+(l-1)*length(Tp) < 10
                fid1 =
fopen(sprintf('C:\\Users\\Ingvild\\Documents\\Skole\\Masters
thesis\\Matlab\\%d\\%s\\JONSWAP\\IR-TXT0%d.out', headings(1,k), deploy, i+(l-
1)*length(Tp)),'r');
            else
                fid1 =
fopen(sprintf('C:\\Users\\Ingvild\\Documents\\Skole\\Masters
thesis\\Matlab\\%d\\%s\\JONSWAP\\IR-TXT%d.out', headings(1,k), deploy, i+(l-
1)*length(Tp)),'r');
            end
            % Extract parameters
            tz = textscan(fid1, '%*s %*s %*s %*s %*s %f',1, 'HeaderLines',
46);
            tz = tz{1,1};
            static = textscan(fid1, '%*s %*s %*s %*s %*s %*s %f', 1,
'HeaderLines', 28);
            static = -static{1,1}/1000;
            min_wire_history = textscan(fid1, '%*s %*s %*s %*s %*s %*s %*s
%f', 1, 'HeaderLines', 36);
            min_wire_history = min_wire_history{1,1};
            max_cranevel = textscan(fid1, '%*s %*s %*s %*s %f',1,
'HeaderLines',3);
            min_cranevel = textscan(fid1, '%*s %*s %*s %*s %f',1,
'HeaderLines',1);
            cranevel(1,1) = max_cranevel{1,1};
            cranevel(1,2) = -min_cranevel{1,1};
            max_craneaccel = textscan(fid1, '%*s %*s %*s %*s %f',1,
'HeaderLines', 3);
            min_craneaccel = textscan(fid1, '%*s %*s %*s %*s %f',1,
'HeaderLines', 1);
            craneaccel(1,1) = max_craneaccel{1,1};
            craneaccel(1,2) = -min_craneaccel{1,1};
            cranemotion = textscan(fid1, '%*s %*s %*s %*s %*s %*s %f',1,
'HeaderLines',20);
            cranemotion = cranemotion{1,1};
            wire = textscan(fid1, '%*s %*s %*s %f', 1);
            wire = wire{1,1};

            %Store parameters in matrixes
            Tz_calc(i+1, l+1) = tz;
            if min_wire_history < static-wire
```

```matlab
                MinWiretension(i+1, l+1, k) = min_wire_history;
            else
                MinWiretension(i+1, l+1, k) = static - wire;
            end
            MaxWiretension(i+1, l+1, k) = static + wire;
            Cranemotion(i+1, l+1,k) = cranemotion;
            Cranevel_max(i+1, l+1,k) =  max(cranevel,[],2);
            Craneaccel_max(i+1, l+1,k) = max(craneaccel,[],2);
            %Overrule two Moonpool output files where results are
            %unreadable for the script
            if Deploy == 2 && headings(1,k) == 0 && Tp(1,i) == 9 && Hs(1,l) ==
4.5
                MinWiretension(i+1,l+1,k) = -50000;
            elseif Deploy == 2 && headings(1,k) == 30 && Tp(1,i) == 9 &&
Hs(1,l) == 4.5
                MinWiretension(i+1,l+1,k) = -50000;
            end
            fclose(fid1);
        end
    end
end
%Display cranemotion if desirable
Cranemotion;

%% Write MACSI2 computed Tz values to Jonswap_Tz
fprintf(fidS, 'Calculated Tz values for the MACSI2 JONSWAP spectrum\n\n');
fprintf(fidS, 'Hs values are given in the top row, Tp values in the first
column\n');
fprintf(fidS, '-----------------------------------------------------------
--\n');
if Deploy == 2
    for i = 1:size(Tz_calc,1)
        fprintf(fidS,'%5.2f %5.2f %5.2f %5.2f %5.2f %5.2f %5.2f\n',
Tz_calc(i,:));
    end
else
    for i = 1:size(Tz_calc,1)
        fprintf(fidS,'%5.2f %5.2f %5.2f %5.2f %5.2f %5.2f %5.2f %5.2f
%5.2f\n', Tz_calc(i,:));
    end
end
fprintf(fidS, '-----------------------------------------------------------
--\n');
fclose(fidS);
end
```

Appendix 13.2.9 "readinfo_TH.m"

```matlab
function [Tz_calc, MinWiretension, Cranemotion, Cranevel_max] =
readinfo_TH(headings, Hs, Tp, Deploy, Tz_calc, MinWiretension, MaxWiretension,
Cranemotion, Cranevel_max, Craneaccel_max, fidS)
%% Open folders where MACSI2 output files are stored
if Deploy == 2
    deploy = 'Moonpool';
else
    deploy = 'Crane';
end


for k = 1:size(headings,2)
    for l = 1:size(Hs,2)
        for i = 1:size(Tp,2)
            if i+(l-1)*length(Tp) < 10
                fid1 =
fopen(sprintf('C:\\Users\\Ingvild\\Documents\\Skole\\Masters
thesis\\Matlab\\%d\\%s\\Torsethaugen\\IR-TXT0%d.out', headings(1,k), deploy,
i+(l-1)*length(Tp)),'r');
            else
                fid1 =
fopen(sprintf('C:\\Users\\Ingvild\\Documents\\Skole\\Masters
thesis\\Matlab\\%d\\%s\\Torsethaugen\\IR-TXT%d.out', headings(1,k), deploy,
i+(l-1)*length(Tp)),'r');
            end
            %Extract parameters
            tz = textscan(fid1, '%*s %*s %*s %*s %*s %f',1, 'HeaderLines',
47);
            tz = tz{1,1};
            static = textscan(fid1, '%*s %*s %*s %*s %*s %*s %f', 1,
'HeaderLines', 28);
            static = -static{1,1}/1000;
            min_wire_history = textscan(fid1, '%*s %*s %*s %*s %*s %*s %*s
%f', 1, 'HeaderLines', 36);
            min_wire_history = min_wire_history{1,1};
            max_cranevel = textscan(fid1, '%*s %*s %*s %*s %f',1,
'HeaderLines',3);
            min_cranevel = textscan(fid1, '%*s %*s %*s %*s %f',1,
'HeaderLines',1);
            cranevel(1,1) = max_cranevel{1,1};
            cranevel(1,2) = -min_cranevel{1,1};
            max_craneaccel = textscan(fid1, '%*s %*s %*s %*s %f',1,
'HeaderLines', 3);
            min_craneaccel = textscan(fid1, '%*s %*s %*s %*s %f',1,
'HeaderLines', 1);
            craneaccel(1,1) = max_craneaccel{1,1};
            craneaccel(1,2) = -min_craneaccel{1,1};
            cranemotion = textscan(fid1, '%*s %*s %*s %*s %*s %*s %f',1,
'HeaderLines',20);
            cranemotion = cranemotion{1,1};
            wire = textscan(fid1, '%*s %*s %*s %f', 1);
            wire = wire{1,1};

            %Store parameters in matrixes
            Tz_calc(i+1, l+1) = tz;
            if min_wire_history < static-wire
```

```matlab
                    MinWiretension(i+1, l+1, k) = min_wire_history;
                else
                    MinWiretension(i+1, l+1, k) = static - wire;
                end
                MaxWiretension(i+1, l+1, k) = static + wire;
                Cranemotion(i+1, l+1,k) = cranemotion;
                Cranevel_max(i+1, l+1,k) =  max(cranevel,[],2);
                Craneaccel_max(i+1, l+1,k) = max(craneaccel,[],2);
                fclose(fid1);
            end
        end
end
%Display cranemotion if desirable
Cranemotion;

%% Write MACSI2 computed Tz values to Torsethaugen_Tz
fprintf(fidS, 'Calculated Tz values for the MACSI2 Torsethaugen
spectrum\n\n');
fprintf(fidS, 'Hs values are given in the top row, Tp values in the first
column\n');
fprintf(fidS, '-----------------------------------------------------------
--\n');
if Deploy == 2
    for i = 1:size(Tz_calc,1)
        fprintf(fidS,'%5.2f %5.2f %5.2f %5.2f %5.2f %5.2f %5.2f\n',
Tz_calc(i,:));
    end
else
    for i = 1:size(Tz_calc,1)
        fprintf(fidS,'%5.2f %5.2f %5.2f %5.2f %5.2f %5.2f %5.2f %5.2f
%5.2f\n', Tz_calc(i,:));
    end
end
fprintf(fidS, '-----------------------------------------------------------
--\n');
fclose(fidS);
end
```

Appendix 13.2.10 "slamming.m"

```matlab
function [Vw, F_slam] = slamming(headings, Hs, Tp, g, Deploy, Tz_calc,
Cranevel_max)
%% Defining parameters
Cs = 5.0;
rho_w = 1025;
As = 12*6*(1-0.05);
Vc = 0.5;
d = 0;

Zeta_a = zeros(1,size(Hs,2));
Zeta_a = 0.9.*Hs;
Vw = zeros(size(Tp,2)+1, size(Hs,2)+1, size(headings,2));
Aw = zeros(size(Tp,2)+1, size(Hs,2)+1, size(headings,2));
Vs = zeros(size(Tp,2)+1, size(Hs,2)+1, size(headings,2));
F_slam = zeros(size(Tp,2)+1, size(Hs,2)+1, size(headings,2));
F_rho = zeros(size(Tp,2)+1, size(Hs,2)+1, size(headings,2));
F_m = zeros(size(Tp,2)+1, size(Hs,2)+1, size(headings,2));
F_hyd = zeros(size(Tp,2)+1, size(Hs,2)+1, size(headings,2));

for i = 1:length(headings)
    Vw(1,1,i) = headings(1,i);
    Aw(1,1,i) = headings(1,i);
    Vs(1,1,i) = headings(1,i);
    F_slam(1,1,i) = headings(1,i);
    F_rho(1,1,i) = headings(1,i);
    F_m(1,1,i) = headings(1,i);
    F_hyd(1,1,i) = headings(1,i);
    Vw(1,2:size(Vw,2),i) = Hs;
    Aw(1,2:size(Vw,2),i) = Hs;
    Vs(1,2:size(Vw,2),i) = Hs;
    F_slam(1,2:size(Vw,2),i) = Hs;
    F_rho(1,2:size(Vw,2),i) = Hs;
    F_m(1,2:size(Vw,2),i) = Hs;
    F_hyd(1,2:size(Vw,2),i) = Hs;
    Vw(2:size(Vw,1),1,i) = Tp;
    Aw(2:size(Vw,1),1,i) = Tp;
    Vs(2:size(Vw,1),1,i) = Tp;
    F_slam(2:size(Vw,1),1,i) = Tp;
    F_rho(2:size(Vw,1),1,i) = Tp;
    F_m(2:size(Vw,1),1,i) = Tp;
    F_hyd(2:size(Vw,1),1,i) = Tp;
end

%% If moonpool deployment estimate moonpool water particle velocities
if Deploy == 2
    [Vel_mp] = M_velocity(headings, Hs, Tp, g, Tz_calc);
end
%% Compute slamming forces
for k = 1:length(headings)
    for i = 2:(size(Tp,2)+1)
        for j = 2:(size(Hs,2)+1)
            if Deploy == 2
                Vw(i,j,k) = Vel_mp(i-1,j-1,k);
            else
```

```
            Vw(i,j,k) = Zeta_a(1,j-1)*(2*pi/Tz_calc(i,j))*exp(-
4*pi^2*d/(Tz_calc(i,j)^2*g));
            end
            Aw(i,j,k) = Zeta_a(1,j-1)*(2*pi/Tz_calc(i,j))^2*exp(-
4*pi^2*d/(Tz_calc(i,j)^2*g));
            Vs(i,j,k) = Vc + sqrt(Cranevel_max(i,j,k)^2 + Vw(i,j,k)^2);
            F_slam(i,j,k) = 0.5*rho_w*Cs*As*Vs(i,j,k)^2/1000; %kN
        end
    end
end


end
```

Appendix 13.2.11 "M_velocity.m"

```matlab
function [Vel_mp] = M_velocity(headings, Hs, Tp, g, Tz_calc)
%% Defining parameters
rho = 1025;
Draft = 7.8;
kappa = 0.46;
neta = 0.19;
A_mp = 105;
M_wp = rho*A_mp*(Draft + kappa*sqrt(A_mp));
K_wp = rho*g*A_mp;
omega0 = sqrt(K_wp/M_wp);

%% Upload Normand Subsea heave transfer functions wave headings 0-180
Gs = load('Gs.txt');
T = Gs(:,1)';
omega = 2.*pi./T;

%Extraxt transfer functions
for i = 1:length(headings)
   Gs_amp(1,:,i) = Gs(:,i*2);
   Gs_phi(1,:,i) = Gs(:,1+i*2)*pi/180;

   %Compute moonpool water plug elevation ratio to wave elevation
   for j = 1:length(Gs_phi(1,:,i))
       if Gs_phi(1,j,i) >= 0 && Gs_phi(1,j,i) < pi/2;
           Real_Gs(1,j,i) = Gs_amp(1,j,i)/sqrt(tan(Gs_phi(1,j,i))^2 + 1);
           Im_Gs(1,j,i) = sqrt(Gs_amp(1,j,i)^2 - Real_Gs(1,j,i)^2);
       elseif Gs_phi(1,j,i) > pi/2 && Gs_phi(1,j,i) < pi;
           Real_Gs(1,j,i) = - Gs_amp(1,j,i)/sqrt(tan(Gs_phi(1,j,i))^2 + 1);
           Im_Gs(1,j,i) = sqrt(Gs_amp(1,j,i)^2 - Real_Gs(1,j,i)^2);
       elseif Gs_phi(1,j,i) >= pi && Gs_phi(1,j,i) < 3*pi/4;
           Real_Gs(1,j,i) = - Gs_amp(1,j,i)/sqrt(tan(Gs_phi(1,j,i))^2 + 1);
           Im_Gs(1,j,i) = - sqrt(Gs_amp(1,j,i)^2 - Real_Gs(1,j,i)^2);
       else Gs_phi(1,j,i) > 3*pi/4 && Gs_phi(1,j,i) < 2*pi;
           Real_Gs(1,j,i) = Gs_amp(1,j,i)/sqrt(tan(Gs_phi(1,j,i))^2 + 1);
           Im_Gs(1,j,i) = - sqrt(Gs_amp(1,j,i)^2 - Real_Gs(1,j,i)^2);
       end
       Ratio_transfer(1,j,i) = sqrt(Real_Gs(1,j,i)^2+Im_Gs(1,j,i)^2);

       Real_Gw(1,j,i) = rho*A_mp*(g*exp(-omega(1,j)^2/g*Draft)-
omega(1,j)^2*kappa*sqrt(A_mp)*Real_Gs(1,j,i));
       Im_Gw(1,j,i) = - rho*A_mp*omega(1,j)^2*kappa*sqrt(A_mp)*Im_Gs(1,j,i);

       freq_rat(1,j) = omega(1,j)/omega0;

       Real_ratio_num(1,j,i) = (Real_Gw(1,j,i)/(rho*g*A_mp)-
Im_Gs(1,j,i)*2*neta*freq_rat(1,j))*(1-
freq_rat(1,j)^2)+(Real_Gs(1,j,i)*4*neta^2*freq_rat(1,j)+Im_Gw(1,j,i)/(rho*g*A_
mp)*2*neta)*freq_rat(1,j);
       Im_ratio_num(1,j,i) =
(Im_Gw(1,j,i)/(rho*g*A_mp)+Real_Gs(1,j,i)*2*neta*freq_rat(1,j))*(1-
freq_rat(1,j)^2)+(Im_Gs(1,j,i)*4*neta^2*freq_rat(1,j)-
Real_Gw(1,j,i)/(rho*g*A_mp)*2*neta)*freq_rat(1,j);
       ratio_denom(1,j,i) = 1-
2*freq_rat(1,j)^2+freq_rat(1,j)^4+4*neta^2*freq_rat(1,j)^2;
```

```matlab
        Real_ratio(1,j,i) = Real_ratio_num(1,j,i)/ratio_denom(1,j,i);
        Im_ratio(1,j,i) = Im_ratio_num(1,j,i)/ratio_denom(1,j,i);
        Ratio_amp(1,j,i) = sqrt(Real_ratio(1,j,i)^2+Im_ratio(1,j,i)^2);
    end

    for j = 1:length(Tp)
        for k = 1:length(Hs)
            [X,Y] = find(T == Tp(1,j));
            RAO_mp(j,1,i) = Ratio_amp(1,Y,i);
            Amp_mp(j,k,i) = RAO_mp(j,1,i)*Hs(1,k)*0.9;
            Vel_mp(j,k,i) = Amp_mp(j,k,i)/(0.5*Tz_calc(j+1,k+1,1));
        end
    end
end

Ratio_transfer;

%% Possible to plot water plug to wave elevation RAO
% for i = 1:length(headings)
% figure(i*400)
% plot((T.*omega0./(2.*pi))', Ratio_amp(1,:,i), '*-')
% xlabel('T/T_0 [s/s]')
% ylabel('Water plug elevation/wave elevation [m/m]')
% grid on
% title(sprintf('Wave Heading %d', headings(1,i)))
% end

end
```

Appendix 13.2.12 "Plot_results.m"

```matlab
function Plot_results(Seastate, Deploy, Hs, Tp, headings, Static_weight,
MinWiretension, F_slam, Vw, Cranevel_max)
%% Compute the slack sling limit
for i = 1:length(Hs)
    limit(1,i) = 0.1*Static_weight;
end

%% Matrixed with Hs values analysed and wire tension when slamming is
considered. Both to be used during plotting
Hsmatrix = zeros(size(Tp,2), size(Hs,2), size(headings,2));
hsmatrix = zeros(size(Tp,2)+1, size(Hs,2), size(headings,2));
Slammingforce = zeros(size(Tp,2), size(Hs,2), size(headings,2));
for j = 1:length(headings)
    for i = 1:length(Tp)
        Hsmatrix(i,:,j) = Hs;
    end
    for i = 1:length(Tp)+1
        hsmatrix(i,:,j) = Hs;
    end
    Slammingforce(:,:,j) = Static_weight-
F_slam(2:size(F_slam,1),2:size(F_slam,2),j);
end

%% Plots
for i = 1:length(headings)
    %Minimum wire tension when slamming at time instance 1
    figure(i*4-3)
    if Deploy == 2
        slammingforce = zeros(size(Slammingforce,1)+1, size(Slammingforce,2),
i);
        slammingforce(1,1:size(Slammingforce,2),i) = limit;
        slammingforce(2:size(Slammingforce,1)+1,1:size(Slammingforce,2),i) =
Slammingforce(:,:,i);
        plot(hsmatrix(:,:,i)', slammingforce(:,:,i)', '*-')
        hold on
        plot(hsmatrix(:,:,i)', limit, 'k-')
        legend('', 'Tp 9', 'Tp 11', 'Tp 13', 'Tp 15', 'Tp 17', 'Limit',
'Location', 'EastOutside')
    else
        plot(Hsmatrix(:,:,i)', Slammingforce(:,:,i)', '*-')
        hold on
        plot(Hsmatrix(:,:,i)', limit, 'k-')
        legend('Tp 7', 'Tp 9', 'Tp 11', 'Tp 13', 'Tp 15', 'Tp 17', 'Limit',
'Location', 'EastOutside')
    end
    axis([2.0 5.5 -3000 2500])
    xlabel('Hs [m]')
    ylabel('Minimum Wire Tension, Slamming Considered [kN]')
    if Seastate == 2;
        title(sprintf('Torsethaugen Wave Spectrum, Wave Heading %d',
headings(1,i)))
    else
        title(sprintf('JONSWAP Wave Spectrum, Wave Heading %d',
headings(1,i)))
    end
```

```matlab
    grid on

    %Minimum wire tension at time instance 2
    figure(i*4-2)
    if Deploy == 2
        MinWiretension(1,2:size(MinWiretension,2),i) = limit;
        plot(hsmatrix(:,:,i)',
MinWiretension(1:size(MinWiretension,1),2:size(MinWiretension,2),i)', '*-')
        hold on
        plot(hsmatrix(:,:,i)', limit, 'k-')
        legend('', 'Tp 9', 'Tp 11', 'Tp 13', 'Tp 15', 'Tp 17', 'Limit',
'Location', 'EastOutside')
    else
        plot(Hsmatrix(:,:,i)',
MinWiretension(2:size(MinWiretension,1),2:size(MinWiretension,2),i)', '*-')
        hold on
        plot(Hsmatrix(:,:,i)', limit, 'k-')
        legend('Tp 7', 'Tp 9', 'Tp 11', 'Tp 13', 'Tp 15', 'Tp 17', 'Limit',
'Location', 'EastOutside')
    end
    axis([2.0 5.5 -3000 2500])
    xlabel('Hs [m]')
    ylabel('Minimum Wire Tension [kN]')
    if Seastate == 2
        title(sprintf('Torsethaugen Wave Spectrum, Wave Heading %d',
headings(1,i)))
    else
        title(sprintf('JONSWAP Wave Spectrum, Wave Heading %d',
headings(1,i)))
    end
    grid on

    %Vertical water particle velocity
    figure(i*4-1)
    if Deploy == 2
        Vw(1,:,i) = zeros(1,size(Vw,2));
        plot(hsmatrix(:,:,i)', Vw(1:size(Vw,1),2:size(Vw,2),i)', '*-')
        legend('','Tp 9', 'Tp 11', 'Tp 13', 'Tp 15', 'Tp 17', 'Location',
'EastOutside')
    else
        plot(Hsmatrix(:,:,i)', Vw(2:size(Vw,1),2:size(Vw,2),i)', '*-')
        legend('Tp 7', 'Tp 9', 'Tp 11', 'Tp 13', 'Tp 15', 'Tp 17', 'Location',
'EastOutside')
    end
    axis([2.0 5.5 0 5.5])
    xlabel('Hs [m]')
    ylabel('Water Particle Velocity [m/s]')
    if Seastate == 2
        title(sprintf('Torsethaugen Wave Spectrum, Wave Heading %d',
headings(1,i)))
    else
        title(sprintf('JONSWAP Wave Spectrum, Wave Heading %d',
headings(1,i)))
    end
    grid on

    %Vertical crane tip/main sheave in MHT velocity
```

```matlab
    figure(i*4)
    if Deploy == 2
        Cranevel_max(1,2:size(Cranevel_max,2),i) = limit;
        plot(hsmatrix(:,:,i)',
Cranevel_max(1:size(Cranevel_max,1),2:size(Cranevel_max,2),i)', '*-')
        hold on
        plot(hsmatrix(:,:,i)', limit, 'k-')
        legend('', 'Tp 9', 'Tp 11', 'Tp 13', 'Tp 15', 'Tp 17', 'Limit',
'Location', 'EastOutside')
    else
        plot(Hsmatrix(:,:,i)',
Cranevel_max(2:size(Cranevel_max,1),2:size(Cranevel_max,2),i)', '*-')
        hold on
        plot(Hsmatrix(:,:,i)', limit, 'k-')
        legend('Tp 7', 'Tp 9', 'Tp 11', 'Tp 13', 'Tp 15', 'Tp 17', 'Limit',
'Location', 'EastOutside')
    end
    axis([2.0 5.5 0 5.5])
    xlabel('Hs [m]')
    ylabel('Crane Tip Vertical Velocity [m/s]')
    if Seastate == 2
        title(sprintf('Torsethaugen Wave Spectrum, Wave Heading %d',
headings(1,i)))
    else
        title(sprintf('JONSWAP Wave Spectrum, Wave heading %d',
headings(1,i)))
    end
    grid on

end

end
```

Appendix 14: Minimum Wire Tension for Residual Wave Headings

Here are the additional plots of minimum wire tension considering both deployment methods and time instances for the residual wave headings not given in Chapter 15.5 Minimum wire tension. These wave headings are 60⁰, 150⁰ and 180⁰ for over the side deployment and 60⁰, 120⁰, 150⁰ and 180⁰ for moonpool deployment.

Appendix 14.1: Crane deployment, time instance 1.
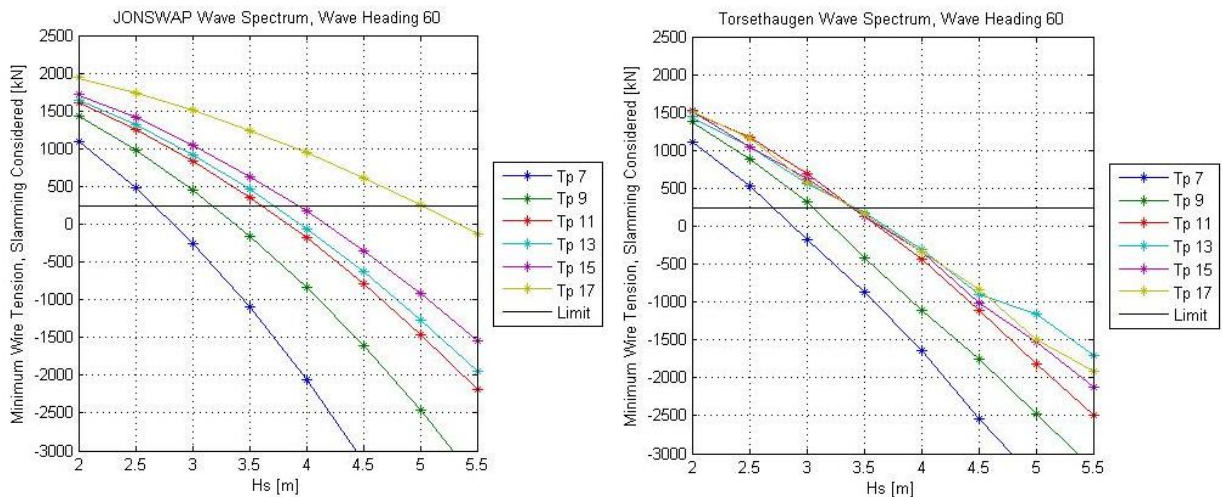
Figure 87: Crane deployment. Minimum wire tension [kN] for JONSWAP and Torsethaugen wave spectra, wave heading 60⁰ at time instance 1.
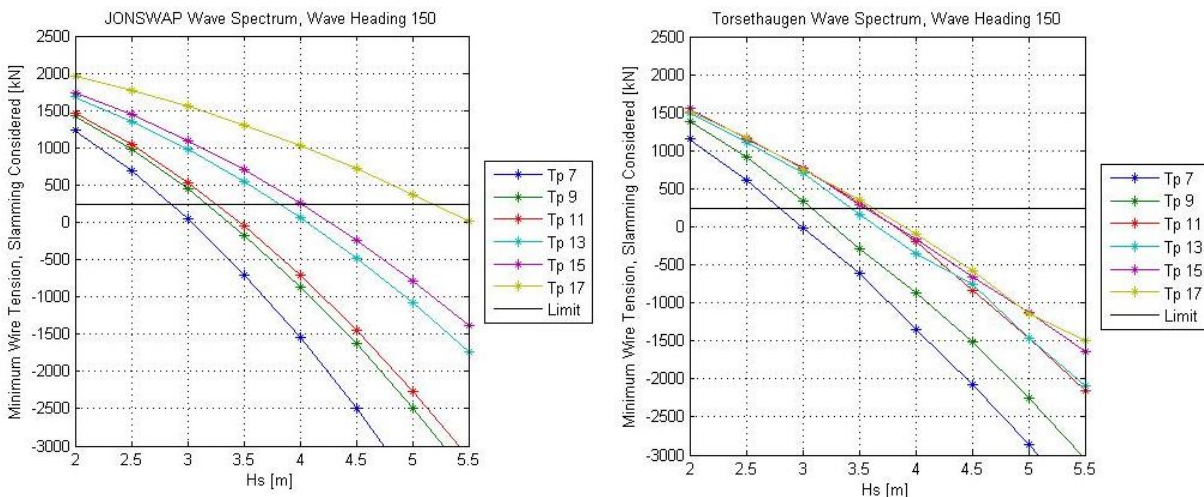
Figure 88: Crane deployment. Minimum wire tension [kN] for JONSWAP and Torsethaugen wave spectra, wave heading 150⁰ at time instance 1.
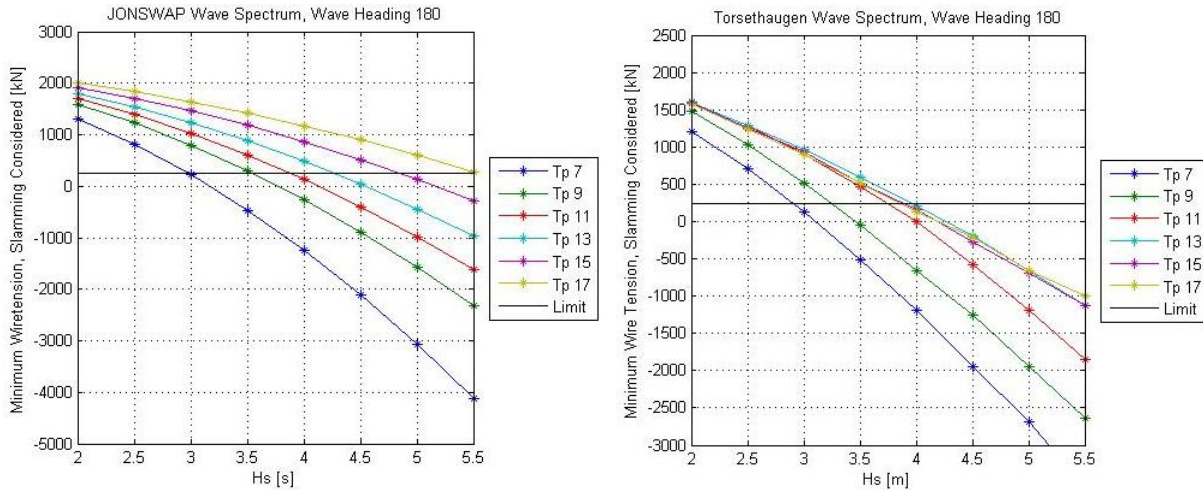
Figure 89: Crane deployment. Minimum wire tension [kN] for JONSWAP and Torsethaugen wave spectra, wave heading 180° at time instance 1.

Appendix 14.2: Crane deployment, time instance 2.
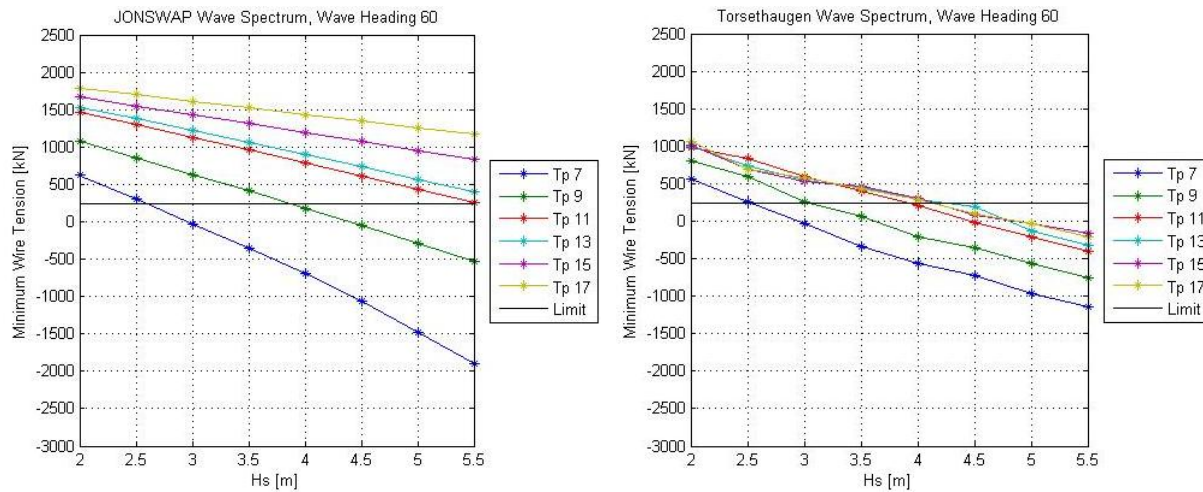
Figure 90: Crane deployment. Minimum wire tension [kN] for JONSWAP and Torsethaugen wave spectra, wave heading 60° at time instance 2.
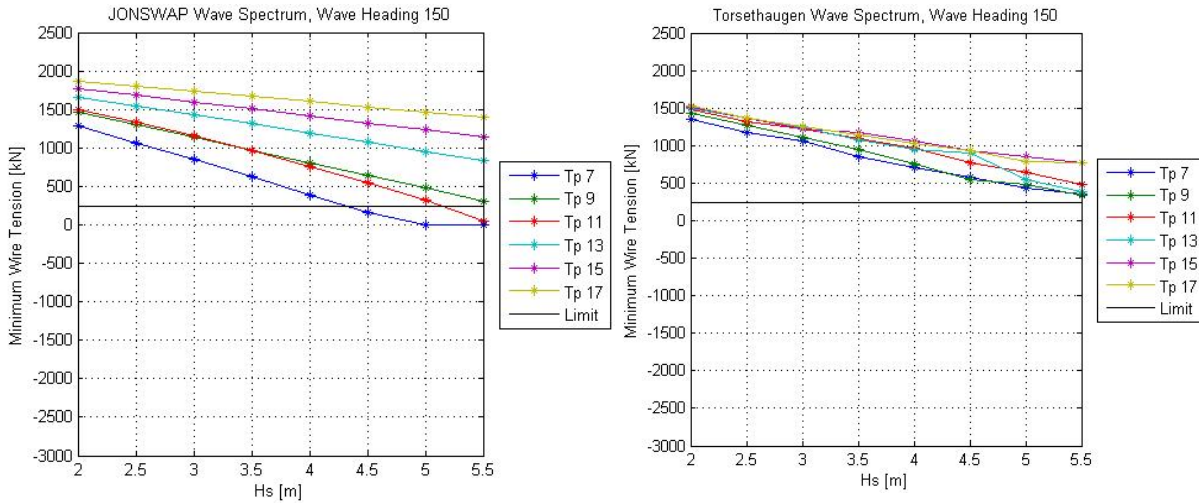
Figure 91: Crane deployment. Minimum wire tension [kN] for JONSWAP and Torsethaugen wave spectra, wave heading 150º at time instance 2.
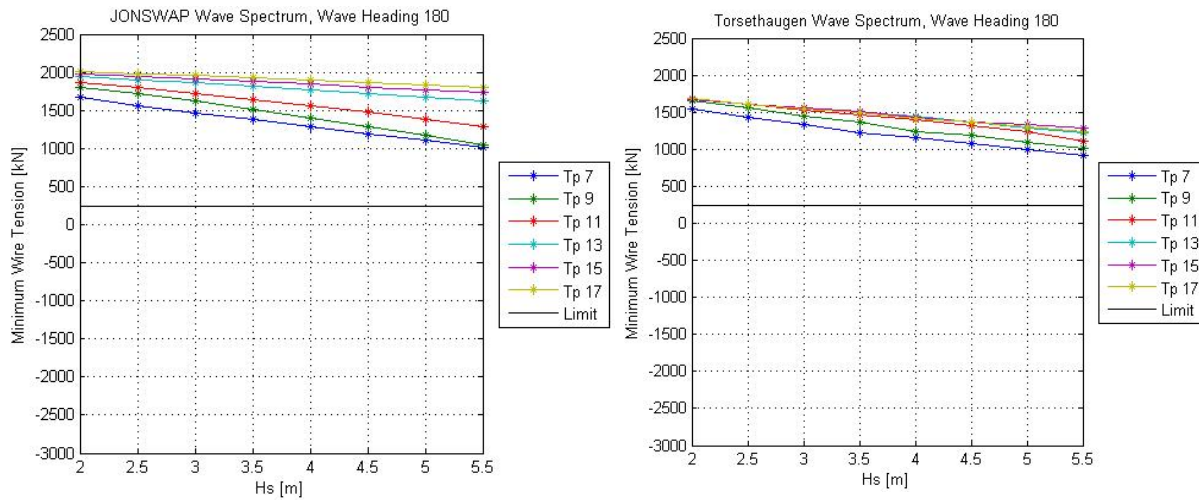
Figure 92: Crane deployment. Minimum wire tension [kN] for JONSWAP and Torsethaugen wave spectra, wave heading 180º at time instance 2.

Appendix 14.3: Moonpool deployment, time instance 1.
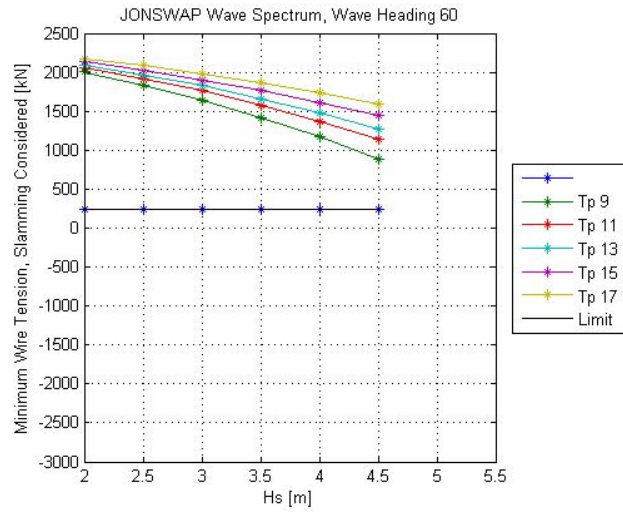
Figure 93: Moonpool deployment. Minimum wire tension [kN] for JONSWAP wave spectrum, wave heading 60⁰ at time instance 1.
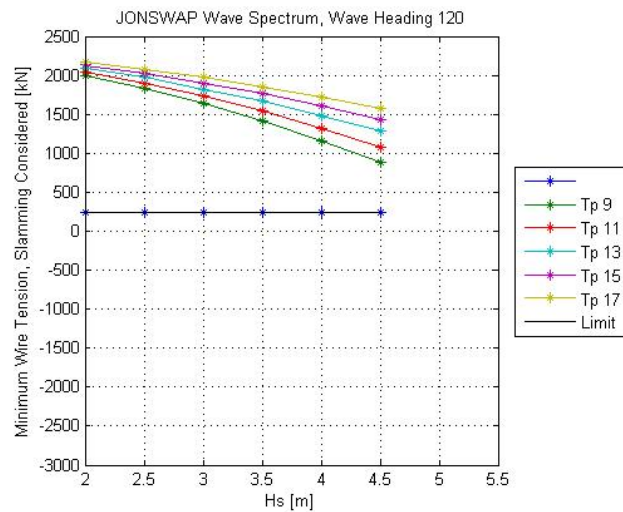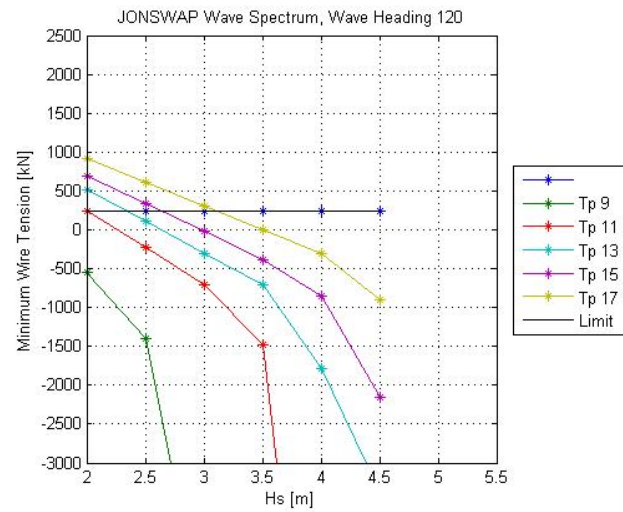

Figure 94: Moonpool deployment. Minimum wire tension [kN] for JONSWAP wave spectrum, wave heading 120⁰ at time instance 1.
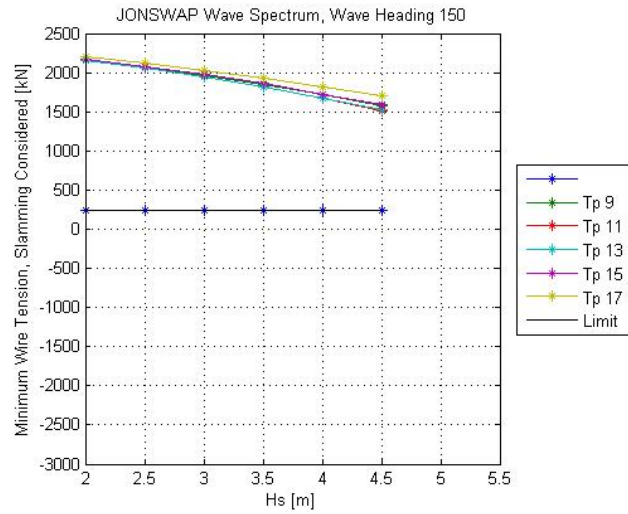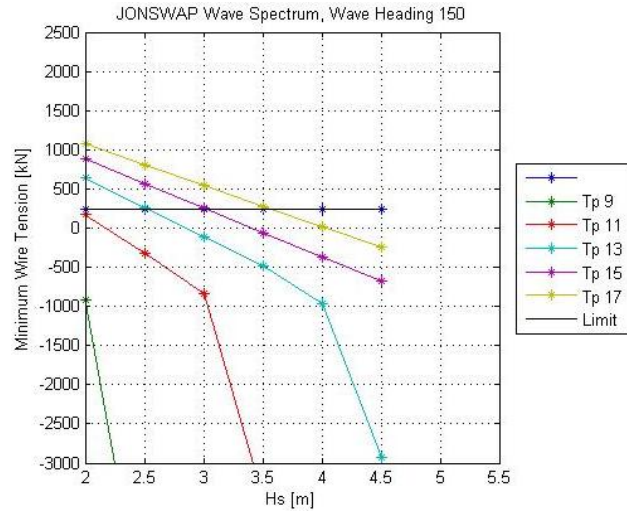
Figure 95: Moonpool deployment. Minimum wire tension [kN] for JONSWAP wave spectrum, wave heading 150° at time instance 1.
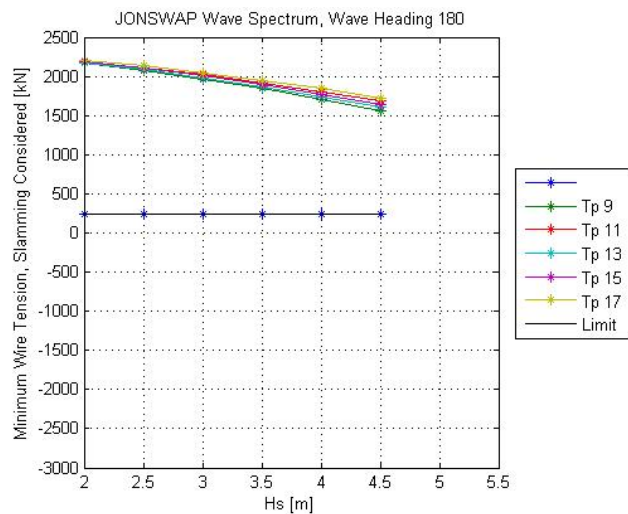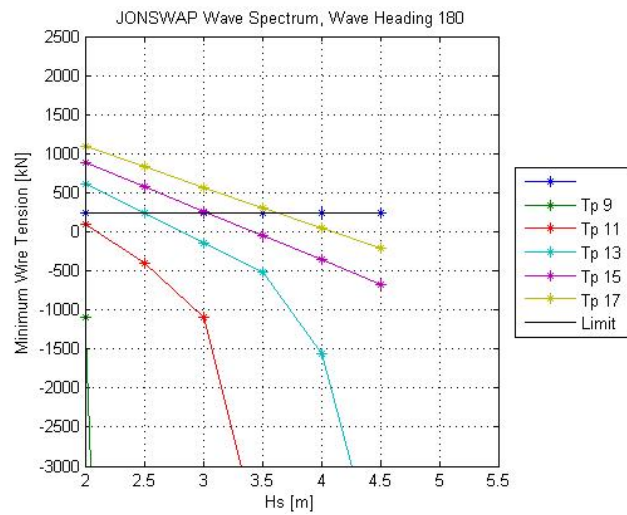

Figure 96: Moonpool deployment. Minimum wire tension [kN] for JONSWAP wave spectrum, wave heading 180° at time instance 1.

Appendix 14.4: Moonpool deployment, time instance 2.
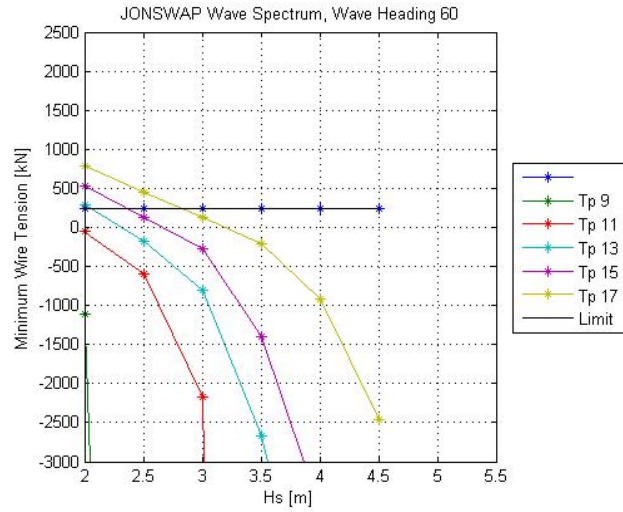
Figure 97: Moonpool deployment. Minimum wire tension [kN] for JONSWAP wave spectrum, wave heading 60° at time instance 2.

Figure 98: Moonpool deployment. Minimum wire tension [kN] for JONSWAP wave spectrum, wave heading 120° at time instance 2.

Figure 99: Moonpool deployment. Minimum wire tension [kN] for JONSWAP wave spectrum, wave heading 150° at time instance 2.

Figure 100: Moonpool deployment. Minimum wire tension [kN] for JONSWAP wave spectrum, wave heading 180° at time instance 2.

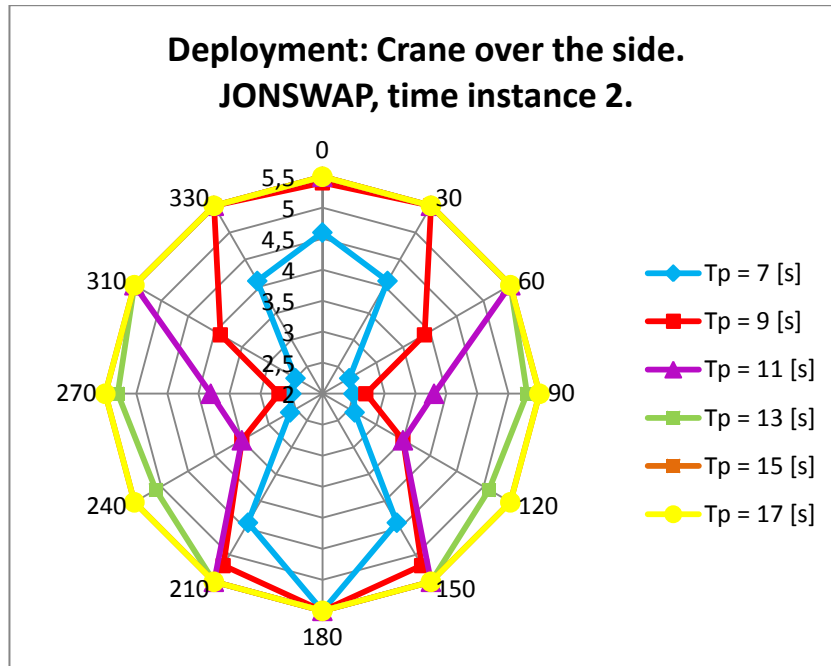## Appendix 15: JONSWAP and Torsethaugen Separate Operability Rosettes

Figure 101: Operability rosette for crane deployment at time instance 2, JONSWAP wave spectrum only. The circles represent design H_s from 2.0 – 5.5 [m].
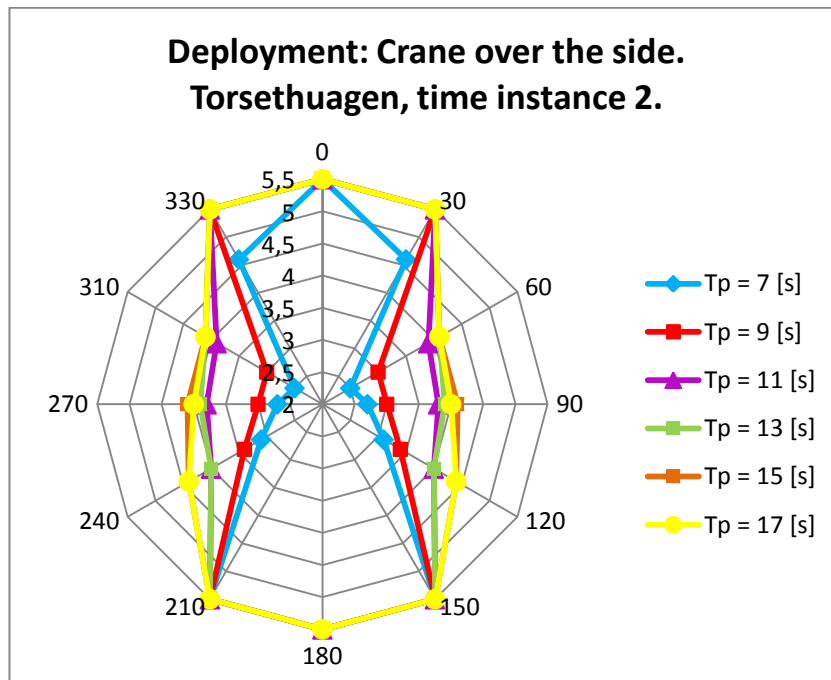

Figure 102: Operability rosette for crane deployment at time instance 2, Torsethaugen wave spectrum only. The circles represent design H_s from 2.0 – 5.5 [m].